

---

**Finding gaps on  
techno-economic assessment on  
Wave Energy Converters: path  
towards commercialization**

---

*Adrián David de Andrés Gutierrez*

*PhD advisors: Raúl Guanche García, Cesar Vidal Pascual*



*Doctor of Philosophy*

UNIVERSITY OF CANTABRIA

2015

*"You are capable of more than you know. Choose a goal that seems right for you and strive to be the best, however hard the path. Aim high. Behave honorably. Prepare to be alone at times, and to endure failure. Persist! The world needs all you can give",*

*E. O. Wilson*

*"Many of life's failures are people who did not realize how close they were to success when they gave up",*

*Thomas Edison*

*"Never doubt that a small group of thoughtful, committed citizens can change the world. Indeed, it is the only thing that ever has",*

*Margaret Mead*

---

# Abstract

---

Nowadays, Wave energy is still on a pre-commercial stage. A lot of interest has been raised during the last decades due to the increasing interest in a blue economy. However although wave energy has proved to be feasible, the prototypes are on the testing phase and no technology has been successfully confirmed to be competitive yet. A lot of different converters with different activating principles are still being considered and no convergence has been achieved. Therefore, a gap on the techno-economic analysis of wave energy converters has been identified. Hence, this thesis attempts to look at the techno-economic issues related to wave energy conversion, in a more thorough manner.

Firstly, due to the lack of long-term power production data for wave energy converter a computationally efficient methodology aiming to obtain the long-term power production series has been developed. This technique was further applied to several converters under different sea state conditions at different locations across the world. Within the use of this methodology the influence of the classic power assessment methodology assumptions regarding the analytical spectra has also been analyzed. The assumption of the analytical spectra was proved to be very inaccurate for resonant devices while it was acceptable for follower devices. In addition, it was confirmed that the use of analytical spectra tends to yield very inaccurate at locations with mixed swell-wind sea states. The methodology was probed to give accurate long term data series for both analytical spectra and actual ones from buoys. The need of long term quality data (buoy or multi-component spectra) has also been highlighted.

Secondly, the influence of met-ocean conditions on the design/operation process of a converter has been analyzed. The latest failures of some actual prototypes show a lack of the understanding of the way the met-ocean conditions influence the design/operation process of a wave-energy converter. In this chapter, the design phase of a generic wave energy converter is analyzed from the location targeting perspective. Secondly, the Operation and Maintenance (O&M) parameters are analyzed on a global basis, in order to find the balance between resource and accessibility. Furthermore, a generic failure analysis is performed in order to target the locations with an adequate balance between resource and the severity of the wave conditions. An assessment of the adequability of the different sites around the world as a function of the stage of development (reliability) is suggested. Finally, a study of the main wave factors that influence array design is performed.

Lastly, an analysis of the current economics of wave energy is performed. The effect of the uncertainties on met-ocean conditions on the finance of a particular wave energy project is further analyzed. Also, the influence of the political uncertainties, regarding feed in tariff, is studied on the cash flow of a particular project, leading to the conclusion of the importance of

the stability of the regulatory markets, so as to provide the adequate tools for the development of wave energy. Finally, an analysis of the Levelized Cost of Energy (LCOE) of two current existing prototype is carried out in order to show some current figures of the real cost of wave energy nowadays.

---

# Acknowledgements

---

First of all, I would like to express my gratitude to my supervisors, Prof. Cesar Vidal, whose expertise, understanding and technical advice have added significantly to my graduate experience and improved this dissertation. Many thanks are due to PhD Raúl Guanche for his dedication, understanding and his technical and non-technical support, which has been beneficial in every way. I would also like to mention that he has believed in me and my potential since I started my research career, and for this reason, I am eternally grateful to him.

Special thanks are due to Prof. Raúl Medina, Íñigo Losada and Javier Lopez Lara. They introduced me into the coastal engineering research through my undergraduate final project, as well as provided me with direction, technical support. Thanks to this opportunity that has paved the way toward a career in coastal engineering research. Furthermore, due to their recommendation and unfaltering support, I was granted a PhD position at IH Cantabria, and for this reason, I owe them a debt of gratitude.

I would also like to thank all members of the Offshore Engineering and Ocean Energy group at IH Cantabria. Lucía, Carlos, Víctor, Jose, Elena, Joseba and Michele, as well as Miguel, Javi and Gema, although they are now embarked on other commitments, thank you very much for your valuable contributions to this thesis and all the good moments that we spent. A very special thanks go to Arantza for being so supportive, helpful and friendly to me whilst working on this thesis, and Fernando and Javi for being there for me during the past three years and for patiently putting up with my ups and downs.

Part of this thesis consists of collaborations with other research institutes from other countries. I would like to thank Ronan Costello, from NUI Maynooth and Jochem Weber from NREL, for the exciting and interesting work we carried out within the scope of this thesis. I also would like to thank Henry Jeffrey and Andy MacGillivray from the University of Edinburgh for their valuable contribution to some parts of this thesis. Many thanks are due to all these people who taught me different ways with which we can approach and solve problems.

I spent four months of the past three years at the Institute of Energy Systems at the University of Edinburgh, and I would like to show my gratitude to the Institute's staff, for welcoming me since my arrival and for making me feel one of them from the very first day. Very special thanks go to Andy MacGillivray for his friendship, all the good moments we spent during my academic journey in Edinburgh and his useful contribution to this thesis. I should never forget Henry Jeffrey, my host supervisor at IES, for the time he had dedicated to me, the useful discussions and his kindness during my time at IES. My sincere thanks are due to Duncan, Sam, Lucy, Andy, Laura, John, George, Atul, Susan, Mark, Nicola, Pauline, Aby, David and Cameron for warmly welcoming me in Edinburgh and for making my stay there enjoyable.

Very remarkable thanks go to INORE, for giving me the opportunity to meet so many interesting people during those important three years. A very special acknowledgement goes to some very smart people I met during those years and who have now become very close friends to me, from across the world: David, Keith, Andy, Duncan, Sam, Cam, Cesc, Simon, Morten, Miren and Antoine, thanks for supporting me during the last stages of my PhD. During the last two years, I served at the INORE Committee, as a way of giving back to INORE for all what I had already received from them. During this time, I learnt very important things, such as dealing with people of different backgrounds/nationalities, as well as managing a large organization. I have also made very good friends at the INORE committee, such as Cam, Morten, Cesc, Michele and Sam, who I would like to thank for the good moments and all the time we had spent discussing how to take INORE to the next level.

Last but not least, I would like to thank my family for the consistent support that they have provided me throughout my entire life, and in particular, I must acknowledge my mum, Maria Jesus and my grandma Dorita whose encouragement and support have been one of the main reasons why I managed to complete this thesis. My thoughts are also with my two grandpas, Jesus and Proculo, who unfortunately are not here to see how I complete this commitment but I know that wherever they are they are supporting me.

To sum up, I strongly believe that this research would not have been possible without the financial assistance of the University of Cantabria. Thus, I would like to express my gratitude for its PhD scholarships program for the funding toward my PhD work.

---

## Declaration

---

I declare that this thesis was composed by myself, that the work contained herein is my own except where explicitly stated otherwise in the text, and that this work has not been submitted for any other degree or professional qualification except as specified.

---

**Adrián David de Andrés Gutierrez**

---

# Contents

---

<b>Abstract</b>	<b>IV</b>
<b>Acknowledgements</b>	<b>VI</b>
<b>Declaration</b>	<b>VIII</b>
<b>Figures and Tables</b>	<b>XII</b>
<b>0 Resumen en castellano</b>	<b>2</b>
0.1 Introducción . . . . .	2
0.2 Estado del arte . . . . .	3
0.3 Objetivos . . . . .	6
0.4 Metodología para el análisis de la producción a largo plazo . . . . .	7
0.5 Influencia de las condiciones meteoceánicas en el diseño y operación de los WECs . . . . .	10
0.5.1 Adaptabilidad de un convertidor de las olas a varias condiciones meteoceanicas . . . . .	10
0.5.2 Estudio de los parámetros de Operación y mantenimiento con una perspectiva global . . . . .	12
0.5.3 Estudio de la fiabilidad de los convertidores de energía de las olas . . . . .	15
0.5.4 Estudio de los factores que afectan al diseño de parques . . . . .	16
0.6 Estudio economico de la energía de las olas . . . . .	17
0.6.1 Riesgos e incertidumbres de la energía de las olas . . . . .	17
0.6.2 Trayectoria hacia un LCOE reducido . . . . .	20
0.7 Conclusiones . . . . .	21
<b>1 Introduction</b>	<b>23</b>
1.1 Introduction . . . . .	23
<b>2 State of the art of wave energy</b>	<b>28</b>
2.1 Introduction . . . . .	28
2.2 Historic Review of Wave energy . . . . .	28
2.3 Description of Wave Energy Extraction Phenomena . . . . .	30
2.4 Classification of Wave Energy Prototypes and Current prototypes . . . . .	31
2.4.1 Oscillating Water Column . . . . .	31
2.4.2 Oscillating Bodies . . . . .	34
2.4.3 Overtopping . . . . .	40

---

2.5	Current State of Wave Energy Development . . . . .	41
2.6	Review of techno-economic assessment on wave energy . . . . .	46
2.7	Conclusions . . . . .	47
<b>3</b>	<b>Objectives</b>	<b>48</b>
3.1	Objectives . . . . .	48
3.2	Thesis structure . . . . .	49
<b>4</b>	<b>Power assessment methodology and applications</b>	<b>50</b>
4.1	Long term power production assessment methodology . . . . .	50
4.1.1	Introduction . . . . .	50
4.1.2	Methodology for long term analysis . . . . .	52
4.2	Influence of sea state characterization on power assessment . . . . .	60
4.2.1	Introduction . . . . .	60
4.2.2	Description of studied parameters . . . . .	62
4.2.3	Methodology . . . . .	69
4.2.4	Results . . . . .	72
4.3	Conclusions . . . . .	84
<b>5</b>	<b>Influence of met-ocean conditions on wave energy converters design and operation</b>	<b>86</b>
5.1	Introduction . . . . .	86
5.2	WEC Design approach: adaptability of a WEC to different weather scenarios	87
5.2.1	Introduction . . . . .	87
5.2.2	Climate data . . . . .	88
5.2.3	WEC Characteristics . . . . .	90
5.2.4	Results . . . . .	96
5.3	Study of O&M Parameters from a Worldwide Perspective . . . . .	111
5.3.1	Introduction . . . . .	111
5.3.2	Climate data . . . . .	112
5.3.3	Accessibility and availability . . . . .	112
5.3.4	Weather windows and waiting period analysis . . . . .	122
5.3.5	Operation and maintenance cost . . . . .	132
5.3.6	Conclusions . . . . .	137
5.4	Linking O&M and Reliability assessment on wave energy converters . . . . .	139
5.4.1	Introduction . . . . .	139
5.4.2	Failure simulation background . . . . .	140
5.4.3	Bathtub curve & O&M . . . . .	142
5.4.4	Maintenance Scenarios . . . . .	146
5.4.5	Conclusions . . . . .	154

---

5.5	Factors that influence array layout on wave energy farms . . . . .	156
5.5.1	Introduction . . . . .	156
5.5.2	Simulations . . . . .	157
5.5.3	Results: sensitivity analysis . . . . .	160
5.5.4	Application to different weather scenarios . . . . .	167
5.5.5	Conclusions . . . . .	173
<b>6</b>	<b>Economics of wave energy</b>	<b>176</b>
6.1	Introduction . . . . .	176
6.2	Risks and Uncertainties on wave energy economics . . . . .	176
6.2.1	Introduction . . . . .	176
6.2.2	Methodology . . . . .	178
6.2.3	Long term production analysis . . . . .	181
6.2.4	Statistical analysis of financial indicators . . . . .	186
6.2.5	Sensitivity analysis: feed in tariff . . . . .	191
6.2.6	Feed in tariff uncertainty . . . . .	193
6.2.7	Conclusions . . . . .	200
6.3	Pathways towards a reduced LCOE in Ocean Energy . . . . .	201
6.3.1	Introduction . . . . .	201
6.3.2	Wave energy prototypes case study . . . . .	202
6.3.3	Conclusions . . . . .	208
<b>7</b>	<b>Conclusions</b>	<b>210</b>
<b>8</b>	<b>Future research</b>	<b>215</b>
<b>9</b>	<b>Scientific contributions of this thesis</b>	<b>217</b>
<b>Appendices</b>		
<b>A</b>	<b>Appendix 1: Time domain model</b>	<b>219</b>
<b>B</b>	<b>Appendix 2: Frequency domain model</b>	<b>224</b>
B.1	Frequency domain model for Section 5.2 . . . . .	224
B.2	Frequency domain model for Section 4.2 . . . . .	226
<b>Bibliography</b>		<b>228</b>

---

# Figures and Tables

---

## Figures

1.1	Cost of Marine Renewables based on Carbon Trust approach (see CarbonTrust (2011)) . . . . .	25
1.2	Learning rate of different energy sources against installed capacity . . . . .	26
2.1	Salter Duck recreation from Edinburgh Wave Power Group webpage . . . . .	29
2.2	Phenomena associated to wave energy conversion from Iturrioz (2014) . . . . .	31
2.3	Wave Energy converter classification based on Falcao et al (2010) . . . . .	32
2.4	LIMPET prototype on the Islay Island (Scotland,UK) from Limpet: the guardian News Ltd . . . . .	33
2.5	OEBuoy in the Galway Bay testing location . . . . .	34
2.6	Ocean Power Technology Power buoy, see Ocean Power Technologies Web page	35
2.7	Wavestar 120 kW in Hanstolm (Denmark) . . . . .	36
2.8	Pelamis P2 at EMEC . . . . .	38
2.9	Oyster 2 at EMEC . . . . .	39
2.10	Wave Dragon at Nissun Brending (Denmark) . . . . .	40
2.11	Development stages of WEC technologies . . . . .	44
2.12	Development path of some WEC technologies, in yellow current path, in green optimum path . . . . .	45
2.13	Developers perceived uncertainty on Operation and Maintenance activities . . .	45
4.1	Analyzed two body heave WEC with dimensions . . . . .	53
4.2	Location of the point selected for the power study . . . . .	53
4.3	Power matrix of the device (kWh) . . . . .	54
4.4	Capacity factor vs Nominal Power . . . . .	55
4.5	Percentage occurrence matrix/occurrence matrix in Santoña (Spain) . . . . .	56
4.6	Schema of the proposed methodology . . . . .	56
4.7	r-squared parameter for the different selection cases and the different number of cases . . . . .	57
4.8	Percentage of relative error with respect mean annual hourly production between methodologies scatter diagram* Power Matrix and power matrix calculated by the model for year 2001 . . . . .	58
4.9	Selected sea states for the two methodologies applied for the year 2001 . . . . .	59
4.10	Mean annual power and standard deviation for the 60 year series at the study with 200 and 1000 cases . . . . .	60

4.11 Selected locations (Longitude, Latitude) . . . . .	62
4.12 Occurrence matrix in % of the selected locations . . . . .	63
4.13 Occurrence of the different sea state types on the different locations . . . . .	64
4.14 Example of the different data sets considered: on the right JONSWAP and IFREMER, on the left buoy data, IFREMER and both JONSWAPs for Bilbao . . . . .	66
4.15 Simulated WECs, from right to left: one body heaving device, two body heaving device, deep water flap . . . . .	66
4.16 Added mass for all the devices, scale normalized, see table 4.5 for more information	67
4.17 Radiation damping for all the devices, scale normalized, see table 4.5 for more information . . . . .	68
4.18 Excitation force transfer function for all devices. Magnitude is normalized see Table 2 for more information . . . . .	69
4.19 Power Matrices in kWh for the three studied devices . . . . .	70
4.20 Mean and standard deviation of the $\varepsilon_0$ for the different number of peak sea states	71
4.21 100 sea states subsets over the whole sea states data series . . . . .	72
4.22 Real power on the whole set vs interpolated power based on the 100 selected sea states . . . . .	75
4.23 Correlation coefficient for the 3 WECs and all the data types at Bilbao . . . . .	75
4.24 Set of consecutive sea states selected for analysis in Denmark, in blue the IFREMER data, in pink JONSWAP . . . . .	77
4.25 Estimated harvest power with the 3 different WECs on the set of spectra selected on Figure 4.24 . . . . .	79
4.26 Capture width ratio vs Spectrum broadness for the selected spectra on Figure 4.24 . . . . .	79
4.27 Scatter of the power estimated with JONSWAP vs Power estimated with IFREMER data . . . . .	80
4.28 Annual Energy production (MWh/year) estimated with the classical method as well as the different sea state data sources outlined . . . . .	83
4.29 Resource estimation(kW/m) with the different sources of sea states data . . . . .	83
4.30 Capture width ratio (%) estimation with the different data sources . . . . .	84
5.1 Mean $T_p$ (s), standard deviation of $T_p$ (s), coefficient of variation of $T_p$ and mode of $T_p$ (s) . . . . .	89
5.2 Average (kW/m), standard deviation (kW/m) and coefficient of variation of wave energy resources . . . . .	91
5.3 Set of floaters analysed as a converter . . . . .	92
5.4 Response amplitude operator of the individual floats for the proposed converters	93
5.5 Power and amplitude of motion as a function of the PTO constant for the 8 s converter (individual float), for the 10.5 s wave period . . . . .	94

5.6	Average Power and selected PTO Constant for each period for the 8 s converter (individual float) . . . . .	95
5.7	Power matrix (kW) of the designed converters (4, 6, 8, 10, and 12 s) . . . . .	95
5.8	Distribution of the converter used on each location for the option C (Tuned converter) in seconds . . . . .	97
5.9	Capture width ratio (%) for option 1, 2 and 3 . . . . .	98
5.10	KWT for the three studied options . . . . .	100
5.11	WEC mass versus the natural period . . . . .	101
5.12	Global WEC power production related to natural frequency . . . . .	101
5.13	Available coastal locations for Scenarios 1 and 2 and the different WEC options .	104
5.14	Percentage of available locations depending on CWR . . . . .	105
5.15	Percentage of available locations depending on the KWT indicator . . . . .	106
5.16	normalized O&M costs per kWh for different turbine ages and sizes, from Jensen <i>et al.</i> (2002) . . . . .	108
5.17	Cost per kWh curves for the different options . . . . .	108
5.18	Optimum option for material cost and normalized O&M costs for different values of $\beta$ and $\lambda$ . . . . .	109
5.19	Availability map in percentage for wave height threshold $H_s = 5m$ . . . . .	115
5.20	Wave energy restrictions with availability restrictions . . . . .	115
5.21	Accessibility (in %) for different wave height thresholds . . . . .	116
5.22	Situation of the sites chosen for further study . . . . .	117
5.23	Cumulative density function of the $H_s$ for Ireland and Australia location . . . . .	118
5.24	Cumulative density function of the wave energy flux for Ireland and Australia location	119
5.25	Mean monthly accessibility for the Denmark, Ireland, Chile and Spain . . . . .	120
5.26	Monthly accessibility for Portugal, Scotland and Australia . . . . .	120
5.27	Average and standard deviation of the number of 6 h weather windows per year for wave height threshold $H_s = 1.5m$ . . . . .	123
5.28	Average and standard deviation of the number of 12 h weather windows per year for wave height threshold $H_s = 1.5m$ . . . . .	124
5.29	Average and standard deviation of the number of 24 h weather windows per year for wave height threshold $H_s = 1.5m$ . . . . .	125
5.30	Mean, standard deviation and 99% quantile waiting period during winter time for a weather window of at least 6 h . . . . .	126
5.31	Mean, standard deviation and 99% quantile waiting period during winter time for a weather window of at least 12 h . . . . .	128
5.32	Mean, standard deviation and 99% quantile waiting period during winter time for a weather window of at least 24 h . . . . .	129
5.33	CDFs of waiting periods on Australia, Denmark, Spain and Ireland . . . . .	131
5.34	Average power production (kW) . . . . .	132

5.35	Normalized O&M costs with 1,3 and 5 fails per year . . . . .	134
5.36	Normalized O&M costs for the different locations with 1,3 and 5 fails per year . . . . .	135
5.37	Normalized O&M costs (for 3 fails per year) and power production . . . . .	137
5.38	Bathtub curve . . . . .	141
5.39	Schema of the simulation . . . . .	143
5.40	Mean downtime for the different aforementioned scenarios . . . . .	144
5.41	Availability(%) for the different aforementioned scenarios . . . . .	145
5.42	Resource and time availability in Denmark, Ireland and Australia . . . . .	148
5.43	Failure rates needed for an average normalized O&M costs of 0.04Euros/kWh . . . . .	149
5.44	Failure rates needed for an average normalized O&M costs of 0.04 Euros/kWh on selected locations . . . . .	149
5.45	Histogram of failures per year for all the coastal locations . . . . .	150
5.46	Recommended areas for wave energy development as a function of failure rates Scenario 1 . . . . .	151
5.47	Stages of development for a wave energy prototype . . . . .	151
5.48	Recommended areas for wave energy development as a function of failure rates Scenario 2 . . . . .	154
5.49	Difference in normalized O&M cost (Euros/kWh) of corrective and annual preventive maintenance with respect just corrective . . . . .	154
5.50	Failure rates needed for an average normalized O&M cost of 0.04Euros/kWh on selected locations Scenario 3 . . . . .	155
5.51	Recommended areas for wave energy development as a function of failure rates Scenario 3 . . . . .	155
5.52	The two bodies heave Converter analyzed . . . . .	158
5.53	The different farms configurations simulated: a)Linear, b)Triangle, c)Rhombus, d)Square . . . . .	159
5.54	Power production vs $H_s$ for different peak periods . . . . .	160
5.55	q factor for the specified separations in the subfigures and the specified incidence direction in the legend over the range of simulated periods . . . . .	161
5.56	$q_m$ factor for 2-body linear configuration . . . . .	162
5.57	$q_m$ factor for 3-body linear configuration . . . . .	162
5.58	$q_m$ factor for 3-body triangle configuration . . . . .	163
5.59	$q_m$ factor for 4-body linear configuration . . . . .	163
5.60	$q_m$ factor for 4-body square configuration . . . . .	164
5.61	$q_m$ factor for 4-body rhombus configuration . . . . .	165
5.62	Comparison of square and rhombus configuration for a 4 WEC wave farm, $0^\circ$ incidence and separation $L_{10}/2$ throughout the range simulated periods . . . . .	166
5.63	KMA clustering: initialization { $v_{10}, \dots, v_{160}$ }, updating tracks and final centroids { $v_1, \dots, v_{16}$ }with their corresponding clusters. Camus <i>et al.</i> (2011) . . . . .	169

5.64	Weather climates types derived from classification taking into account wave height, the peak period, the wave energy flux and the deviation of directionality . . . . .	172
5.65	$q_r$ factor maps for the linear(above), square(center) and rhombus(bellow) configuration . . . . .	173
5.66	Occurrence matrices and Direction Rose of Climates selected for comparison 2,6,7 and 8 . . . . .	174
5.67	Probability density functions for $q$ factor (gain factor) for rhombus and square configurations . . . . .	174
6.1	Two body heave converter analyzed . . . . .	179
6.2	Location of the wave farm and yearly mean wave energy resources around La Palma Island extracted from IHCantabria (2011) . . . . .	179
6.3	Occurrence matrix (in percentage) and 196 selected sea states for the selected site	180
6.4	Diagram of the energy production model . . . . .	181
6.5	Yearly production of the 4 WECs 4 MW wave farm 1948 to 2008 . . . . .	182
6.6	Process of generation of the life-cycles for the statistic analysis (Monte Carlo) . .	182
6.7	Distribution of cost items for the EPCI budget for the selected wave energy farm	184
6.8	Mean cash-flow for the 10000 generated life-cycle. . . . .	187
6.9	Mean, standard deviation and coefficient of variation of wave flux . . . . .	188
6.10	Comparison between 2 life-cycles: top panels, the yearly accumulated production and lower panels associated the cash flow . . . . .	189
6.11	Cumulative distribution function for the IRR with a lognormal distribution . . . . .	189
6.12	Cumulative distribution function for the NPV with a lognormal distribution . . . . .	190
6.13	Cumulative distribution function for the PBP with a extreme value distribution . .	190
6.14	Internal rate of return and Net present value vs different feed in tariffs . . . . .	193
6.15	Internal rate of return vs number of units and feed in tariff for the different scenarios (optimistic, medium and pesimistic) proposed (the gross lines represent the isolines of IRR) . . . . .	194
6.16	Curves of iso-internal rate of return for number of units produced vs feed in tariff applied . . . . .	194
6.17	PDF of IRR for the different feed in tariffs . . . . .	195
6.18	Level and duration of support for RES-E plants commissioned 2008 . . . . .	196
6.19	Contracts for difference schema from Renewable UK <i>et al.</i> (2013) . . . . .	197
6.20	Feed in tariff Scenario 1 . . . . .	198
6.21	Feed in tariff Scenario 2 . . . . .	198
6.22	Cash flow associated with Feed in tariff Scenario 1 . . . . .	199
6.23	Cash flow associated with Feed in tariff Scenario 2 . . . . .	199
6.24	LCOE for the different cases . . . . .	206
6.25	Cost of Energy on the different selected locations . . . . .	206

6.26	Yearly power production for the two analyzed converter . . . . .	207
A.1	Simplified model . . . . .	219

---

**Tables**

2.1	Characteristics of the LIMPET prototype . . . . .	33
2.2	Characteristics of the OE Buoy prototype . . . . .	34
2.3	Characteristics of the OPT Powerbuoy prototype . . . . .	36
2.4	Characteristics of the Wavestar prototype . . . . .	37
2.5	Characteristics of the Pelamis prototype taken from SIOcean (2013) . . . . .	38
2.6	Characteristics of the Oyster prototype taken from SIOcean (2013) . . . . .	39
2.7	Characteristics of the Wave Dragon prototype taken from SIOcean (2013) . . . . .	41
2.8	TPL-TRL metrics from Weber et al (2012) . . . . .	43
4.1	Annual mean power in kWh calculated with the methodologies selected for year 2001 . . . . .	57
4.2	Summary of power production figures . . . . .	59
4.3	Geometry Characteristics of the WECs selected for study . . . . .	67
4.4	Maximum values used to normalize previous curves . . . . .	68
4.5	Position constraints applied to damping optimization . . . . .	68
4.6	Combination of parameters for simulation . . . . .	73
4.7	Errors with the different data sources. Note: the errors are computed with respect the Exact case for each option . . . . .	82
5.1	Characteristics of the proposed options . . . . .	93
5.2	Analysis of CWR values for the different options . . . . .	99
5.3	Mean and standard deviation for the kW/Ton . . . . .	102
5.4	Proposed scenarios for the study . . . . .	103
5.5	Percentage of nodes on different availability levels . . . . .	113
5.6	Proposed scenarios for the study . . . . .	117
5.7	Percentage of nodes with the different accessibility levels . . . . .	117
5.8	Percentage of nodes that satisfy a minimum waiting period . . . . .	130
5.9	Mean (M), standard deviation (S) of the number of weather windows and Mean (M), standard deviation (S) and percentile 99% (P99) of waiting periods for the selected locations . . . . .	130
5.10	Type of best fit for each waiting period distribution . . . . .	132
5.11	Combination of parameters for simulation . . . . .	143

---

5.12	Combination of parameters for simulation . . . . .	147
5.13	Simulation sets, referring the symbols in array configuration to Linear (L), Triangle (T), Rhombus (R) and Square (S) . . . . .	159
5.14	Climate parameters and mean $q_r$ for each climate type for the configurations specified . . . . .	170
6.1	Budget for the considered 4 WECs 4 MW wave energy farm . . . . .	183
6.2	Coefficient of variation of wave flux, wave production IRR and PBP . . . . .	188
6.3	FIT needed to obtain the same NPV than reference case in Figure 6.8 . . . . .	197
6.4	FIT needed to obtain the same NPV than reference case in Figure 6.8 . . . . .	200
6.5	Characteristics of the selected devices . . . . .	204
6.6	FIT needed to obtain the same NPV than reference case in Figure 6.8 . . . . .	204
6.7	WEC characteristics for case studies . . . . .	206

# Resumen en castellano

---

1

## 0.1 Introducción

La energía del oleaje deriva de la energía solar ya que la radiación del sol calienta los océanos y debido a las diferencias de presión se produce el viento. Este viento al interactuar con la superficie libre del mar produce las olas. El Consejo Mundial de la energía ha estimado que el recurso total de energía de las olas es de 2 teravatios, más del doble del consumo actual eléctrico mundial. Por tanto esta energía puede considerarse una de las más prometedoras en el futuro cercano debido a:

- El recurso de energía de las olas es un recurso predecible (mas que el recurso eólico)
- Los impactos medioambientales son fácilmente gestionables
- El impacto visual es mínimo debido a que la mayoría de los dispositivos están parcialmente sumergidos y la distancia a la costa es suficientemente elevada
- La disponibilidad de localizaciones para la construcción de parques de energía de las olas es muy grande

Además, el incremento de la población, junto con el consiguiente previsto aumento de la demanda mundial de energía y la vida limitada de los combustibles fósiles ha llevado a la construcción de una "blue economy" basada en las energía renovables.

Dentro de estas energías renovables nóveles se encuentran las energías oceánicas, es decir la eólica marina, la mareomotriz y la provenientes de las olas. Esta tesis desarrolla específicamente esta última. Aunque las predicciones marcan que esta energía será muy importante en el mix energético en el futuro cercano, en la actualidad su coste es de alrededor de 0.5 Euros/kWh, CarbonTrust (2011), que está lejos del coste actual de las fuentes de energías convencionales. Éste mismo estudio ha predicho que, cuando se llegue a una capacidad instalada mundial

---

1. In order to accomplish the University of Cantabria regulations regarding thesis format a summary in spanish is included before the body of the thesis

de 46.5 GW, el coste de la energía de las olas (incluyendo el aprendizaje correspondiente) descenderá hasta 0.1 Euros/kWh.

En la actualidad, cientos de prototipos han sido ensayados, sin embargo no se ha apreciado todavía una convergencia hacia una tipología de prototipo concreta. Por tanto, la adecuada selección de los convertidores de energía de las olas basada en criterios técnico-económicos cobra una gran importancia en la actualidad del sector. Además, otra de las razones por las cuales la energía de las olas no es aún comercial, es por los fallos que han tenido algunos prototipos en los últimos años. De ello se desprende que un estudio de detalle de las condiciones meteorológicas que afectan el comportamiento, la operación y mantenimiento y la supervivencia de los convertidores es clave para el diseño de convertidores de energía de las olas.

## 0.2 Estado del arte

La primera tarea que se realizó en esta tesis doctoral es la revisión de la bibliografía existente sobre la energía undimotriz.

La primera patente sobre un convertidor de energía del oleaje proviene de Girard e hijo, en 1799 en Francia. Sin embargo, el japonés Yoshio Masuda es considerado en la actualidad el "padre" de la energía de las olas. Él desarrolló en los años 60 los primeros prototipos de columna de agua oscilante. Además desarrolló el dispositivo Kaimei, un barco compuesto de una serie de cámaras de OWC.

Debido a la crisis petrolífera de los años 70 muchos investigadores como Stephen Salter, Johannes Falnes y John Newman empezaron a profundizar en la investigación de la energía del oleaje. De esta manera Stephen Salter desarrolló el Salter Duct (ver figura 6.1 y Edinburgh Wave Power Group webpage), un convertidor con un giróscopo en su interior que convertía su movimiento de precesión en electricidad. Así mismo, algunos prototipos de OWC fueron desarrollados en Noruega en los años 80. En 1980 el prototipo LIMPET fue construido en Escocia y estuvo funcionando hasta 1999 cuando un prototipo con una mayor potencia se construyó cercano al prototipo antiguo.

Antes de la década de los 90 la mayor parte del trabajo en la energía de las olas estuvo dedicado a la investigación debido a la dificultad del problema y la escasez de fondos. Sin embargo la situación cambió cuando en 1991 la comisión europea decidió incluir la energía del oleaje en su programa de I+D+i de energías renovables.

En la actualidad existen cientos de prototipos diferentes, con distintos principios de actuación. A su vez existen diferentes maneras de clasificación, atendiendo a la distancia de la costa, basados en el tamaño y basados en el principio de actuación. Sin embargo la clasificación más

útil en la actualidad es la proporcionada por Falcao (2010), ver Figura 2.3. Esta clasificación divide a los prototipos en los siguientes tipos:

- **Columna de agua oscilante**

En estos dispositivos, una estructura hueca, abierta por el fondo o lateralmente, atrapa una columna de agua y una cámara de aire, comunicada esta última con la atmósfera a través de una turbina de aire. La excitación del oleaje hace que la columna de agua oscile y actúe como un pistón sobre la cámara de aire, bombeando el mismo a través de la turbina. Esta tipología de prototipos puede ser fija (en dique) o flotante. En cuanto a ejemplos de prototipos fijos se puede destacar la planta LIMPET, desarrollada en Escocia en los años 80 (ver tabla 2.1 y figure 2.4), o Pico en las islas Azores. En cuanto a ejemplos de prototipos flotantes existen por ejemplo el Aquabuoy o el OE Buoy desarrollada en Irlanda (ver tabla 2.2).

- **Cuerpos oscilantes**

Se trata de cuerpos que extraen energía del movimiento relativo de un cuerpo con respecto a un punto de referencia (Seabased por ejemplo) o el movimiento relativo entre varios cuerpos (OPT Powerbuoy). Dentro de este grupo los prototipos se pueden clasificar en flotantes o sumergidos dependiendo de su posición relativa con respecto a la superficie libre. Como ejemplo de este grupo podemos destacar OPT powerbuoy formado por 2 cuerpos flotantes que extraen energía del movimiento relativo entre ambos. Este prototipo ha sido ya probado en Hawái, Atlantic City (USA), Santoña (España) y Escocia.

Otro de los prototipos en esta categoría que se ha desarrollado mucho en los últimos años es el Pelamis, que consiste en una serie de tubos cilíndricos separados por juntas. En este caso se extrae energía del movimiento relativo entre los cilindros. Este prototipo ha sido probado en Portugal en su primera versión y posteriormente en las islas Orcadas (Escocia) en su segunda versión.

Otro de los ejemplos en este grupo, pero en la categoría de sumergidos es el prototipo Oyster desarrollado por Aquamarine Power. Este prototipo consiste en un cuerpo articulado anclado al suelo que extrae energía de su movimiento de rotación (ver figura 2.9 y tabla oystertabla). Este prototipo se encuentra instalado a una profundidad de 10-15 m y por tanto supone que es un prototipo que se encuentra cercano a la costa. Este prototipo ha sido probado en su versión 1 y 2 en las islas Órcadas en Escocia.

- **Dispositivos de rebasa**

Estos dispositivos aprovechan el agua que asciende por un talud con el oleaje y rebasa sobre un depósito cuyo nivel está sobreelevado con respecto al nivel del mar. Esta energía potencial es transformada en mecánica cuando el flujo de agua atraviesa una turbina. Este grupo a su vez se puede dividir en flotantes y fijos en estructura.

Un ejemplo de un convertidor de este grupo es el Wave Dragon. Este concepto consiste en un dispositivo flotante formado por dos reflectores que concentran las olas hacia una rampa, donde el agua rebasa sobre un tanque donde esta energía potencial se transforma

en mecánica a través de una turbina. Otro ejemplo de dispositivo de rebase pero fijo corresponde al dispositivo Sea-wave Slot-cone Generator, de Vicinanza *et al.* (2014) y Vicinanza *et al.* (2012), que consiste en un grupo de tanques a distintas alturas asociado a un dique.

Como se ha demostrado en las últimas décadas, extraer la energía del oleaje es posible, por ejemplo el dispositivo Oyster ha transmitido hasta ahora 12 MWh a la red (ver Doherty (2014)) o el Wavestar ha transmitido 53.5 MWh en sus 3 años de operación (ver Kramer *et al.* (2013)). Sin embargo, por otro lado, algunos fallos importantes han ocurrido en los últimos años en algunos convertidores, lo que ha generado desconfianza al sector. Por ejemplo el Pelamis P1 falló durante su fase de pruebas en Agucadoura (Portugal) en el año 2009, el dispositivo CETO desarrollado por Carnegie se hundió durante el ciclón Bejisa cerca de la Isla Reunión (Australia). También el dispositivo Aquabuoy se hundió por razones aún inciertas.

Como se ha podido demostrar, existen todavía riesgos e incertidumbres por estudiar en cuanto a la energía del oleaje y es necesario una investigación detallada para obtener dispositivos económicamente competitivos y una alta fiabilidad. El análisis técnico-económico ha de ser considerado tanto en el proceso de selección de dispositivos como en el diseño de los mismos.

Weber (2012) resumió algunos de los puntos claves del estado/ evolución de los prototipos de energía del oleaje:

- Aún WECs muy diferentes están siendo considerados con distintos principios de actuación y por tanto no hay evidencias de la convergencia de las tecnologías.
- Todavía se necesitan muchas mejoras a nivel económico (sin considerar aún las economías de escala).
- En la actualidad el grado de desarrollo de las tecnologías:
  - Los prototipos a escala real aún requieren unas inversiones muy grandes y es necesario intentar comprometer a importantes inversores para alcanzar Technology Readiness Level (TRL) 9.
  - Falta de conocimiento del comportamiento de los prototipos en condiciones ambientales severas.
  - No hay flexibilidad en el diseño de los conceptos.

Basado en estos puntos, Weber (2012) propuso un nuevo método para el desarrollo de prototipos de conversión de las olas. Este método se basa en dos parámetros, el TRL que se define como la madurez de la tecnología, y el TPL que se define como el rendimiento de la tecnología (su capacidad comercial), ver figura 2.8. En esta figura se ve como la trayectoria amarilla es la seguida hasta ahora por la mayoría de prototipos donde se alcanzan inversiones millonarias a pesar de que el coste de la tecnología por kWh producido está muy lejos de ser competitivo y por tanto las tecnologías se estancan en TRL altas sin llegar nunca a TPL alta. Sin embargo, la trayectoria óptima correspondería a la verde donde al principio, gracias a la flexibilidad del diseño, se alcanzan TPL moderadas en un tiempo muy corto y después cuando el nivel de

inversión aumenta su transición hasta TRL 9 conlleva un incremento mucho menor de TPL.

En cuanto a la localización del desarrollo de convertidores de energía de las olas, también González-Reguero (2013) realizó un extensivo estudio del recurso de las olas a nivel práctico en las diferentes áreas del mundo y mostró como las diferentes condiciones meteorológicas oceánicas en la Tierra dan pie al diseño de distintos convertidores. A su vez también investigó las tendencias a largo plazo en la seguridad en el diseño de WECs (período de retorno de 100 años), concluyendo que hay determinadas zonas en el globo, cuyos parámetros de fiabilidad, cambiarán en el próximo siglo, y por lo tanto se tendrá que tener en cuenta a la hora del diseño de parques en estas áreas.

Por tanto, queda demostrado que existen todavía riesgos e incertidumbres por estudiar en cuanto a los convertidores de la energía del oleaje. Una de ellas, por ejemplo, estudiada en Davey *et al.* (2009), es la incertidumbre existente en los costes de Operación y Mantenimiento percibidos por los desarrolladores. Esta incertidumbre, y otras muchas asociadas al proceso de diseño y operación de los convertidores de energía del oleaje serán estudiadas en esta tesis. De esta manera todos los aspectos técnico-económicos relevantes en la selección y diseño de prototipos serán analizados con detalle en esta tesis.

### 0.3 Objetivos

Como se ha analizado en el anterior capítulo la energía del oleaje está aún en un estado pre-comercial y todavía los prototipos no han alcanzado la competitividad deseada con respecto a las demás energías renovables. Se ha identificado un vacío en el análisis técnico-económico de los prototipos de energía de las olas, ya que existen riesgos e incertidumbres que todavía no han sido analizados. Por tanto, el objetivo principal de esta tesis es rellenar el vacío existente en algunos aspectos técnico-económicos relacionados con el diseño y operación de convertidores de energía del oleaje.

Analizados los vacíos existentes en esta evaluación técnico-económica, como objetivos específicos de esta tesis se presentan:

- El desarrollo de una metodología para el estudio de la serie de potencia producida a largo plazo
  - Estudio de la influencia de la caracterización de los estados de mar en el estudio de la producción energética. Análisis del método clásico y sus hipótesis.
- El estudio de la influencia de las condiciones meteorológicas oceánicas en el diseño y operación de convertidores de energía del oleaje
  - Investigación del proceso de diseño de un WEC desde el punto de vista de adaptación de las dimensiones geométricas a las condiciones meteorológicas locales
  - Estudio de los parámetros de Operación y Mantenimiento de una manera global

- Estudio de la afección del nivel de fallo a la adecuación de las diferentes localizaciones costeras para los diferentes niveles de desarrollo de un WEC
- Estudio de la influencia de las condiciones meteoceánicas en el diseño de parques de captadores de las olas
- La profundización del conocimiento del análisis económico en la energía de las olas
  - Identificación de la influencia de la incertidumbre de las condiciones meteoceánicas y del marco regulatorio (subvenciones) sobre la viabilidad financiera de parques de captadores de energía de las olas
  - Análisis del coste actual de determinados captadores de energía de las olas e identificación de las áreas con un mayor potencial de reducción de coste

#### 0.4 Metodología para el análisis de la producción a largo plazo

En la actualidad, pocos prototipos han estado durante largos periodos de tiempo en el agua, por tanto no existen series de datos de suficiente longitud para un estudio de detalle de la producción de energía. Además a la hora de la evaluación técnico económica, es necesario disponer de la serie temporal de producción, para tener un estudio de detalle.

Normalmente, el estudio de la producción se hace basado en Pitt (2009), con el método clásico de multiplicación de la matriz de ocurrencias (% de ocurrencia anual de las combinaciones de estados de mar  $H_s$  y  $T_p$ ) por la matriz de potencias (Energía en kWh producida para cada combinación de estados de mar  $H_s$  y  $T_p$ ), dando así la producción media anual en MWh/año. Esta metodología asume un espectro analítico para el desarrollo de la matriz de potencia. Este es el método sugerido por el comité de estándares IEC/TC 114/PT 62600-1, en el que se usa la matriz bidimensional ( $H_s - T_e$  en este caso) de ocurrencias y la matriz de anchura de captura (CWR) para determinar la producción de un dispositivo en una localización concreta.

Uno de los últimos intentos de estandarizar y mejorar el estudio de la potencia corresponde a Kofoed *et al.* (2013).

En esta tesis se ha desarrollado una metodología computacionalmente eficiente para la estimación de la potencia a largo plazo. Esta metodología se basa en trabajos previos relacionados con el downscaling estadístico de las condiciones meteoceánicas a localizaciones costeras, ver Camus *et al.* (2011). Esta metodología trata de resolver los problemas relacionados con el método clásico anteriormente explicado. En primer lugar, en el método clásico, muchos de los estados de mar usados para la matriz de ocurrencia son inútiles ya que su probabilidad de ocurrencia es cercana a cero. Por otro lado, al dividir la matriz de ocurrencias y la de potencias en grupos de celdas se supone una interpolación lineal y por tanto la curvatura real de ambas matrices no es aproximada con exactitud.

Por tanto la metodología propuesta consiste en primer lugar en una técnica de selección, Max-Diss, de Snarey *et al.* (1997), que consiste en seleccionar los estados de mar más representativos

del total de la base de datos meteocéanicos de una ubicación determinada. Estos estados de mar seleccionados se introducen en un modelo numérico para así obtener la potencia asociada a estos estados de mar. Por último se utiliza una técnica de interpolación no lineal (Radial Basis Function) de Franke (1982) para reconstruir la serie de potencias a largo plazo (de la misma longitud que la serie de parámetros espectrales que se utiliza como entrada en la técnica de selección). Esta metodología está resumida en la figura 6.4.

Esta metodología se aplica a un convertidor formado por 2 cuerpos, en los que se extrae energía del movimiento relativo en alteada entre ambos en una localización al Norte de España (Santofía), cuya serie de datos ha sido obtenida de la base de datos Global Ocean Waves (GOW) de Reguero *et al.* (2012) . La complejidad de esta metodología se justifica en términos de precisión y rapidez computacional. Como comprobación se han comparado los distintos pasos de la metodología para un año concreto de datos (2001). Estos datos se muestran en la tabla 5.5. Como se puede apreciar el método clásico subestima la producción real ya que debido al tamaño de celda no se aproxima bien la curvatura de ambas matrices. Como se puede observar, con el mismo esfuerzo computacional (196 estados de mar) el error es reducido de un 46 % con el método clásico a un 11 % con la metodología propuesta. Como se puede apreciar la técnica de selección propuesta selecciona una nube de estados de mar que cubre una variabilidad del 90 % del total de estados de mar.

En la sección 4.2 esta metodología es aplicada a varios convertidores en varias localizaciones con 2 objetivos principales, por un lado analizar el comportamiento de la metodología para otros dispositivos y condiciones meteocéánicas y por otro lado analizar la influencia de la caracterización de los estados de mar y las hipótesis del método clásico en la estimación de la potencia a largo plazo.

Para este estudio se escogieron tres convertidores distintos, primeramente un prototipo de un cuerpo que extrae energía en alteada, similar a Seabased, por otro lado un dispositivo formado por 2 cuerpos que extrae energía del movimiento relativo en alteada entre ambos, similar a Ocean Power Technologies Web page y Seactricity . Por último se simuló un dispositivo formado por un "flap" que extrae energía de su balanceo. Estos dispositivos se simularon con un modelo en el dominio de la frecuencia desarrollado en el Apéndice 2. Como se puede apreciar en las matrices de potencia de la figura 4.19, los 3 dispositivos tienen un comportamiento muy diferente. El primero con una matriz de potencia suave, característica de un seguidor, el segundo con una matriz picuda en 10 s característica de un convertidor resonante, y el tercero, con una matriz picuda alrededor de 6 s.

Se han propuesto 4 localizaciones distintas: Norte de España, Oeste de Dinamarca, Oeste de Irlanda y Centro-oeste de Chile. Como se puede apreciar en la figura 4.12, las matrices de ocurrencias son muy diferentes. La matriz de ocurrencias de Bilbao está concentrada alrededor de 10 s y alturas menores a 2 m. En el caso de Dinamarca las ocurrencias están concentradas en periodos alrededor de 6 s y alturas cercanas a 1.5 m. En el caso de Irlanda las ocurrencias

están mucho más esparcidas alrededor de 10 s y alturas cercanas a 2 m. En el caso de Chile la matriz de ocurrencias es muy concentrada en 12 s y alturas cercanas a 2.5 m.

En cuanto a los datos usados para este estudio para la localización de Bilbao se usaron los datos pertenecientes a la boya del puerto de Bilbao, en las otras localizaciones se usaron los datos de IFREMER de Rasle and Arduin (2013a) y Rasle and Arduin (2013b). Estos consisten en 12 componentes de los espectros de oleaje con una separación de 3 h.

En estas localizaciones se estudió la tipología de estados de mar basados en la metodología de Wang and Hwang (2001). Como se aprecia en la figura 4.13 las localizaciones son muy diferentes con respecto a la formación de los estados de mar. Por ejemplo, Dinamarca destaca ya que el 60% de los estados de mar son de más de un pico, por tanto los espectros analíticos típicos (swell) solo representarían el 40% de los mismos. Esto es debido a la alta combinación de swell y wind sea. Por otro lado en Irlanda el swell tiene una mayor importancia y por tanto los estados de mar con un sólo pico corresponden al 60% de las ocurrencias.

En este estudio con estos 3 convertidores y 4 localizaciones se aplica la metodología explicada anteriormente. Como diferencia con el caso anterior, en este caso, al tener datos de espectros reales o pseudoreales la selección se hace en base a 3 parámetros,  $H_s$ ,  $T_p$  y  $\epsilon_0$ , que representa la anchura del espectro .

En primer lugar se comparan los resultados para la localización de Bilbao, para los diferentes grupos de simulación definidos en la tabla 4.6. Así se demuestra que la metodología es válida para todos los tipos de convertidores, aunque se alcanza un mayor grado de exactitud para convertidores seguidores (ver figura 4.23). Se aprecia además que para espectros reales la metodología funciona bien con una selección basada en 3 parámetros, sin embargo para espectros analíticos 2 parámetros son suficientes para la selección y la inclusión del parámetro de anchura del espectro distorsiona la selección.

Por otro lado, se comparan los resultados estado de mar a estado de mar y en la producción energética anual. En cuanto a la comparación estado de mar a estado de mar como se puede apreciar en la figura 4.25, la diferencia entre JONSWAP y la producción en los estados de mar bimodales es muy alta, hasta con un 200% de diferencia. En la figura 4.26 se representa la anchura de captura (CWR) frente a la anchura espectral. Como se puede ver en la figura la tendencia es decreciente, a mayor anchura espectral menor CWR. Además esta tendencia es más marcada en los convertidores resonantes.

Por otro lado, se comparan todos los grupos de datos estudiados en cuanto a la energía producida anual (AEP) en las figura 4.28 y tabla 4.7. En estas tablas se puede identificar como el procedimiento clásico de la power matrix subestima la producción anual en un rango de -44 a -7%. Como se puede apreciar los mayores errores se encuentran en la localización de Bilbao ya que en este caso los datos son reales. Por otro lado, en cuanto a las aproximaciones con JONSWAP con  $\gamma = 3,3$  y el mejor ajuste de  $\gamma$ , los mayores errores recaen en la localización de

## **0.5. Influencia de las condiciones meteoceánicas en el diseño y operación de los WECs9**

Dinamarca en el WEC 3 debido a que en esta localización existen gran porcentaje de estados de mar bi y trimodales. Además coincide que el WEC 3 su periodo de mayor producción es 6 s, que corresponde al periodo más probable de la matriz de ocurrencias.

Por tanto, se concluye que la metodología propuesta es computacionalmente eficiente y que permite aproximar la serie de potencias a largo plazo para cualquier tipo de WEC en cualquier tipo de localización. Además se demuestra la validez parcial de la metodología clásica para la aproximación de la energía producida anual. El método de la matriz de potencias tiene que ser tomado con cautela ya que la hipótesis del uso de espectros analíticos es una hipótesis que en ciertas localizaciones tiene una validez limitada ya que el porcentaje de estados de mar que no son unimodales es muy alto. Por otro lado, se concluye que a la hora de estimar la producción energética anual en una determinada localización es muy importante contar o con datos de boyas o por otro lado con datos de espectros multicomponente.

## **0.5 Influencia de las condiciones meteoceánicas en el diseño y operación de los WECs**

En esta sección se han estudiado varios temas relacionados con el diseño y la operación de los convertidores de energía de las olas, concretamente la importancia que tiene el estudio y definición de las condiciones meteoceánicas en cada uno de estos temas.

### **0.5.1 Adaptabilidad de un convertidor de las olas a varias condiciones meteoceanicas**

Normalmente, los WECs se diseñan para que su producción en la localización de estudio sea máxima. Para ello, la técnica que se suele aplicar es diseñar el WEC de manera que su periodo resonante (es decir el periodo en el que su producción es máxima) para que coincida con el periodo más probable de las olas en la localización de estudio. Por ejemplo Goggins and Finnegan (2014) estudiaron un algoritmo para adaptar la geometría de un WEC genérico al espectro más probable de una determinada localización. Otra estrategia posible es la aplicación de un control externo reactivo para así adaptar en cada estado de mar el periodo propio de oscilación del dispositivo.

En esta sección, primeramente se muestra la variabilidad de las condiciones climáticas en el mundo. Como puede verse en la figura 5.1, proveniente de una base de datos de reanálisis (GOW 1.0) de Reguero *et al.* (2012) y Gonzalez-Reguero (2013) se puede concluir que la variabilidad del periodo de las olas es muy grande en las distintas zonas del globo. Hay zonas como la costa oeste de Sudamérica, caracterizada por swells muy fuertes con periodos de las olas muy altos (12-14 s) y otras zonas con fetchs mucho más cortos como los mares semicerrados como el Mar Mediterráneo caracterizado por periodos mucho más cortos (4 - 6

## **0.5. Influencia de las condiciones meteoceánicas en el diseño y operación de los WECs10**

s). Por tanto uno de los objetivos de esta sección es demostrar si rediseñar geoméricamente los WEC para cada localización es conveniente o no lo es.

En este estudio se propuso un WEC genérico como el de la figura 5.3 formado por un cuerpo fijo central y una serie de flotadores en sus lados a los que sólo se les permite moverse en alçada. Se plantean 3 opciones distintas para el análisis (ver tabla 5.1):

- La opción 1 es un convertidor en el que los flotadores están adaptados geoméricamente para un periodo característico de mares cerrados (4 s)
- La opción 2 es un convertidor en el que los flotadores están adaptados geoméricamente para un periodo característico del swell atlántico (8 s)
- La opción 3 es un convertidor en el que los flotadores están adaptados geoméricamente para el periodo más probable de cada nodo de estudio. Es decir a cada nodo de estudio se le aplica la subopción correspondiente al periodo más probable en la tabla 5.1.

Cada una de las opciones son modeladas con un modelo en el dominio de la frecuencia descrito en el Apéndice 2. En la figura 5.7 las matrices de potencia de cada una de las subopciones correspondientes a la Opción 3 están representadas.

Los resultados de este estudio se representan en cuanto a dos indicadores la anchura de captura (CWR) y el kW/Ton.

El indicador CWR indica la eficiencia de la conversión de energía con respecto al flujo de energía incidente. En la figura 5.9 se muestran los mapas correspondientes al CWR para cada una de las 3 opciones. Se puede apreciar como para la opción 1, el CWR es muy bajo en la mayoría de las partes del mundo (excepto en los mares cerrados). Por otro lado la opción 2 muestra un CWR alto en muchas localizaciones, ya que 8 s es el periodo medio de las olas en todo el mundo. Por otro lado la opción 3 (adaptable) muestra cómo el rediseñar el convertidor para cada localización y adaptarlo a las condiciones locales mejora el CWR, ya que se puede apreciar como el CWR es alto en casi todas las localizaciones en este último mapa.

Por otro lado el indicador kW/Ton tiene en cuenta la producción con respecto a la masa de los flotadores necesaria para cada opción. En la figura 5.10 se muestran los mapas correspondientes a este indicador para cada una de las opciones. Como se puede apreciar a simple vista, la escala de los colorbar es diferente en los 3 mapas. En la opción 1, el indicador kW/Ton es mayor en todas las áreas del globo que en cualquiera de las otras 2 opciones (opción 2 y opción 2). Se ha de subrayar que en la opción 3 el valor del indicador kW/Ton es muy bajo para casi todas las localizaciones. Esto quiere decir que el incremento de masa que se necesita para adaptar los flotadores para periodos de oleaje altos no es compensado por un incremento en la producción en la misma proporción. El incremento de la producción cuando el flotador está adaptado a las condiciones locales por tanto es menor que el incremento necesario en la masa para poder alcanzar estas condiciones. Se concluye por tanto que no es necesario adaptar la geometría de los convertidores a cada localización sino que el diseño debería ir encaminado a estructuras pequeñas.

## **0.5. Influencia de las condiciones meteoceánicas en el diseño y operación de los WECs11**

Sin embargo en este estudio sólo se ha tenido en cuenta el coste del material. En un estudio completo habría que tener en cuenta que a menores potencias instaladas que los dispositivos pequeños y de baja potencia instalada tienen unos costes de O&M mayores que un número menor de dispositivos grandes con mayores potencias instaladas. En la figura 5.17 se puede apreciar como las curvas del coste del material por kWh y la de O&M por kWh son opuestas. Se muestra una curva conjunta en la que se puede apreciar que existe un mínimo, es decir una opción en la que el coste total es mínimo.

Se concluye por tanto que en general, si sólo atendemos al coste del material, se aconsejan las estructuras de un tamaño pequeño aunque no estén adaptadas a las condiciones climáticas locales. Sin embargo hay que puntualizar que en el caso de considerar otros costes, como los de O&M el resultado puede ser distinto.

### **0.5.2 Estudio de los parámetros de Operación y mantenimiento con una perspectiva global**

En el proceso de selección de emplazamientos para el desarrollo de parques para la captación de energía de las olas normalmente se escogen aquellos sitios con un mayor recurso (kW/m). Sin embargo se ha de tener en cuenta que los dispositivos tendrán fallos y por tanto necesitarán unas operaciones de mantenimiento. A la hora de llevar a cabo estas operaciones se ha de tener en cuenta que las condiciones del oleaje deben mantenerse por debajo de un cierto límite.

O'Connor *et al.* (2013b) y O'Connor *et al.* (2013c) investigaron la importancia de la disponibilidad y accesibilidad en el presupuesto de un parque de captadores y llegaron a la conclusión de que puede llegar al 30% del coste inicial del mismo. En esta sección se analizan las distintas localizaciones del globo con respecto a los parámetros de O&M. Para el estudio que se ha llevado a cabo en esta sección solamente se ha considerado la altura de ola significativa como parámetro limitante para la O&M, aunque en un estudio más detallado deberían ser considerados otros parámetros como la velocidad del viento o el periodo de las olas.

Primeramente se estudian los parámetros de accesibilidad y disponibilidad. Se define disponibilidad como el porcentaje de tiempo que un dispositivo está totalmente operativo y se encuentra produciendo energía. Por otro lado se define accesibilidad como el porcentaje de tiempo en el que un dispositivo es accesible para las tareas de O&M. En la tabla 5.5 se pueden apreciar los distintos niveles de disponibilidad en función del límite en  $H_s$ . Este límite considera el nivel en el que el dispositivo entraría en estado de supervivencia. Como se puede apreciar, para un límite de supervivencia de 5 m de  $H_s$ , el 76% de las localizaciones tienen una disponibilidad en entre el 99% y el 100%. Si el límite de supervivencia se sitúa en 8 m de  $H_s$ , el 97% de las localizaciones se sitúan en la banda anterior de disponibilidad.

En cuanto a la accesibilidad en la figura 5.21 se representan diferentes mapas de accesibilidad para diferentes límites de  $H_s$ . Como se puede apreciar para límites de altura de ola cercanos a

## **0.5. Influencia de las condiciones meteoceánicas en el diseño y operación de los WECs12**

1 m en la mayoría de localizaciones la accesibilidad es menor del 20 %, excepto en algunas localizaciones correspondientes a mares cerrados donde el recurso es muy bajo. Por otro lado, en los límites altos como 3 m la accesibilidad es cercana al 100 % en casi todas las localizaciones, excepto en algunas localizaciones de oleaje extremo como Chile, el sur de Australia o el Norte de Europa.

Dentro de este estudio se detallan las diferentes situaciones en varias localizaciones donde el interés en el desarrollo en la energía del oleaje está creciendo en los últimos tiempos. Los resultados se detallan en la tabla 5.6. Como se puede ver existen localizaciones como Dinamarca con una accesibilidad muy buena para todos los límites, y localizaciones como Australia o Chile con accesibilidades muy bajas para todos los límites. Destaca la comparación entre Irlanda y Australia. Ambas tienen el mismo recurso medio (62 kW/m), sin embargo la accesibilidad en Irlanda es 70 veces mayor para el caso de la limitación de 1 m. Esto es debido a la forma de la función de distribución de la altura significativa (ver figura 5.23). En esta figura se puede apreciar como para alturas de ola menores al punto de intersección entre ambas curvas (3.7 m), la probabilidad de ocurrencia de alturas de ola bajas es mayor en Irlanda que en Australia. Por tanto se puede ver como las condiciones en Australia son mucho más agresivas para la O&M que en Australia, aún teniendo el mismo recurso.

También la estacionalidad es analizada en estas localizaciones en las figuras 5.25 y 5.26. Como se puede apreciar aquellas localizaciones más cercanas al Ecuador, como Chile, tiene una estacionalidad baja y las condiciones son similares en verano y en invierno. Sin embargo ha de apuntarse el hecho de que el Atlántico Norte es mucho más estacional que el Pacífico sur, por la presencia de las masas continentales y la no existencia de un continente helado en el Polo. Las localizaciones Europeas por el contrario muestran una estacionalidad muy clara y la accesibilidad se triplica en los meses de verano.

Aun habiendo estudiado la accesibilidad en las distintas localizaciones hay que tener en cuenta que al realizar las tareas de O&M se necesita un intervalo de tiempo con unas condiciones climáticas determinadas durante el tiempo que tarda la operación. A esto se le llama ventana de operación mientras que al intervalo de tiempo entre ventanas de le llama tiempo de espera.

En esta sección se analizaron el número de ventanas anuales para diferentes duraciones de ventanas, para un límite de operación de  $H_s$  de 1.5 m. En el caso de ventanas de 6 h la media y la desviación estándar se detallan en la figura 5.27. Como se puede apreciar los lugares con los recursos más bajos son los lugares con mayor número de ventanas de operación (Mar Mediterráneo, Mar de Japón). En otros lugares como por ejemplo la costa este de Argentina o la costa este de USA el número de ventanas de operación es muy alto también. En cuanto a las ventanas de operación cabe destacar que zonas como Irlanda o el Mar Mediterráneo tienen una desviación estándar parecida, aunque el número de ventanas de operación es muy diferente. En las figuras 5.28 y 5.29 se representan el número de ventanas de operación para las duraciones de 12 h y 24 h respectivamente. La distribución es similar a la figura 5.27, con la diferencia de

## **0.5. Influencia de las condiciones meteoceánicas en el diseño y operación de los WECs13**

que la diferencia entre las zonas menos agresivas y las más agresivas es acentuada.

Así mismo en las siguientes figuras 5.28, 5.29 , 5.30 se han representado los periodos de espera. En este caso se representa la media, la desviación estándar y el percentil del 99% que podría representar las condiciones más agresivas en invierno. En el caso de de las ventanas de 6 h si analizamos el percentil del 99% las diferencias entre las distintas zonas quedan muy resaltadas. Por ejemplo, se puede apreciar como en las zonas más agresivas como Chile, Australia o Sudáfrica existe un 1% de probabilidad de que la espera supere los dos meses. Por otro lado si comparamos el periodo de espera medio como el percentil del 99% se puede ver como en el caso de la media todas las zonas en Europa tienen unos periodos de espera similares, de igual manera que la costa oeste de norte América y Centroamérica. Si comparamos el periodo de espera medio con el del percentil del 99%, vemos que este segundo destaca claramente aquellas zonas con clima marítimo mas agresivo, como sucede en los casos de la costa sur de Chile, Sudáfrica y Australia.

Por último en esta sección se ha analizado el coste de las actividades de O&M por kWh. Para este estudio se han usado las cifras de producción globales obtenidas en la sección anterior. A la hora de calcular los costes asociados a la O&M se han definido una serie de hipótesis:

- Un coste horario de 625 Euros mientras el barco está esperando para realizar las tareas de mantenimiento
- Un coste fijo de movilización de 7000 Euros
- Un coste por hora mientras el dispositivo está siendo reparado de 1250 Euros
- Se asume que durante el tiempo de espera el dispositivo se encuentra en estado de supervivencia y la producción de energía es nula
- Se asume que la vida del dispositivo es de 25 años

Se simula un numero de fallos aleatorio al año para obtener 10.000 ciclos de fallo distintos a la hora de obtener una estadística fiable. Por tanto en la figura 5.35 se muestra el coste de O&M por kWh para 1, 3 y 5 fallos al año. Se puede ver como hay zonas con un coste muy alto de O&M, ya sea por la inexistencia de ventanas (Sur de Australia) o por la baja producción energética. Por otro lado se pueden identificar áreas como por ejemplo Nueva Escocia (Canadá)o Dinamarca en las que el balance entre accesibilidad y recurso da como resultado costes de mantenimiento bajos.

Estos resultados se detallan en la figura 5.36 donde se muestran detalladamente los resultados para las localizaciones de estudio para los diferentes niveles de fallo. Se puede apreciar como para un numero de fallos al año bajo (1 por ejemplo), la diferencia entre localizaciones como Dinamarca e Irlanda es muy baja, mientras que a medida que el numero de fallos aumenta esta diferencia se hace mas grande. Esto es debido a que si el numero de fallos aumenta es muy probable que en una localización bastante agresiva como Irlanda uno o varios de los fallos se sitúen en periodos de inaccesibilidad. Se concluye por tanto que cuando un convertidor está en una etapa muy temprana de su desarrollo (con muchos fallos) se recomiendan localizaciones

## **0.5. Influencia de las condiciones meteoceánicas en el diseño y operación de los WECs14**

no muy agresivas. Una vez que el convertidor llega a un nivel de desarrollo avanzado y el nivel de fallo es bajo se pueden situar en localizaciones más energéticas como el Oeste de Irlanda.

### **0.5.3 Estudio de la fiabilidad de los convertidores de energía de las olas**

La fiabilidad ha sido identificada como uno de los factores clave para el desarrollo de los convertidores de energía de las olas. En la actualidad el nivel de fallo de los componentes de la mayoría de convertidores es aún incierto.

De acuerdo con Thies (2014), muchos de los componentes de los WECs son iguales que los componentes de industrias como el oil&gas y el offshore wind. Sin embargo, estos componentes están sometidos a ciclos de cargas diferentes, con lo cual los datos de nivel de fallo no pueden usarse para la energía de las olas. Por tanto, la información referente a los fallos de los componentes de los WECs bajo condiciones de oleaje reales es prácticamente inexistente. Una de las pocas aproximaciones a este problema es la de Thies *et al.* (2011a), donde propone unos niveles de fallo para cada uno de los grandes grupos que forman un WEC (estructura, PTO, anclajes y transmisión).

Normalmente, para el análisis de la fiabilidad de cualquier componente se suele usar la distribución de Weibull, dada su flexibilidad. La curva de la bañera simula el comportamiento de los componentes durante su ciclo de vida, teniendo en cuenta tres partes (infancia, desarrollo y deterioro). En esta sección, en primer lugar se hizo una simulación con la curva de la bañera teniendo en cuenta diferentes escenarios, descritos en la Tabla 5.11. En este caso se simula por un lado un fallo muy frecuente pero con una reparación rápida, un fallo poco frecuente pero con una reparación muy lenta y un fallo intermedio. Los resultados de estas simulaciones para varias localizaciones se muestran en las figuras 5.41 y 5.40. Se puede apreciar como si se analiza el tiempo medio de espera, el fallo 2 (poco probable pero reparación muy larga) tiene en la mayoría de las localizaciones un tiempo mayor de espera, especialmente en las localizaciones con un clima severo como Australia. Por el contrario, si se analiza la disponibilidad, esta está directamente correlacionada con la tasa de fallo, independientemente de la longitud de la ventana necesaria para su reparación. Por otro lado, respecto a las diferentes partes de la curva de la bañera se puede ver cómo, en términos medios, los resultados son muy similares. Se puede concluir por tanto que, cuando la incertidumbre en la tasa de fallo es alta y no se disponen de datos concretos de la vida de los componentes, una simulación con una distribución exponencial (parte central de la curva de la bañera) es suficiente.

Por otro lado, en esta sección se realiza una simulación con los escenarios descritos en la tabla 5.42 para determinar qué zonas son adecuadas para cada nivel de fiabilidad. En este caso se determinan tres escenarios distintos con diferentes tipos de mantenimiento y diferentes costes. En las figuras 5.46 5.48, 5.51 se muestran cada una de las zonas adecuadas para cada nivel de fallo. Las zonas con una fiabilidad baja (zonas verdes) corresponden con zonas con un recurso medio y una accesibilidad alta. Estas zonas se caracterizan por un buen balance entre

## **0.5. Influencia de las condiciones meteoceánicas en el diseño y operación de los WECs15**

estos dos parámetros, y por tanto se puede concluir que son zonas adecuadas para los primeros ensayos en mar abierto de los prototipos. Estas áreas corresponden a la costa Pacífica de Méjico, Nueva Escocia en Canadá, la parte este de Nueva Zelanda y la costa de Brasil. Una vez que los prototipos se han ensayado en estas zonas, y su nivel de fiabilidad ha aumentado estos se puede ensayar en las zonas con un nivel de fiabilidad medio y posteriormente en las de fiabilidad alta. Estas últimas zonas normalmente son localizaciones con un desequilibrio entre recurso y accesibilidad. Por ejemplo el mediterráneo (muy bajo recurso-accesibilidad media) o zonas como Australia (recurso muy alto pero accesibilidad muy baja). Por tanto, en esta sección se ha propuesto un mapa de ruta en cuanto a los ensayos a escala 1:1 en mar abierto, con el objetivo de tener unos costes de O&M relativamente reducidos en todas las fases de desarrollo de un WEC.

### **0.5.4 Estudio de los factores que afectan al diseño de parques**

Aunque los WECs se encuentran aún en desarrollo está previsto que en un futuro estos se desarrollen en forma de parques. A la hora de disponer los WECs en forma de parque se ha de tener en cuenta la interacción entre ellos, de manera que esta interacción puede ser destructiva si la producción total del parque de  $N$  WECs es menor que  $N$  veces la producción de un WEC, o constructiva en el caso de que la producción del parque sea mayor que  $N$  veces la de un WEC. La relación entre la producción del parque y  $N$  veces la producción de un WEC se denomina factor de interacción o factor  $q$ . Algunos de los últimos estudios que tienen en cuenta este indicador corresponden a Babarit (2010) y Borgarino *et al.* (2012). Ellos investigaron varias configuraciones de parques con diferentes convertidores y diferentes condiciones de oleaje. También Wolgamot *et al.* (2012) estudió el impacto de la direccionalidad en un parque de cilindros flotantes en alteada concluyendo que la direccionalidad del oleaje es muy importante a la hora de conseguir interacción constructiva.

En esta sección se analizan diversos factores que afectan a la colocación de los parques de WECs basado en un grupo de simulaciones (ver tabla 6.1). Estas simulaciones corresponden al WEC de la figura 5.52. Basados en el grupo de simulaciones previamente seleccionado se analizan las siguientes variables (ver figuras de 5.56 a 5.61):

- Numero de captadores: en las figuras se aprecia como cuando existe interferencia constructiva el incremento del número de dispositivos es positivo, mientras que cuando la interferencia es destructiva un incremento del número de captadores hace disminuir el factor de interacción
- Distancia entre captadores: en cuanto a la distancia entre dispositivos se ensayaron 4 distancias distintas dependientes del periodo de resonancia del sistema ( $L_{10}$ ). En todas las gráficas se muestra como para una distancia de  $L_{10}/2$  se alcanza un máximo en el factor de interacción. Además todas las curvas muestran una pendiente negativa de  $L_{10}$  a  $2L_{10}$ , lo que quiere decir que la interacción deja de existir a esa distancia.

- Distribución en planta de los captadores: se probaron 4 distribuciones en planta, triangular, cuadrado, lineal y rombo. En general la configuración lineal es la que peor comportamiento presenta ya que aquí la interacción es sólo unidireccional. Respecto a las otras configuraciones ensayadas su comportamiento depende mucho de la dirección de incidencia.
- Dirección de incidencia del oleaje: La influencia de la dirección de incidencia del oleaje es muy importante y muy dependiente de la distribución en planta de los captadores. En el caso de la distribución lineal la influencia es muy grande ya que se cambia de terminador a atenuador. En el caso de atenuador la interferencia es destructiva ya que la ola va perdiendo energía a medida que pasa por los WECs. En la configuración en terminador la interferencia es constructiva. Por otro lado, en las configuraciones triangular y de rombo se alcanza la interferencia constructiva cuando la dirección de las olas es paralela a uno de los lados del triángulo. En el caso de la configuración en cuadrado la influencia de la direccionalidad es menor y se alcanza la interferencia constructiva cuando los lados del cuadrado son paralelos a la dirección de incidencia.

Posteriormente, se hace un estudio de la adecuación de los distintos tipos de parques definidos anteriormente para distintos escenarios climáticos. Así, en la figura 5.64 se clasifican los distintos climas en el globo en 10 tipos diferentes atendiendo al flujo medio de energía, la altura de ola significativa media y la desviación estándar de la dirección de propagación media mediante la técnica de clusterización K-medias. Se presenta por tanto la tabla 5.14 donde se dan los factores de interacción medios para cada uno de los climas clasificados anteriormente. Se puede apuntar por ejemplo que el clima 7 es muy multidireccional y por tanto se la configuración triangular muestra un factor de interacción mayor. En el caso del clima 9 por ejemplo, éste se muestra muy unidireccional y por tanto la interacción es máxima cuando se alcanza la interferencia constructiva. Por tanto se puede concluir como la direccionalidad es mucho más importante en los parques de forma cuadrada que en los triangulares y por tanto los parques de forma triangular, estarían más recomendados para climas multidireccionales.

## 0.6 Estudio económico de la energía de las olas

### 0.6.1 Riesgos e incertidumbres de la energía de las olas

En esta sección se estudian cómo las distintas incertidumbres y riesgos relacionadas con la energía del oleaje afectan a la viabilidad económica de estos proyectos. A su vez se ha identificado una falta de una metodología para el análisis de todas las variables que influyen en el flujo de caja y la viabilidad económica en los proyectos de energía del oleaje.

Hasta el momento sólo algunos autores han estudiado la viabilidad económica de proyectos de energía del oleaje. Por ejemplo, Teillant *et al.* (2012) estudió el impacto económico de

simulaciones operacionales en un convertidor genérico. Por otro lado Dalton *et al.* (2012) hizo un estudio del impacto de la curva de aprendizaje, las curvas de demanda y abastecimiento y el coste futuro del dinero. Se concluyó que las feed in tariff actuales son insuficientes para el estado de la tecnología. También O'Connor *et al.* (2013a) estudió 2 tipos de tecnologías diferentes en varias localizaciones y analizó el impacto de las distintas condiciones meteoocéánicas en la viabilidad económica.

Sin embargo no existen estudios que lleven a cabo un análisis de la sensibilidad de todos los riesgos e incertidumbres que afectan a la energía del oleaje desde una perspectiva económica. Este estudio tiene una gran importancia, ya que desde la perspectiva del inversor los dos puntos claves son el momento de recuperación de la inversión y que riesgos existen.

Por tanto en esta sección se propone un caso de estudio consistente en un captador formado por 2 cuerpos que extrae energía en alteada (el mismo que en el capítulo 4, ver figura 6.1). Este parque se encuentra situado en el Norte de la Isla de la Palma (España).

El primer objetivo de este estudio es analizar la influencia de la variabilidad climática en la viabilidad económica. Para ello se ha de obtener una serie de producción del parque seleccionado a largo plazo. Para esta tarea se utiliza la metodología explicada en la sección 4.1 basada en la técnica de selección de estados de mar y de interpolación no lineal.

Una vez obtenida esta serie a largo plazo (60 años) de potencia del parque se ha de crear una serie de ciclos de vida suficientemente amplios para que puedan representar la variabilidad climática. Para ellos, se utiliza la técnica del bootstrapping estadístico de Espejo *et al.* (2011). Éste consiste en una recomposición de 10.000 ciclos de vida de 25 años a partir de la serie de 60 años obtenida anteriormente obteniéndolas de manera aleatoria.

Teniendo los 10.000 ciclos de vida de producción anual, el próximo paso es la elaboración del presupuesto del proyecto. En la tabla 6.1 se detallan los costes asociados a cada uno de los conceptos.

Después se realiza un análisis del flujo de caja, para analizar la viabilidad económica del proyecto. Para ellos se asume:

- El precio de la energía queda fijado en 0.1 Euros/kWh
- Se fija un interés neto del 8% y una inflación del 5%
- Se supone que todos los costes se pagan en el año 0, no necesitando por tanto financiación
- Se asume que el OPEX es un 5% del coste inicial del proyecto
- Se asume una subvención inicial de 0.55 Eur/kWh aunque se analizará la influencia de este parámetro

Se presenta la figura 6.8 en la que se muestra el flujo de caja medio, el mínimo y el máximo. Como se puede ver la incertidumbre es bastante amplia, y la desviación estándar media del Valor Presente Neto (NPV) es de 600.000 Euros. Esta incertidumbre en el NPV viene dada por la variabilidad interanual. Esta se puede ver en la figura 6.10 en la que se muestran 2 ciclos

de vida, uno con unas producción es relativamente altas, que concluyen en un flujo de caja positivo y otra con una serie de producciones relativamente bajas con un flujo de caja negativo.

En las figuras 6.12, 6.11, 6.13 se muestran las funciones de distribución de los parámetros Valor Presente Neto NPV, la tasa de retorno (IRR) y el periodo de amortización (PBP), y como se puede apreciar la variabilidad climática causa una gran incertidumbre en la viabilidad económica del proyecto, que debe ser tenida en cuenta desde el principio.

Por otro lado se analiza la influencia de la subvención y la curva de aprendizaje en el resultado del proyecto. En la figura 6.14 se puede ver como sólo se consiguen NPV positivos a partir de 0.55 Eur/kWh. En cuanto a la IRR sólo se obtienen IRR de 10% a partir de 0.6 Eur/kWh, por tanto se puede concluir que no las subvenciones actuales en general no son suficientes para el estado de la tecnología.

Por otro lado se analizó en la figura 6.17 la influencia de la subvención en la incertidumbre del parámetro IRR. Como se puede apreciar a medida que la subvención aumenta la PDF de la IRR se hace más ancha, lo que quiere decir que la incertidumbre aumenta también con la subvención. Por tanto, un incremento de las subvenciones tampoco es bueno en cuanto a la incertidumbre.

Por otro lado, en cuanto a la subvención también se estudió cómo un cambio de las condiciones de estabilidad de la misma influyen en la incertidumbre financiera. Por ejemplo, en Reino Unido en el último año se ha cambiado la política de subvenciones de las Renewable Energy Obligations a los Contracts of Difference. Esto ha conllevado un recorte en el periodo de la subvenciones de 20 años a 15 años. Este cambio ha sido analizado en el caso de estudio que se ha estudiado.

Del análisis de los 2 escenarios realistas que se muestran en las figuras 6.20 y 6.21 se puede concluir que el recorte de la longitud de la subvención por debajo de la duración del ciclo de vida del proyecto es muy negativo y afecta en gran medida a la incertidumbre en el proyecto. Un recorte de 5 años por ejemplo supondría un necesario aumento de la subvención en un 8% si se quiere mantener el mismo nivel de apoyo. Por otro lado en la tabla 6.4 se puede apreciar como la influencia de la estabilidad de los mecanismos de subvención (representados por el Escenario 1 y 2) en la incertidumbre de la viabilidad económica es mayor que la incertidumbre representada por la variabilidad interanual de las condiciones meteoceanicas. Se puede concluir por tanto que una estabilidad del marco regulatorio es muy importante para reducir los riesgos e incertidumbres intrínsecas a la energía del oleaje.

### 0.6.2 Trayectoria hacia un LCOE reducido

En esta sección se ha analizado el coste actual de 2 prototipos reales y las mejoras previstas para el futuro cercano y su influencia en el coste nivelado de la energía (LCOE). En este caso se analizan 2 prototipos cuyas características se detallan en la tabla 5.9. Un prototipo es un absorbedor puntual múltiple, analizado en Hanstholm (Dinamarca) y otro que es un atenuador, estudiado en EMEC (Reino Unido).

En la tabla 6.7 se proponen ciertas mejoras a cada prototipo y en la figura 6.24 se muestra la influencia de cada una de estas mejoras en el LCOE. En el caso del absorbedor puntual múltiple (MPA) el caso inicial es muy caro (5 Eur/kWh) y por tanto al estar en una etapa más temprana de su desarrollo cada una de las mejoras tiene un impacto muy grande en el LCOE. Por ejemplo una mejora de la eficiencia hidráulica del PTO reduce el LCOE en un 200%. También el cambio de un control resistivo a un control reactivo lleva a una reducción del LCOE de un 50%. En el caso del atenuador al ser un prototipo más desarrollado sus mejoras tienen una influencia menor en el LCOE. Por ejemplo, el cambio del material de acero a hormigón de alta resistencia produce una reducción en el LCOE de un 30%. En ambos casos, las mejoras en el control junto con la aplicación de materiales más baratos tienen un impacto muy importante en el LCOE.

Por otro lado, estos convertidores fueron analizados en dos localizaciones distintas, sin embargo para dar una comparación más justa se analizaron los 2 prototipos en 5 localizaciones distintas. Los resultados en cuanto al LCOE se muestran en la figura 6.25. Se puede ver como aunque la localización con un mayor recurso es Chile la localización que muestra mejores resultados es Humboldt Bay debido a que la disponibilidad en Chile es menor debido a sus condiciones extremas. Por otro lado llama la atención la diferencia en el comportamiento de ambos prototipos en las diferentes localizaciones. Por ejemplo en SEM-REV la diferencia entre ambos es de 0.3 Eur/kWh. En todas las localizaciones el MPA tiene un LCOE más bajo que el atenuador excepto en EMEC. Esto es debido a que el atenuador tiene una matriz de potencia en la que solo se alcanzan potencias altas para estados de mar muy severos con alturas de olas muy altas, mientras que el MPA está diseñado para trabajar en unas condiciones menos agresivas y alcanza potencias altas con estados de mar menos severos. Esta figura nos lleva a la conclusión de que no todos los prototipos son adecuados para todas las localizaciones sino que es importante definir el tipo de prototipos que se adaptan a cada una de las localizaciones en el mundo.

## 0.7 Conclusiones

Esta tesis ha tratado diversos temas relacionados con el análisis técnico-económico de convertidores de energía del oleaje. El objetivo de esta tesis es obtener una serie de consejos/reglas aplicables al diseño y operación de los convertidores de energía undimotriz teniendo como tema principal la influencia de las condiciones meteoceánicas en el diseño, operación y viabilidad económica de convertidores de energía undimotriz.

En el capítulo 2 se ha realizado una revisión el estatus actual de los prototipos para la conversión de la energía del oleaje, además de un repaso de los estudios técnico económicos que se han llevado a cabo. Se ha concluido que existen todavía muchos prototipos en pruebas con diferentes principios de funcionamiento, sin que se haya producido una convergencia de la tecnología. Además en los últimos tiempos ha habido fallos importantes en algunos prototipos en el mar. Además, se ha identificado una falta de aplicación de los estudios técnico-económicos en todas las fases desde el diseño hasta la operación de un convertidor de energía del oleaje. Esta tesis por tanto intenta cubrir esta falta y por tanto se han investigado varios temas relacionados con el análisis técnico económico.

Primeramente, debido a la falta de datos de producción de convertidores durante periodos de tiempo largos se ha desarrollado una metodología para el análisis y obtención de la serie de potencias a largo plazo de un convertidor en una localización concreta. Esta metodología ha sido validada y ha demostrado ser computacionalmente eficiente y precisa. Se ha probado esta metodología para diferentes dispositivos en distintas localizaciones y se ha concluido que aunque funciona bien para todos los dispositivos alcanza un mayor precisión con un número menor de casos en dispositivos seguidores que en dispositivos resonantes. También, esta metodología se aplicó a espectros reales. Se concluyó que el uso de la metodología clásica para la obtención de la producción media anual es parcialmente inexacta en algunos casos, especialmente en el caso de dispositivos resonantes y localizaciones con un gran porcentaje de estados de mar combinados swell-wind sea (como por ejemplo en Dinamarca). Así mismo también se concluyó que para una adecuada estimación de la serie de potencias, y la potencia media anual es preciso contar con datos de espectros reales o espectros de reanálisis de multicomponente en la medida de lo posible.

También se estudio la influencia de las condiciones meteoceánicas en todas las etapas desde el diseño hasta la operación de un WEC. En primer lugar se analizó la fase de diseño de un prototipo genérico desde el punto de vista de la localización optima. Se llegó a la conclusión de que no es necesario adaptar geoméricamente un prototipo a las condiciones locales de cada lugar sino que el diseño debe estar enfocado a estructuras pequeñas (desde el punto de vista de producción versus masa). Seguidamente se estudiaron también los parámetros más útiles de Operación y Mantenimiento en las localizaciones costeras del mundo. Se concluyó que existen áreas con condiciones muy agresivas y recursos muy altos (como Chile o el sur de Australia), sin embargo su accesibilidad es muy limitada durante todo el año y las ventanas

de operación son muy escasas o casi inexistentes. Por otro lado existen localizaciones con recursos muy altos también pero con una accesibilidad más alta y con un número mayor de ventanas de operación al año (por ejemplo Irlanda). Por otro lado existen localizaciones que desde el punto de vista del coste de O&M por kWh que tienen un balance adecuado en términos de recurso y accesibilidad, como la zona de Nueva Escocia en Canadá o la zona Noroeste de Dinamarca. En este contexto se realizó una calificación de la adecuación de las distintas zonas costeras para los diferentes estados de desarrollo de un WEC (teniendo en cuenta su tasa de fallo). Finalmente se llevó a cabo un estudio de los factores meteoceánicos que influyen en la colocación de los parques de captadores de energía del oleaje. Se analizaron varios factores como la separación entre captadores, la colocación en planta de los mismos, el número de captadores y la direccionalidad del oleaje incidente. Además se clasificaron los distintos climas marítimos en el mundo teniendo en cuenta estas variables y así se hizo un estudio del tipo de colocaciones óptimas para cada tipo de convertidor.

Por último se estudió la afectación de los riesgos e incertidumbres actuales en la viabilidad económica de los proyectos de energía del oleaje. Se analizó la influencia de la variabilidad interanual de la producción en el flujo de caja, demostrando su alta influencia en los indicadores financieros. Además se analizó cómo las subvenciones influyen en la viabilidad económica. Se llegó a la conclusión de que las subvenciones actuales no son suficientes. Además se concluyó que la estabilidad del marco regulatorio es importante y la prolongación de las subvenciones durante toda la vida útil del proyecto es también clave para eliminar riesgos.

Por último se estudiaron dos prototipos reales y se analizó el impacto de distintas mejoras en los prototipos en el LCOE. Además se analizó el comportamiento de los prototipos en distintas localizaciones del mundo llegando a la conclusión que es importante determinar que tipología de dispositivos se adaptan a cada localización ya que no todos ellos se adaptan a las condiciones climáticas de distintas localizaciones.

## Introduction

---

### 1.1 Introduction

Wave energy is a concentrated form of solar energy transmitted to the oceans. The sun heats the atmosphere and because of the pressure differences among the different locations the wind is produced and its energy is transferred to the ocean surface producing the waves. Winds generated by pressure differences caused by the sun heat represent an average power flow typically up to about five times denser (about  $0.5 \text{ kW}/\text{m}^2$ ) than in the solar radiation reaching the surface of the earth (about  $0.1\text{-}0.3 \text{ kW}/\text{m}^2$ ). In the transition from wind blowing over the ocean surface to waves the energy flow intensity it is again concentrated about five times, up to  $2\text{-}3 \text{ kW}/\text{m}^2$  in the upper layer of the oceans. Thus, although only a small part of the solar irradiation ends up as wave power, it is quite a concentrated form of renewable energy, something which should give prospects for efficient harvesting.

The World Energy Council has estimated that approximately 2 terawatts (2 million megawatts), about double current world electricity production, could be produced from the oceans via wave power. Therefore, wave energy could be considered one of the most promising renewable energy forms because:

- Wave energy is a predictable resource, as waves originate a long way from shore, computer models of wave propagation allow us to accurately forecast incoming waves up to five days in advance. In comparison with wind energy, it is easier to accurately predict how much energy can be generated by waves. In addition, the peaks and troughs of wind and wave energy do not always coincide. This means there are times when there is an abundance of wave energy and little wind. This diversity helps even out the fluctuating nature of some renewable energy sources. When combined with other renewable energy forms, such as offshore wind, it helps provide a more predictable and steadier renewable energy mix.
- Assuming marine biological impacts are found to be negligible or readily manageable, WEC devices may offer a very environmentally benign form of power generation.
- Visual impact is nearly negligible because the devices would be placed far enough from the coast and they have low profile. Compared to offshore wind the visual impact is much lower and the social acceptance is expected to be higher.

- There are significant permitting and technical advantages in locating wave energy sites on the Outer Continental Shelf (OCS), including deeper water. This fact highlights the great availability of wave energy around the world coast and the possibility of building wave energy farms in a lot of locations around the world.

Apart from the advantages of wave energy some political/economic issues should be taken into account. Then, based on the population growth curves proposed by the United Nations (see United Nations (2009)), the Earth population will have increased to 9 billion people by 2050. This fact also indicates an exponential growth of energy demand. The world electricity demand is estimated to have achieved 35 TW by 2050 based on CERN (2008), which doubles the energy consumption of the 1960s.

This exponential energy consumption growth summed to the limited life of the fossil fuels is leading towards the building of a green economy led by renewables. Nowadays, some governments are supporting renewables in order to reduce the dependency on the fossil fuels. There is a global awareness of the need for transition to a lower carbon energy system. Carbon dioxide ( $CO_2$ ) and other greenhouse gas (GHG) emissions are recognized factors in climate change, and as such, decarbonisation of the energy sector is receiving a lot of support in international energy policy. Low carbon technological innovation is fundamental in achieving the targets that have been set.

Within the field of renewables, some novel energy forms are also supported and they are trying to be introduced into the energy mix. The offshore renewables (offshore wind, tidal, wave and OTEC) are found within this group of novel renewable energies and its interest on them has been growing in the last decades. On the one hand, Offshore wind is one of the most developed offshore renewables. By January 2014, 69 offshore wind farms had been constructed in Europe with an average annual rated capacity of 482 MW in 2013, see EWEA (2014) and as of January 2014 the United Kingdom has by far the largest capacity of offshore wind farms with 3,681 installed MW. Offshore wind is now on the commercial phase and it is competitive with the other renewables.

On the other hand, Tidal energy is a form of hydropower that converts the energy of tides into useful forms of power, mainly electricity. It is now on demonstration phase and several prototypes are being tested (both floating and fixed ones), however no commercial deployments has been found yet. The first full scale tidal prototype was deployed in 2009 in Strangford Lough in Northern Ireland. The SeaGen Turbine has been producing electricity since the deployment and it remains the world's first and largest's offshore tidal generator. It is expected to be commercial and competitive with the other renewables in the foreseeable future.

Despite the several advantages outlined before and the prospects of supplying large amounts of electricity in the future, wave energy, which is the main topic of this PhD thesis has not become commercial yet. Based on Carbon Trust 2011 estimation (see CarbonTrust (2011) and Figure 1.1), nowadays wave energy has an average cost of 50 Eurocents per kWh, that is far from the

cost of fossil fuels energy sources (between 1 and 4 Eurocents per kWh). However this cost is expected to get lower due to the economies of scale, the optimization of the prototypes and the learning by doing process. Based on Carbon Trust, wave energy cost will achieve 10 Eurocents per kWh around the year 2050 when the global deployment achieves 46.5 installed GW .

Learning rates are essential to understand how mass production influences the cost of novel energy sources. In Figure 1.2 the learning curve of several energy sources is plotted. As it can be inferred from these curves a learning of 70 % to 110% could be expected. However, prior to experiencing this drop on the cost of energy due to mass production some R&D is still needed on the sector in order to achieve reliable designs. This thesis then will summarize all the techno-economic aspects needed on the wave energy assessment and will propose new methods to facilitate this assessment. Nowadays, there are lots of prototypes being tested, receiving large amounts of funding by the governments. However, no convergence has been perceived yet on the wave energy sector and it is not clear which technologies (if any) will prevail. Also it is not clear if there will be a technology for specific sites or a global generic technology convenient for all the locations. Because of this reason, prototype selection becomes a key issue on wave energy development and looking at the techno-economic analysis of WECs in depth turns into a priority for the sector.

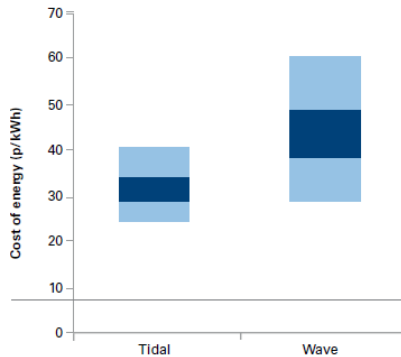


**Figure 1.1:** Cost of Marine Renewables based on Carbon Trust approach (see CarbonTrust (2011))

In addition, another reason why wave energy has not become commercial yet is reliability. Nowadays, prototypes have not proved to be reliable yet and very few successful deployments have been achieved. When designing a Wave Energy Converter (WEC) the environment needs to be carefully taken into account and its design procedure needs to be focused on power maximization, easiness of operation and survivability. This thesis will study the design process of the WECs in order to provide some guidance to designers so as to design a reliable, efficient

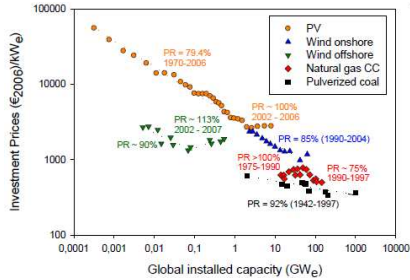


**Figure 1.2:** Learning rate of different energy sources against installed capacity

and competitive WEC.

Chapter 2 describes the state of the art of wave energy technologies. On this chapter the history of the beginning of wave energy as well as the current wave energy prototypes are thoroughly outlined and elaborately described. The techno-economic study behind wave energy prototypes are presented too and all the pre-existent knowledge previous to this thesis is reviewed.

Chapter 3 presents the main objectives of this PhD thesis, which essentially consists of creating a design procedure for the wave energy converter in order to create reliable and economically viable WECs. The structure of this thesis is presented in this chapter.

Chapter 4 presents the methodology in order to estimate the long-term performance of WECs. Due to the absence of long-term sea trials, the estimation of the harvested power during the life-cycle of a converter is extremely important. This chapter also proposes a computationally efficient methodology in order to estimate the long-term performance of a WEC and it also addresses the details of sea state characterization into power assessment.

Chapter 5 presents an overview of the influence of met-ocean conditions on the different aspects, regarding wave energy converter design. Firstly, the design approach in terms of tuning a WEC is studied and some recommendations are proposed. Secondly, the Operation and Maintenance of converters around the world coast are assessed and convenient locations for wave energy development are highlighted. Thirdly, a reliability study is performed, in order to study the convenience of some locations for wave energy development, depending on the state of the technology. Finally, the factors that influence array layout on wave energy farms are analyzed.

Chapter 5 focuses on the economics of wave energy. Firstly, the uncertainties regarding the financial returns of wave energy projects are investigated. Finally, an analysis of the elements affecting LCOE is presented and the areas with room for improvement in order to achieve lower costs are identified.

To sum up, chapter 7 summarizes the main concluding remarks of this work, while chapter 8

---

presents the future research plans, as well as the gaps of this work that could be studied in the future.

# State of the art of wave energy

---

## 2.1 Introduction

In this chapter, a review of the status of wave energy will be presented. Firstly, the story of how wave energy started on the last century is presented. Secondly, the principles of wave energy absorption are outlined and the different types of converters are also presented, as well as some current prototypes. Afterwards, the state of development of wave energy is reviewed and the current state of wave energy, with respect to other renewables, is also stated. Finally, a review of the techno-economic studies performed in relation to wave energy is presented.

## 2.2 Historic Review of Wave energy

The possibility of harvesting energy from the oceans was identified long time ago. The first wave energy patent was presented in 1799 in France by Girard father and son. Then again, in 1910 in Paris Bochaux Praceique asked Government to use this power to light his house. However, it was not until 1973 when the interest in wave energy was increased because of the oil crisis and the desire to find novel and efficient sources of energy.

However, nowadays Yoshio Masuda might be considered as the father of modern wave energy technology. He developed an autonomous navigation buoy powered by wave energy. He was the inventor of the first oscillating water column prototype. These buoys were commercialized in Japan and USA afterwards. Masuda was also the inventor of the Kaimei device (Kaimei website), a large barge (80x12 m) formed by several Oscillating Water Columns Chambers (OWCs) however the power levels achieved on these prototypes were quite modest due to the early stage of the technology.

Due to the oil crisis that occurred in 1973 many research scientists from renowned universities started working on wave energy such as Stephen Salter, Johannes Falnes, and John Newman. Stephen Salter, see Salter (1974), invented the Salter Duck in 1974. In small scale controlled tests, the Duck's curved cam-like body can absorb 90 % of wave motion and can convert 90% of that to electricity. The wave impact induces rotation of gyroscopes located inside a pear-shaped "duck", and an electrical generator converts this rotation into electricity , see Edinburgh Wave

Power Group webpage and Figure 2.1. A prototype attempt to use the device was constructed in 1976 off Dores Beach. It was used to provide 20 kW of power. However, because of the 1980s oil success, the perceived need for immediate alternative energy sources declined and, in 1982, the UK Wave Energy Program was discarded. This ended the hope of having Salter's duck becoming a reality in the alternative energy mix. After later investigation, it was discovered that the Energy Technology Support Unit's cost determinations had mis-estimated the cost of building Salter's duck by more than double the actual cost.

In addition in the 1980s two small OWC prototypes (350 kW and 500 kW) were built near the coast of Bergen in Norway. However their success was limited. Also, in the early 90s another OWC prototype was built on the Scottish island of Islay. The LIMPET prototype was rated at 75 kW and it worked until 1999 when the prototype was decommissioned because a larger prototype (500 kW) was installed 400 m from the original one, Whitakker *et al.* (2006). In Spain the OWC was also first started with studies carried out by Vidal (1984).

Before the 90s almost all the work on the wave energy field remained in the R&D scenario because of the difficulty of the problem and also because of the scarcity of funding. However, this situation changed in 1991 when the European Commission decided to include wave energy in their R&D program on renewable energies.

In the next subsection a brief description of the wave energy extraction phenomena is explained prior to the the classification of the current wave energy converters. Examples of the current existing prototypes that are nowadays in a precommercialization stage are described on section 2.4.



**Figure 2.1:** Salter Duck recreation from Edinburgh Wave Power Group webpage

## 2.3 Description of Wave Energy Extraction Phenomena

In order to extract energy from the waves the law of conservation of energy requires the extracting device to interact with the waves so as to reduce the amount of energy in the system. It is then assumed that the device needs to create a wave that interferes destructively with the incoming wave. The widely used sentence to describe this process is: " In order for an oscillating system to be a good wave absorber it should be a good wave generator". Then, it is clearly stated that in order to absorb the wave on an optimum way the device has to oscillate with a certain amplitude and phase. One of the first premises for an absorber is that for a single oscillating body that interacts with sinusoidal wave train, the optimum phase is obtained at resonance. If the body is sufficiently large, then its bandwidth for obtaining optimum phase for a bunch of frequencies is also large. However, when the body is smaller (with a more reasonable size) this bandwidth is narrow and then external control systems are needed in order to approach optimum phase, see Falnes (2007).

Floating bodies move in 6 degrees of freedoms and then in order to obtain optimum absorption, different forces should be applied for the different degree of freedoms. Therefore the wave energy conversion process could be explained in 2 steps: in the first step the energy is transferred from the sea to the oscillating system and in the second step, this potential/mechanical energy is converted by a machinery into useful one (i.e. electricity).

Wave energy converters then usually extract some energy of the waves associated with the three phenomena shown on figure 2.2. The first phenomenon has to do with the push of the wave (mainly drag forces). Based on this phenomenon, the converters do not usually use the radiation absorption mechanism aforementioned. One of the types of devices that use this phenomenon is the oscillating wave surge converter (i.e. Oyster) that will be further explained in the next section. The second motion has to do with the free surface variation, which is the principal phenomenon used by converters for energy extractions. Heaving converters, such as Sea-based or OPT Power buoy (further explained in the next subsection) use this phenomenon, and their wave energy extraction is based on the aforementioned radiation problem. The third phenomenon used by some converters is the pressure change under the free surface. Some converters, such as the CETO (by Carnegie), use this phenomenon for wave energy extraction, see Carnegie Web page.

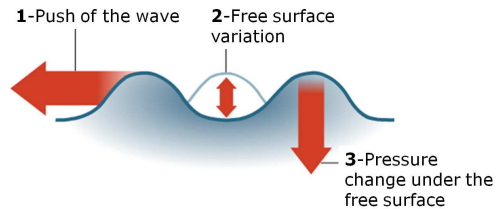


Figure 2.2: Phenomena associated to wave energy conversion from Iturrioz (2014)

## 2.4 Classification of Wave Energy Prototypes and Current prototypes

Nowadays there is still a great variety of wave energy converters. No convergence has been achieved yet by the wave energy sector and then there are still a lot of prototypes being tested nowadays. Because of this variety there is also several ways to classify the converters, based on the locations (nearshore-offshore) or based on their size-principle (point absorbers-attenuators-terminator). However the classification on this thesis is based on the working principle, Falcao (2010). The classification is shown on Figure 1 and it is based on three main types of converters: Oscillating Water Columns, Oscillating bodies and overtopping converters. In the next subsection every class is further explained and some real examples are presented. It was decided to include more examples in the oscillating bodies class due to their present abundance of them nowadays.

It should be noted that in tables from 2.1 to 5.3 summarize the specific characteristics of the WEC prototypes.

### 2.4.1 Oscillating Water Column

The oscillating water column consists of a hollow caisson open to the sea that traps a column of water and an air chamber inside. Incident waves excitate the vertical motion of the water column, that acts as a piston on the air chamber. The chamber could be located on a fixed structure in an isolated way (LIMPET) or as a part of a breakwater (Mutriku). Since the beginning of prototypes in Norway in the 1980 there have been many examples of fixed OWC such as Pico plant in the Azores, Limpet in Scotland or Osprey in Scotland too. Some of the most recent ones (Mutriku) are attached to a breakwater, having the advantage of sharing construction costs and facilitating maintenance. On the other hand the chamber could be also located on a floating barge (OE buoy, Mightly Whale). The floating prototypes were initiated by Masuda in the 1970s as mentioned before, however there are quite a lot of examples of them such as the Aquabuoy in Portugal, the Mightly Whale in Japan or the Oceanlinx in Australia.

Two selected prototypes of each category are going to be described:

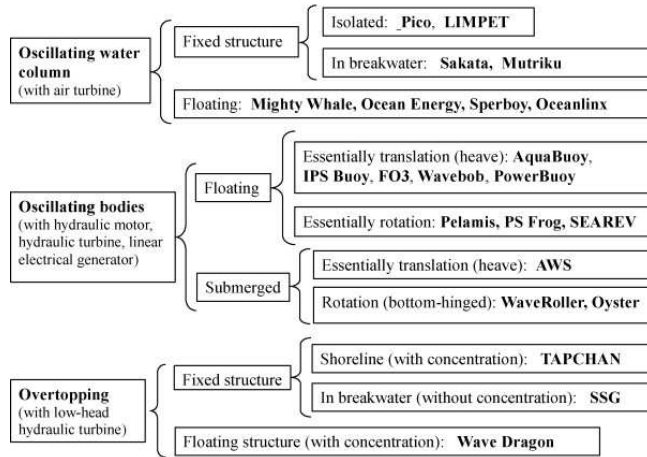


Figure 2.3: Wave Energy converter classification based on Falcao et al (2010)

#### Fixed Oscillating Water Column example: LIMPET

LIMPET (Land Installed Marine Powered Energy Transformer) is a shoreline based Oscillating Water Column energy converter located on the island of Islay, on the west coast of Scotland, see Figure 2.1. This device was installed in 2000 and it has a peak power output of 500 kW. Islay LIMPET was developed by Wavegen in cooperation with Queen's University Belfast. The device is comprised of three water columns contained within concrete tubes each measuring internally 6 m by 6 m and inclined at  $40^{\circ}$  to the horizontal giving a total water surface area of 169 m<sup>2</sup>. The upper part of the tubes is inter-connected and power conversion is performed via a single turbine generator unit connected to the central column. The water columns with an external width of 21 m are located 17 m inland from the natural shoreline in a man-made recess with a water depth of 6 m at mean water level. The sides of the recess are virtually parallel and vertical, see Whitakker *et al.* (2006).

The power take off system is comprised of a single 2.6 m diameter counter-rotating Wells turbine in which each plane of blades is directly mounted on the shaft of a modified wound rotor induction generator rated at 250 kW, giving an installed capacity of 500kW.

Islay LIMPET was the worlds first commercial wave power device connected to the United Kingdom's National Grid.



**Figure 2.4:** LIMPET prototype on the Islay Island (Scotland,UK) from Limpet: the guardian News Ltd

Country of Origin	UK, Germany
Rated Power Output	300 kW, 500 kW
Water depth Min/ Max	15 m nominal mean
Mooring Type	Shored based structure
TRL	7
Number of devices deployed	2
Target market	Near shore
PTO	Pneumatic, wells turbine and induction generator
Deployment vessel	N/A
Maintenance strategy	Due to the location of the device, all maintenance and major repairs can be carried out onshore
Projects to Date	Islay, UK

**Table 2.1:** Characteristics of the LIMPET prototype

#### **Floating Oscillating Water Column example: OE Buoy**

The OEBuoy device continues the work started with the Backward Bent Duct buoy in the last decades. It uses wave energy to compress air in a plenum chamber and pump it through an air turbine. One advantage of this prototype is that the power conversion system is isolated from the seawater. The device is a floating system with the opening of the OWC facing opposite from the oncoming wave direction. This fact facilitates resonance and power production is maximized.

The OE Buoy has undergone three full phases of scaled testing, from 1:50 scale to 1:4 scale. Initial testing of the OE Buoy concept was carried out at the Hydraulics and Maritime Research Centre (HMRC) in University College Cork, Ireland. The three-quarter scale OEBuoy was deployed at the scale test site in Spiddle, near Galway, Ireland, for data collection purposes as part of the EU funded CORES project. OE Buoy has only one moving part and has completed

over 3 years of testing in Atlantic waves. A full scale OE Buoy is planned for deployment at the Wave Hub test facility in UK in 2014.



**Figure 2.5:** OE Buoy in the Galway Bay testing location

Country of Origin	Ireland
Rated Power Output	Unknown )
Water depth Min/ Max	Unknown
Mooring Type	Slacked moored
TRL	6
Number of devices deployed	1
Target market	Deep offshore
PTO	Pneumatic,wells turbine and indusction generator
Deployment vessel	Tug boat
Maintenance strategy	Minor maintenance:on site; Major Maintenance:return to base
Projects to Date	Spiddle, Galway, Ireland

**Table 2.2:** Characteristics of the OE Buoy prototype

### 2.4.2 Oscillating Bodies

Oscillating bodies consists of systems that extract energy from the movement of a single body with respect to a point of reference (i.e Seabased) or by the relative motion among several bodies (i.e OPT Powerbuoy). These systems are generally located offshore, which gives them the opportunity to capture more energy than nearshore. In this class the prototypes can be classified based on floating or submerged depending on its position with respect to the water surface. Also in this category the devices can be divided depending on their energy extraction principle (either translation or rotation).

Nowadays there are several prototypes on this class and because of this reason three examples are described on this category.

#### **Floating Oscillating body translation example: OPT Power buoy**

OPT's PowerBuoy is a semi-submerged floating device consisting of a toroidal float that moves with respect to an inertial stable spar structure moored to the sea bed. This device is a self reacting heaving buoy, slack moored in deep water. The mechanical heaving motion of the buoy relative to the spar is converted to an electrical output via a power take-off driving an electrical generator. In extreme waves, the structure can enter on survival mode locking the hinge, protecting the device in the event of storm waves. To date, OPT have deployed the 150 kW variant of the PowerBuoy in various wave climates, see figure 2.6. OPT are currently developing a 500 kW PowerBuoy device. Some characteristics of the OPT prototype are found in Table 2.3.



**Figure 2.6:** Ocean Power Technology Power buoy, see Ocean Power Technologies Web page

#### **Floating oscillating body translation example: Wavestar**

The Wavestar device consists of two rows of round floats attached to a bridge structure, secured to the sea bed by the use of steel piles, which are cast into concrete foundations. All moving parts are therefore above normal seawater level. The device is installed with the structural bridge supporting the floats directed towards the dominant wave direction. When the wave passes, the floats move up and down driven by the passing waves, thereby pumping hydraulic fluid into a common hydraulic manifold system which produces an even flow of high pressure

Country of Origin	USA
Rated Power Output	150 kW,(500 kW)
Water depth Min/ Max	55 m/ 250 m
Mooring Type	Slacked moored
TRL	7
Number of devices deployed	4
Target market	Deep offshore
PTO	Direct drive
Deployment vessel	Buoy tender, tug boat, crane or A-frame vessel
Maintenance strategy	Return to base
Projects to Date	Altantic city(USA), 1X40kW; Oahu(Hawaii), 1x40kW; Santoña(Spain), 1x40kW; Scotland(UK), 1X150 kW

**Table 2.3:** Characteristics of the OPT Powerbuoy prototype

oil into a hydraulic motor that directly drives an electric generator. When the significant wave height exceeds a certain limit the machine automatically enters storm protection mode. Storm protection involves un-ballasting the floats and retracting the hydraulic cylinders which thereby pull the floats out of the water. The test prototype in Hanstolm had 2 floats and a rated power of 110 kW. However the next planned prototype would have 20 floats with 5 m diameter each. The arm length is 10 m and the overall structure is 1600 Tons. The nominal power would be 1 MW (it should be noted that in Table 2.4, the rated power among brackets refers to the full scale 20 float Wavestar). Some figures from the Wavestar prototype are summarized in 2.4.



**Figure 2.7:** Wavestar 120 kW in Hanstolm (Denmark)

Country of Origin	Denmark
Rated Power Output	110 kW (1 MW )
Water depth Min/ Max	15 m/ 35 m
Mooring Type	Pilot
TRL	6
Number of devices deployed	2
Target market	Nearshore
PTO	Hydraulic
Deployment vessel	Tug boat
Maintenance strategy	On site
Projects to Date	Nissun Brending, Hanstolm

**Table 2.4:** Characteristics of the Wavestar prototype

#### **Floating oscillating body rotation example: Pelamis**

Pelamis is a semi-submerged wave energy converter consisting of individual tubular sections, each linked to neighboring smaller PTO system by joints, see figure 2.5. Motion is induced in each section as a wave passes down the length of the device; movement between neighbouring segments will be resisted by hydraulic rams, which pump hydraulic fluid through pressure smoothing accumulators and then to a hydraulic motor. This motor is connected to a electric generator. Pelamis is expected to be moored in water depths exceeding 50m, and the design of the device is such that it is able to weathervane to face oncoming waves - a self-referencing mechanism that allows the device to maintain a directional heading perpendicular to the oncoming wave direction. The weathervane concept also allows the Pelamis device to enter a survival mode in which the WEC rides underneath extreme waves which would otherwise impart extreme forces.

The current model of device, the P2, has a rated power output of 750 kW. At present, there are two Pelamis P2 machines undergoing grid-integrated testing at the European Marine Energy Centre in Orkney, UK. Two utility companies, E-On and ScottishPower Renewables, have entered into an agreement to carry out joint testing of their respective device, with knowledge gained over the course of the testing being shared between the two utilities. Pelamis have recently secured an order for a third device from the Swedish utility company Vattenfall.

Pelamis is involved in the development of array projects in the Pentland Firth (Marwick Head) and Shetland (Aegir) together with utility partners, in addition to the development of two sites autonomously, Farr Point and Bernera (UK, Scotland).



**Figure 2.8:** Pelamis P2 at EMEC

Country of Origin	UK
Rated Power Output	750 kW )
Water depth Min/ Max	50 m/ 250 m
Mooring Type	Slacked moored
TRL	7
Number of devices deployed	6
Target market	Deep offshore
PTO	Hydraulic
Deployment vessel	Tug boat, anchor handling vessel
Maintenance strategy	Return to base
Projects to Date	Agucadoura, 3x750 kW (P1) ; EMEC, 2X750 kW (P2)

**Table 2.5:** Characteristics of the Pelamis prototype taken from SIOcean (2013)

#### **Submerged oscillating body rotation example: Oyster**

The Oyster developed by Aquamarine Power, is a near-shore hydroelectric wave energy converter that consists of a hinged flap attached to the seabed at depths of between 10 and 15 metres, around half a kilometer from the shore. This location is often referred to as the nearshore.

Oyster's hinged flap, which is almost entirely underwater, pitches backwards and forwards in the nearshore waves due to the draft forces. The movement of the flap drives two hydraulic pistons which push high pressure water onshore via a subsea pipeline to drive a conventional hydro-electric turbine.

A 315 kW Oyster device has been operated at sea at the European Marine Energy Centre (EMEC) in northern Scotland between 2009 and 2011. The second-generation 800 kW Oyster 800 began operation testing at sea in June 2012 when it produced first electrical power to the

grid. Planned installation of a third-generation Oyster 801 machine is scheduled 2013. The first and second generation Oyster devices were constructed of steel. The next-generation Oyster 801 is to be constructed from fibre-reinforced polymer (FRP).



**Figure 2.9:** Oyster 2 at EMEC

Country of Origin	UK
Rated Power Output	800 kW
Water depth Min/ Max	10 m/15 m
Mooring Type	Bottom fixed/ pin pile
TRL	7
Number of devices deployed	2
Target market	Near shore
PTO	Hydraulic, high pressure water pumped from device to a shore based Pelton turbine
Deployment vessel	Tug boat
Maintenance strategy	Electrical PTO components and hydroelectric turbine located onshore. Calm weather window required for any maintenance work. Major maintenance: return to base
Projects to Date	EMEC, UK- 1X315 kW, 1X800 kW

**Table 2.6:** Characteristics of the Oyster prototype taken from SIOcean (2013)

### 2.4.3 Overtopping

These prototypes work with a very different mechanism compared to the previous ones. They are based on the overtopping phenomenon that depends on taking the water that is closed to the wave crest and introducing it into a reservoir whose level is higher than the surrounding free surface area. This potential energy is transformed to mechanical energy through a low-head hydraulic turbine. Some authors actually consider this type of WEC as an offshore hydraulic dam. Within this type of converter it can be distinguished between fixed structure and floating. The TAPCHAN prototype was the first prototype of this class (fixed overtopping), it was built during the 80s in Norway and tested during several years. As an example the Wave Dragon prototype is further explained. Within the fixed subgroup the Sea-wave Slot-cone Generator (SSG), see Vicinanza *et al.* (2014) and Vicinanza *et al.* (2012), employs several reservoirs placed on top of each other, in which the energy of incoming waves is stored as potential energy. Then, the captured water runs through turbines for electricity production.

#### Floating overtopping example: Wave Dragon

The Wave Dragon is a floating slack-moored wave energy converter of the overtopping type. It basically consists of two wave reflectors focusing the waves towards a ramp. Behind the ramp there is a large reservoir where the water that runs up the ramp is collected and temporarily stored. The water leaves the reservoir through hydro turbines that utilize the head between the level of the reservoir and the sea level. The prototype in a 1/4 scale is shown in Figure /refWD, the characteristics of this prototype are also summarized in Table 5.3.



Figure 2.10: Wave Dragon at Nissun Brending (Denmark)

Country of Origin	Denmark
Rated Power Output	20 kW, (4 MW)
Water depth Min/ Max	25 m/unknown
Mooring Type	Slacked moored
TRL	6
Number of devices deployed	1
Target market	Intermediate offshore
PTO	Direct drive permanent magnet generator
Deployment vessel	Tug boat
Maintenance strategy	Maintenance and major repair works can be carried out at site
Projects to Date	Nissun breeding, Denmark

**Table 2.7:** Characteristics of the Wave Dragon prototype taken from SIOcean (2013)

## 2.5 Current State of Wave Energy Development

Wave energy has been demonstrated to be possible and feasible and during the last decades: Oyster has delivered more than 12 MWh to the grid (Doherty (2014)), Pelamis has delivered up to 10 MWh from their P1 machine and up to 190 MWh with their P2 machines, see Yemm (2014), Wavestar has delivered 53.5 MWh to the grid up to December 2012, see Kramer *et al.* (2013), Pico delivered 52 MWh and Mutriku 200 MWh so far (Fernandez-Chozas (2013)). These figures demonstrated that extracting energy from the waves is possible. Furthermore, there have been some converters that have survived to very harsh conditions, for instance OE Buoy and Wave Dragon have survived three winters, see Fernandez-Chozas (2013), as well as Wavestar, during two winter in operation.

However, some important failures happened to some of the full-scale testing prototypes, which lead to a distrust of the prospective investors and governments, and spread some doubts about the commercial ability of wave energy in the foreseeable future. Some of these recent failures are as follows:

- The OSPREY prototype, that was planned to be deployed off to Dounreay (Scotland) failed in 1996 because of some problems relating to the harsh environment on the installation phase.
- Pelamis installed three P1 energy converters off the Portuguese coast in September 2009, and planned to add 22 more for a total of capacity of 21 MW. The cost of these three prototypes led to 9 million Euros. However, The initial three converters had to be removed in December due to leaks in the buoyancy tanks. A slew of more technical problems followed, and eventually Pelamis lost its financial backing.
- Oceanlinx, an Australian developer tried to tow their new multi OWC device off to Fleirieu Peninsula in Australia. The unit, which was being towed by a tug boat, suffered

serious damage to the airbags supporting the 3,000-tonne structure, which led to its sinking.

- CETO device, developed by Carnegie deployed their prototype off to Reunion Island (Australia). The prototype was swept away and damaged during the cyclone Bejisa. The buoy was damaged and even the foundations were found adjacent to a nearby reef.
- Aquabuoy sank for unknown reasons
- OPT powerbuoy, deployed off Santona (Spain), had a leak in the hydraulic system, what led to a flooding of the electronics of the device.
- Pelamis and Aquamarine recently had financial problems, being the first one put into administration recently due to the slow technology development

These failures demonstrate that reliability is a key factor on wave energy development and that devices and their deployment/maintenance techniques need to be in accordance with the met-ocean conditions of the deployment location.

Then, these previous examples demonstrated that wave energy technology development has not delivered the desired progress and success hoped for. It is still on the prototype testing stage and no prototype has successfully proved to be commercial. As stated in the previous section the cost of energy for the current devices is more than 25 times greater than standard energies and then the investor engagement is still very challenging.

Nowadays, a wide diversity of technology types still exists with prototype implementations far from converged optima. Techno-economic performance in terms of cost of energy (CoE) requires considerable improvement for profitable commercial application beyond the essential cost reductions associated with learning rates by bulk manufacturing (cost of energy reduction of more than 70 %). The situation can be explained in the next points, see Weber (2012):

- Very different WEC technologies are still being tested today
- No evidence of convergence of technology implementation nor operational principles has been achieved yet (tidal energy for instance has achieved convergence on the three blade turbines)
- High cost of energy (CoE) projections. Techno-economical performance still requires large improvements for profitable economical application even if the expected cost reductions associated with economies of scale and learning curves are taken into account
- Technology developments are:
  - Full scale prototypes requires a large amount of investment and it is necessary to engage a big investor to achieve TRL 9
  - High risk of investments due to repeated failures as well as the ignorance of prototype's behavior in harsh conditions
  - No flexibility on concept development

The development path of a prototype from invention to commercialization is long and it normally includes several models used for different sizes (scaling ratios). The outcome of this

phased analysis is that some specific aspects of the device are investigated in order to collect some information. This leads to the continuation and the development and investigation of the potential concept through the next phases. The characteristics of the different development phases are presented in figure 2.11 taken from Pecher (2012). The first phase looks at the proof of concept, where the invention is proved to work. It allows quick and fast modifications on the structure or other aspects of the model. It consists of a proof of the performance of the device and a first optimization. This phase is normally cheap in terms of budget and normally around 50.000 Euros. Phase 2, the design and feasibility study consists of the tests validation of Phase 1 tests and fine-tune some parameters, but not to make any drastic modifications to the device, so the results given at the end of this phase lead to the final design. Phase 3 looks at the testing of the prototype on a medium scale on a benign open sea site. The manufacturing, deployment, commissioning and actual operation will give a very good approach to the full-scale equivalent and therefore be highly valuable. A grid connection and use of power electronics are also strongly recommended as it might be part of the control strategy, and the quality of the electricity supply is an important parameter in the wave-to-wire model. This phase is the most challenging in terms of budget because it requires a step towards the millions of Euros figures. At the end of this development phase, a good estimation should be possible of the overall cost of the full-scale device, the wave-to-wire performance model and of the control of the system. Moreover, valuable experience should have been gained in the required equipment and the main complications related to the construction and commissioning of the full-scale device. The last development phase includes a fully-functional prototype on the device installed on open sea conditions. In Phase 5, Economics, after the successful development of the device, it is time to demonstrate the economic viability and the operation of a large project of full scale and possibly with several WECs. This relatively small array of WEC devices will be composed of the individual devices that have been technically proven and thereby should bring a relatively low technical risk. The devices should also have been proven able to produce the expected levels of energy at the end of the previous stage.

Apart from this development path, Weber (2012) proposed a new way to classify this trajectories based on a new metrics. He suggested that the development trajectories for the Wave energy converters have not been well-developed and then he proposed another method to achieve a successful development trajectory for a prototype. His proposed system is based on the following parameters:

Metric	Defines	Directly associated with
TRL	how ready a technology is	commercial ability of the technology
TPL	how well a technology performs	economic ability of the technology

**Table 2.8:** TPL-TRL metrics from Weber et al (2012)

Until today the developers have only cared about TRLs and quite a lot of technologies have been tested in a large scale, however most of them have demonstrated poor technology per-

	Phase 1 Proof of concept	Phase 2 Design and feasibility	Phase 3 Functional model	Phase 4 Demonstration	Phase 5 Economics
Technical Readiness Level	1. Confirmation of operation 2. Performance 3. Device optimisation	4. Sub-systems assessment	5. Sub-assembly bench tests 6. Full system sea	7. Solo, sheltered, grid emulator 8. Solo, exposed grid	9. Multi-device array (3 - 5)
Scale	1:20 - 1:100	1:10 - 1:50	1:3 - 1:10	1:1 - 1:2	Array (1:1)
Location	laboratory	Laboratory	Benign site	Open seas	Open seas
Time [months]	1 - 6	3 - 12	6 - 24	6 - 24	12 - 60
Budget (€, 000)	1 - 50	50 - 250	1000 - 2500	10000 - 20000	25000 - 75000
Model	Idealized setup Load-adaptable PTO Standard mooring	Final design Mooring layout Simulated PTO	Full fabrication True PTO and Electrical generator	First fully operational device	First multi-device
Objectives	Concept validation	Performance estimation	Real sea performance	Operation and procedures	Array interaction
	Performance estimation	Parametric study	Wave-to-wire model	Electrical quality and grid supply	Production line
	Design variables	Detailed numerical calculation	Control strategy	Overall performance	Economics
	PTO & mooring characteristics Loads & movements estimations	Estimates on cost Feasibility study	Mooring forces Survival & sea keeping Marine environment	Control strategy Survival	Service schedules Components life

**Figure 2.11:** Development stages of WEC technologies

formance. These technologies have been able to raise funds for sea testing of their full scale prototypes, however techno-economic analysis is carried out once large amounts of money have been spent on full scale prototypes. On figure 2.12 two development path are shown. The yellow path and the blue dots represents technologies that exist in reality. As can be seen, their economic performance is far from commercialization. The suggestion proposed by Weber (2012) is to assess the economic viability of converters on each of the design phases to reach high TPLs from the very beginning of the WEC development to be able to modify/stop the project before the high investments necessary for the commercial devices.

The Equimar project, see Davey *et al.* (2009) (Equitable Testing and Evaluation of Marine Energy Extraction devices in terms of Performance, Cost and Environmental Impact) tried to provide a guidance and some protocols on techno-economic assessment of wave energy devices. On workpackage 7 the cost model used by developers was reviewed. Four developers were interviewed in order to provide some information about their economic assessment methodologies. All of them used the net present value approach. The risk was taken into account by differentiating between discount rates. A need of improving for risk assessment is perceived and suggestions are made to apply stochastic approaches to consider uncertainties. The project report showed that uncertainty ranges for Operation and Maintenance costs are perceived as being relatively high by the developers. The O&M strategies (accessibility, cost of vessel and operating limits) seemed to be an important uncertainty cost center of the device. The figure

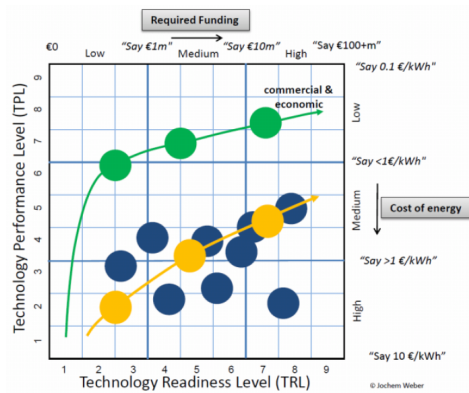


**Figure 2.12:** Development path of some WEC technologies, in yellow current path, in green optimum path

showed the uncertainty perceived by four developers (A,B,C and D) on the different O&M aspects. For three of the developers the uncertainty was perceived on more than 25 % for all the issues.

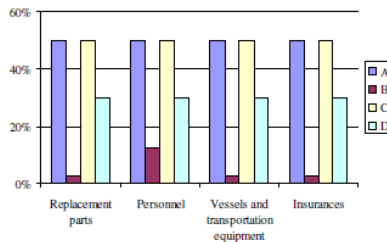


**Figure 2.13:** Developers perceived uncertainty on Operation and Maintenance activities

Therefore, it should be noticed that there are still quite a lot uncertainties on marine energy assessment and the risk associated is one of the reasons why it is not yet commercial. This thesis reviews the current risks and uncertainties related to wave energy development from a techno-economic perspective. In addition, on the next subsection the state of the art on techno-economic assessment of wave energy projects will be investigated in more detail and it will be the baseline for this thesis.

## 2.6 Review of techno-economic assessment on wave energy

The techno-economic assessment of Wave Energy devices is quite a recent discipline considered on wave energy development but its importance has been highlighted by quite a lot of experts in the past decade.

Firstly, one significant thesis to highlight is Gonzalez-Reguero (2013). In one of the chapters three tasks related with wave energy were addressed. Firstly, the evaluation of the global wave energy resources, describing its spatial-temporal variability throughout different scales; and secondly a risk analysis of absorbed wave power for four offshore Wave Energy Converters (WECs) with a twofold scope: resources change in a life-cycle and survivability risk from expected variations in the 100-yr wave height. It was concluded that the global offshore wave power is estimated in the range of 1 to 10 Twh (between 9,000 and 90,000 Twh/yr). A recent estimation was made in 32,000 Twh/yr considering all possible directions. In this work a new approach was developed, through a computation of the resources on a hourly basis in the period from 1948 to 2008 and only taking into consideration the transverse directions onshore. The global gross theoretical wave power is hence estimated approximately in 16,000 Twh/yr (corresponding with 1.8 Twh power). Also it was concluded that different devices are prone to show different performance depending on the wave climate types at different locations. Site-specific optimized design and comparison of technologies is a must for installation analysis.

Furthermore, some projects that led to important conclusions regarding the techno-economics assessment of WECs are, the Navitas tool from HMRC, see NAVITAS web page, that was a initiative to facilitate techno-economic assessment of wave, tidal and wind projects. The COE Tool from Fernandez Chozas, see Julia Fernandez Chozas web page, is an excel sheet that facilitates assessment of converters for early stages of development. Also TEOWEC, from Maynooth tried to integrate economic assessment with operational modeling, see Teillant *et al.* (2012).

Several authors have carried out studies regarding the economic performance of wave energy projects such as Beels *et al.* (2011), Dalton *et al.* (2012), O'Connor *et al.* (2013a)), almost all of them concerning a specific type of technology. Beels *et al.* (2011) were one of the first to study several arrangements for the Wave Dragon device taking into account the operational and maintenance costs as a function of the marine climate.

Beels *et al.* (2011) studied the economical performance of a generic wave energy device through operational simulations. However, generally, all the studies published to date base their cash flow analysis on the power matrix.

Several authors have studied the economic feasibility of wave energy projects reaching the same conclusion, namely that current feed in tariffs are not sufficient to make the development of wave energy farms cost-effective. A sensitivity analysis of the inputs of the economic analysis were performed and optimal locations for specific technologies are suggested as a

function of these parameters (O'Connor *et al.* (2013d)).

O'Connor *et al.* (2013a) also studied the implications of operational costs on the economic analysis taking into account the concepts of accessibility and availability of a specific location. Brown *et al.* (2010) differentiated the concepts of survivability and reliability on the context of wave energy. A metric for survivability was developed taking into account the number of hours that a certain wave condition is exceeded within a year.

Finally Dalton *et al.* (2012) performed a case study sensitivity analysis taking into account the impact of the learning curve, supply and demand curves and future cost of cash. The conclusion of this study was that the current feed in tariffs for wave energy in countries such as Ireland is insufficient to develop cost-effective projects. Ireland feed in tariff, available until 2015, has been set to 0.22 Euros/kWh and spans a 15-year project. However this tariff has been shown to be insufficient for the currently available devices, specifically for the Pelamis Device studied by Dalton *et al.* (2012). A feed in tariff of 0.45 EUR/kWh was found to be more realistic and reliable reaching an attractive internal rate of return.

## 2.7 Conclusions

Wave energy has been demonstrated to be technically feasible due to the last achievements by some full-scale prototypes in the last decade. However, it has also been demonstrated to be far from commercialization due to the high current Levelized Cost of Energy (LCOE) and the relatively low reliability of the prototypes. Techno-economic assessment has been shown to be a key issue on wave energy development, and then its evaluation is crucial on every stage of development. Reliability, survivability and O&M procedures are all still aspects that cannot be accurately measured and then a better understanding of the influence of these points, mainly the influence of the met-ocean conditions on WEC design is the key to success. This thesis pretends to obtain a better understanding of wave energy conversion from the techno-economic point of view, and it intends to give some guidance through the investigation of several technical issues of some current WECs with different met-ocean conditions.

# Objectives

---

### 3.1 Objectives

The current state of the art of wave energy development is explained in chapter 2. It is concluded that wave energy is still at a prototype testing stage, there is not technology convergence yet and the commercial stage has not been achieved. There are still some unanswered questions in regard to certain issues, such as power assessment, reliability and failure analysis, O&M strategies and uncertainties on economic analysis on Wave Energy converters. Afterward, this thesis attempts to address these topics that have not been investigated, yet in order to provide some guidance for wave energy developers, so as to design reliable and economic WECs.

The main objective of this thesis is to fill the current gaps on techno-economic and feasibility studies of Wave Energy converters from a design-oriented perspective. Then, the specific objectives related to this thesis are as follows:

- Development of new methods for wave power assessment (section 4.1).
  - Development of a methodology for long-term performance assessment. As there is not extensive experience on full-scale prototype testing, it is essential to find a computationally efficient methodology, regarding the long-term power assessment on WECs. This thesis addresses this gap and proposes a new methodology for power assessment.
  - Investigation of sea state characterization influences power assessment on WECs (section 4.2) For power assessment on WECs, normally some assumptions are made regarding the shape of the sea spectrum and its distribution. The influence of these assumptions of annual energy production is assessed.
- Investigation of the influence of met-ocean conditions on the different issues related with WEC development
  - Geometric adaption of a Wave Energy converter to global locations (section 5.1). Designers normally focus their device, in order to harvest the maximum possible energy on a particular site. However, as a method to maximize profitability, the converter should be adaptable to several locations. The best design strategies for that are investigated.

- Deepening the O&M strategies understanding from a global perspective (section 5.2)  
O&M is demonstrated as one of the important gaps and uncertainties on wave energy development, and then it is investigated from a global perspective
- Investigate reliability and failure analysis on Wave Energy converters (section 5.3)  
Reliability and failure analysis is important on the different stages of development of a WEC. An analysis of the areas with the most favorable conditions for wave energy development, in terms of failure and survivability is carried out.
- Study the met-ocean factors that influence farms layout (section 5.4)  
Wave energy converters are planned to be deployed as farms. However, it is not clear how the marine environment will influence the possible and feasible configurations. A study of the different factors that affect array configurations is conducted
- Deepen into the understanding of economic analysis on wave energy conversion
  - Identify the cost areas with a higher uncertainty (section 6.1)  
One of the main gaps on ocean energy is that the uncertainty is very high. The different uncertainties are outlined and their influence on the financial indicators on project feasibility studies is assessed. The influence of the different push pull mechanisms is also investigated and the level of current uncertainty on wave energy projects is identified.
  - Identify the possible prototype improvements path for a lower LCOE (section 6.2)  
It is apparent that technologies need to be improved in order to achieve a lower LCOE. However, it is not clear on what R&D areas the investment should be focused, in order to accelerate marine energy deployment. A study based on two actual and current prototypes is performed.

## 3.2 Thesis structure

Then, based on the aforementioned objectives, the Thesis is organized as follows:

- Chapter 1: Introduction
- Chapter 2: State of the art of wave energy
- Chapter 3: Objectives
- Chapter 4: Long term power production assessment
- Chapter 5: Influence of met-ocean conditions on WEC design
- Chapter 6: Economic analysis of wave energy
- Chapter 7: Further research
- Chapter 8: Conclusions
- Chapter 9: References

# Power assessment methodology and applications

---

## 4.1 Long term power production assessment methodology

In this chapter, a new methodology used for estimating the long-term performance of a Wave Energy converter on a certain location is presented and validated. Also, the classical power assessment method based on the power matrix approach is compared with this new approach. In the second section of this chapter, certain assumptions on the classical power assessment method are reviewed and the influence of the sea state characterization on power assessment is studied.

### 4.1.1 Introduction

Power assessment of Wave Energy Converters is a key step on techno-economic analysis. In order to calculate the performance of a WEC on economic terms (EUR/kWh) both the costs of the device and on the other side the income received from the power production of the device are needed to be taken into account. Then, power assessment is an important step to consider. There have been some attempts to standardize the power assessment on WECs. For instance, Smith and Taylor (2009) proposed a method to collect standard data for power assessment. They set a list of parameters to be measured and listed on power assessment regarding resource characterization and device measurement. Also, Pitt (2009) proposed a most updated way to standardize power assessment on Wave Energy Converters. They set a methodology in order to estimate the Annual Energy Production as well as the capture length. They presented the power matrix as the most common way of representing the output power of a device. The power matrix is a bivariate histogram of  $H_s$  and  $T_e$  in which each cell contains the average value of the power output of the WECS for all the sea states falling within that cell. The measured power matrix may be presented to give an overall picture of the performance of the WECs during the test period which has the advantage of familiarity. It is recommended that the cells of the matrix should be 0.5 m wide for  $H_s$  and 1.0 s for  $T_p$ , but these may vary depending on the local wave climate. In this report they also presented the occurrence matrix that is also a bivariate

histogram of probability of occurrence of the pair of sea states falling in between a certain  $H_s$  and  $T_e$  range. The classical method of estimating the Annual Energy production (AEP) suggests multiplying the Power matrix by the occurrence matrix. On the other hand, Pitt (2009) analyzed some WECs sea trial performance data trying a common approach for all of them. Also, the last attempt to standardize power assessment corresponds to the International Energy Committee within the IEC/TC 114/PT 62600-1 and IEC/TC 114/PT 62600-102. In this case they propose the use of the bi-dimensional scatter diagram ( $H_s$ - $T_e$  in this case) and the capture width instead of the power matrix, in order to be able to compare devices easily regardless of the rated power.

One of the last attempts to standardize power assessment corresponds to the Equimar project, further explained in Kofoed *et al.* (2013). They propose a new method for power assessment within the Equimar project consisting of three main parts. The first part intends to pre-process the environmental data (e.g. waves, tides, wind, etc.) and the performance data (e.g. mechanical power, electricity transmitted to the grid, etc.). This consists of establishing the environmental matrix that contains all parameters used to characterize the environmental climate at the test site. This environmental matrix has to be based on long-term data, typically 10 years or more for wave data, in order to cover all the long and short term variability of the individual parameters. This can then be simplified into the scatter diagram, determined by  $H_{m0}$  and  $T_e$ . The performance of the WEC at the conversion stage of interest, in terms of power output (P) or available power, is processed relative to its corresponding environmental conditions so as to obtain the non-dimensional performance values of the WEC, and from the basis of the procedure. If various energy conversion steps or other device dependent or environmental parameters are investigated, then these must also be included in the data from the outset. Due to the fact that these factors will impact the later development of the process, it is necessary to capture their impact on the initial data.

The processing of the environmental and performance data is carried out by clustering the data into zones. Each zone is delimited by a specific range of the environmental matrix (typically in terms of  $H_{m0}$  and  $T_e$ ) and includes a certain amount of performance data points. For each zone, a non-dimensional power performance (zone) will be calculated, together with the corresponding uncertainty based on a selected subset of the performance data points that are included in the zone. The size and the location of the zones on the environmental matrix are defined corresponding to the available data and overall environmental matrix. The selection of the data points that represent a zone has to be carefully done, as it influences the stated zone and its related uncertainty, which are at the basis of the calculation of the Annual Energy Production (AEP) of the WEC.

However, all the aforementioned methods only estimate the Annual Energy Production. For an accurate power assessment and in order to be considered the input for an economic analysis the long-term power data series of the prospective device in a potential location is essential. The classical method is only able to estimate one isolated figure of the power production. However

the inter-annual variability should be taken into account. This classic approximation, then, is not totally precise and then further research on this topic is needed. Also due to the lack of long term power field data it is highly important to find a computationally efficient method to estimate the long-term power production series through an easy and quick approach. This section presents a new approach used for obtaining the long-term power estimation of a WEC. This approach focuses on a sea state selection technique, a numerical model and non-linear interpolation technique.

It should be noticed that in this piece of research the peak period is used instead of the energy period. This is due to two reason:

- When dealing with buoy data, some of the buoys do not retain the whole spectrum, they keep some spectral parameters in order to save space. When saving spectral parameters normally the significant wave height and the peak period are the most widely used. If the energy period needs to be obtained through this data some assumptions regarding the shape of the spectrum needs to be made. Therefore, it is preferred to work with the data directly obtained from buoys, without additional assumptions.
- When dealing with combined swell-wind sea spectra the energy period can be located in a part of the spectrum with a low amount of energy and it does not represents the location of none of the energy groups within the spectrum. On the other hand, the peak period represents at least the location of one of the energy groups within the wave period scale.

For these two reasons, as well as the standard use of the peak period within harbor and coastal engineering applications, it is decided to use the peak period from now on in this thesis.

#### 4.1.2 Methodology for long term analysis

The final goal of this section is to obtain the power production time series and power statistics of the modeled WEC when installed in a given location. The goal of this subsection is produce a new methodology for the analysis of the long term power performance of a device, validate it and compare it with the classical method of computing the Annual Energy production. This methodology is based on a sea state selection technique and a non-linear interpolation technique. For this section, a two-body heaving WEC, taken from Babarit *et al.* (2012), was selected for analysis, see figure 6.1. It is formed by a submerged buoy and a floating torus. This WEC extracts the energy of the relative motion between the two bodies. This WEC is assumed to be installed on the Cantabrian Sea, near the village of Santoña, north Spain, obtained from Reguero *et al.* (2012). This location was selected because the local Government has been developing a testing area for WECs there. The point selected is  $3.46^{\circ}W$  and  $43.56^{\circ}N$  with a depth of 100 m and yearly averaged power of  $24 \text{ kW}/m$ . Figure 4.2 shows the location of the selected point of study while Figure 4.5 shows the  $H_{m0} - T_p$  scatter diagram of the marine climate at this point. In order to compute the power matrix, the  $C_{PTO}$  used is the optimum one

for each sea state explained in the next subsection.

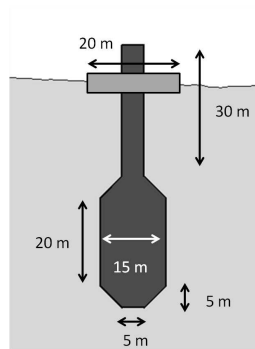


**Figure 4.1:** Analyzed two body heave WEC with dimensions



**Figure 4.2:** Location of the point selected for the power study

Figure 4.3 shows the power matrix of the analyzed WEC. In order to compute this power matrix a linear time domain model based on a state space approach was developed for this purpose. This numerical model is further explained in Appendix 1. In order to compute this matrix the model was run for three 1 h sea states presented in Figure 4.5. In the computation of Figure 4.3 it was assumed that the WEC will enter in survival mode for  $H_{m0} > 6m$  and then the power production for the sea states with  $H_{m0} > 6m$  is assumed to be zero. As Figure 4.3 shows, the power production increases as the wave height increases and the peak period approaches the natural period. The annual production of the device is obtained multiplying this power matrix by the scatter diagram (see Figure 4.5) giving an annual energy production of 1414 MWh/year.

The Net Capacity Factor (NCF) of a power plant is the ratio of the actual output of a power plant over a period of time and its potential output if operating at full nominal power the entire

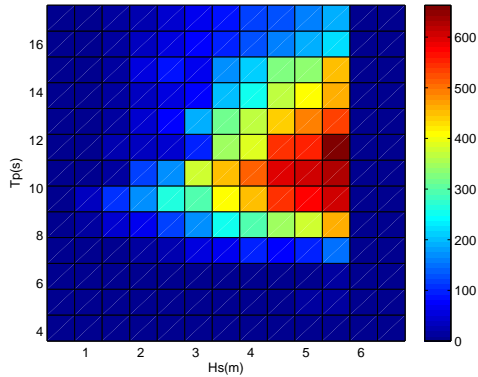


**Figure 4.3:** Power matrix of the device (kWh)

time. The WEC's NCF depends on the PTO nominal power and should increase as the PTO nominal power decreases. Taking into account that electrical machines can support overcharges over short periods of time, to compute the NCF the Babarit *et al.* (2012) assumption was used: If the power is between one or two times the nominal power, the generated power will be the nominal one, but if the power exceeds two times the nominal power then the generated power will be zero.

Figure 4.4 shows the NCF for the analyzed WEC. The slope represents the net increase of the NCF in terms of the nominal installed power. The optimum installed capacity should be that which presents the maximum slope, because it means then installed rated power is used more efficiently. As shown in Figure 4.4, this maximum slope is around an installed capacity of 1 MW (a detailed study with a higher resolution was performed in order to select the nominal power). Furthermore, the decision about the nominal power of the device is based on the state of the art of similar devices. This installed power has been used in the following analysis of the WEC.

The yearly averaged optimal energy production of the heave device in a given wave climate is usually obtained by multiplying the optimized power matrix by the  $H_{m0}-T_e$  scatter diagram. If a sea state time series is available at a given location, the sea state time series of optimal energy production can be obtained interpolating each time series sea states on the optimal power matrix.

The previous approach has two main sources of inefficiency: 1) many of the sea states computed to build the optimal power matrix are useless because their probability of occurrence is zero and 2) if a linear interpolation is used for computing the time series of sea states of optimal

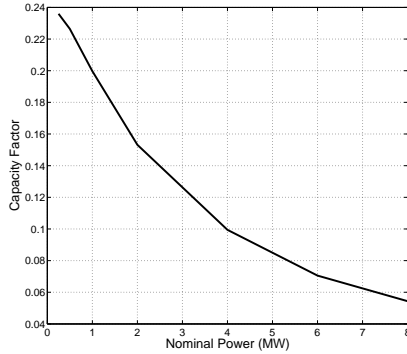


**Figure 4.4:** Capacity factor vs Nominal Power

power, the changes in the slope on the production matrix are not taken into account. To avoid these inefficiencies, a new methodology to calculate the sea states time series of optimal energy production is proposed below. The methodology is explained on the next paragraphs and it is summarized in figure 6.4. This methodology is applied to a node of the 60-year reanalysis data base, Global Ocean Waves (GOW) from Reguero *et al.* (2012) located near Santoña (North Spain) made up of hourly sea states with the pairs  $H_{m0}$  and  $T_p$ .

The first source of inefficiency is addressed using a selection technique to separate a subset of sea states from the whole data base that best represent all the data base sea states. In this methodology, the MaxDiss algorithm from Snarey *et al.* (1997) is proposed because it efficiently represents the boundaries of the data base in a multidimensional domain. It is based on a selection that computes the distance between points in a multidimensional space and selects the most distant points in order to cover the whole variability of the set. For the second inefficiency source, the Radial Basis Function (RBF) interpolation method from Franke (1982) is used. This methodology has been used and proven previously in Camus *et al.* (2011) to study the downscaling of wave climate to coastal areas. This methodology has been proved to be one of the best interpolation methodologies for multidimensional data.

The first sea state of the MaxDiss selection procedure is given by the user. Usually, one sea state on the multidimensional data base boundary is chosen (i.e. the sea state of the time series with the maximum  $H_{m0}$ ). In this case the time series is 2-dimensional ( $H_{m0}$ - $T_p$ ) and as the objective is the power production, four criteria for the starting sea state are tested, corresponding to the sea state with maximum:

- $H_s$  significant wave height

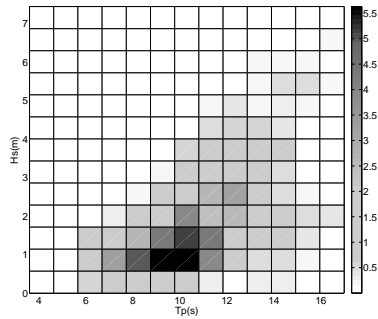


**Figure 4.5:** Percentage occurrence matrix/occurrence matrix in Santoña (Spain)

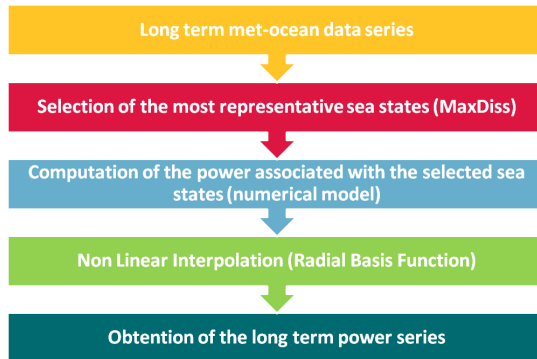


**Figure 4.6:** Schema of the proposed methodology

- $H_s^2$  square significant wave height
- $H_s^2 T_p$  Energy Flux
- $T_p$  (optimal) Peak period

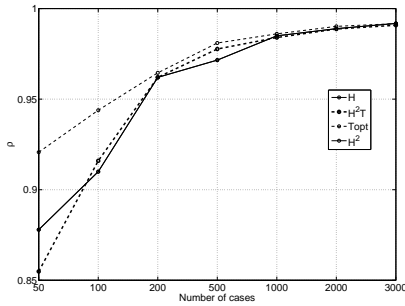
In order to check the best initial sea state criteria and the optimal size of the selected subset of sea states, a year-long time series of sea states (year 2001, 8737 sea states) of energy production has been computed with the numerical model and with the proposed methodology, using different sizes (50 to 3500) of the MaxDiss subset of sea states and the four criteria indicated above for the initial sea state and the RBF interpolation technique to rebuild the full time series of energy production.

Figure 4.7 represents the linear correlation coefficient  $\rho$ , between the two data sets obtained by, computing the 8737 sea states and, using the proposed methodology (MaxDiss-RBF) com-

Model	274
Power Matrix*Ocurrence matrix	147
Equally spaced Power Matrix+RBF	190
MaxDiss+RBF	245

**Table 4.1:** Annual mean power in kWh calculated with the methodologies selected for year 2001

puting only a subset of sea states of different sizes and with different starting criteria. As can be seen in the figure, the best criterion for the Max-Diss starting sea state is that one using the maximum  $H_{m0}^2 T_p$  sea state. Also note that with subset sizes larger than 200 sea states, all four criteria for the starting sea state provide similar accuracy. Therefore, the influence of the starting criteria become negligible with large subsets of sea states.



**Figure 4.7:** r-squared parameter for the different selection cases and the different number of cases

The complexity of the MaxDiss+RBF methodology is justified here in terms of precision with respect to the traditional method of multiplying the frequency and power matrices. To compare the accuracy of the proposed methodology with the traditional one, the 2001 year series was reconstructed by interpolating each time series sea states on the  $14 \times 14 = 196$  sea states of the power matrix using the RBF technique, through the proposed methodology with a MaxDiss subset of sea states with the same size as the power matrix (196 cases) and rebuilding the full year time series using the RBF technique.

The correlation coefficients between the true time series of sea states power production and the reconstructed ones were 0.96 for the proposed methodology and 0.7 for the one using the power matrix and the RBF interpolation technique. In Table 4.1, the yearly averaged energy production is computed using: 1) the time series of sea states energy production obtained

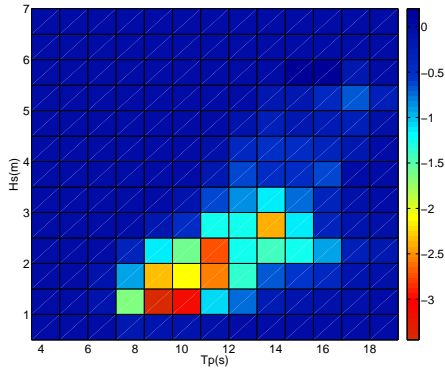


**Figure 4.8:** Percentage of relative error with respect mean annual hourly production between methodologies scatter diagram\* Power Matrix and power matrix calculated by the model for year 2001

by computing all 8737 sea states, 2) the product of power and frequency matrices, (196 sea states computed) 3) the time series of sea states energy production reconstructed using the power matrix and RBF (196 cases computed) and 4) the proposed MaxDiss+RBF methodology computing 196 cases. As shown, the percentage difference between each method and the exact (full time domain computation) is 46% for method 2, 31% for method 3 and 11% for the proposed methodology. Figure 4.8 shows the contribution of each sea state of the scatter diagram to the relative error on the yearly averaged energy production computed using method 2. The maximum error is located around the 10 s peak period, where the power matrix has a local ridge and the scatter diagram nears it maximum and the concavity of the power production matrix that provides the interpolation of each sea state energy production is always below the true one. Finally, figure 4.9 illustrates the MaxDiss selected subset of sea states concentrated on the  $H_{m0}-T_p$  region where sea states are probable (192 points on the 90% probability volume) while using the equally-spaced power matrix, only 121 points are in the same volume.

Taking into account that the proposed methodology only computes 2% of the sea states of the data set, the advantage of the new methodology is obvious. Moreover, the inaccuracy of the traditional methodologies used to compute the yearly-mean of energy power production to rebuild the full time series has been demonstrated.

If the range of the sea state variables ( $H_{m0} - T_p$ ) does not change, the number of sea states on the MaxDiss subset does not either. For example, the full 60-year hourly sea states time series

Nominal Power	1MW
Average power	300kW
Capacity factor	30%
Mean annual production	2602MWh/year

**Table 4.2:** Summary of power production figures

of energy production can be rebuilt with similar accuracy computing the energy production of only 200 sea states with the numerical model. Figure 4.10 represents the yearly mean and the standard deviation of the 60 year rebuilt time series using 200 and 1000 subset of sea states in the MaxDiss selection. Furthermore, there is no noticeable difference between the two curves. The average power produced by the device is 300kW, with the year 1962 being the worst in terms of production with 260kW and 1960 being the best with 340kW . Therefore, with the methodology presented in this section the most important statistics of the life cycle of a wave converter can be obtained in a reliable manner.

Finally, in order to clarify and summarize all the quantities related to power production Table 4.2 is presented:

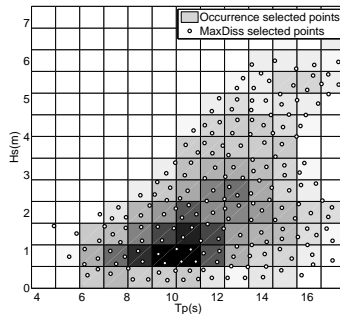


**Figure 4.9:** Selected sea states for the two methodologies applied for the year 2001

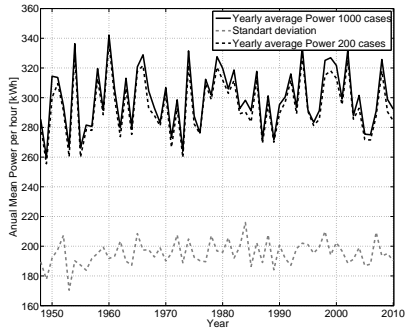


**Figure 4.10:** Mean annual power and standard deviation for the 60 year series at the study with 200 and 1000 cases

## 4.2 Influence of sea state characterization on power assessment

### 4.2.1 Introduction

As stated in the previous subsection, during a classical power assessment of WECs, normally the average annual power is computed with the multiplication of the occurrence matrix (% of occurrences of a set of sea states) by the power matrix (power of the converter on a set of sea states), as stated on the previous section. However, as it has been demonstrated, this method can only provide a figure with the average power production and it is partially inaccurate. Furthermore, when evaluating a particular wave energy converter development from the economic point of view, the interannual variability is essential to estimate the profitability of a project. Then, a methodology to estimate the long term performance of a wave energy converter in a locations with low computational requirements is very valuable tool for WEC development and optimization.

The methodology presented in the previous subsection assumes that a long met-ocean data series is available with the most important spectral parameters. In the previous subsection the methodology was validated with a two-body heaving converter and a location in the North of Spain. However, it is considered that the investigation of the sensitivity of the methodology to different parameters could be useful for future developments.

Currently, there are several types of wave energy converters with different working principles and power characteristics. Babarit *et al.* (2012) studied eight different types of converters on different locations and as can be concluded from this paper the different mechanic principles of WECs provoke different power matrices. One of the factors that will be studied on this subsection is how the different power matrices affect the methodology and the long term

performance of a WEC.

A further consideration, beyond sea state selection and device characterization, is the frequency spectrum of the sea states. When computing the power matrix of a device analytic spectra are often supposed (i.e JONSWAP or Bretschneider). However this assumption influences the performance of a WEC and sometimes the real spectra on open sea conditions do not fit with the analytical spectral representation. Some authors, e.g. Kerbiriou *et al.* (2007a) and Kerbiriou *et al.* (2007b) studied how an improved characterization of sea states influences the performance of a WEC. They stated that analytical spectra are erroneous by 63% due to the existence of sea states with more than one peak. They concluded that the sea state characterization with analytical spectra could provoke a large error in the power production results. With respect the SEAREV device on the SEMREV site they concluded that the analytical spectrum led to an under-estimation of the harvested power by the device.

Also Saulnier *et al.* (2011a) studied the sensitivity of the wave groupiness and spectral width for some wave energy converters. They concluded that the sensitivity of a WEC to spectral width is more significant when the mean period is near the resonance period of the device and also when the response of the WEC is broad. Saulnier *et al.* (2011b) studied the distribution of the different sea states that occur on the Portuguese coast in terms of the number of modes and directionality. Then it is clear that the sea state characterization significantly influences the numerically calculated power performance of a converter. Thus, it is clear that the sea state characterization is a key parameter that influences long term power performance of WEC and an accurate approach is needed in order to estimate the Annual Energy production of WEC.

Also, the met-ocean conditions are very variable and then the occurrence matrixes fluctuate. In section 4.1 a location in the north of Spain was set to develop the methodology. However, as stated beforehand the broadness and the peakness of the occurrence matrix greatly influences the long term performance of a wave energy converter and it is a parameter that should be studied for future uses of the methodology.

This subsection focuses on the influence of the type of WEC, the occurrence matrix type and the different spectra data types available in order to define the influence of each aspect on the ultimate power production. Also, the influence of the assumptions regarding the spectral shape on the power matrix will be investigated. Firstly the numerical model used will be explained, secondly the different sets of factors analyzed (WEC, location and spectrum data type) will be explain and thirdly the methodology consisting of the set of simulations run will be stated and finally the results will be presented.

### 4.2.2 Description of studied parameters

In this subsection the different options in terms of locations, data and wave energy converters will be described:

#### Locations

Four different locations are selected for this study. These locations have very different characteristics due to the different position around the globe and the different atmospheric dynamics governing them. On Figure 4.11 the locations are shown on the Globe map. The locations are North of Spain (Bilbao, near BIMEP), North-West of Denmark (near Hanstolm), West of Ireland and South-Central Chile. The met-ocean data used in each location are thoughtfully described in the next subsection.

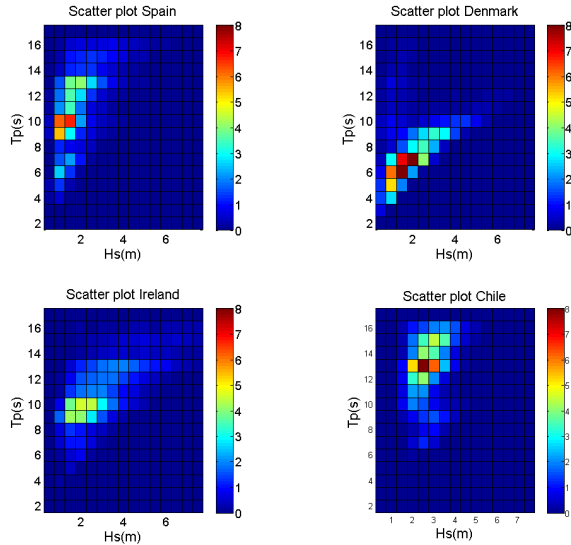


Figure 4.11: Selected locations (Longitude, Latitude)

In Figure 4.12 the occurrence matrices of the locations are shown (percentage of occurrence over time). Bilbao location is characterized by an occurrence matrix concentrated around 9 s and with relatively low wave heights. Denmark is characterized by low peak periods and a very concentrated occurrence matrix around low wave heights. On the other hand, Ireland has a very broad occurrence matrix characterized by very energetic sea states, with high wave heights and peak periods around 10 s. Chile has an extremely concentrated occurrence matrix with quite high peak periods and wave heights around 2.5 m.

Also, an investigation about the sea state type on each location has been performed in relation to the number of peaks of the spectra and on the type of component (swell and wind sea). This separation of the components has been performed based on the steepness method proposed by Wang and Hwang (2001) computing a separating frequency when distinguishing between wind sea and swell based on the moments of the spectrum.

Figure 4.13 represents the sea state spectral distribution on the different locations (see next subsection for the data type for this figure). Firstly, in Bilbao there are almost 50% of one peak sea states (42% swells and 6% seas), while the 50% left are combined sea states with a predominance of swell+sea sea states. In Denmark, the percentage of one peak sea states is lower (around 45%, 15% of swells and 30% of seas). However the percentage of more than



**Figure 4.12:** Occurrence matrix in % of the selected locations

one peak is quite high (around 65% having 30% of sea+swell sea states). On the other hand Chile and Ireland have both a high percentage of swells (40 %) and only 40% of the sea states corresponds to more than one peak spectra.

It should be noted that the plot from Denmark reflects the conclusion of Guedes-Soares (1992) and Rodriguez *et al.* (2004) regarding the occurrence of the two-peaked spectra on the occurrence matrix: wind dominated sea states tend to be on the low period area while strong swells tend to be on the high period area.

### Data type

For this study four different data types have been selected, although not all the data types are available for all the locations. For instance, buoy data was available just for the Bilbao site. This buoy, that is from the SeaWatch model, corresponds to the buoy located off Bilbao port. It is located on the coordinates  $3.05^{\circ}$  West and  $43.64^{\circ}$  North, on a depth of 600 m and it provides directional spectrum components of hourly sea states from 2009 until today.

The second data source is the IFREMER spectral data base, available for all the locations .This database provides the spectral parameters with a 0.5 degree resolution grid, 3-hour time

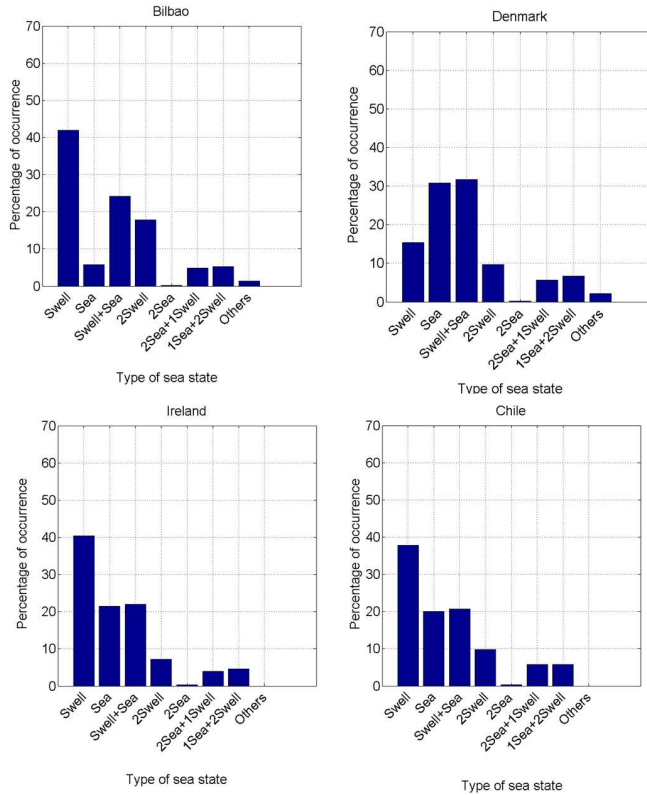


**Figure 4.13:** Occurrence of the different sea state types on the different locations

step, covering the years 1994-2012; see Rasclé and Ardhuin (2013a) and Rasclé and Ardhuin (2013b)). This database splits the spectrum into individual wave fields (1 sea and 5 swells) using the method of Hanson and Phillips (2001) as described in Tracy *et al.* (2007). The selected points in this database are less than 100 km distant from shore and less than 200 m deep. The use of this database provides smoothed spectra of more than one peak on the selected locations. For this IFREMER data base the spectra are available from 1994 to 2012. These sets then account for 58,440 sea states. For the Bilbao location the coincident dates between the buoy data and the IFREMER data base were taken. These dates are from 2009 until 2012 with a 3 h span, which accounts for 9469 sea states.

When simulating the performance of WECs some analytical spectra such as Brechneider,

JONSWAP or Pierson Moskowitz are used because they are very similar to a perfect swell sea state. Normally JONSWAP spectrum is one of the widely used spectra. This spectrum has a peak enhancement factor called  $\gamma$  that is usually set to 3.3, usually set for storms, however it could be changed from 1 (typical for wind seas and broad spectra) to more than 6 (typical of long Atlantic swell, for very thin spectra). The third set of data in this study consists of the JONSWAP spectra with the same wave height ( $H_{m0}$ ) and the same peak period ( $T_p$ ) as the IFREMER data. The fourth data set consists of JONSWAP spectra with the gamma parameter chosen to give a best fit to the IFREMER sea states.

For the Bilbao location, all the data sets will be used, on the other hand for the rest locations, only three data sets will be used (no buoy data). It should be pointed out that the buoy location does not perfectly match the IFREMER data points and then an interpolation between two IFREMER data points was taken for comparison with the buoy data in order to reduce the spectral errors due to shoaling and refraction effects.

One of the aims of this subsection is to analyze the influence of the one peaked spectrum assumptions on the final power of the device. Figure 4.14 shows two examples for the different selected data sets of how one peak spectra fit to real spectrum. In the left panel a spectrum from the IFREMER data base (red) is compared with a JONSWAP spectrum with gamma 3.3 for the same  $H_{m0}$  and the same  $T_p$ . It should be noted how the JONSWAP spectrum only fits with the swell component and not with the wind sea peak. On the right panel the four different data types for the Bilbao location are represented. Here the blue line represent the buoy data, while the green line represents the IFREMER data. As it can be seen the correspondence is very good and the IFREMER data picks the two spectra peaks. With the red line and the black line the JONSWAP with gamma 3.3 and the best gamma fit respectively are represented. As shown in these spectra, the JONSWAP fit does not correctly represent the multi-peaked or multi component nature of the measured spectrum. The influence of this fact on the power production assessment will be investigated.

### Description of WEC devices

Three different Wave Energy Converters (WEC's) were studied in this section. These devices were, at first, a heaving buoy with bottom reference, then a two body heaving buoy with power production in relative heave, and lastly a deep water hinged flap with power take off in pitch. These devices are generic and are not related to any particular commercial design, but the relevance of these generic devices is borne out by the many devices that have been proposed and/or promoted and are conceptually close to these generic devices. Real world devices operating on similar principles to WEC 1 include Seactricity and Seabased as well as many others, devices operating on similar principles to WEC 2 include Ocean Power Technologies Web page and devices operating on similar principles to WEC 3 include S.H.Salter (1992) and Fronde WEC . Representations of the geometries used are given in figure 4.15 and the geometrical parameters

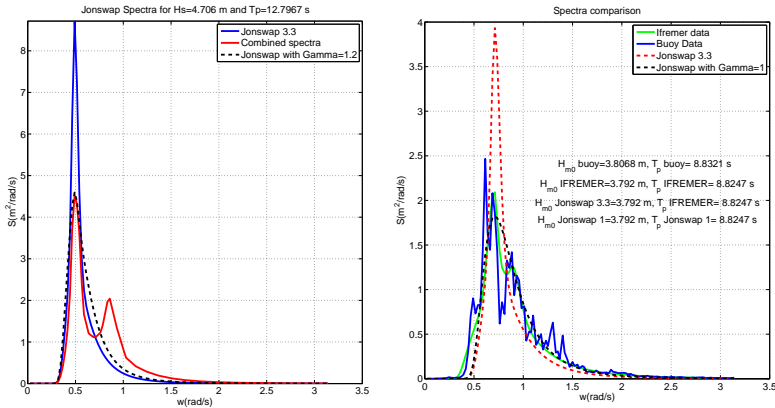


**Figure 4.14:** Example of the different data sets considered: on the right JONSWAP and IFREMER, on the left buoy data, IFREMER and both JONSWAPs for Bilbao

are summarized in Table 4.3.

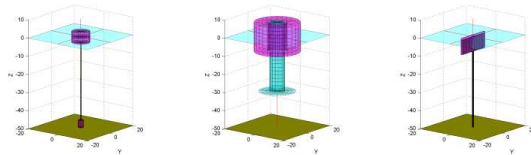


**Figure 4.15:** Simulated WECs, from right to left: one body heaving device, two body heaving device, deep water flap

In order to proceed with the simulation of these devices a frequency domain model was used. This model, which is further explained in Appendix 2, is common for the three devices but with certain specifications. The linear hydrodynamic properties of the three devices were calculated using Wamit(see DNV (2008)). The solution to the Radiation problem is presented in figure 4.16 and the solution to the diffraction problem is presented in Figure 4.17. In all three graphs the ordinate is normalized by dividing each curve by its maximum value, these maxima are presented in table 4.4.

The power take off machinery was represented by the power take off damping and spring matrices,  $b_{pto}$  and  $c_{pto}$  that are further explained on Appendix 2. For all three devices  $c_{pto}$  was set to zero, i.e. the power take off force was assumed to be purely linear damping with no spring component. The value of  $b_{pto}$  is calculated from  $b_{pto} = b \cdot \pi$  where  $b$  is a scalar damping coefficient and  $\pi$  is a pattern matrix. In our case  $b$  is a trial value supplied on each iteration by

WEC 1		WEC 2		WEC 3	
Diameter	10 m	Torus OC	25 m	Width	20 m
Draught	3 m	Torus ID	10 m	Draught	8 m
Freeboard	3 m	Torus draught	8 m	Thickness	0.7 m
		Column OD	8 m	Freeboard	1 m
		Plate OD	20 m		
		Column draught	30 m		
		Freeboard	8 m		

**Table 4.3:** Geometry Characteristics of the WECs selected for study

the optimization while the pattern matrix is a device specific constant. For WEC 1 and WEC 3 the power producing modes of motion coincide with the axis of the co-ordinate system so that by suppressing the non-power producing modes of motion the equations are reduced to a scalar equation and  $\pi = 1$ . For WEC 2 the power production is in relative heave, the equations are reduced to 2  $\times$  2 dimension (heave of body 1 and heave of body 2) and the PTO pattern matrix is set to

$$b_{pto} = \begin{bmatrix} 1 & -1 \\ -1 & 1 \end{bmatrix}; \quad (4.1)$$

The motion of each device was constrained using the methodology introduced in the previous section. The constraints for the each WEC are summarized in Table 4.5.

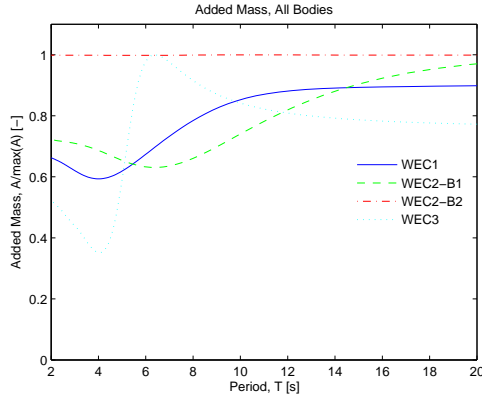


**Figure 4.16:** Added mass for all the devices, scale normalized, see table 4.5 for more information

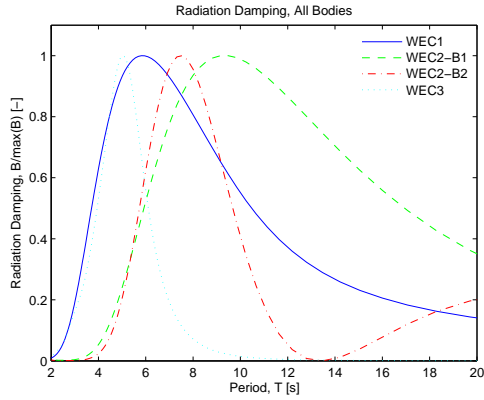


**Figure 4.17:** Radiation damping for all the devices, scale normalized, see table 4.5 for more information

	A	B	C
WEC1	$3.395 \times 10^5$	$7.627 \times 10^5$	$7.827 \times 10^5$
WEC2-B1	$3.464 \times 10^5$	$5.443 \times 10^5$	$4.108 \times 10^5$
WEC2-B2	$3.606 \times 10^5$	$2.95 \times 10^5$	$3.3954.987 \times 10^5$
WEC3	$3.790 \times 10^5$	$2.011 \times 10^5$	$3.3957.113 \times 10^5$

**Table 4.4:** Maximum values used to normalize previous curves

The power matrices that result from this calculation are given in 4.19. WEC 1 shows a low response in sea-states with peak periods below its natural period in heave and a wave follower behavior in sea states with peak periods above its natural period (wave follower means that amplitude and phase of body motion approach wave amplitude and phase). This behavior is consistent with the shape of the excitation force curve (see figure 4.18) and the arrangement of absolute PTO reference. WEC 2 shows a peak power absorption in sea states with peak periods of approximately 9 s with lower absorption at higher and lower periods. The peak at 9 s corresponds to the natural period of the device in the 'locked bodies' condition. The power increases with period up to this point and after this point the decrease in power is related to the decreasing phase angle of the relative heave motion of the two bodies in the device. At

	$x_{98\%}$	Units	Mode
WEC1	2	m	Heave
WEC2	4	m	Relative heave (B1-B2)
WEC3	0.3	m	Pitch

**Table 4.5:** Position constraints applied to damping optimization

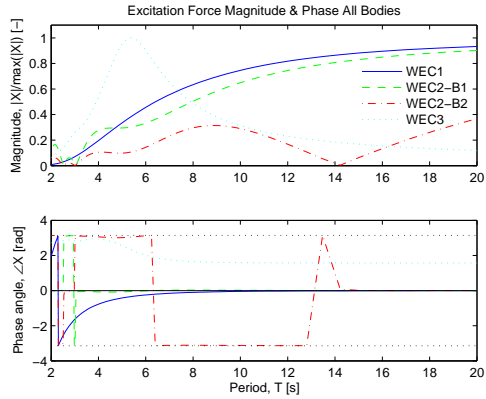


**Figure 4.18:** Excitation force transfer function for all devices. Magnitude is normalized see Table 2 for more information

very large periods the two bodies will move together as wave followers (motion amplitude and phase of each body approaching wave amplitude and phase). WEC 3 power peaks at sea-states with peak periods of about 6s. Unlike WEC 2 this peak is not related to the natural period of the device but to the wave forces which have a maximum in this period range. The natural period of the flap in pitch about an axis on the sea floor is in fact much longer than 6 s. The wave forces indicated for WEC 3 by the excitation and radiation damping curves in Figure 4.16 and Figure 4.17 peak at approximately 5 s.

It should be clarified that for the sake of simplicity only unidirectional waves have been considered in this study. The inclusion of a directional spreading functions will difficult the analysis and then it was decided to consider only unidirectional waves, although it is known that the directions of waves will heavily influence some devices (such as device 3). Then the influence of the wave direction within this methodology will be carried out in future research.

### 4.2.3 Methodology

#### Selection and interpolation methodology

As explained in the previous subsection the methodology used to obtain the long-term performance of a wave energy converter consists firstly of a sea state selection technique, secondly of calculation of power production in those selected sea states and thirdly of application of a non-linear interpolation using radial basis functions to give power estimates for any required sea state not limited to the selected sea states. The sea state selection technique is used to extract a representative subset of sea states from the database.

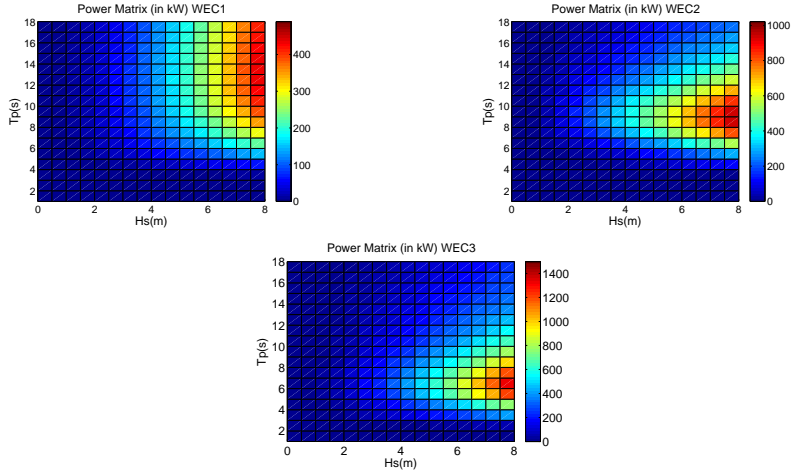


**Figure 4.19:** Power Matrices in kWh for the three studied devices

In the previous subsection the selection technique was applied over the parameters  $H_{m0}$  and  $T_p$  because in that section the spectra were assumed to be JONSWAP and 2 parameters were enough to characterize the sea states variability. For this subsection a selection approach based on three parameters is chosen due to the fact that the spectra are not single peaked and a parameter relating to the shape of the spectrum is needed. From Saulnier *et al.* (2011a) it was concluded that the broadness or bandwidth parameter  $\epsilon_0$  is well suited for the representation of the peakness and broadness of the spectrum. In Saulnier *et al.* (2011b) it was also found that the parameter  $\epsilon_0$  is strongly correlated with the device power and capture width.

$$\epsilon_0 = \sqrt{\frac{m_0 \cdot m_{-2}}{m_{-1}^2} - 1} \quad (4.2)$$

This parameter measures the peakness and broadness of the spectra. A set of real spectra from the Bilbao buoy set was analyzed. Each sea state was identified as single, double or triple peaked and the value of  $\epsilon_0$  was calculated for each sea state, the mean and standard deviation of  $\epsilon_0$  was calculated for each category of peakedness. In Figure 4.20 the wide columns give the mean values and the error bars give  $\pm$  standard deviation. It is evident that the single peaked sea states have a lower mean value of  $\epsilon_0$  and a much lower standard deviation.

For this study a sea state selection based on  $H_{m0}$ ,  $T_p$  and  $\epsilon_0$  was computed. The whole data set

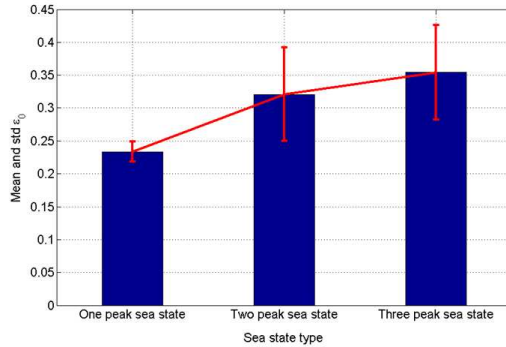


**Figure 4.20:** Mean and standard deviation of the  $\epsilon_0$  for the different number of peak sea states

used consisted of 58,460 sea states for the Ireland, Chile and Denmark locations and 9469 sea states for the Bilbao location (a reduced number of sea states were used for Bilbao to match the time period for which buoy measurements were available). In Figure 4.21 a selection of 100 sea states are represented over the whole set of sea states. The colorbar represents the value of the  $\epsilon_0$  parameter. As it can be seen this methodology selects the most different and distinct sea states with respect to the three chosen parameters  $H_{m0}$ ,  $T_p$  and  $\epsilon_0$ . In all the plots it could be seen how the sea states with higher  $\epsilon_0$  accumulates generally on the area with low wave height. This is due to the fact that combined sea states of swell and wind sea are correspond to sea states with low wave height and low period as suggested by Guedes-Soares (2001).

After the selection process, the power production of this selected sea states is computed with a numerical model (explained in Appendix 2) and then the whole series of power production is computed with a non-linear interpolation technique, as explained in the previous subsection. After this non-linear interpolation technique the power production time series along the time where the met-ocean conditions are known is computed. The results with the different data sets are explained in the next section.

### Simulation sets

One of aims of this section is to make a comparison between the power production computed using the full sea state time series data base and the power production obtained computing only a selected subset of sea states and interpolating the rest of the time series of sea states on this computed selected subset.

For Ireland, Chile and Denmark sites, power production of each device was calculated for the 58,640 sea states, assuming 2- a 3- parameter JONSWAP spectra. The same was done for Bilbao but using only 9,469 sea states for both the IFREMER and buoy data sets. This

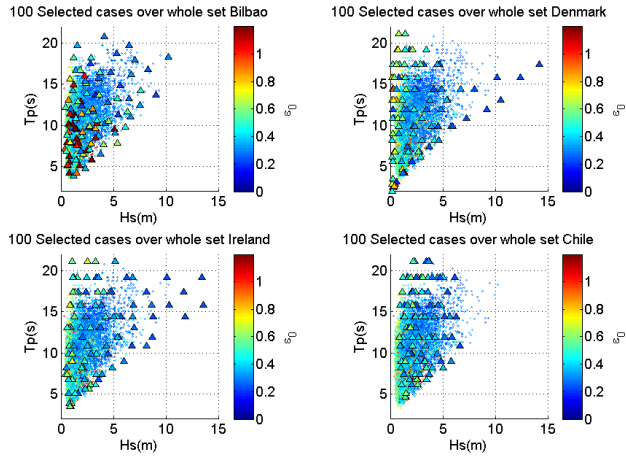


**Figure 4.21:** 100 sea states subsets over the whole sea states data series

exhaustive calculation of all sea states is regarded as the best possible estimate of power production of the selected devices from the given data and the quality of estimates based on selected subsets of sea states may be gauged by comparison.

Several subsets of the sea states of different sizes were evaluated, these were 100, 500, 1000 and 2000 sea states. Table 4.6 gives a summary of the combinations of devices, locations, sea state characterizations and sea state subset selection size that were evaluated. Ultimately, for the locations of Ireland, Chile, Denmark locations the annual energy yield for each device was assessed using 15 different wave resource descriptions (3 sea state characterizations x 5 sea state selected subsets) and for Bilbao the annual energy yield for each device was assessed using 20 different wave resource descriptions (4 sea state characterizations x 5 sea state selected subsets).

#### 4.2.4 Results

In section 4.2.4.1 and for the sake of simplicity, only results for the 20 Bilbao site power production computations will be presented. (four spectra types x five subset sizes). (buoy, IFREMER, JONSWAP  $\gamma = 3.3$  and JONSWAP  $\gamma$  best fit).

In section 4.2.4.2 the effect of sea state characterization (spectral shape and then the different data sources) on the power production of each device in each location is investigated by comparison of annual energy yield calculated from each sea state characterization. These two approaches were separated in order to evaluate the sources of error separately. In the first

Location	Database	Sea state characterization	Selection size
Ireland	Ifremer	IFREMER	All; 58640
Chile		JONSWAP	2000
Denmark		JONSWAP best $\gamma$	1000
			500
			100
Bilbao	Ifremer+ buoy	All buoy comp	All; 9469
		IFREMER	2000
		JONSWAP	1000
		JONSWAP best $\gamma$	500
			100

**Table 4.6:** Combination of parameters for simulation

section the goodness of the methodology will be probed. On the other hand on the second part, taking only the long subsets (9469 sea states for Bilbao and 58460 for the others) the influence of sea state characterization and the use of analytical spectra will be analyzed.

#### 4.2.4.1. Sea state by sea state analysis

In this first subsection the results of the long-term power production assessment with the different data sets proposed in the previous sections are presented. As explained on the previous subsection, the whole number of sea states is run for all the sets and also the cases with the selected sea states so as to compare the performance of the select-evaluate-interpolate methodology with the exhaustive evaluation. In Figure 4.22 the "best estimate" of power on the y axis (obtained from running the whole set of sea states) is plotted against an estimate of power reconstructed by interpolation between the 100 selected sea states for the Bilbao location for the buoy data. Here the power of the set of 9469 sea states for both real and reconstructed power are represented. In this case it can be seen that the correspondence between real and interpolated data is significantly obvious. The correlation coefficient is 0.98 and the scatter index is 0.02. The scatter index represents the spreading of the data with respect the real data. In this case tends to be very low, which means that the correspondence is excellent. It can be concluded that the proposed methodology of selecting a small data set of sea states (using the MaxDiss algorithm) and interpolating the full data set on this computed subset (using the RBF technique) reproduce with high reliability the long-term power production with very low computational effort.

Figure 4.23 shows the correlation coefficient of the power series obtained with the proposed methodology with respect to the real power obtained by the running of the whole set of sea states (9860 sea states). The different curves correspond to the four spectrum definition used: blue for the spectrum components obtained from the buoy data, red for the multiple spectra definition of IFREMER, green for JONSWAP 3.3 spectrum and pink for JONSWAP best gamma fit spectrum. Looking at the buoy and IFREMER correlation coefficients (blue and

red lines, respectively) it can be concluded that good results could be obtained using only three parameters to define the sea state ( $H_{m0}$ ,  $T_p$  and  $\epsilon_0$ ) and that a selection subset of sea states of 500 cases is enough for rebuilding the whole time series by interpolation (correlation coefficient  $>0.97$ ).

In the case of one-peaked spectra, green and pink lines of figure 4.23, the correlation coefficient do not increase as the size of the selected subset of sea states increase. This fact means that the selection is not appropriate for one-peaks spectra because the inclusion of the epsilon parameter within this cases masks the other important parameters (and the good selection). The epsilon parameter is good when dealing with real sea states of more than one peak because this parameter takes the broadness of the spectrum. However when dealing with analytical spectra of just one peak the parameter  $\epsilon_0$  is not appropriate for sea state selection. This is demonstrated with the dotted black line in the WEC 2 plot. This line corresponds to the JONSWAP 3.3 spectra but with the selection taking just into account  $H_s$  and  $T_p$  (as considered in the previous section for one peak spectra). As can be seen with this selection the validity of the comparison increases as the number of cases gets higher. Then, it is demonstrated that the MaxDiss selection procedure with 3 parameters is fine in order to represent real spectra of more than one peak. However when selecting the representative sea states of a one peaked sea spectra the selection process should be conducted with 2 parameters only.

When comparing the different WECs the WEC 1 is the WEC that gets higher  $r^2$  in all numbers of cases. This is due to the smooth slope of the power matrix. WEC 1 is a follower and the power matrix is quite smooth in the peak period axis as it does not achieve resonance. Then, it is logic that WEC 1 achieve the highest  $r^2$ .

WEC 2 and 3 they are both resonant WECs and the power matrix is sharp around the natural period of the device. WEC 3 has a slightly higher  $r^2$  due to the sea state selection. Bimodal sea spectra are found on the low period area, and then the selection of sea states with low periods (around 6 s) is abundant. As the WEC 3 is resonant around the area of low period, then the correlation is slightly higher.

However, it can be concluded from these previous figures that, the methodology works well for the different types of converters and for the various occurrence matrices and data type. It is concluded also that a lower number of sea states is needed in order to achieve good  $r^2$  for follower WECs. It should be noted how the sea state selection process works well for the real sea states with 3 spectrum parameters and how the representation of the spectrum variability is easily handled with this methodology. Furthermore, in general, with 500 cases the validity of the fit is very good and then the computational time is significantly reduced in order to obtain the whole power production on a long-term basis. For instance computing the power of the 500 selected sea states and doing also the non-linear interpolation lasted for 2 h while the whole set of 9469 sea states lasted for 1 day.

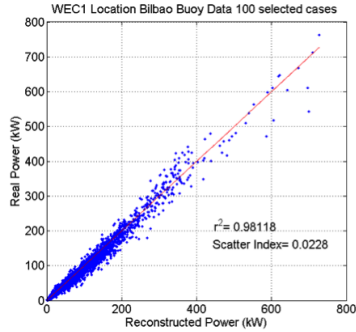


Figure 4.22: Real power on the whole set vs interpolated power based on the 100 selected sea states

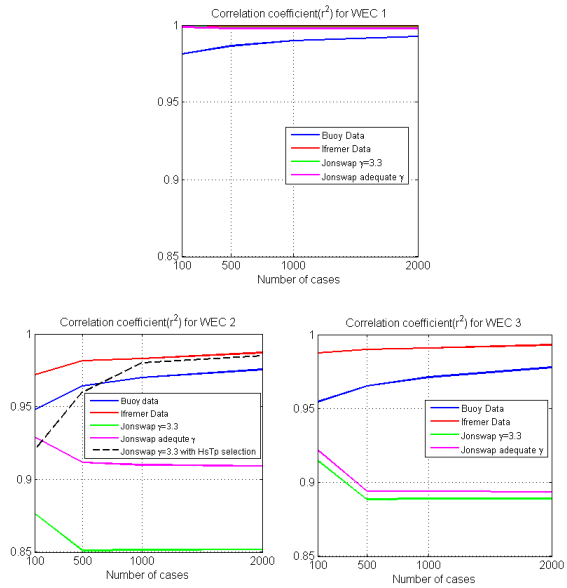


Figure 4.23: Correlation coefficient for the 3 WECs and all the data types at Bilbao

#### 4.2.4.2. Influence of sea state characterization on power production

One of the aims of this section was to demonstrate how the assumptions regarding the sea state spectrum characterization influence the power production. Then, four data sets (buoy, IFREMER, JONSWAP with gamma 3.3 and JONSWAP with best gamma fit) will be compared in terms of the power production. Firstly, they will be compared on a sea state by sea state basis and secondly the annual energy production for the different sets will be compared.

For this case a set of sea states with a combination between swell and wind sea has been selected. On Figure 4.24 the selected spectra for comparison are shown. On blue the IFREMER data is represented and the JONSWAP with the best gamma is represented by the pink. This set of spectra correspond to the location of Denmark and they are dated between the 12-3-1996 and the 15-3-1996. The data compared here are the IFREMER data base and the two JONSWAP approaches. As shown this period of time is a combination between swell+sea that starts with a more predominant swell, continuing with a more important wind sea and it finishes with a perfect wind sea.

The power production in this range of time was computed with the aforementioned sets and it is shown in Figure 4.25. The IFREMER data is illustrated in blue and in red there is the JONSWAP with gamma 3.3 and finally the power with the best gamma is shown in black. As seen in the figure the difference between the different series is higher on the first period of time. For WEC 1 the power obtained by the bimodal sea states is 14 kW and on the other side the power obtained by the JONSWAP spectra is 26 kW, this corresponds to a 85% of difference. This fact highlights the importance of taking into account bimodal sea states because the difference between considering real and analytical spectra is very high.

Analyzing the different WECs the higher differences appear on WEC 2, where the differences of the bimodal spectra (IFREMER) and the JONSWAP are up to 100%. The JONSWAP spectra overestimates the power production for the first and second WECs. When the sea states changes to one peaked sea states on the 15-3-1996 at 6 h the correlation between the different series is much better and the correspondence is much higher. In Figure 4.24 the capture width ratio of the three WECs is represented for the 3 different spectral types considered. The capture width ratio represents an efficiency of the power conversion with respect the incident wave resource. It is calculated according to the next formulae:

$$CWR(\%) = \frac{\text{Power absorbed by the device (kW)}}{(\text{Wave Resource (kW/m)} * \text{Device working dimension (m)})} \quad (4.3)$$

In the figure 4.26, the IFREMER spectra are represented with blue dots and the JONSWAP with gamma 3.3 and gamma best fit with red and green dots respectively. As seen the bimodal spectra have values of the broadness between 0.2 and 0.7. However the JONSWAP spectra have very

low values (around 0.2). The fact that the highest points where capture width is higher or lower also correspond to low and high values of the  $\epsilon_0$  parameter, that cannot be approximated by the JONSWAP spectra and then the CWR is infra-estimated or overestimated in this cases.

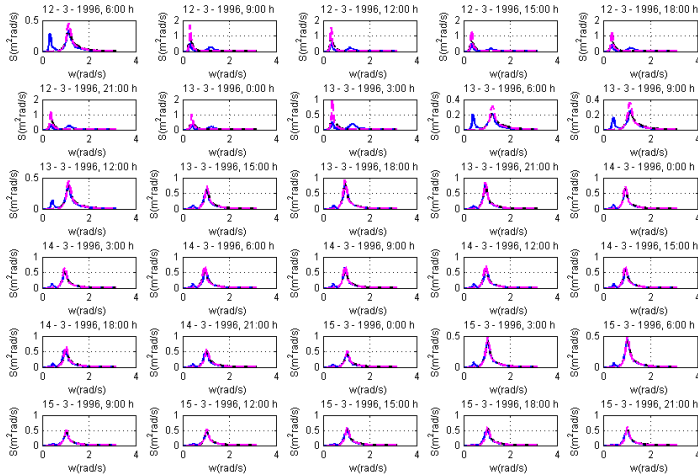


**Figure 4.24:** Set of consecutive sea states selected for analysis in Denmark, in blue the IFREMER data, in pink JONSWAP

It is also important to highlight how the blue data points from IFREMER data base have a descending tendency as the  $\epsilon_0$  increases for all the WECs. It means that as the spectrum gets broader the efficiency of the conversion is lower. This fact makes sense because generally the converters are designed to work well in an area of a specific period and when the spectrum is broader the converter is not able to capture all the energy of the spectrum. Also, if the three plots are compared it can be seen that WEC 1 has an approximate slope of -11, the WEC 2 -104 and the WEC 3 a -66.6. It is concluded that the influence of the broadness of the spectrum has a higher influence on the resonant converters (WEC 2 and 3) than in the follower converter (WEC 1). This is expected as the follower converter has a similar performance on a large range of periods and on the other hand the resonant converters have a much narrower performance for frequency band of good performance.

From this point the comparison is made for the four locations, plotting the concordance of all the series in Figure 4.27, the IFREMER data base (on the x axis) and the JONSWAP with  $\gamma = 3.3$  are plotted. The colorbar represent the broadness of the sea state that corresponds to the

power represented with the dots. As seen Denmark is the location where the correlations are the lowest for all the devices (the r-squared parameter is 0.99, 0.87 and 0.71 for WEC 1, WEC 2 and WEC 3) respectively. This result was expected as Denmark was demonstrated to have just 40% of one-peaked sea states. Also the way the points that are further from the bisectrix are the ones with higher 0 can be noted. This is also expected as the broader the spectrum the larger the error when assuming analytical spectra. It can be also highlighted that the WEC with lower correlations is WEC 3 (as well as WEC 2) because they both have a peaky response and then it is more affected by the spectrum broadness. Also, WEC 3 correlation is little but lower than WEC 2 because WEC 3 is tuned for a period near 6 s and the broadest spectra are usually found in this area (see Figure 10). Also in terms of WECs, the WEC 1 is the one with highest correlation for all the locations. As previously explained, this is also coherent as WEC 1 is a follower and then its performance is less dependent on the spectrum shape.

From these plots it could be concluded that the influence of using standard unimodal spectra to describe real sea states, that are normally much broader or even bi- or multimodal, when calculating the power production is very high. When assuming an analytical spectrum for a bimodal spectrum the error is large on instantaneous terms and the power production could be over or infra estimated on a 200%. The parameters  $H_s$  and  $T_p$  are demonstrated to be insufficient to represent two peaked spectrums. These types of spectra should be considered in power assessment and more parameters, such as the ones proposed by Guedes-Soares (2001) (Intermodal distance and the sea-swell energy ratio)

In addition, the capture width ratio is not well estimated assuming one peaked spectra. A clear tendency is found, then the highest the spectrum broadness the lowest the efficiency of the conversion, however this tendency is not captured with one peak spectra and then it is over estimated.

The influence of the groupiness of the spectra on the power production on an instantaneous basis has been investigated in the previous explanations. One of the objectives of this section is estimating the influence of these assumptions on the classical method of power assessment for the annual energy production. The classical method of power assessment consist on the multiplication of the power matrix (kWh) by the occurrence matrix (in percentage) assuming analytical spectra for the representative sea states on the power matrix. As demonstrated in the last paragraphs only between 30% and 60% of the real states fit with these analytical shapes and then the real power production is not accurately estimated with the classical power production assessment.

From now on, the influence of these hypothesis on the Annual energy production are investigated. Therefore four approaches are compared: 1) the classical method of multiplying the power matrix by the occurrence matrix, 2) the computations of the whole series of sea states (9469 sea states for Bilbao and 58460 for the other sites) with the IFREMER data base (taking into account smoothed bi and tri modal spectra as well)3) and the JONSWAPs with  $\gamma = 3.3$  and

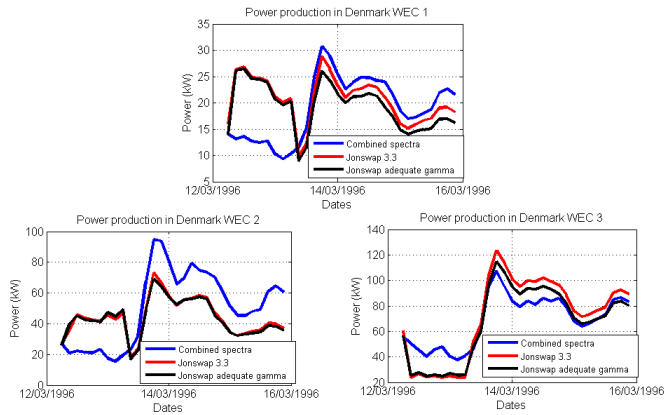


Figure 4.25: Estimated harvest power with the 3 different WECs on the set of spectra selected on Figure 4.24

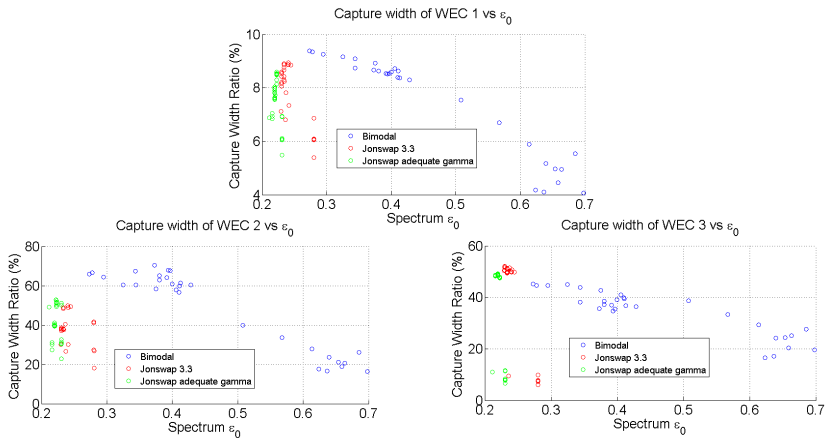
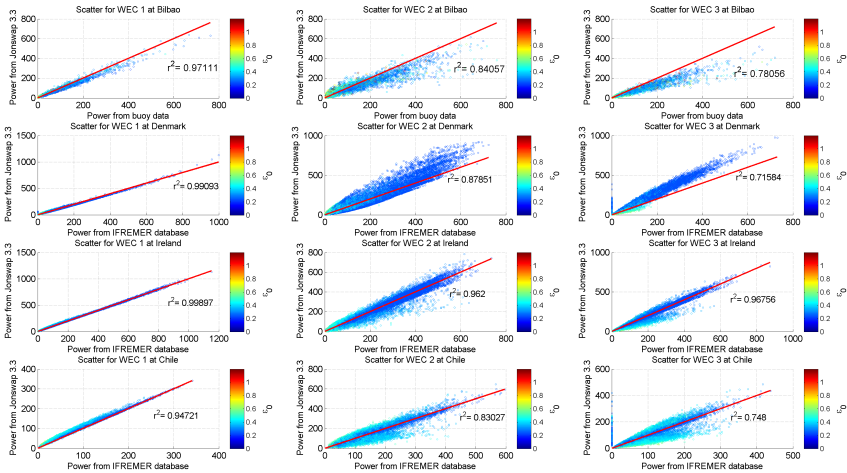


Figure 4.26: Capture width ratio vs Spectrum broadness for the selected spectra on Figure 4.24

4) the best  $\gamma$  fit. The annual energy production for each alternative is represented on Figure 4.28. As expected the highest power production on the three WECs corresponds to Ireland. The lowest power production corresponds to Denmark for the WEC1 and WEC2 . However for the WEC3 case the lowest power production corresponds to Chile because it is tuned with



**Figure 4.27:** Scatter of the power estimated with JONSWAP vs Power estimated with IFREMER data

a climate that is close to the site of Denmark. The differences on the results of the AEP for the different methods are shown in a percentage from in Table 4.7. It should be noted that the percentages are calculated against the most exact case for each location. Then, in Bilbao the percentages are calculated against the buoy data and in the rest of locations the percentages are calculated against the IFREMER data. As shown the highest differences exist on the site of Denmark. This is due to the fact that Denmark is the location with the highest percentage of more than one peak sea states (nearly 60%). Also the differences are higher for the WEC 3 in the Denmark site. This WEC is tuned to a period near the 6 s which is the most probable on this site and also the most probable for the sea states of more than one peak and then this differences are expected. For WEC 3 in the location of Denmark the JONSWAP spectrum overestimate the mean annual power production on a 30%.

With respect to the rest of WECs and locations for the location of Denmark the WEC 1 and WEC 2 power production are underestimated with the JONSWAP spectra. This is due to the fact that on this location the selected sea states are found on the low periods section and this WECs are either tuned for a higher period (WEC2) or do not have a resonance period (WEC1). For the rest locations, Ireland is the site where the differences are lower. This is due to the fact that the percentage of more than one peak sea states is lower. Also the difference of the power matrix method with the rest approaches should be highlighted. As seen in all the cases, the

highest differences corresponds to Bilbao, where it is compared with real data. The difference goes from -23% for WEC 1 to -32% in WEC 2 and also -44% for the WEC 3. The highest difference correspond to the WEC 3 because its power matrix peak is on the 6 s area, and the most of one peak spectra are also located around this area.

In the other power matrix cases the differences are found on a range of -13% to -7%. The differences are also high in the Ireland case. This is due to the fact that the Ireland occurrence matrix is very broad, and then in order to get a better definition a smaller cell range would be needed. It should be noted that these differences of the annual energy production are very high, and then this uncertainty should be taken into account when analyzing the techno-economic viability of a device. The power matrix has been demonstrated to be a quick and simple method to obtain the Annual Energy Production, however, as demonstrated here it is partially inaccurate and then, more accurate methods such as the methodology presented beforehand are required. With respect the IFREMER case, as it is taken as the most exact for Denmark, Chile and Ireland the comparison is only valid for the Bilbao case. As shown in Figure 4.28 and table 4.7, the error percentages goes from 9% to 13 %, that are quite low compared with the power matrix ones. Then, it could be concluded that the IFREMER data base could be taken as basis in order to obtain the AEP, as it contents realistic sea states.

Both the JONSWAP with  $\gamma = 3.3$  and JONSWAP with the best  $\gamma$  fit generally have a better approximation to the exact Annual Energy Production than the power matrix method. The highest overestimation with these 2 approaches correspond to Denmark with the WEC 3 case. As previously explained this WEC has a peak on the 6 s area and then as this is the most probable period in Denmark the overestimation is very important. Among the other WECs, the underestimation is lower for the WEC 1 case, as it works as a follower and its power matrix is smoother.

When comparing different types of devices one important parameter is the capture width ratio, that measures the efficiency of the conversion with respect the incident resource (see equation 4.3).

Figure 4.29 shows the average resource in the four locations analysed using the aforementioned four spectral definition methods: 1) spectral components obtained by Bilbao buoy (only for Bilbao site), 2) multimodal spectra obtained from the IFREMER data base, 3) unimodal JONSWAP 3.3 spectra fitted to the IFREMER data and 4) unimodal JONSWAP best gamma fitted to the IFREMER data. As can be seen in the figure, for Denmark, Ireland and Chile the wave resource is heavily over-estimated by the JONSWAP spectra. On average, the wave energy resource is overestimated on a 30% using a JONSWAP with  $\gamma = 3.3$ . Also, as seen, the other JONSWAP approximation (with an adequate  $\gamma$  fit) has a lower underestimation of the resource (around 20%). For the Bilbao location (that is the only one with buoy data) the resource is underestimated with the buoy, IFREMER and the JONSWAP data. This could be due to the fact that the buoy point does not coincide exactly with the IFREMER point. In all

	Locations	Buoy Data	Ifremer data	Power Matrix (with JONSWAP $\gamma = 3.3$ )	JONSWAP $\gamma = 3.3$	JONSWAP best $\gamma$
WEC 1	Bilbao	Exact case	-12%	-23%	-5%	-8%
	Denmark		Exact case	-13%	-6%	-14%
	Ireland		Exact case	-17%	1%	-2%
	Chile		Exact case	-7%	12%	9%
WEC 2	Bilbao	Exact case	-9%	-32%	-11%	-8%
	Denmark		Exact case	-13%	-8%	-16.5%
	Ireland		Exact case	-13%	-2%	5%
	Chile		Exact case	-10%	-6%	18.2%
WEC 3	Bilbao	Exact case	-13%	-44%	-26%	-20%
	Denmark		Exact case	-14%	31%	30%
	Ireland		Exact case	-16%	-2%	13%
	Chile		Exact case	-16%	-2%	12%

**Table 4.7:** Errors with the different data sources. Note: the errors are computed with respect the Exact case for each option

locations, the JONSWAP with the best gamma fit approach better the reference Annual Energy Production with the relative differences depending on the proportion of unimodal spectra in the site, being the lowest at Bilbao site (highest proportion of unimodal spectra) and the highest at the Denmark site (lowest proportion of unimodal spectra).

In Figure 4.30 the Capture width ratio is represented for all the computation methodologies. It should be pointed out that on the capture width estimation both the power production errors and the resource are mixed and then the comparison between the different sources is expected to be worse.

On average terms the WEC 1 has a CWR around 8%. It is quite low due to the fact that is a follower and as it is not designed to resonate their performance is low. For the second converter their average CWR goes to 60%, that is quite high due to its resonance. However it is suspected that this CWR is overestimated due to the fact that the model used for this computation is linear. In reality, this type converter would have a lower performance. For the WEC 3, its average CWR goes to 25%, which is standard on these type of devices.

With respect to the comparisons between the different CWR for the different type of data it can be seen how the JONSWAP spectra underestimate heavily the average CWR. This fact is coherent as in general the power production is underestimated by the JONSWAP and the resource is heavily overestimated. Then, the CWR is heavily underestimated by the JONSWAP series. The highest differences correspond to Denmark, which is, as specified before the location with the highest occurrence of bi and tri-peaked sea spectra.

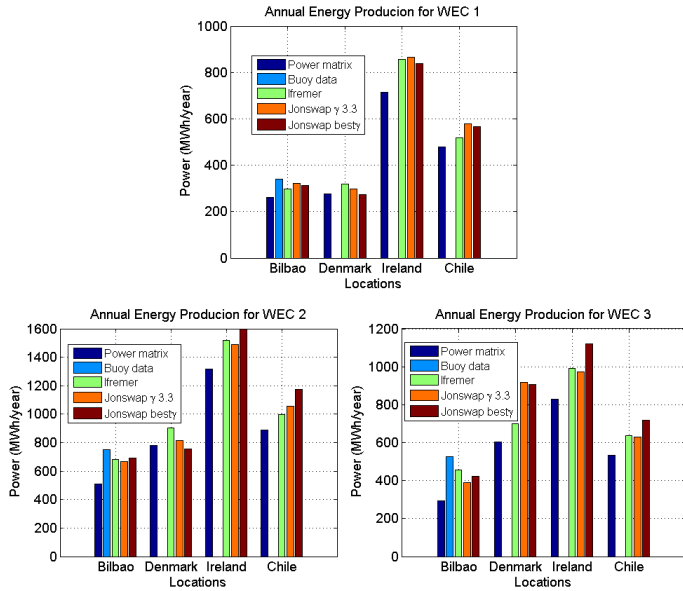


Figure 4.28: Annual Energy production (MWh/year) estimated with the classical method as well as the different sea state data sources outlined

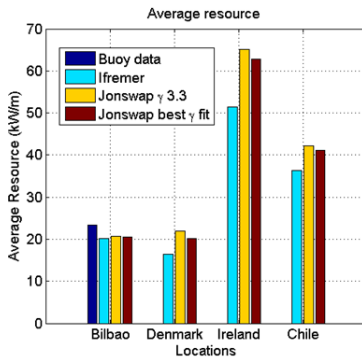


Figure 4.29: Resource estimation(kW/m) with the different sources of sea states data

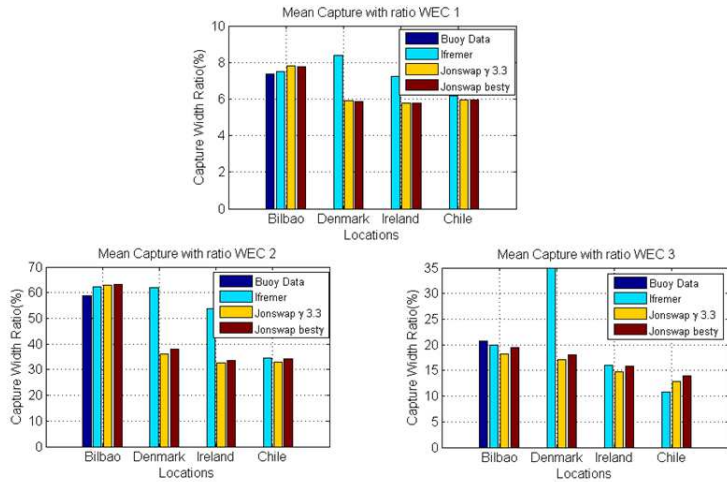


Figure 4.30: Capture width ratio (%) estimation with the different data sources

### 4.3 Conclusions

In this chapter, firstly a new computationally efficient methodology for estimating the long term power performance of a wave energy converter on a particular location having a long met-ocean series have been developed and validated. This methodology uses a sea state selection technique in order to select the most distinct and representative sea states from a sea state spectral long term time series. These selected sea states are the input for a numerical model and the power production for the cases is assessed. Afterwards a non-linear interpolation technique (RBF functions) is used in order to reconstruct the whole power production series along the met-ocean data series. In the first part of this chapter the methodology was validated for a specific converter in a particular location.

In the second part of this chapter, the influence of several factors on the aforementioned methodology has been investigated. In this work three types of WECs, a one body heaving converter (follower), a two body heaving converter (resonant) and a deep water flap have been investigated. Regarding the locations 4 different locations with different occurrence matrix and sea-states distribution characteristics were assessed (Bilbao- North of Spain, West of Denmark, West of Ireland and Chile). A set of simulations was run in order to investigate the influence of these factors on the methodology.

The methodology was found to work well with the different types of WECs, locations and types of data. It was concluded to work more accurately with non-resonant converter (such as

WEC 3), as its response is uniform for all wave frequencies, so a smaller subset of sea states are necessary to attain good results. With respect the data types a selection based on  $H_{m0}, T_p$  and  $\varepsilon_0$  was found to be very efficient for the real spectra with more than 1 peak. However for the JONSWAP cases a selection based on two parameters  $H_{m0}$  and  $T_p$  was found to be enough because the  $\varepsilon_0$  masked the variability of the data (as all of them were one-peaked spectra).

On the other hand, in this chapter the influence of the real spectra in contrast to the analytical ones (JONSWAP), was also investigated. On sea state by sea state basis the differences were very high (+/-200%). Also the inaccuracy of the classical method of computing the Annual Energy Production was investigated on this thesis. This approach was compared with the computation of Annual Energy production with buoy data, multi-component spectral data (IFREMER) and JONSWAP fit. The power matrix method was found to underestimate the Annual Energy Production on all the locations from -45% to -7%. Also the effect of the theoretical spectrum used to define the sea states was investigated. In the case of using unimodal spectra as JONSWAP, the underestimation of the Annual Energy Production was between -20% and -5%, depending on the site. The critical location for this comparison was found to be Denmark, as the percentage of one peaked sea states is just 40 %. The classical power matrix method was found to be very inaccurate on this kind of locations.

Also the resource estimation with different spectral data sources was investigated in this research. The assumption of JONSWAP spectra for an specific  $H_{m0}, T_p$  set took to an overestimation of the resource of a 30% in all the locations. Besides, the CWR estimation was found to be very inaccurate due to the errors on the resource and the power production. In all the locations an infra-estimation was carried by the JONSWAP approaches.

To sum up, the classical method of power production assessment was found to be very inaccurate in those area with high percentage of multimodal spectra (combined SEA and SWELL sea states). In this case, the use of multimodal theoretical spectra or the measured/computed spectrum components is recommended.

# Influence of met-ocean conditions on wave energy converters design and operation

---

## 5.1 Introduction

In this section the influence of wave climate on the behavior of Wave Energy Converters is studied. The order of the subsections on this chapter follows the design/operation process of a wave energy converter.

- First, the design process of a wave energy converter regarding the tuning/matching strategy is explained. The premise of matching the natural period of the converter with the most probable wave period is further investigated and some rules of thumb are provided.
- Secondly, once the converter is designed and it is operating at open sea conditions the Operation and Maintenance issues become important. Availability and accessibility parameters will be studied around the world coast's and the cost of O&M are detailed for different locations.
- Thirdly, a failure assessment is performed and some recommendations regarding the deployment location as a function of the converter reliability level are given.
- Lastly, as the converters are expected to be deployed in an array, the factors that affect array layout are analyzed. Optimum configurations depending on the local wave climate are studied.

Due to the contrast among the different sub-section in this chapter, every subsection will have an introduction in order to explain the state of the art on wave energy on this particular sub-topic and also some conclusions are given for each subsection.

## 5.2 WEC Design approach: adaptability of a WEC to different weather scenarios

### 5.2.1 Introduction

By contrast to wind energy, an abundance of technologies exist in the wave energy sector, and a dominant technology has not emerged. Many developers are testing inventions and simultaneously optimizing the power absorption characteristics to achieve commercial prototypes. Nevertheless, uncertainty remains for this topic, and it is not clear yet if the solutions could be either global or site-specific.

In the optimization process, a key parameter is the wave power absorbed by the device. To maximize the Wave Energy Converter (WEC) power absorption, the local wave climate must be considered. The main assumption for the optimization scheme is that the maximum annual power absorption is obtained when the WEC natural period matches the most probable wave period at the point of interest (see Goggins and Finnegan (2014)).

Extensive research investigating the optimization and tuning of wave energy converters has been performed in recent years. For instance, two main methods for tuning a device were previously studied: geometry tuning (which affects the natural period of the device) and the Power Take Off (PTO) control (which has the ability to alter the absorption characteristics over time) Price *et al.* (2009). A previous study investigated the geometry tuning procedure; Flocard and Finnigan (2012) tuned a bottom hinged flap to the prevailing wave frequency by experimenting with modifying the inertia. The sensitivity of the resonant frequency to slight changes in the geometry was analyzed using a new numerical model Renzi and Dias (2012). Finally, a procedure for optimizing the geometries of a generic heaving wave energy converter was presented by Gilloteaux and Ringwood (2010). One of the latest pieces of work on this topic corresponds to Goggins and Finnegan (2014). They implemented/studied an algorithm in order to design geometrically a WEC depending on the most probable spectrum on each location. All these investigations demonstrated that optimizing the geometry of the tuning process is a key step in maximizing the power absorption of any WEC.

The annual power production of a WEC depends on the local wave climate and the power matrix of the WEC. As indicated above, the hypothesis for power production maximization is to match the most probable sea states with higher production in the power matrix. This matching is achieved by tuning the resonant frequency of the WEC with the most probable sea state frequency.

Apart from tuning the resonant frequency of the WEC with the most probable frequency, the shape and characteristics of the power matrix also greatly influence the performance of a WEC at a given location. Different types of WECs were studied Babarit *et al.* (2012), and the displayed differences on power matrices resulting from the WEC type depended on the

absorption principle and the geometry of the converter.

Therefore, in the design and optimization of a WEC, the met-ocean conditions of the potential deployment sites must be considered. To maximize the potential economic revenue, WECs should be able to be deployed in as many locations as possible. Each site has different met-ocean conditions; therefore, maximizing the number of potential deployment sites (varying the power characteristics of the device and adapting them to the different local wave conditions) may be attained through geometrically tuning WECs.

Globally, wave climate conditions are highly variable, and wave parameters (i.e., significant wave height,  $H_s$ , and peak period,  $T_p$ ) have different values depending on the location. To date, no study has investigated the best adaptability strategy of WECs to different ocean climate scenarios. Whether a unique solution for all locations or a customizable design (variable depending on the location) is appropriate has not been addressed. Currently, no analysis is available investigating which of the following methods is economically favorable: 1) developing WECs tuned for each location, 2) deploying unique broadband WEC that are valid for a high number of locations or 3) implementing site-tunable WECs.

This section investigates the geometric adaptation of a generic WEC to different global climate scenarios. Two non-adaptive solutions and a customizable solution (variable resonant characteristics) are globally tested to analyze the improvements in power production resulting from the tuning mechanism. Performance is assessed based on two parameters: the capture width ratio (CWR) and the kW/Ton indicator.

### **5.2.2 Climate data**

A global climate database is required to analyze WEC power production in global terms. In this study, a global wave reanalysis database is used (GOW1.0) Reguero *et al.* (2012) Espejo (2011). GOW 1.0 is based on a NCEP/NCAR atmospheric forcing reanalysis, see Kalnay *et al.* (1996), which constitutes one of the longest and most up-to-date global re-analyses. This database provides spectral sea-state parameters (significant wave height ( $H_s$ ), mean period ( $T_m$ ), peak period ( $T_p$ ) and mean direction ( $\theta_m$ ) and directional spectra components,  $S(f, \theta)$ , along the coast. GOW 1.0 covers the period 1948-2008 at a  $1^\circ \times 1.5^\circ$  global resolution. This database has been globally calibrated with satellite data and validated with buoy data.

In this study, the following three sea state parameters are used:

- Significant or zero moment wave height ( $H_s$ ).  $H_s$  is notable because the wave energy is related to the square of the wave height.  $H_s$  is also important in terms of WEC survivability because WECs must be designed to survive extreme conditions.
- Mean Wave incident direction ( $\theta$ ). The performance of several WECs depends on the wave direction, and the performance of wave energy farms also depends on the spatial distribution of WECs relative to wave direction.

- Peak period ( $T_p$ ). The performance of the floating WECs depends on the matching the wave period of the incoming waves with the natural period of the floating device.

Although all of these variables are important and necessary in the study of wave energy converters, the direction and wave height are not key variables regarding the tunability of a wave energy converter. The peak period will be the key parameter investigated in this study.

The GOW database offers global information. WEC farms will be first deployed on continental shelves away from the breaking zone. For this study, 1188 GOW 1.0 nodes located between 50 and 100 m of water depth around global coastlines have been selected. In this analysis, the prospective wave energy farm is assumed to be deployed in deep water (>50 m), consequently the GOW database can be used without further propagation modeling. Although some shoaling and refraction effects might be noticed by some large period waves, these effects are neglected in this work and for the sake of simplicity the propagations effects are not considered.

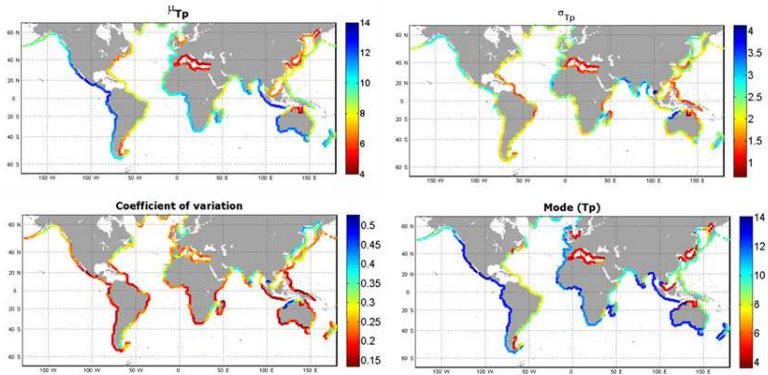


**Figure 5.1:** Mean  $T_p$ (s), standard deviation of  $T_p$ (s), coefficient of variation of  $T_p$  and mode of  $T_p$  (s)

Figure 5.1 shows several statistical parameters used to characterize the  $T_p$  of the selected nodes. The upper left panel shows the average peak period,  $T_p$ . Globally, the variability of  $T_p$  is high. The lowest values of  $T_p$  (less than 5 s) are found in enclosed seas (i.e., the Mediterranean) that are dominated by low fetch SEA waves; whereas the highest values (higher than 12 s) are found along coasts that are dominated mainly by SWELL waves (Indian Sea Indonesia; Pacific Central America) or by highly developed SEAS (Southwest Australia). Intermediate to low values (between 6 and 9 s) are found in the east-oriented oceanic coasts that are attacked primarily by long fetch SEA waves (Atlantic North and South America; Pacific Japan, New Guinea and Australia). Finally, medium to high periods (between 9 and 12 s) are encountered on west-oriented oceanic coasts attacked by SEA and SWELL waves (Atlantic Europe and

Africa; Pacific North America and Southern Chile).

The upper right and the lower left panels of figure 1 show the standard deviation,  $T_p$ , and the coefficient of variation of the peak periods, respectively. Both parameters are relevant in the understanding of the variability in the peak period parameter and the shape of the distribution. The lowest values,  $CV=0.2$ , correspond to those south- and west-oriented coastlines that are governed by constant SEAs or SWELLs and are exposed to the southern Pacific waves generated by the roaring forties or in those eastern-oriented Atlantic, Indian and Pacific coasts submitted to the developed SEAs generated by the trade winds. Intermediate CV values between 0.2 and 0.4 correspond to of the majority of the remaining coastline. These values indicate that the variability of the peak period is higher in these areas, and although tuning of a WEC is possible, the influence of the wave period on WEC design is higher and should be considered. The highest values,  $CV>0.4$ , are found in enclosed seas (i.e., the Timor Sea coast in northwest Australia), along which the SEAs display a higher rate of variability.

Finally, the bottom right panel of figure 5.1 shows the modal value of the peak period. Comparing this panel with the mean  $T_p$ , the modal value of  $T_p$  is higher than the mean globally, indicating a positive skewness of the  $T_p$  distribution (a longer upper tail than the lower tail).

Spectral parameters in the database can be used to compute the global energy resource in deep waters (assuming seas have a Pierson-Moskowitz spectrum with  $T_p \simeq 1.4T_z$ ) by using the International Energy Agency's formula for the sea state mean energy flux:

$$F_e \approx 577 \cdot H_s^2 \cdot T_z \approx 412 \cdot H_s^2 \cdot T_p \quad (5.1)$$

Figure 5.2 shows the average, the standard deviation, and the coefficient of variation, of the wave energy flux,  $F_e$  (kW/m). The variability in the wave energy resource is high around the globe. The areas with the highest energy resource (60-80 kW/m) correspond to the high latitudes (Northwest Europe, Northwest America and the Southwest portion of America, Africa and Australia). The tropical and subtropical areas have lower power resources and the lowest variations. The coefficients of variation in the high latitudes of the Northern hemisphere and in the enclosed seas show the highest variability.

### 5.2.3 WEC Characteristics

The selected WEC resembles the Wavestar prototype, see Steenstrup (2006), consisting of a central body that is fixed or floating and a series of floaters on both sides of the central body (figure 5.3). These floats are connected to the main body with arms and are allowed to move only in heaving motions. A hydraulic piston acts on the arms to transfer the motion of the floaters into mechanical energy. The main difference with the Wavestar prototype is that the motion is not circular and the floaters are assumed to only move in heaving motions. To simplify

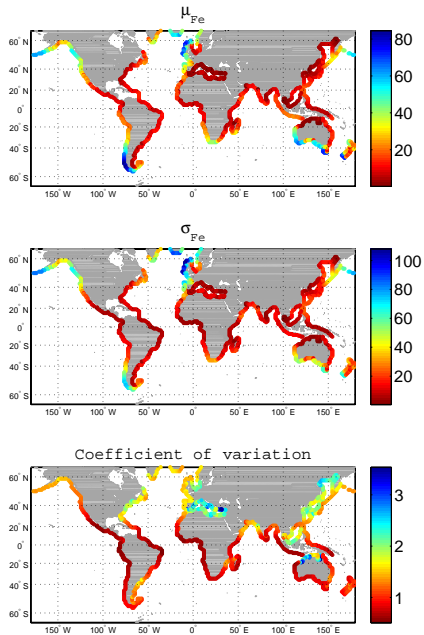


**Figure 5.2:** Average (kW/m), standard deviation (kW/m) and coefficient of variation of wave energy resources

the analysis and the tuning process of the floats, a set of cylinders is selected for this study. This simple design was selected to easily tune structures because the objective of this chapter does not include studying the feasibility or behavior of this design.

This prototype was simulated with a frequency domain model further explained on Appendix 2. This numerical model was based on Falnes (2002). The power matrix of a device can be built based on the results of irregular sea states on this numerical model applying the optimum PTO Constant for each sea state. The optimum PTO constant means the constant that leads to the highest energy harvest during a sea state (normally it is found in an optimization loop).

Three geometric options are analyzed. First, floaters with a heave natural frequency of 4 s that are near resonance for small enclosed seas and will behave as wave followers for larger wave periods; second, floaters with 8 s natural frequency (matching the most probable periods in North Atlantic waters); and third, a tunable converter, designed to resonate at 4, 6, 8, 10 and 12 s. Each of the sub-options are applied for the most probable period of each location to match the converter with the local met-ocean conditions for each site.

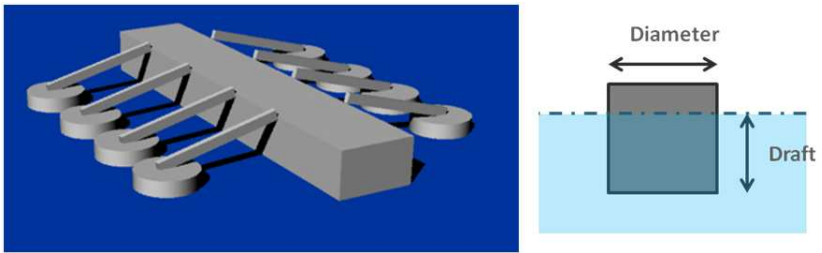


**Figure 5.3:** Set of floaters analysed as a converter

For this stage of research, a cylinder is then selected with a height equal to its diameter. The dimensions of the cylinders change for each option. Different draft/diameter ratios may lead to "lighter" structures; in this study, however, this ratio has been kept constant for the sake of simplicity and to limit the number of options. As expected, the natural period increases with the dimensions of the cylinder. Consequently, larger structures with a high draft are used when a high natural period is required. Table 1 presents a summary of the main parameters considered in this analysis.

In this research, it is assumed that waves propagate always with their fronts perpendicular to the line of floats (head seas) so wave direction is a constant. Floats are separated by  $1.5 D$  ( $D$ : Diameter), and the two rows of floats are separated by  $5 D$ . A BEM software by HydroD (DNV) frequency domain numerical model is used for this analysis: see DNV (2008). This DNV program provides the coefficients required to perform the frequency domain analysis and to construct the power matrices (for details see Appendix 2). The central body that supports the

## 5.2. WEC Design approach: adaptability of a WEC to different weather scenarios 92

cylinders is assumed to be fixed and emerged, so only the cylinders interact with the waves.

Characteristics	Option 1	Option 2	Option 3				
			4 s	6 s	8 s	10 s	12 s
Natural Period	4 s	8 s	4 s	6 s	8 s	10 s	12 s
Diameter of the float	4 m	15 m	4 m	8 m	15 m	20 m	28 m
Draft	3.5 m	14 m	3.5 m	8 m	14 m	19 m	27 m
Mass	38 Ton	2170 Ton	38 Ton	308 Ton	2170 Ton	6100 Ton	16308 Ton

**Table 5.1:** Characteristics of the proposed options

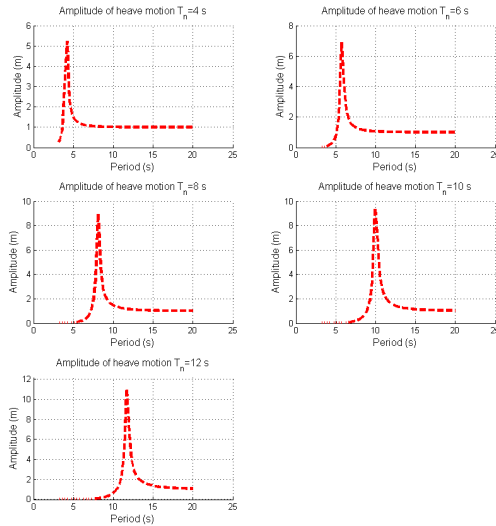


**Figure 5.4:** Response amplitude operator of the individual floats for the proposed converters

Figure 5.4 shows the response amplitude operator (RAO) for all considered floats. Although these figures show the heave behavior of the individual floats, the computation of the power matrices considers the interaction between floats.

Using the previously mentioned frequency domain model and further detailed on Appendix 2, the power matrix of each option is calculated. This power matrix has been obtained using the PTO damping constant that maximizes the extracted power for each period. To do that, a sweep of PTO damping constants is carried out for each period. Figure 5.5 shows the WEC power absorption in terms of the damping constant of an 8 s converter for regular waves with period

10.5 s. A maximum power production is achieved for a PTO constant of  $1.2 \times 10^6$  Nm/s. The observed motion amplitude at the optimum damping value is 0.9 m. This procedure is replicated for every period to obtain each individual optimum PTO constant (figure 5.7). Because a linear theory is applied, the optimum PTO constant does not depend on the incident wave amplitude.

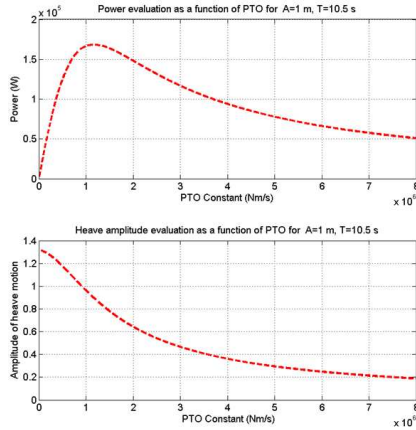


**Figure 5.5:** Power and amplitude of motion as a function of the PTO constant for the 8 s converter (individual float), for the 10.5 s wave period

After calculating the optimum damping constant, the power matrices of all geometries are computed. These values are calculated by applying the optimum damping that corresponds to a period equal to the peak period assigned to the bin of the  $H_s-T_p$  matrix. Figure 5.7 shows the power matrices that are obtained without any restriction in terms of nominal power or maximum vertical motion. Although figures 5 and 6 are shown for a single cylinder, the power matrices displayed in figure 5.7 are obtained by considering the interaction between cylinders.

Each matrix shows a peak in power production in the corresponding natural period. For each power matrix, the power production reaches a minimum for periods lower than the natural period. This result also coincides with the trends displayed in figures 5.4 and 5.6. However, as the dimensions of the cylinders increase, the power production increases. In the next section, the results are computed in terms of capture width ratio to avoid the influence of the diameter of the cylinder on power performance.

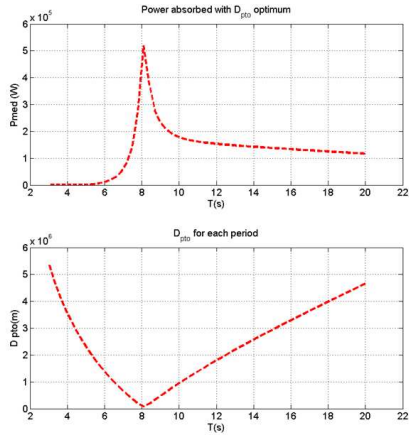


Figure 5.6: Average Power and selected PTO Constant for each period for the 8 s converter (individual float)

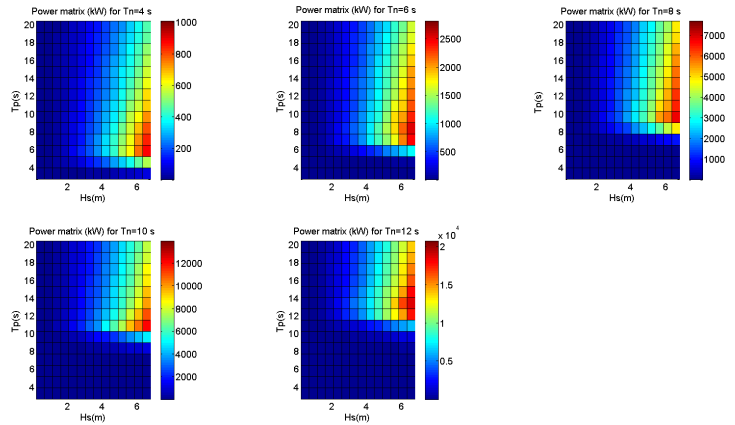


Figure 5.7: Power matrix (kW) of the designed converters (4, 6, 8, 10, and 12 s)

### 5.2.4 Results

Local wave climate characteristics have not been previously considered in this analysis. With the power matrices for all geometries computed, the mean annual power absorbed by each WEC option at each location has been calculated by multiplying the  $H_s-T_p$  occurrence matrix in % at each node (obtained from the GOW1.0 database) by the power matrix.

$$\text{AnnualMeanEnergyProduction}(kWh) = \text{OccurrenceMatrix}(\%) \cdot \text{PowerMatrix}(kWh) \quad (5.2)$$

where the occurrence matrix corresponds to the percentage of occurrence of the set of sea states  $H_s-T_p$  in the analyzed period of time and the power matrix corresponds to the average power in kWh for the set of sea states  $H_s-T_p$ . It should be noticed that oppositely to the power assessment methodology developed in Chapter 4, in this particular case the classical power method was chosen for the sake of simplicity and in order to use the standardized method.

To compare the effects of tuning on the efficiency of the devices, the results are shown in terms of capture width ratio (CWR) for a virtual cylinder with the WEC diameter. This parameter is calculated with the following formula:

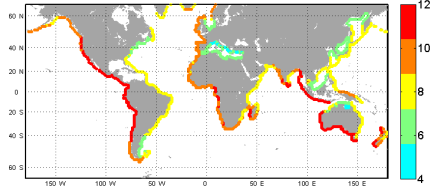
$$\text{CWR}(\%) = \frac{\text{Annualmeanpowerproduction}(kWh)}{\text{WaveEnergyresource}(kW/m) \cdot \text{Numberoffloats} \cdot \text{Widthofthefloats}(m)} \quad (5.3)$$

Figure 5.8 shows the global distribution of the most productive WEC option for WEC type 3 (tunable option). It has been assumed that the most productive option is the one that has its natural period nearest to the most probable period in the considered node. Almost 35% of the nodes are tuned for the 8 s option (this value is the most probable global wave period), approximately 28 % for the 6 s option, 23% for the 10-s option, 15% for the 12 s option and 5 % for the 4 s option. Geometries with natural periods of 6 s, 8 s and 10 s are predominant. Figure 5.9 shows the CWR for the 3 options considered. As observed in the upper panel, the 4 s geometry has the only acceptable CWR values that range between 15 and 18% in several of the enclosed seas dominated by short SEA waves. In other oceanic areas, the 4 s geometry behaves as wave followers, and the capture ratio decreases as the predominant wave period increases; the CWR is still 10% in oceanic coastal areas oriented to the East with predominant SEA waves.

The middle panel of figure 5.9 shows the CWR for the 8 s geometry. In this case, the natural period for the converter better matches the mix of the ocean SEA and SWELLS encountered in the western ocean margins and the SWELLS of tropical coasts with CWRs between 15 and 20%. The maximum CWR values (>20%) correspond to tropical coasts oriented to the south in the Arabian Sea and on the Pacific coast of the Philippine Islands. As shown in Figure 5.1, these

areas are characterized by a most probable period of 8 s; therefore, the CWR is at a maximum. As this WEC geometry performance decays rapidly for wave periods below 8 s, the enclosed seas have low CWR values (<5%).

Option 3, Tuned converter, chosen converter (Tn) on each location



**Figure 5.8:** Distribution of the converter used on each location for the option C (Tuned converter) in seconds

The bottom panel of figure 5.9 shows the CWRs obtained with the tunable device. In this case, the CWR is medium to high in almost all areas. The maximum values of close to 25% are encountered in coastal areas under a constant SWELL or fully developed SEAs, such as the coasts north and west of the Iberian Peninsula, the west coast of Chile, the south and west coasts of Australia or the southwest coast of Indonesia. Coastal areas of very variable wave climates as the Eastern continental margins have lower CWR values because the high variability of wave periods.

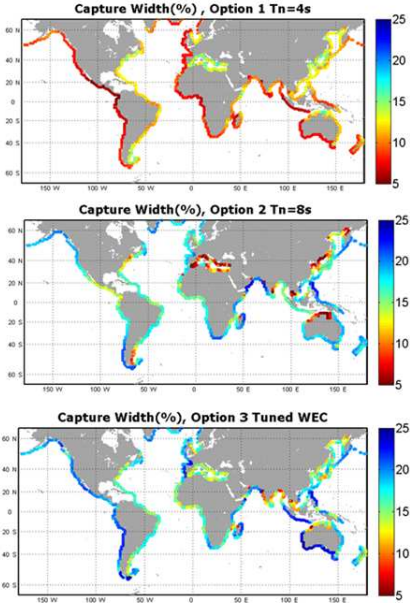


Figure 5.9: Capture width ratio (%) for option 1, 2 and 3

## 5.2. WEC Design approach: adaptability of a WEC to different weather scenarios 98

Tuning a WEC for each location (and each climate characteristics) therefore improves the CWR. For example, in the Mediterranean Sea, the 4 s geometry has a 12% average CWR; the 8 s geometry has a 5% average CWR and a 17% average CWR if the WEC is tuned for that climate. In the case of Southern Chile, the average CWR for the 4 s geometry is 7%; the 8 s geometry has a 20% average CWR and a 25% average CWR if the WEC is tuned for that climate. Table 5.3 shows the mean, standard deviation and several useful percentages of the CWR parameter computed for the entire set of nodes. Globally, option 1 has the lowest average CWR (10%). Option 2, tuned for a period near 8 s, has an average CWR of 15%. The tuned option has a 19% CWR. The percentages of nodes within certain CWR ranges are also shown. For a CWR higher than 15%, option 3 displays a 72% value, indicating a high conversion efficiency at many points. However, the percentages of nodes with a CWR higher than 15% corresponds to 67% for option 2. Consequently the tuned option improved the CWR by 4% and 9% with respect to option 2 and 1, respectively. However, if the results were analyzed from a local perspective, the tuned option would display higher differences with respect to the other two options. Therefore, redesigning a WEC for the climate of the deployment site improves efficiency.

Parameters	Average CWR (%)	Standard deviation CWR (%)	% nodes with CWR >5%	% nodes with 5% < CWR < 15%	% nodes with CWR > 15%
Option 1	10	3	0.001	94	5.99
Option 2	15	5	3	30	67
Option 3	19	3	0.01	27	72.99

**Table 5.2:** Analysis of CWR values for the different options

Although the CWR parameter is an indicator of the WEC energy capture efficiency, this value does not provide any information about the economic performance of the device.

From an economic perspective, the cost of the WEC structure is one of the key factors in the WEC budget. According to previous studies, the marine structure accounts for nearly 40% of the budget of a WEC. To establish an indicator of the economic performance of the three proposed options, the indicator of kW/Ton (KWT onwards) will be used. This parameter relates the power produced to the WEC mass and has been previously used as an indicator of the economic performance (Babarit *et al.* (2012)). Numerically higher factors indicate a better economic performance.

Figure 5.10 shows the KWT maps for the three proposed options. The upper panel of figure 5.10 displays the case of the 4 s geometry; the highest value of this indicator appears in South Chile, with a KWT of approximately 0.7 kW/T. High KWT values (between 0.4 and 0.6) are also found in South and Southwest Australia, West Ireland, West Scotland, the northwest of France and Spain, South Iceland, West Canada and the Pacific Shores of the Aleutian Islands. However, the device is not tuned for these wave climates; the lightness of the structure and

the capability of the WEC wave follower allow this option to be competitive in these high-energy/high-period areas. The areas in which the WEC is tuned to the wave climate (i.e., the Mediterranean or North Sea) have low KWT values (0.05 kW/Ton) because of low energy production. The middle panel shows the KWT map for the 8 s WEC geometry. In this case, the KWT values are approximately one order of magnitude lower than the 4-s geometry case. Discarding the general KWT drop, the map is similar to the 4 s geometry map.

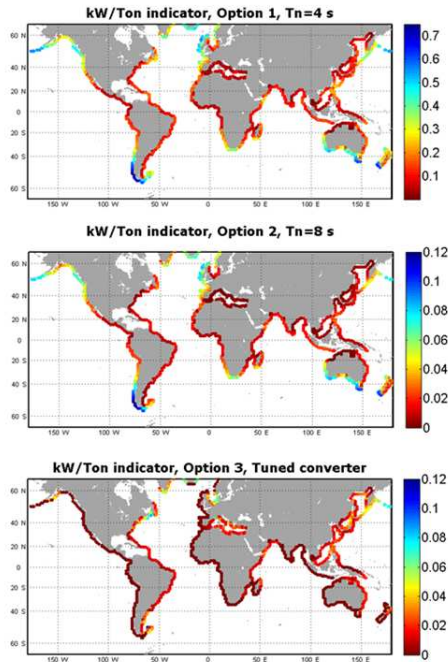


Figure 5.10: KWT for the three studied options

The bottom panel shows the KWT map for the tuned converter. In this case, the values are low. Most of the enclosed seas that are tuned to 4-6 s (low WEC mass, see figure 5.11) have low energy fluxes (i.e., low production, see figure 5.12), and coasts with high energy fluxes are tuned to high periods, indicating high structural costs. Only small areas, such as the coasts of Holland, Germany and Denmark along the North Sea, have slightly better values. The North Sea is well suited for the 4 s device, and the energy flow is not as low as other enclosed seas. To support this analysis, figure 5.11 shows that the increase of WEC mass depends on the WEC natural period (a cubic fit is included in the figure). From this analysis, smaller structures are

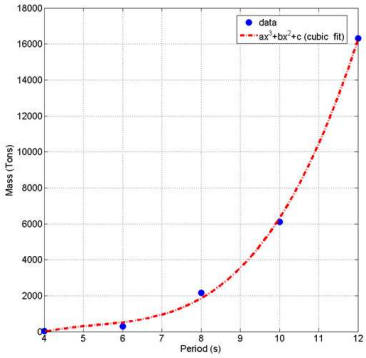


Figure 5.11: WEC mass versus the natural period

advantageous when considering the power production versus mass. It should be highlighted that if this analysis is performed for OWC prototypes the results may change. In that case, the mass is provided by the water (that is costless) and then heavier structure would not lead to costly prototypes.

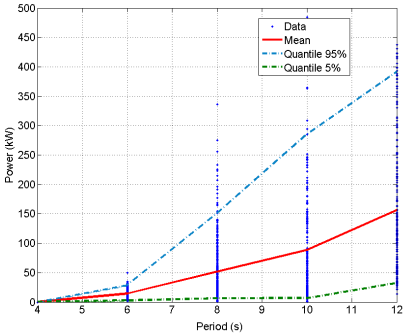


Figure 5.12: Global WEC power production related to natural frequency

Figure 5.12 shows the average production, the 5% percentile and the 95% percentile of the global KWT values in terms of the WEC natural period. Table 5.3 shows the KWT mean and standard deviation.

The revenue from the increase in power production obtained by tuning the WEC to the mean peak period does not offset the cost increase of the structure of the WEC. The increase in power

Parameters	Average KWT	Standard deviation KWT
Option 1	0.16	0.13
Option 2	0.02	0.019
Option 3	0.025	0.02

**Table 5.3:** Mean and standard deviation for the kW/Ton

production of a tuned over a non-tuned converter (wave follower) is approximately 20% to 40%. However, a higher increase in the mass of the structure is required for high peak periods. Therefore, tuning the WEC to the mean peak period is not necessary (except if the mean peak period is low), and the design of the converter should be directed to small marine structures that are wave followers.

The KWT parameter described above could be used as an indicator of the economic viability of the WEC in the studied location. However, it is known that in order to give an accurate estimation of the cost of a device the levelized cost of energy should be used. As this is considered an intermediate step, this indicator was for the sake of simplicity. A thorough analysis of the LCOE is carried out on the next chapter. Regarding the KWT, in order to transform this indicator into Euros/kWh (EurkWh), the following assumptions are drawn:

- Only the mass of the WEC floats are considered. These floats are supposed to be constructed with reinforced concrete.
- The WEC operative life is 25 years
- The cost of reinforced concrete is 500 Euros/m<sup>3</sup> (high performance concrete)

With these assumptions, the KWT is converted to a EurkWh indicator. This indicator is not a valid parameter for economic analyses because numerous additional costs should be considered to assess the real WEC cost. However, the EurkWh parameter could be used to compare different locations.

From the point of view of a developer, the goal of the design of a WEC is to obtain a converter that could be deployed with a good performance in as many locations as possible. Therefore, two scenarios are imposed to determine appropriate locations for wave energy farms. The following two conditions are imposed (see Table 5.4):

- In terms of CWR, a minimum value is selected. A previous study (see Babarit and Hals (2011)) investigated the CWR for a set of converters using numerical modeling and experimental testing. For the case of small heaving buoys, a range in CWRs (from 9% to 14 %) was achieved. For the large buoys, a CWR range of 19 to 41% was attained. In this analysis, a 10% CWR minimum is used for the two proposed scenarios.
- In terms of KWT, different minimum values are used for each of the two scenarios to study which locations comply with the restriction: 0.01 KWT (0.1 EurkWh) and 0.1

## 5.2. WEC Design approach: adaptability of a WEC to different weather scenarios 102

KWT (0.01 EurkWh). The second restriction could be near the current energy cost scenario in numerous locations.

Parameters	Average KWT	Standard deviation KWT
CWR	>10%	>10%
KW/TON	>0.1 / >0.01	>0.01 / >0.1

**Table 5.4:** Proposed scenarios for the study

Locations that satisfy these conditions are suitable for wave energy farms (YES), otherwise areas labeled with a NO. Finally a sensitivity analysis in terms of the percentage of available locations restricted by the CWR and KWT is performed. This analysis is shown in Figure 5.14 and Figure 5.15.

Panels on the left-hand side of Figure 5.13 show the available coastal locations for Scenario 1 and the different WEC options. For option 1 (4 s natural period; upper panel), approximately all locations satisfy the conditions. If option 2 is selected (8 s natural period, middle left panel), those regions with peak periods far from 8 s (i.e., the Mediterranean) with low peak periods and low energy waves or the West coast of Central America with high peak periods and low energy waves do not satisfy condition 1. Finally, for option 3 (tuned converter; bottom left panel), the locations that do not satisfy condition 1 are those areas with high peak periods and low wave energy (i.e., tropical Pacific America, Tropical Atlantic Africa or the southern coast of Arabia, India or Indonesia).

Panels on the right-hand side of figure 5.15 show the available coastal locations identified by the more restrictive, in terms of KWT, condition 2 and the different WEC options. For option 1 (upper right panel), those areas with low wave energy (enclosed seas as the Mediterranean and several tropical areas) do not satisfy the conditions. the Mediterranean Sea and other enclosed seas do not satisfy condition 2 despite the good CWR in the oceanic areas because of the high peak periods. If option 2 is selected (middle right panel), only those areas with high mean wave energy fluxes and medium to high peak periods (Northwest Europe, South Iceland and Greenland in the Atlantic; Alaska, part of Aleutian Islands and Southwest Chile in the Pacific; South Africa, Southwest Australia and New Zealand) comply with condition 2.

Finally, if an option 3 device is selected (tunable; bottom right panel), several coastal areas display medium energy with low peak periods of approximately 6 s (the North African Mediterranean Coast of Tunisia and Libya, southern coasts of the North Sea, the south coast of Newfoundland and other small areas). Regions with high wave energy fluxes and high periods that were acceptable for Scenario 2 for WECs tuned for 8 s (option 2) are unacceptable when tuned for the location peak period. Tuning for the location is unacceptable because of the high cost of the structure. However, for option 3 on the Mediterranean, several differences are shown

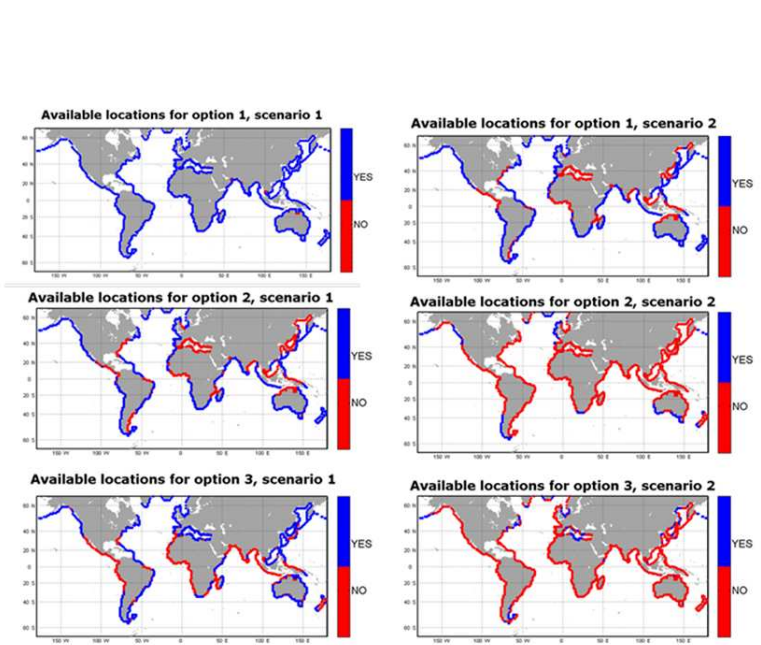


Figure 5.13: Available coastal locations for Scenarios 1 and 2 and the different WEC options

## 5.2. WEC Design approach: adaptability of a WEC to different weather scenarios 104

for scenario 2. This is because the most probable period of these locations ranges from 4 to 7 s, and then when option 3 is applied, different sub-options are applied for different points.

Option 1 (4 s converter) has the most possibilities in terms of availability of locations, and tuning a converter for each met-ocean condition does not provide a positive effect on the cost of the extracted energy. In other words, smaller floaters produce higher KWTs. This statement should be taken with care because other costs (PTO costs, normalized O&M costs, etc.) that may decrease as the floater size increases have not been considered in this analysis.

Finally, to separate the influence of the two studied variables (CWR and KWT), a sensitivity analysis is performed. This analysis is conducted in terms of the percentage of locations at which the CWR or the KWT is lower than a certain value.

Figure 5.14 shows the percentage of available locations with a CWR higher than a selected value for the three WEC geometries. As observed in the figure, the tuned converter always displays higher CWRs than the other two options. Option 2 is slightly below the tuned converter for medium to high CWRs but is well below the tunable option for medium to low CWR. This behavior is because the 8-s tuning restricts those locations with low mean peak periods. Finally, the option 1 curve (4 s WEC natural period) falls below the other two because the 4 s converter is only tuned for a few locations. For instance, in the case of an option 1 WEC, 5% of locations have CWRs higher than 15% whereas the percentage of locations are 12% and 75% for option 2 and 3, respectively.

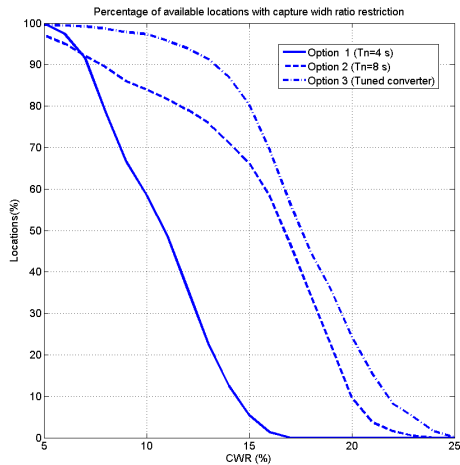
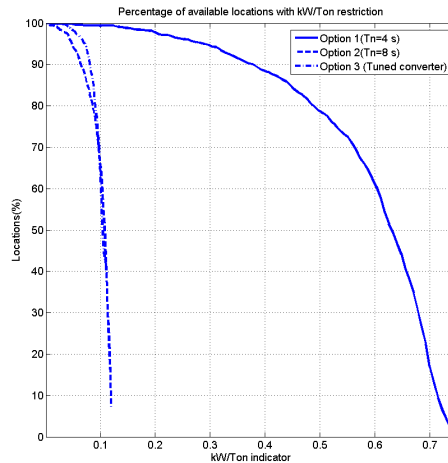


Figure 5.14: Percentage of available locations depending on CWR



**Figure 5.15:** Percentage of available locations depending on the KWT indicator

Figure 5.15 shows the percentage of available locations with KWT values higher than a selected value for the three WEC geometries. As observed in the figure, the differences between option 1 (WEC with 4-s natural period) and the other two options are notable. Option 1 is applicable to many more locations than the other two options. The difference between the curves for options 2 and 3 and the curve for option 1 is due to the low mass required by option 1 compared with the other two. Option 2 (8 s converter) and 3 (tunable option) display similar curves. Both of these curves converge to an identical KWT of 0.12 (0.09 Euros/kWh). Option 2 and option 3 converge when the percentages of locations lowers. This is because the value was inferred for section 1 and the most probable period around the world coastlines is 8 s. Therefore, the convergence is unsurprising.

In this last subsection, in order to provide an order of magnitude of the importance of selecting one of the options presented on this study a conversion to Eur/kWh was made. This "conversion" was based on a set of assumptions explained before. One of the conclusions from this study is that, in general design should be focused on small structures although they are not tuned with the local wave climate. However this quote should be taken with care, as only the cost of the material was taken into account. Then, on this section an ascending curve (Eur/kWh) was presented as the natural period (diameter and rated power as well) increases.

However, there is a curve that also influences the cost of the device that is opposite to the aforementioned curve. The O&M decreases as the rated power of device increases. For example

## 5.2. WEC Design approach: adaptability of a WEC to different weather scenarios 106

if a wave energy farm of 10 MW is being planned, it is easier to maintain 10 devices of 1 MW each than 100 devices of 100 kW each. Then, this curve also should be taken into account when analyzing the whole picture of device design/selection.

Regarding this curve there is no data for wave energy devices as only few of them has been tested and no more than one rated power per device has been analyzed yet. Regarding wind energy there is few data comparing the decrease on the normalized O&M costss for different rated powers. Jensen *et al.* (2002) presented the curves of normalized O&M costs per kWh for different turbines (see figure 5.16).

If the cost for the 3 year old turbine are fitted to an exponential the expression would be:

$$Cost = 1133.3454 \exp(-0.98138 \cdot RatedPower) \quad (5.4)$$

For this case study and due to the lack of data the same expression will be assumed for wave energy with correction factors alpha and beta:

$$Cost = 1133.3454 \cdot \beta \exp(-0.98138 \cdot \lambda \cdot RatedPower) \quad (5.5)$$

In figure 5.17 the material cost, the normalized O&M costs as well as the sum curve are represented for a node with  $\beta = 10$  and  $\lambda = 0.1$ . It should be noticed that this investigation is specific to this study, with this converter and conditions applied on the previous section. In the x-axis instead of the rated power of the devices, the natural period has been plotted in concordance to the previous section. In this specific study the higher the natural period the higher the rated power of the device, but this statement should not be generalized. If it is required to plot the cost versus the rated power instead of the natural period the concordance would be: 4 s-1000 kW, 6 s-2600 kW, 8 s-7500 kW, 10 s-13500 kW, 12 s-20000kW.

Here it could be seen how both material and O&M curves have an opposite behavior. The sum curve has a minimum and then this would be the optimum point taking into account material cost and normalized O&M costs. If the material cost is the only thing taken into account the lightest option (4 s) will be the optimum. In Figure 5.18 the optimum option for all the set of nodes is plotted for different values of  $\beta$  and  $\lambda$ . These graphs shows how when the O&M increases the optimum option goes towards higher rated power (natural period). This means that the higher the normalized O&M costs, the higher the percentage of nodes with a higher natural period, indicating that larger WECs become more economically efficient.

This small example highlights the importance of the other associated costs and then the result and conclusions of this section should only be applied to the cost of the material.

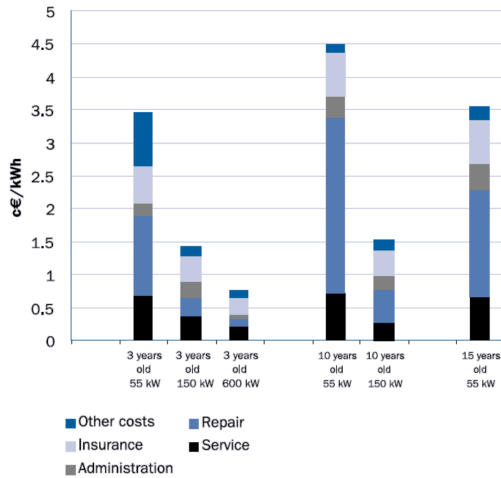


Figure 5.16: normalized O&M costs per kWh for different turbine ages and sizes, from Jensen *et al.* (2002)

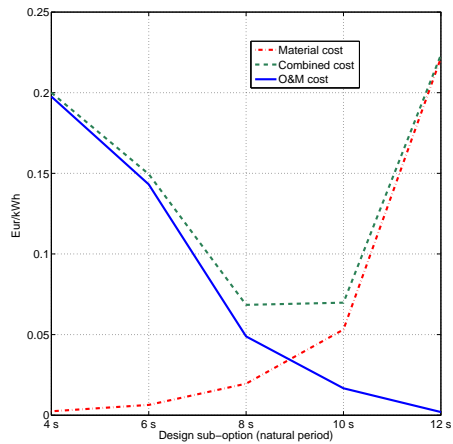
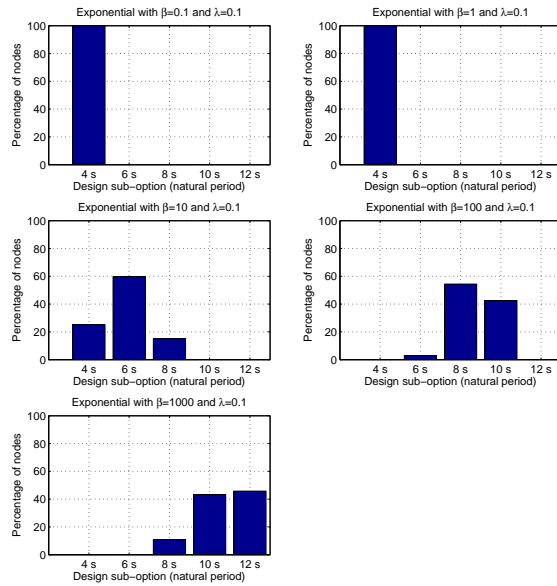


Figure 5.17: Cost per kWh curves for the different options



**Figure 5.18:** Optimum option for material cost and normalized O&M costs for different values of  $\beta$  and  $\lambda$

**Conclusions**

In this study, an analysis of the adaptability of a generic Wave Energy Converter (WEC) to different climate conditions was conducted. The studied converter mimics the Wave Star device and consists of two rows of cylinders aligned in the wave propagation direction to absorb energy during heaving motion. Three options are proposed: a converter tuned to a period typical of the enclosed seas (option 1; 4 s converter), a converter tuned to the typical Atlantic swell (option 2; 8 s converter) and a tunable option (option 3; variable converter 4, 6, 8, 10 and 12 seconds). The power matrices are calculated with a frequency domain model. The adaptability of these options to the global coastal wave climate is studied using the met-ocean data extracted from the global reanalysis database GOW 1.0 (see Reguero *et al.* (2012)). For this analysis, two indicators (Capture Width Ratio (CWR) and kW/Ton (KWT)) are assessed to analyze the advantages and disadvantages of tuning the WEC natural period to the prevailing sea state peak period.

The CWR indicator represents the efficiency of the converter with respect to the available resources at the location. Because option 1 is tuned to low-peak period locations that are typical of enclosed seas, the CWR for this option in ocean locations with medium- to high-peak periods is low. However, option 2 (8 s converter) has good CWR values on these oceanic coasts with medium to high peak periods, whereas these converters perform poorly in low-peak period environments in the enclosed seas. Logically, the tunable WEC, option 3, adapts the best to all wave scenarios in terms of CWR.

The KWT indicator represents a type of "economic viability" indicator. The structure cost is related to the mass. The mass of the resonant WEC increases by a cube of the WEC natural period (see figure 11). Therefore, tuning the WEC to high periods implies heavy and costly structures. Globally, the higher KWT values are found for WEC option 1 although the converter is not tuned with the majority of the climates (in most cases, the floater follows the free surface). For example, the structure of an option 2 device is 80 times heavier than an option 1 structure, and the power production is only 30% higher at locations in which option 2 is tuned to its natural 8-s period. For option 3 (WEC tuned to the peak period), the KWT indicator is low in almost all locations, notably in locations characterized by high peak periods in which the tuning requires large structures without a comparable increase in power production.

Therefore, tuning a converter for each location is positive in terms of power conversion efficiency but not advantageous in economic terms (KWT indicator). Considering that the cost of the other factors that influence the overall cost of WECs (the number of PTOs for a given power, O&M) increase for smaller WECs, the main goal of a WEC design should be to select for structures with a moderate size even if not tuned with the local wave climate.

## 5.3 Study of O&M Parameters from a Worldwide Perspective

### 5.3.1 Introduction

As explained in the last section normalized O&M costs are an important part of the cost pie on the device total budget ranging from 5% to 25% of the initial budget. Therefore an understanding of how these costs work is essential when selecting sites for wave energy development.

When looking for a location for WEC installation, developers usually aim for sites with maximum wave energy resource. From this perspective, countries like Scotland, Ireland or Portugal have made great effort to include this energy source in their energy mix due to their high untapped potential.

However, higher wave energy resource usually means rougher sea conditions. When choosing a location for the deployment of a WEC, the installation, operation and maintenance activities should be taken into account. One of the primary causes of unsuccessful marine operations is due to poor marine conditions. According to the International Energy Agency one of the key issues related to offshore marine energy is the shortage of the suitable deployment vessels for adverse weather conditions and the long waiting periods that should be waited for the maintenance operations. In the case of offshore wind energy, wind turbines could be deployed in areas with high wind resource but "mild" wave conditions. However in the case of WEC farms, high resource means harsh sea conditions; so the location should be chosen with these conditions in mind.

The research carried out in O'Connor *et al.* (2013b) and O'Connor *et al.* (2013c) concluded that accessibility and availability factors have a significant impact with respect to the financial return of wave energy technology. They concluded that intensive and high normalized O&M costs should be expected in locations with adverse climate. These normalized O&M costs have an impact of around a 30% of the total cost of the WEC. A method for the assessment of weather windows in order to manage marine operations was presented in Walker *et al.* (2011). They concluded that the primary influencing factor that affects normalized O&M costs is related with is the amount of available weather windows on a particular location, so this is an important point when choosing the deployment location of a wave energy project. With respect to the geospatial analysis of wave energy deployment constraints in Nobre *et al.* (2009) seven criteria were considered for choosing a suitable area for energy conversion: Sea bottom geology, distance to shore, ports and power grid, average wave height, period and power. The analysis in this paper was performed only for UK waters. There are no studies related to the optimum location for wave energy development from a worldwide perspective, taking into account the normalized O&M costs.

This subsection presents a study of the suitability for wave energy development from a global perspective with emphasis on normalized O&M costs. This sub section has been structured as follows: first, the wave climate databases are described; second, the availability and accessibil-

ity indicators around the world are shown; third, the O&M main parameters (weather windows and waiting period between weather windows) are presented; finally, the worldwide influence of the normalized O&M costs on the energy cost are analyzed for a WEC composed by a set of heaving cylinders (previous chapter).

### 5.3.2 Climate data

For the global analysis of weather windows and their durations, a long term global meteocean database is needed. The same database as in the previous chapter (GOW  $1^{\circ}\times 1.5^{\circ}$  coverage), based on the NCEP/NCAR reanalysis atmospheric forcing is used from Reguero *et al.* (2012).

For the study of O&M indicators some of the sea states parameters should be highlighted. According to O'Connor *et al.* (2013c) and Walker *et al.* (2011) the main sea states parameters for O&M are:

- Wave height ( $H_s$ ), it is the most important variable because the O&M activities are usually limited by this parameter. According to O'Connor *et al.* (2013c) there is a limit on the working wave height depending on the type of vessel used for the operation and the type of offshore structure to be boarded (wind turbine, WEC...). For offshore wind turbines the range of operating wave heights goes from 1.5 m for Catamarans to 3 m with the Amplemann system. For WECs, the range of wave height limit is around 1.5 or 2 m according to O'Connor *et al.* (2013c).
- Peak period ( $T_p$ ): according to Walker *et al.* (2011) there is a range of operating periods for each type of barge. Normally, the limiting periods for usual barges for O&M activities are from 4 s to 16 s depending on the relative direction between barge and wave propagation direction.
- Other parameters as wind speed or current speed are important in order to study the access limits for the different vessel types. According to O'Connor *et al.* (2013c) the wind speed access limits vary between 8 m/s to 15 m/s.

### 5.3.3 Accessibility and availability

Accessibility and availability are two parameters that are crucial in order to understand the behavior of a WEC depending on weather conditions. Availability is the percentage of the time that a WEC (or turbine in the case of wind energy for instance) is ready to produce electricity. Usually depending on met-ocean conditions and type of converters; WECs have a wake up level, an operational range and finally a survival mode. As few prototypes are still at open sea conditions the information about these levels is scarce. For instance, according to Rashid and Hasanzadeh (2011) the Pelamis enters the survival mode at a significant wave height of 8 m, the C5-600 Wave Star prototype works until a wave height of 6 m, see Vidal *et al.* (2012) and the survival limits for SEAREV and AWS devices is 8 m and 6.5 m, respectively, see Saulnier

(2004). Less information is still available about the wake up level, so  $H_s = 0m$  is assumed for that level in the following.

Thresholds	Availability(%)			
	<90%	90%-95%	90%-99%	99%-100%
$H_s < 5m$	4%	6%	14%	76%
$H_s < 6m$	0%	3%	12%	85%
$H_s < 8m$	0%	0%	3%	97%

**Table 5.5:** Percentage of nodes on different availability levels

In this study, a conservative value of  $H_s = 5m$  was set for the survival mode level. Figure 5.19 shows the percentage of time that WEC devices would be in the operative range around the Earth's coastlines. As can be seen in the figure there are lot of coastal regions closer to 100% availability, many of them coinciding with low resource areas. There are also some low availability coasts coinciding with high wave energy resource, for instance the east coast of Ireland and the south-east part of Chile. Although these areas show a very high resource, availability rates should be taken into account in a wave energy project development. In these areas a hypothetical device availability would be around 82% (18% of the time would be in survival mode). From these figures, and only from the operation perspective it should be noted that although some locations have a extremely high resource, due to the survivability requirements of the devices the most powerful sea states cannot be exploited. In this respect, figure 5.20 shows the average available power around the world coastlines with different survivability  $H_s$  thresholds. As can be seen some sites with very high resource (like the east coast of Ireland) have similar available resource as other areas with lower total resource (like the west coast of Portugal) when a lower wave height threshold is considered for the availability study. Regarding this, table 5.5 shows the percentage of coastal nodes that accomplish certain levels of availability. As can be seen, the availability is quite high for all the considered thresholds.

On the other hand, accessibility is the percentage of time when the device could be accessed for maintenance operations. The accessibility is device specific too and it also depends on the met-ocean conditions and on the type of vessel used for the operations. In this work the accessibility is only analyzed as a function of  $H_s$ , however in the future research it will be analyzed according to the methodology developed by North Atlantic Treaty Organization (2000), Dobie (2000) and Crossland and Rich (2000) taking into account the specific sea keeping conditions for staff performing O&M on floating structures. As demonstrated by O'Connor *et al.* (2013c) the wave height limits goes from 1 m to 3 m depending on the type of vessel. Figure 5.21 shows the accessibility levels (in % of the year) assuming that wave height were the only variable involved in the accessibility. As illustrated on the figure the wave height threshold has great influence on the accessibility level and its spatial distribution. For instance, for  $H_s = 1m$  threshold almost all the ocean coastal areas have low accessibility levels with values near the 30% except for

enclosed seas like the Mediterranean or the Baltic, where the accessibility levels for this low  $H_s$  threshold are much higher (nearly 80%), however wave resource at those sites is low.

For the case of  $H_s = 1.5m$  threshold, many more locations show acceptable accessibility levels. For instance, in Europe, the levels range from 68% in Denmark's North Sea coast, to a 45% accessibility for Spain or Portugal North and West Atlantic coasts or 20% in the open Atlantic coasts of Ireland or Scotland. In Pacific coasts of America, the accessibility levels range from almost 90% in Central America to 30%-40% in Canada and USA coasts to 20% in Chile. If the threshold is incremented to  $H_s = 2m$  the accessibility levels of some coastal areas change significantly as is the case of Europe, where the accessibility levels range from 60% in Spain and Portugal, to 35% in Ireland and Scotland. There are some areas like Chile and the South coast of Australia that still have very low accessibility levels (20%). With respect the East (Atlantic) coast of America the levels of accessibility there are quite high, near 90%. Finally for the 3 m threshold the accessibility levels around the globe are much higher. Except for some rough areas, including Ireland, Chile and South part of Australia the rest of the coast have an availability of 90% or over.

Table 5.7 shows the percentage of nodes corresponding to the indicated range of accessibility level for different  $H_s$  thresholds. As shown, for a wave height threshold of 1 m, 50% of the nodes have accessibility levels lower than 25% (very limited accessibility for O&M). As the  $H_s$  threshold increases the percentage of nodes with the lowest accessibility level decreases. For instance for the  $H_s = 2.5m$  threshold 1% of the nodes have accessibility levels below 25% and 7% of the nodes have accessibility levels between 25% and 50%. Table 2 also includes the mean wave energy flux resource corresponding to the percentage of nodes that are on the given accessibility level range. It should be noted that for the most restrictive thresholds the nodes with high accessibility (75%-100%) have very low resource (just 2 kW/m). In order to see an equilibrium between resource, accessibility and amount of locations that accomplish the conditions the higher  $H_s$  thresholds need to be studied. For instance for  $H_s = 2m$  threshold, the percentage of nodes with accessibility between 50% and 75% is 24% and the mean wave energy resource of these nodes is 18 kW/m. For  $H_s = 2.5m$  and  $H_s = 3.0m$  and the same accessibility level range. These values are 15% and 26 kW/m and 11% and 36 kW/m, respectively. From the investor perspective a balance should be achieved in terms of resource, accessibility and available locations.

For a more detailed analysis, seven reference sites have been selected, see Figure 5.22 illustrating: the North-West of Denmark, the West of Ireland, Chile, the North of Spain, West-Portugal, South-West of Australia and West-Scotland. The selected sites are areas with tradition and interest on wave energy. Table 5.6 summarizes key numbers in terms of resource and accessibility at each site. From this table it can be concluded that locations with very high resource (Chile and Australia) have very poor accessibility levels. In the case of Australia for instance, even for the 3 m threshold the accessibility as low as 50%. For the case of Chile,

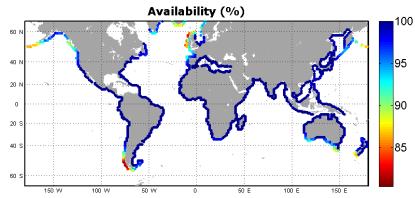


Figure 5.19: Availability map in percentage for wave height threshold  $H_s = 5m$

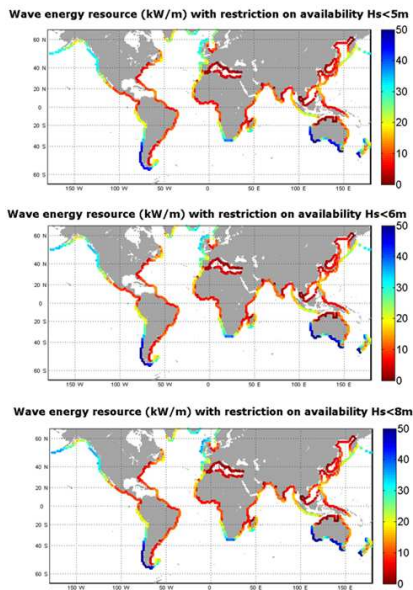
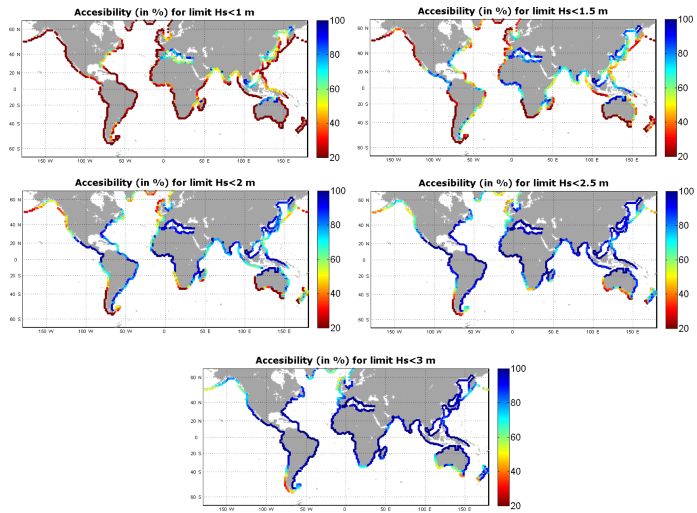


Figure 5.20: Wave energy restrictions with availability restrictions



**Figure 5.21:** Accessibility (in %) for different wave height thresholds



**Figure 5.22:** Situation of the sites chosen for further study

Locations	Longitude	Latitude	Mean wave energy resource (kW/m)	Accessibility (%)				
				1m	1.5m	2m	2.5m	3m
$H_s$ thresholds								
North-West Denmark	7.5	57	12	44	64	77	85	90
West of Ireland	-10.5	53	62	7	19	34	47	59
Chile	-73.5	36	34	1	9	32	61	81
North of Spain	-3	44	28	25	47	64	75	83
West Portugal	-9	40	29.5	18	42	60	73	82
South of Australia	115.5	-35	62	0.01	1	10	29	51
West Scotland	-4.5	59	50	8	23	38	52	64

**Table 5.6:** Proposed scenarios for the study

Thresholds	Accessibility(%)			
	0-25%	25%-50%	50%-75%	75%-100%
	Percentage of nodes/ Mean Wave energy resource			
$H_s < 1$ m	50% / 23 kW/m	20% / 9.35 kW/m	21% / 5 kW/m	9% / 2 kW/m
$H_s < 1.5$ m	18% / 35 kW/m	24% / 18 kW/m	26% / 10 kW/m	32% / 4 kW/m
$H_s < 2$ m	6% / 48 kW/m	12% / 30 kW/m	24% / 18 kW/m	58% / 7 kW/m
$H_s < 2.5$ m	1% / 55 kW/m	7% / 42 kW/m	15% / 26 kW/m	77% / 9 kW/m
$H_s < 3$ m	0% / 0 kW/m	2% / 53 kW/m	11% / 36 kW/m	83% / 11 kW/m

**Table 5.7:** Percentage of nodes with the different accessibility levels

the accessibility is low too, but an abrupt change on accessibility is noted from the 2 m to 2.5 m threshold, accessibility changes from 32% to 61% due to local wave height distributions. Due to this fact similar sites, with very similar resource may show very different accessibility rates depending on wave height distribution functions. If attention is focused on Ireland and South Australia the differences are noticeable. Both points have the same resource (62 kW/m), however the levels of accessibility for all the thresholds are much higher in Ireland.

This case is further investigated in figures 5.23 and 5.24. In these figures the Cumulative Dens-

ity Function of the significant wave height and the wave energy flux are represented. Figure 5.23 explains why the accessibility is much lower in Australia with the same wave energy resource. The shape of the distribution is different and both tails have different behaviors. The distribution for Australia is more skewed than the one for Ireland. For low wave heights (in order to measure accessibility) the probabilities are much higher in Ireland than in Australia. However, for high wave heights (once the curves intersect,  $H_s > 3.8m$ ) the probability of having extreme waves is higher for Ireland than Australia. It could be concluded that in terms of accessibility Ireland has more probable periods of time where the vessel could access the devices, however in terms of reliability and availability Ireland has more extreme waves than Australia and then its variability is higher.

In Figure 5.24 the CDF of the wave energy flux is represented. Here, the probability of having low wave energy resource is much higher for Ireland than for Australia. For instance, the percentile 5% in Ireland corresponds to a resource of almost 3 kW/m while in Australia corresponds to 14.72 kW/m. This means that the probability of having low resource waves(not interesting from the harvesting point of view) is higher in Australia than in Ireland. If the upper tail of the distribution is analyzed the distribution shows that extreme wave resources are more probable in Ireland than in Australia, which corroborates the conclusions extracted from figure 5.23.

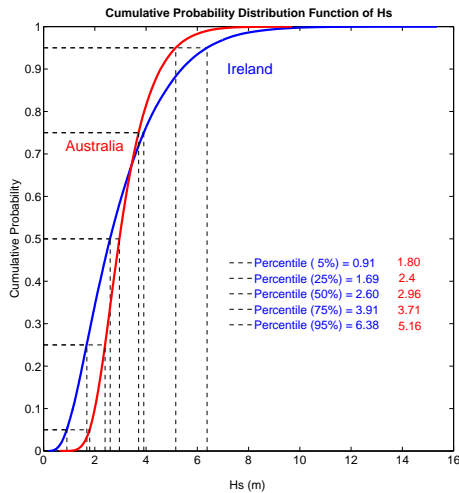


**Figure 5.23:** Cumulative density function of the  $H_s$  for Ireland and Australia location

On the other hand, locations like Denmark, with a low wave energy resource have, very high

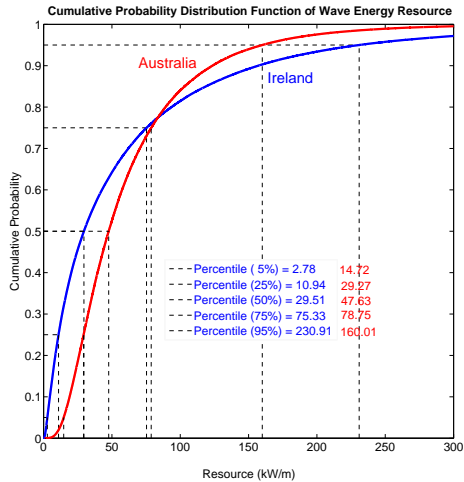


**Figure 5.24:** Cumulative density function of the wave energy flux for Ireland and Australia location

accessibility levels. There are also some intermediate situations, like in Spain and Portugal, as both locations have a similar resource and similar accessibility levels: the mean wave energy resource is around 30 kW/m and the accessibility levels range from 25% for the 1 m threshold to the 83% at the 3 m threshold. Also in Europe, the case of Scotland should be highlighted. The wave energy resource here is high (50 kW/m), however the levels of accessibility are low (from 8% at the 1 m threshold until 64% at the 3 m threshold).

Also the monthly accessibility levels were analyzed on each location in order to study the seasonal changes. Figure 5.25 and Figure 5.26 presents the monthly accessibility curves for each location and each wave height threshold. As expected all the curves show much lower accessibility during the winter months than summer. Also, the sites closer to the Equator (for instance Chile) show smaller differences in between winter-summer accessibility levels than the locations that are at higher latitudes. In the case of the site of Denmark it can be seen that its accessibility levels are medium to high even at winter months. For a threshold of 1.5 m for instance the accessibility in winter months is around 45%, which is acceptable compared to other locations.

It should be highlighted that in Chile the accessibility has a stronger dependence on the threshold than the rest of the locations. In contrast, in the Australia site, located at similar Southern latitude, the seasonal variability is higher and during the winter, accessibility levels are very low for all the considered thresholds. Wave height distribution on this particular site is significantly

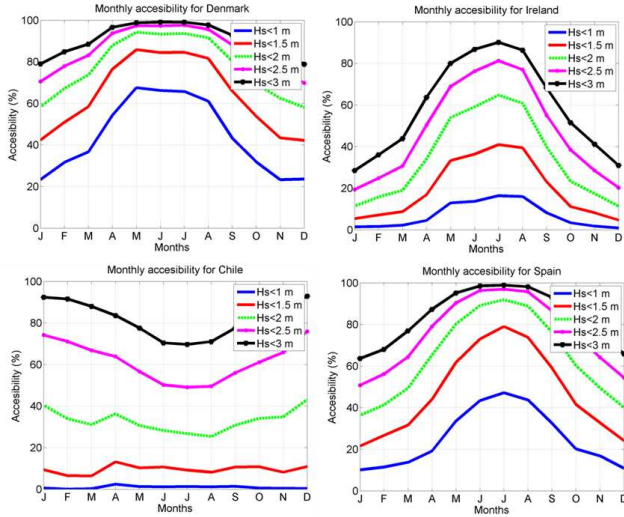


Figure 5.25: Mean monthly accessibility for the Denmark, Ireland, Chile and Spain

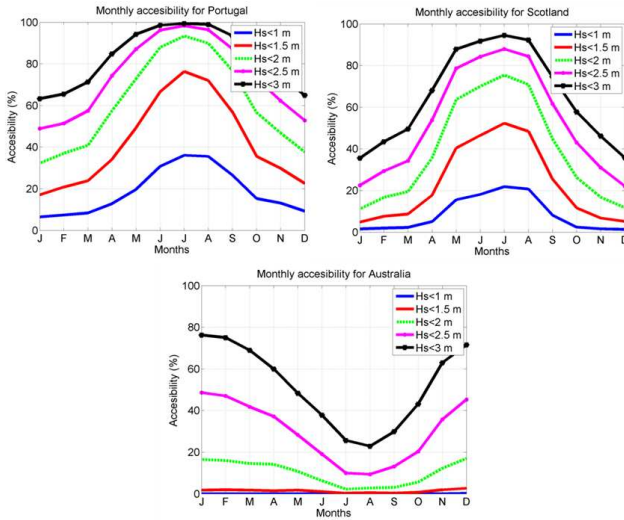


Figure 5.26: Monthly accessibility for Portugal, Scotland and Australia

different from the Chilean site, and even with a similar resource both sites are different from a strategic wave energy development point of view. However the seasonal variations are very low in Chile, because this locations is less storm dependent and wave conditions tends to be rather constant along the year. This fact is positive for wave energy development in Chile, because as failures are expected during the winter time, then the lower the seasonal variation is, the better, more regular and planned maintenance activities it stimulates.

In the case of the European Atlantic locations (Scotland, Ireland, Spain and Portugal), all the curves show a similar behavior. The difference on accessibility between winter and summer months is high and very dependent on the  $H_s$  threshold level chosen. If the attention is focused on winter months (where O&M activities could be needed because of failures) the differences are high among the different locations. For instance for a threshold of 2 m the accessibility levels are 40% for Spain, 15% for Ireland, 38% for Portugal and 15% for Scotland. This means that the winter accessibility levels in Ireland and Scotland are very low and that there would be a lot of time during winter when maintenance operations will be impossible. This fact has two main implications: 1) if a failure happens and corrective maintenance is not possible during a long time period then the converter should be stopped and will not produce energy and 2) the device damage could increase during this period.

From Table 5.6 and Figure 5.25 and Figure 5.26 it can be concluded that there are some locations with a high energy potential and harsh sea conditions (e.g. Australia, Ireland or Scotland). If a wave energy converter is deployed, then the reliability of the WEC should be very high in order to avoid failures (and then corrective maintenance) during winter months. On these sites the maintenance strategy should be focused on preventive maintenance on summer months, where accessibility levels reach 60%. However, wave energy is still on a prototype testing stage and wave devices have not affronted open sea conditions enough time to assure high reliability levels.

There are also some areas with high accessibility and low wave energy resource (Denmark) that are therefore less dependent from O&M issues. Finally there are some locations with medium wave energy resource (Spain and Portugal) and acceptable accessibility levels even during winter months (around 40% for 2 m threshold, 220% higher than in Ireland or Scotland) where installation of first WEC farms would be easier.

### 5.3.4 Weather windows and waiting period analysis

In the previous section the WEC availability and accessibility around the coasts of the world were analyzed. However from the O&M point of view an analysis of weather windows is crucial since O&M activities requires some time with certain sea state conditions to be carried out. For instance, from DONG energy experience, at the offshore Borkum cluster (located far from shore) a weather window of 12 h is needed for a 6 h of effective net maintenance work time.

The analysis carried out in this section is focused on the influence of the wave height on the O&M activities; nevertheless this study could be applied to installation and decommissioning procedures. Apart from the wave height there are other parameters that influence the O&M operations: wind speed, tides, wave period, etc. that have not been taken into account. For this study a common, conservative 1.5 m wave height threshold has been chosen based on Rashid and Hasanzadeh (2011) and O'Connor *et al.* (2013c). For each node the number of weather windows of at least 6 h, 12 h and 24 h per year were calculated. As the GOW is a 60 year reanalysis database, 60 values were obtained for each node. Average and the standard deviation of the number of weather windows per year were represented on each map. It should be pointed out that for this analysis the number of consecutive periods of x h weather windows has been considered. Then for instance if there is a period of 36 h with accessible weather conditions 6 weather windows of 6 h, 3 of 12 h and 1 of 24 h will be considered with the applied criteria.

#### Annual number of weather windows analysis.

Figure 5.27 shows the number of 6 h weather windows per year. It should be noted that the maximum number of weather windows 6 h weather windows per year is 1460. Then, the maps shows some areas such as the Mediterranean or the sea around China (mainly enclosed seas) where the number of weather windows per year is nearly the maximum 1460. These locations are characterized by a large accessibility and low resource.

The average number of weather windows shows that some areas in Europe have around 300 weather windows per year in average. The Atlantic coast or Ireland and in the west coast of South America however remains with a very low number of weather windows (around 100). On the other hand there are some areas with a very high number of weather windows per year. This is the case of the Argentinean coast, the southern coast of Brasil and the coasts of Nova Scotia in Canada. In Argentina the average number of weather windows is around 1200 and around 1000 in Nova Scotia . Also it should be remarked that the differences on the weather windows number on the west coast of America, from 300 at the California Peninsula, to 1200 in the west coast of Central America to the 100 around the Chilean coast.

The standard deviation of the number of weather windows is shown on the bottom panel of Figure 5.27. The standard deviation shows the variability of the weather windows along the

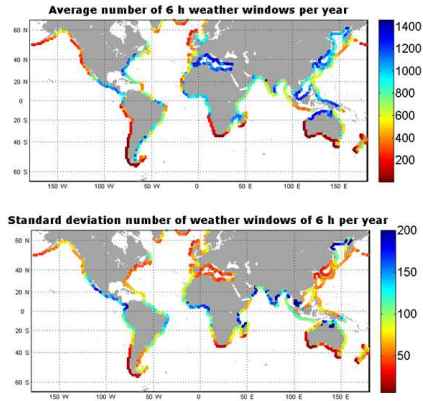


**Figure 5.27:** Average and standard deviation of the number of 6 h weather windows per year for wave height threshold  $H_s = 1.5m$

year. The maximum standard deviation is near 200 per year, then we can assume that the number of weather windows per year is quite constant throughout the time. The locations with highest standard deviation usually correspond also with locations with high number of weather windows. However, if the coefficient of variation is computed, it can be seen how the variability in Australia (0.25) is extremely high compared to the Mediterranean for instance (0.041). If the European coasts are compared the way the standard deviation of the Mediterranean coasts and the Irish west coast are very similar is remarkable, with a standard deviation around 50 weather windows per year. However, the ratio between standard deviation and mean shows that both sites have a highly different performance. Irish waters show a higher variability than the Mediterranean. It is also remarkable how the west coast of India has a high standard deviation (around 200) compared with its mean (700). Also in terms of comparison it should be pointed out how two areas with similar average number of weather windows, their standard deviation is very different, having around 200 for the Guinean Gulf and just 50 for the Mediterranean. This means that the variability of the accessibility in the gulf is much higher than in the Mediterranean.

In Figure 5.28 the number of weather windows 12 h duration is studied. In this case 780 weather windows would correspond to a full year accessibility. In this case the number of locations with full availability is lower than in the 6 h case. If the differences among the maps are highlighted it should be noted that the number of nodes with weather window accessibility higher than 80% (calculated as the number of weather windows divided by the maximum number of weather windows on a year) is 25% for the 6 h while in the case of 12 h weather windows this percentage

is lowered until 20%.

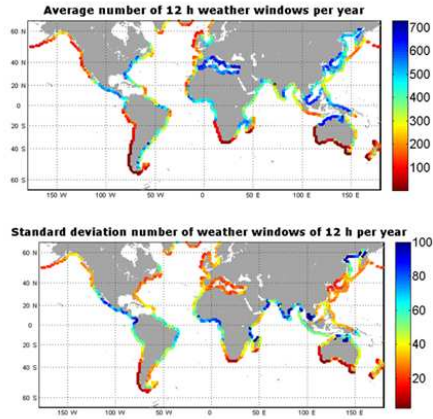


**Figure 5.28:** Average and standard deviation of the number of 12 h weather windows per year for wave height threshold  $H_s = 1.5m$

With respect to the distribution of the number of weather windows on the map this is quite similar to the 6 h map and the only difference is that the areas with lowest and highest number of weather windows are highlighted in the 12 h map and then the differences among the low and high accessibility areas are reinforced.

Finally the corresponding maps of weather windows of 24 h duration are presented on Figure 5.29. For this case the maximum possible number of weather windows per year is 390. In this case, as expected the number of locations with high number of weather windows is reduced and only 15% of the locations have accessibility values (calculated as specified before) greater than 80%. In geographic terms the distribution of the weather windows is similar to the 6 h and 12 h maps. With respect the standard deviation map at the bottom panel of the figure the standard deviation of the 24 h is very similar in geographic terms with the 6 h and 12 h too.

Table 5.9 shows the weather windows results for the selected sites with focus on wave energy. With respect the average values Denmark is the location with higher number of weather windows, until 904 (maximum is 1460) weather windows of 6 h. Spain and Portugal have very similar number of weather windows (around 600). For the case of Scotland and Ireland the average number of weather windows is around 300. In the case of Australia and Chile it should be pointed out that for the 6 h window Australia has around double the number of weather window than Chile. This relationship is also kept for the 24 h weather windows. Also, in terms of comparison among some locations the standard deviation of the number of weather windows is very similar for the case of Denmark and Spain (around 38 for the 12 h duration), however

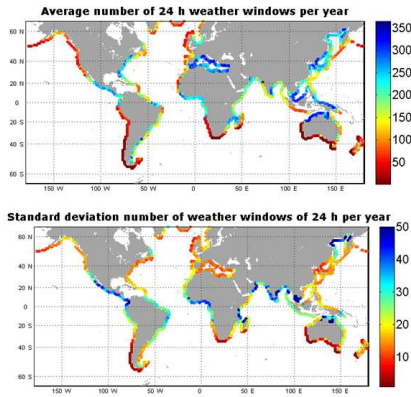


**Figure 5.29:** Average and standard deviation of the number of 24 h weather windows per year for wave height threshold  $H_s = 1.5m$

their number of weather windows is quite different (319 for Spain and 436 for Denmark) and then the coefficient of variation is computed (0.087 for Denmark and 0.11 for Spain) it shows that the variability of the weather windows is higher in Spain than in Denmark.

### Waiting period analysis

Also the periods of inaccessibility are assessed in this section. It is one of the most important variables in order to plan an O&M strategy. Once a failure occurs at an offshore structure, a maintenance operation is needed. Then, the maintenance team has to wait until a weather windows is available in order to carry out the repair.

As suggested by O'Connor *et al.* (2013c) the periods of inaccessibility are more probable to occur during winter months. The waiting period is defined then as the period of time among weather windows (that satisfy a certain wave height threshold for this case) of at least certain duration. The weather window definition is taken as in the previous subsection. The database is cut in  $X$  hours( 6 h, 12 h and 24 h) portions and then the analysis is performed in the  $X$  h new database instead of the hourly data.

Then, in the next figures the average, standard deviation and the 99% percentile of the waiting period for a 1.5 m  $H_s$  weather window of at least 6 h is calculated. It should be pointed out that the waiting periods are calculated for each year and then, from the yearly waiting periods the statistical parameters are calculated. Then, the statistical values show the seasonal variability of the waiting periods intrinsically.

On Figure 5.30 the waiting period is shown for the weather window of at least 6 h. On the top panel the mean waiting period is represented. It should be noticed here that the mean, the standard deviation and the 99% quantile are calculated for each year and then, the average value for the mean, standard deviation and 99% quantile for the whole data base are calculated. That means that the values shown in the figures are the average of the waiting period yearly mean (that is equal to the waiting period mean for all the database) the average of the waiting period yearly standard deviation and the average of the waiting period yearly 99% percentile. As can be seen in this top panel, a lot of areas have less than 1 day for waiting period. Regarding the European coastlines it should be pointed out that the difference among these areas is relatively low. The Mediterranean or Denmark has around 0.3 days of average waiting period, while the West Irish coast has waiting periods around 1.2 days.

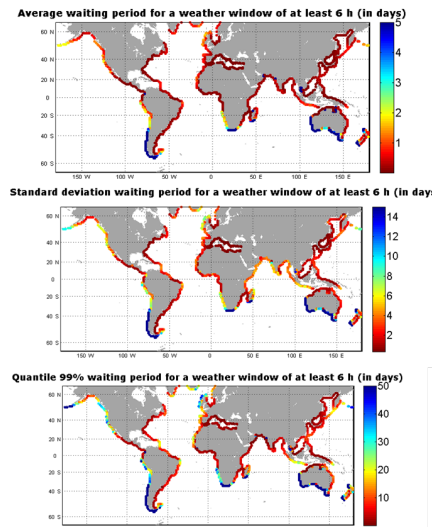


**Figure 5.30:** Mean, standard deviation and 99% quantile waiting period during winter time for a weather window of at least 6 h

The areas with the highest waiting periods (more than 4 days) correspond to the Chilean coast as well as the South coast of Australia. Apart from these areas with high waiting periods the majority of the areas around the East and West coast of America have waiting periods lower than 2 days.

In the middle panel the average of the yearly standard deviation of the waiting period is represented. As seen if the European coasts are compared the differences are much more reinforced. The Mediterranean coasts have an standard deviation lower than 2 days while the

west coast of Ireland have standard deviation around 10 days. This fact highlights the variability of the waiting periods in the Atlantic coast of Ireland and the UK, and it also demonstrates the high variability between summer and winter. On the other hand, as expected the areas with a higher variability are the Chilean coast and the South part of Australia with standard deviations around 15 days.

On the bottom panel of the figure the average of the yearly 99% probability percentile is shown. It shows the waiting period with a probability of occurrence of 99% during the year on average (average waiting period that is only exceeded by 1% of the waiting periods of the year). Then, it highlights the extreme events that normally occur during the winter. In this case the differences among the different areas in the world are much more reinforced. The areas with lowest waiting period correspond to the Mediterranean, the West coast of Central America, as well as the East coast of South America and the majority of the locations in the Indic ocean. All these locations have an average 99% quartile of less than 10 days. If the attention is focused on the locations with high waiting periods, it should be pointed out that unlike from the average plot at the top of the figure, the Atlantic coast of Ireland is characterized by very high waiting periods of around 40 days. For the case of Chile and South of Australia, as expected they have very high waiting periods of more than 50 days.

In Figure 5.31 the mean, standard deviation and the 99% percentile waiting periods are represented for the 12 h weather window. It should be pointed out that the geographic distribution is very similar to the 6 h figure. The main differences relate to the West coast of Ireland and the West coast of the US. In both places the average waiting period was quite low, however for the 12 h this average waiting period is higher. For this 12 h case the average waiting period goes to 3 days in both areas. This fact means that the weather windows in this area are generally short, and when the duration of the weather windows gets longer the waiting periods are much higher. For the middle panel the standard deviation plot for the 12 h weather window is shown. In this case the geographic distribution is very similar to the plot of the 6 h weather window. As seen in the bottom panel of figure 5.31, the 99% quartile of the waiting period for the 12 h weather window is very similar to the corresponding figure for the 6 h weather window (bottom panel of figure 5.30), although a general increase of the waiting period is observed as expected. Differences are explained later in Table 5.8.

In Figure 5.32 the mean, standard deviation and 99% of the waiting period for the 24 h weather window are represented. Despite being geographically very similar to the 6 h and the 12 h plots the way the North-West coast of UK and Ireland and the West coast of USA are much rougher than in the previous plots should be pointed out. This means that the weather windows tend to be short in these areas and when a longer weather window is needed then the waiting period increase dramatically. It should be pointed out that these areas with an average waiting period of 8 days and a standard deviation of 15 days, then it means that the variability between summer and winter is high and that it could go from 0 waiting periods during the summer to 23 (8+15)

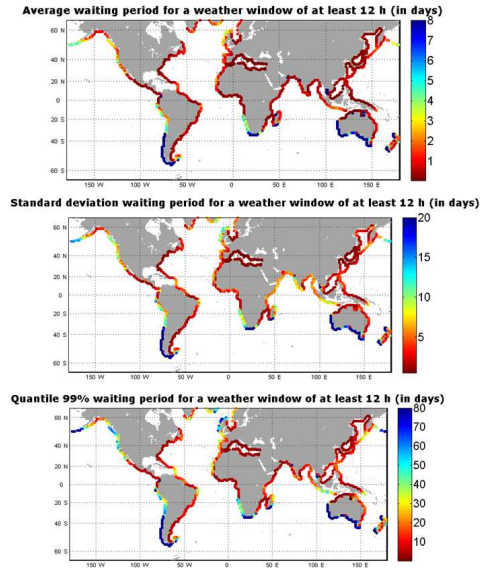


**Figure 5.31:** Mean, standard deviation and 99% quantile waiting period during winter time for a weather window of at least 12 h

days during the winter. The percentile plot is similar to the plots for 6 h and 12 h weather windows (but with a general scale increase as the weather window time increases). Differences are highlighted on Table 5.8. Here the percentage of nodes with waiting period of less than a certain figure for both the average and the 99 % percentile is represented.

As shown in table 5.8, 81% of locations have an average waiting period of less than 1 day for a weather window of at least 6 h. However for the 12 h and the 24 h only 67 % and 45 % nodes satisfy this condition respectively. This drop in the percentage of nodes is less dramatic for an average waiting period smaller than 7 days, that is less restrictive. In the case of the 99 % percentile percentile, 86% of the nodes have this waiting period percentile smaller than 30 days while only 60% of the nodes satisfy this waiting period percentile for a weather window of at least 24 h. It highlights the importance of having a clear picture of the necessary length of the weather window in order to do your maintenance operation.

On Table 5.9 the results of the waiting period for the selected locations are summarized. With respect to the European locations all of them have similar waiting periods for the average 6 h weather window. Differences are highlighted when longer weather window are used. For instance some locations such as Ireland have much larger waiting periods than other locations

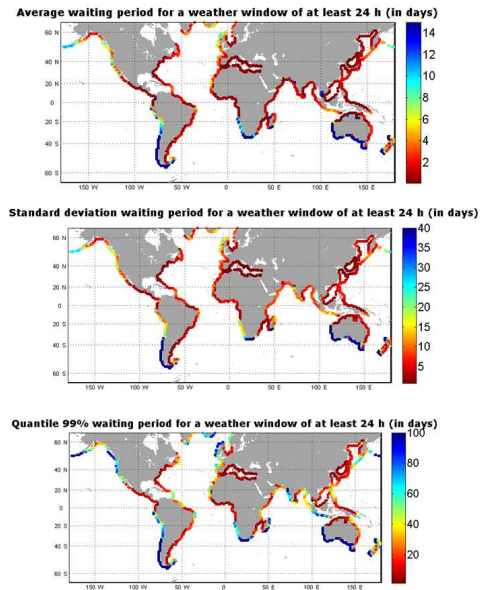


**Figure 5.32:** Mean, standard deviation and 99% quantile waiting period during winter time for a weather window of at least 24 h

(Spain and Portugal). For instance for the 24 h weather window duration the Ireland has a waiting period four times higher than Spain. However if the attention is fixed on the 99% percentile Ireland has a waiting period only 3 times higher than Spain. This means that the severe storms are more frequent in Ireland than in Spain, but the magnitude of the storms is similar on both locations. The fact that for a 6 h weather window Scotland has a 24 days waiting period for the 99% percentile, while Ireland has a 30 days waiting period should be also pointed out. However is opposite for the 24 h span because Scotland has a 30 days waiting period while Ireland is characterized by 24 days. This means that the length of the weather window is more important in Scotland than in Ireland.

On the other hand there are some locations like Chile or Australia where the waiting periods are very long compared to the ones in Europe. For instance in Australia for the shortest weather window duration the average waiting period is 3.18 days and for the case of Chile 7 days. On the other hand it should also be pointed out that waiting periods in Chile are much more constant during the year as the standard deviation is just 2.5 times the mean, while in Denmark for instance this number is 4.5 times. Having calm period during the summer however could help for the preventive maintenance activities.

Parameters	Waiting period for a 6 h weather window	Waiting period for a 12 h weather window	Waiting period for a 24 h weather window
Average waiting period <1 days	81%	67%	45%
Average waiting period <7 days	93%	91%	85%
Percentile 99% waiting period <30 days	86%	77%	60%
Percentile 99% waiting period <60 days	92%	89%	80%

**Table 5.8:** Percentage of nodes that satisfy a minimum waiting period

Both in Southern Chile and Australia, the 99% waiting period is very high, near two months in Australia and three months in Chile for the 6 h weather window, increasing to more than four months in both locations for the 24 h weather window. This fact shows the usually high reliability levels needed for a device deployed in these areas, as the periods of inaccessibility in winter are very long and then the devices should be designed to avoid failures and maintenance in the winter months. This is a difficult situation for wave energy prototypes due to the early stages of development and then these locations are less suitable for testing wave energy devices. Once the technology is mature enough to bear with these rough conditions then these locations become an interesting option for wave energy development. Nowadays, these sites are risky in terms of O&M.

Locations	Weather Windows per year									Waiting period (in days)								
	6 h			12 h			24 h			6 h			12 h			24 h		
	M	S		M	S		M	S		M	S	P99	M	S	P99	M	S	P99
North-West Denmark	904	79		436	39		203	20		0.15	1	4	0.34	1.4	7	0.8	2.51	13
West of Ireland	267	44		125	21		54	10		1.14	6	30	2.5	8	50	6	14	75
Chile	67	33		29	16		11	6		7	18	86	15.6	28	103	41	48	135
North of Spain	663	73		319	36		148	18		0.3	2	8	0.6	3	13	1.5	5	26
West Portugal	586	67		282	33		129	17		0.4	2	10	0.8	3.4	16	1.85	6	30
Scotland	313	50		146	24		64	12		1	5	24	2	8	44	5	14	78
South of Australia	116	38		51	18		19	8		3.2	10	55	7	17	85	20	33	126

**Table 5.9:** Mean (M), standard deviation (S) of the number of weather windows and Mean (M), standard deviation (S) and percentile 99% (P99) of waiting periods for the selected locations

It should be noted that on this waiting period analysis some differences have been noted between the average, standard deviation and percentile values among the different locations. This is due to the shape of the waiting period distribution on the different locations. For the 7 selected locations the whole set of waiting periods over the 60 year life cycle excluding the

zero values have been fitted to several probability distributions. In table 5.10 the best probability distribution fit for each locations is shown. It should be noted that all the locations fit either to log normal distribution or weibull min distribution. The difference between these distribution relies on the shape of the upper and lower tails. The lognormal distribution is characterized by a steep lower tail when the values are close to zero, on the other hand the weibull min distribution is characterized by a milder lower tail and a steeper upper tail when the values are high. In figure 5.33 the CDFs of the waiting periods for Australia, Denmark and Ireland are shown as well as the best fit for each one.

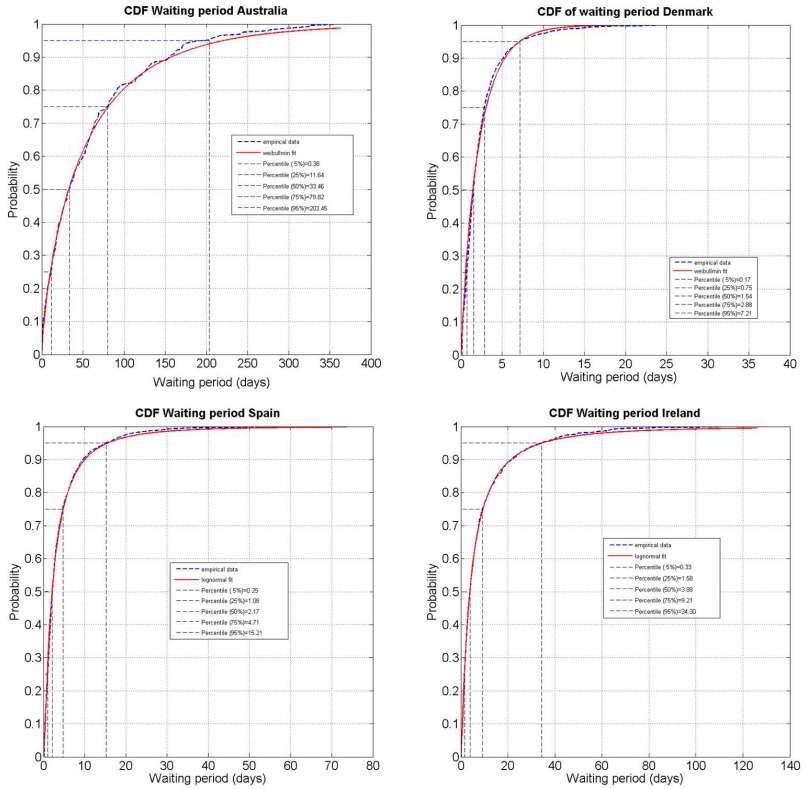


Figure 5.33: CDFs of waiting periods on Australia, Denmark, Spain and Ireland

Location	Distribution type
Denmark	Weibull min
Ireland	Log normal
Chile	Weibull min
Spain	Log normal
Portugal	Log normal
Scotland	Weibull min
Australia	Weibull min

**Table 5.10:** Type of best fit for each waiting period distribution

### 5.3.5 Operation and maintenance cost

In the last section, the weather windows and waiting periods were analyzed with respect to the maintenance operations. As previously explained the locations with rougher climate have larger wave energy resource, however they also have more difficult access for maintenance. In this section the influence of O&M parameters will be investigated in order to find out how the accessibility influences cost of energy and which locations have a good balance between harvesting energy and availability for maintenance operations.

For this purpose a generic wave energy device is taken from the previous subsection that is similar to Wavestar device (see Vidal *et al.* (2012)). Several variations of this device have been studied in the last subsection. From the three different types, the first one (tuned to a period of 4 s) is used again in this subsection.

In Figure 5.34 the average power production is shown. As expected, the highest power production is located in Southern Chile, North of Europe and South of Australia. However, these areas have rough climate in terms of O&M and then the periods of inaccessibility could deteriorate the economic performance of these sites

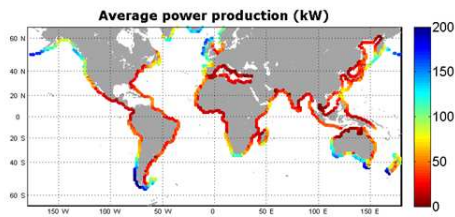


**Figure 5.34:** Average power production (kW)

For this study only corrective maintenance has been considered. Preventive maintenance is characterized by a long term planning and it is usually scheduled for summer months and therefore it is not the most useful indicator about how wave climate affects over productivity

and viability. This section is built according to a sequence of failure and corrective maintenance. It is assumed that after each failure all the maintenance team is ready to perform the operations as soon as a weather window is available.

A random set of failures has been simulated along the year and when the failure occurs the waiting period starts counting until a weather window takes place. Here, as in the other sections a wave height threshold of 1.5 m was chosen following O'Connor *et al.* (2013c) and O'Connor *et al.* (2013b). Also for the weather window required a length of 6h was chosen following Abdulla *et al.* (2011) from the experience gained with some WECs.

The cost per kW has been calculated dividing the cost of O&M by the harvestable power production during its life cycle. This energy is obtained multiplying the scatter plot of the harvestable sea states (available) by the power matrix of the device by the number of hours the device is harvesting energy along the year. For the cost of energy the O&M was taken into account with a combined approach:

The cost of the maintenance activities has been split up on three main costs:

- A cost per hour while the vessel is waiting to start the maintenance activities (during the waiting period) of 625 EUR/h
- A fixed cost referred to the mobilization of the vessel of 7000 EUR
- A cost per hour while the device is being repaired of 1250 EUR/h
- During the waiting period and the weather window while the maintenance operation is happening the device is supposed to be stopped. This means that during this time the device is not producing energy and it would be in survival mode.

Then, when a failure occurs the normalized O&M costs will be evaluated in terms of Euros/kWh taking into account the real cost of the operations and the time that the device will not be producing energy because it will be stopped. The climate database used for this study have 60 year wave data and then in order to get credible figures the life cycle of the WEC is assumed to be 25 years. Therefore a bootstrapping technique, based on Espejo *et al.* (2011), is performed in order to obtain 10.000 lifecycles of 25 years each obtained from the set of 60 year based climate database.

For the simulation of the failure events, the following simplification hypothesis are assumed:

- Three scenarios with 1, 3 and 5 failure events per year are considered for all locations, independently of the wave climate severity.
- The hour of failure is a random event with uniform distribution (between 0 and 8760). No seasonal influence on the failure time has been taken into account.

Then, on Figure 5.35 the maps of the normalized O&M costs are shown for 1, 3 and 5 failures per year. It is named as normalized because this cost just takes into account the O&M and the its only a pseudo-real cost. The average normalized O&M costs are divided by the power

production in each location to obtain the average normalized O&M costs in Eurocents/kWh shown in the figures.

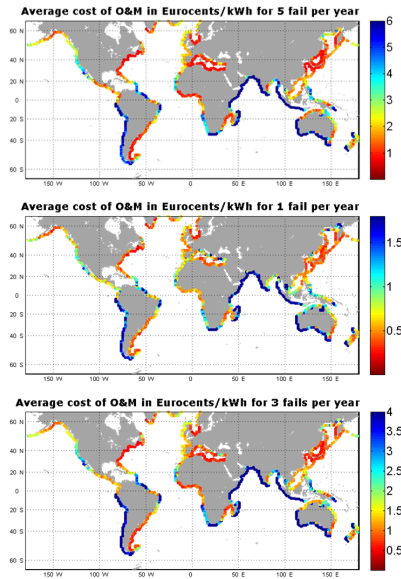


**Figure 5.35:** Normalized O&M costs with 1,3 and 5 fails per year

At the top of the figure the map for the normalized O&M costs for 1 failure per year is shown. As expected some areas (Mediterranean, Japan, East coast of the North America) with very low resource have very low cost (0.5 Eurocents per kWh). This is due to the absence of periods of inaccessibility and then when a failure occurs it can be repaired almost immediately. On the other hand there are some sites with very high resource and very high power production (i.e. Chile or South coast of Australia), however the number of weather windows is very low in these sites and the device could be stopped during a long time per year, and then the cost of O&M is large in these locations (more than 2 Eurocents/kWh). If figures 5.34 and 5.35 are compared it can be seen that while Southern Chile and Ireland have similar power production, O&M costs in Chile are three times higher than in Ireland because of the different accessibility levels. This is due to the similar resource figures but very different accessibility levels. On the other hand if the attention is focused on the west coast of India, the power production is low, while the normalized O&M costs is high due to the high waiting periods compared to the resource.

Some European locations have very good values for O&M, for instance all the North and West coast of Spain and Portugal have values around 0.5 Eurocents per kWh. There are also some

locations like the coast of Nova Scotia with medium resource levels (around 25 kW/m) and low costs in terms of O&M (0.2 Eurocents/kWh). These locations for instance are a good example of an excellent combination of resource and availability. Also the North West coast of Africa (Morocco) has low values for normalized O&M costs (near 0.6 Eurocents/kWh).

Figure 5.36 also represents 3 fails per year and 5 fails per year scenario. As the number of failures gets higher the possibility of distributing the failures along the year is higher. Then, the locations with mild climates (Mediterranean, East coast of USA) get lower values for the normalized O&M costs compared with the locations with rougher climates that may have available weather windows only in summer months, so that differences are reinforced.

In Figure 5.36 the normalized O&M costs are analyzed for the different selected locations. On the first figure the mean and the standard deviation are shown for 1 failure. There are two locations that stand out for the high cost. Australia and Chile have very high mean and maximum values for the normalized O&M costs. This is due to the absence of weather windows during long periods mainly during winter. This cost is very high for all the failure rates compared with the rest locations (for instance Spain has normalized O&M costs 1/3 lower), and then these locations would have more difficulties during the early stages of development.

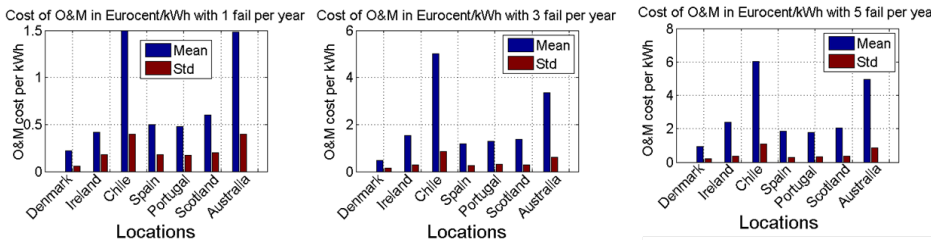


**Figure 5.36:** Normalized O&M costs for the different locations with 1,3 and 5 fails per year

For the European locations the lowest cost corresponds to Denmark with 0.22 Eurocent/kWh. As explained before the availability in this location is around 65% and the combination between resource and availability gives a low cost of O&M. For higher number of failures the cost remains the lowest for these locations as the availability varies from 40% during winter months to 80% during summer months.

On the other hand, there are some locations like Ireland or Scotland with low values of normalized O&M costs but due to the high resource in these locations. For the case of Ireland 0.4 Eurocents/kWh and 0.6 Eurocents/kWh for Scotland. These costs come from the balance between high power production and medium to low availability. It should be highlighted that when the number of failures gets higher the situation changes and the cost of O&M is higher for Ireland (1.8 Eurocents/kWh) compared to the 1.6 Eurocents/kWh in Scotland.

Other locations with milder climates as Spain and Portugal have a good combination between

resource and availability resulting on reasonable O&M costs (0.57 and 0.53 Eurocents/kWh, respectively). As the failure rates gets higher these locations achieve lower costs in comparison with the more energetic locations (i.e. 1 Eurocents/kWh in Spain compared to the 1.6 Eurocents/kWh of Ireland for the 3 fails per year scenario). This is also due to the redistribution of failures all along the year as the failure rate grows, and then locations like Portugal or Spain with high availability levels during summer (around 50%) achieve lower costs than more energetic locations with lower availabilities (30% for summer months in Ireland for instance).

This fact proves that milder locations like Denmark, Spain or Portugal could be good for early stages of technologies. In these stages the technologies are expected to have a higher failure rate, and then it could be proved that the normalized O&M costs is lower for these locations than the most energetic locations. However, once a technology is mature and its failure rate is low it could be deployed in the more energetic locations, like Ireland.

Then, it could be recognized how the higher the failure rate the more difference among mild and rough locations. If the failure rate is high then the probability of having a failure during winter months and the having a long waiting period is higher and then the mild locations with short waiting times get much lower values for the normalized O&M costs per kWh.

Finally, although locations with a mild climate have the lowest cost in terms of O&M a balancing want to be achieved by developers between absorbed power and O&M. To help this purpose Figure 5.38 is presented.

Here the normalized O&M costs for 3 fails per years versus the power production is represented. The goal here is obtaining the location with the highest power production and the lowest cost in terms of O&M. The location with the lowest power production and also the lowest cost is Denmark, and then it is taken as a base for comparison with the rest locations. For instance, Ireland has a cost for O&M that is 450% higher than in Denmark. However, in terms of power production it is 293% higher than in Denmark. If Scotland is taken for comparison it has a cost 381 % higher than in Denmark and a power production 255 % higher too.

On the other hand, locations such as Chile with a cost 900 % higher than in Denmark but a power production just 210%, or Australia with a cost 1011% higher than in Denmark but just 175 % higher in terms of power production. These locations then seemed not very recommendable for wave energy development because although the power production is high, the increment on the normalized O&M costs with respect to other locations is very high.

When analyzing the milder locations in Europe, as Spain is characterized by a power production that is 132 % higher than in Denmark, and the normalized O&M costs are 308 % higher. In Portugal these figures are similar, the power production is 143 % bigger and the cost is 361 % higher too. It can be inferred that although an increment on power production means also an increment on the cost of O&M this relationship is not linear.

From these figures it can be concluded that all the European locations can be considered as

sites recommended for wave energy conversion because all of them have reasonable figures in terms of O&M. However there are some differences that need to be considered. Denmark has a extremely low cost in terms of O&M, but the power production is low. This location could be useful for instance for the early development stages of new technologies.

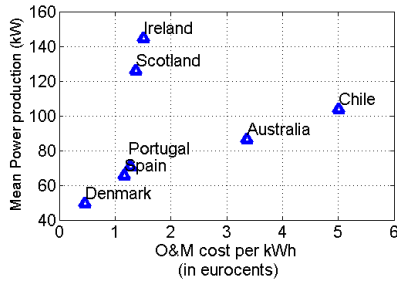


**Figure 5.37:** Normalized O&M costs (for 3 fails per year) and power production

On the other hand, Ireland has very high power production but a quite mild normalized O&M costs. This location is the most energetic one in the European set and then it would be a good location when a technology is mature and the failure rate is low.

Apart from the studied locations from the maps it could be inferred that apart from the European locations there are some very good sites in terms of power production and normalized O&M costs. For instance for the 3 failure rate the coast of Nova Scotia has a power production of 91 kW with a normalized O&M costs of 1.1 Eurocents per kW. This location has a perfect balance between the resource and weather windows for O&M. Also in the West coast of North America, for instance in the Oregon coast the power production values are quite high (91 kW) and the cost of O&M is medium (2.5 Eurocents/kW).

### 5.3.6 Conclusions

In this section an analysis of the O&M main parameters is performed from a global perspective. The met-ocean data is taken from a 60 year global reanalysis database extracted from Reguero *et al.* (2012). This database contents 1188 nodes all along the coastline of the globe with hourly sea state parameters.

Firstly the availability and accessibility levels are studied in the different regions of the world. From this study it is concluded that the accessibility has a extremely high dependence on the wave height threshold. For very restrictive thresholds (1 m or 1.5 m) the accessibility in the regions with high resource (high latitudes) is very low (less than 20%). Here, locations with very high resource (Chile and Australia) have very poor accessibility levels. In the case of Australia for instance, even for the 3 m threshold the accessibility is 50%, that is poor for this

limit. If Ireland and South Australia are compared, the differences are noticeable. Both points have the same resource (62 kW/m), however the levels of accessibility for all the thresholds are much higher in Ireland (60%).

There are also some intermediate situations, in the case of Spain and Portugal, both locations have a similar resource and similar accessibility levels. The mean wave energy resource is around 30 kW/m and the accessibility levels range from 25% for the 1m threshold to the 83 % at the 3 m threshold. In the case of Scotland, the wave energy resource is high (50 kW/m), however the levels of accessibility are low (ranging from 8 % at the 1m threshold until 64 % at the 3m threshold). For the seasonality the difference on accessibility between winter and summer months is high, almost doubled, depending on the threshold level chosen. If the attention is fixed on winter months (where O&M could happen because of failures) the differences are high among the different locations. For instance for a threshold of 2 m the winter accessibility levels are 40% for Spain, 15% for Ireland, 38 % for Portugal and 15% for Scotland.

Secondly, a study of persistence of weather conditions is performed for the weather window and waiting period analysis. A difference is found when the duration of the weather windows is elongated. The difference between mild climates and rough climates is highlighted as the length of the weather window gets higher. From this study it is also concluded that all the coastline around the Indic ocean is hard in terms of high waiting periods. Also the East coast of South America is characterized by a low number of weather windows and waiting periods of several months.

Finally, the cost of O&M for a device extracted from previous subsection in this chapter was assessed. This cost was evaluated with different failure rates assuming failure like a random event along the year. For low failures rates some locations like Ireland show a low normalized O&M costs per kWh. However as the failure rate gets higher these sites have higher cost compared to milder climates (Spain or Portugal). In these terms some sites are found to have a good balance between power production and normalized O&M costs. For instance Scotland with a cost of 1.8 Eurocents/kWh and a power production of 130 kW. On the other hand some locations like Australia or Chile are found to have very high normalized O&M costs compared with other locations with power production not so high in percentage. For example, Nova Scotia, with a resource of 25 kW/m and O&M cost of 1.2 Eurocents/kWh has a good balance between availability and resource.

From this study it is also concluded that there are some sites with a very high resource, for instance the East coast of Ireland (55 kW/m) that are valid for mature technologies with low failure rates. However, for prototype testing when failures are much more probable milder locations are suggested (Spain, Portugal) because they would have lower normalized O&M costs for these failure rates. Next section further investigates the relation between reliability and met-ocean conditions with the goal of targeting locations for wave energy development.

## 5.4 Linking O&M and Reliability assessment on wave energy converters

### 5.4.1 Introduction

In the previous section, the importance of O&M has been highlighted in the different coastal areas of the globe. Balancing resource, availability and accessibility was identified as a key step in order to determine the areas with best characteristics for wave energy development. O&M is identified as the consequence of component obsolescence and component reliability and then an identification of the state of development of reliability studies within the marine energy industry becomes significant for the purpose of this thesis.

Reliability assessment on wave energy converters has been identified as one of the most important challenges of the marine energy industry nowadays (see UKERC (2007) and Department of Energy and Climate Change (2010)). Mackay *et al.* (2010) identified three main sources of uncertainty that influence the estimates of achievable annual electricity production:

- Uncertainty regarding energy resource conditions at the project site.
- Conversion uncertainty, i.e. variations and unknowns along the conversion chain wave to wire.
- Uncertainty about the device availability.

While the uncertainty of wave resource conditions can be estimated, the availability of devices is regarded as perhaps the most difficult to quantify ; Mackay *et al.* (2010) . The main reasons are that (i) it is difficult to predict failures for a new technology and (ii) operational experience is scarce. In particular, even the application of proven components and equipment in a harsh dynamic marine environment under significantly altered load conditions, implies large uncertainties regarding failure mechanisms and frequency. These uncertainties may lead to either costly design safety factors or field failures both of which would impede project viability.

Reliability assessment on wave energy devices is still a topic under R&D and a limited number of studies have investigated this topic. On the last years the main advancements rely on different techniques to proceed with failure simulation on Wave Energy Converters. For instance, Thies *et al.* (2011b), showed how a generic reliability test approach employed in other industries could be used to provide evidence of component reliability under specific operational (test) conditions. The case study for a mooring component test applied a rainflow analysis procedure to available tank test data in order to establish a possible accelerated component test regime, in this way one year operational loads under the assumed wave tank conditions could be simulated in approximately 60 h of testing. Also, Thies *et al.* (2012) investigated some sources of uncertainty on failure rates on wave energy converters. The modeled examples show how failure rate distributions are influenced through the incorporation of engineering knowledge and test data. They concluded that the application of the Bayesian method helps to reduce

the uncertainty of component failure rates and to improve the confidence in system reliability estimates for emerging technologies.

Some of the latest studies refer to Ambühl *et al.* (2014a). On this paper one example of an ultimate limit state modeling a structural failure mode of WECs is shown. The example focuses on sliding of the gravity based foundation due to extreme wave and wind loads including extreme loads due to failure of mechanical and electrical components as well as the control system. In addition, Ambühl *et al.* (2014b) concluded that the uncertainties related to wave loads have larger impact on the structural reliability compared with wind loads. Therefore, for wave energy converters stochastic modeling of wave conditions is more important compared with wind modelling.

However, there are few studies so far that link the simulation of failure and repair operation continuously. This section addresses this gap and simulates different failure and repair scenarios along the coast of the globe, identifying then the target areas for different reliability levels. Therefore, an assessment of the adequacy of certain local met-ocean conditions for the the different reliability levels is presented. A roadmap for wave energy developers regarding the best areas to test the devices depending on the achieved reliability level is presented on this section, adding some steps to the classical development pathway.

#### 5.4.2 Failure simulation background

Reliability is usually defined as the ability of an item to perform a required function under stated conditions for a stated period of time. The qualitative interpretation is that the item is free from operational failures. One of the most studied topics in the last decades was the statistical approach to risk and reliability analysis. A key point is selecting the adequate distribution in order to have a correct and accurate failure simulation. Although lots of distributions have been proposed in literature the most common correspond to the exponential and Weibull distribution.

In this piece of work the Weibull distribution is used. The Weibull distribution is one of the most widely distributions used in reliability applications as it is very flexible and the choice of different shapes thus provides a good statistical fit to most of the data collected in the field. The probability of failure is then described by a 3 parameter Weibull:

$$F(t, \alpha, \beta, \lambda) = 1 - e^{-\left(\frac{t-\lambda}{\beta}\right)^\alpha} \quad (5.6)$$

where  $t$  represents the time.

The distribution characteristics of the distribution are controlled by each parameter. The exponent  $\beta$  governs the shape of the distribution at it is usually named shape parameter. The scale of the distribution is controlled by the scale parameter  $\alpha$ . The location, or  $x$ -offset of

the distribution (sometimes called guaranteed life) is controlled by parameter  $\lambda$ . In reliability applications, normally a 2 parameter Weibull is used and then the parameter  $\alpha$  is assumed to be equal to 1, see Thies *et al.* (2011b).

The mean time to failure (MTTF, or failure rate) is defined for a Weibull distribution as (for detailed explanation see Thies *et al.* (2011b)):

$$MTTF = \int_0^{\infty} (1 - F(t, \alpha, \beta, \lambda)) dt = \lambda + \alpha \Gamma\left(\frac{\alpha+1}{\alpha}\right) \quad (5.7)$$

when  $\Gamma$  is the gamma function and the three parameters Weibull distribution is simplified to a two parameter distribution assuming  $\alpha = 1$  then the  $MTTF = \frac{1}{\lambda}$ , that is known as failure rate as well.

When simulating failures along the life cycle of a component, the bathtub curve is normally used due to its excellent representation of the life of mechanical components. It comprises a hazard function consisting of three differentiated parts, that are modeled with three Weibull distribution with different  $\beta$  parameters:

- Early infant mortality failure; with a decreasing failure rate ( $\beta = 0.5$ )
- Constant random failures ( $\beta = 1$ ); corresponding to an exponential distribution
- Wear-out failures; with an increasing failure rate ( $\beta = 3$ )

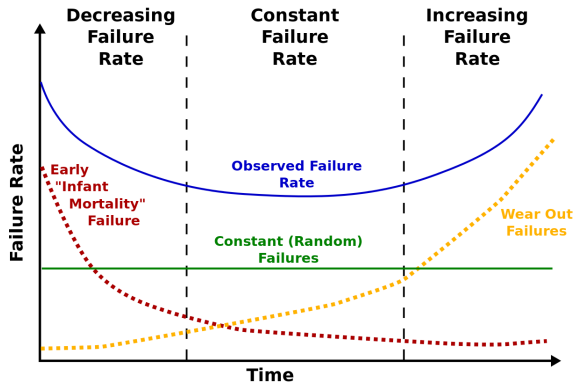


Figure 5.38: Bathtub curve

Once a failure in any component has happened, the next step is the repair of the damaged system. Normally the repair operation can be also modeled with a statistical distribution. Often, the lognormal distribution is used within this purpose (see Bovaïrd and H.Zagor (2006)).

### 5.4.3 Bathtub curve & O&M

In mature industries, such as the oil and gas industry, there is a considerable history and experience in the use of specific mechanical components, and consequentially a large volume of reliability data is available. In some cases this has been collated in databases (such as Reliability data handbook (OREDA)), which are consulted by reliability analysis for use in simulations.

On the other hand, while this data includes several components which are regularly employed in the design of new wave energy converters, there are several problems with the application of these data in reliability analyses for these new systems. The most common problem is often the novel use of an existing technology, either with a new duty cycle, or in a new environment. Such changes in the way a component is employed will have a large impact on the time to failure and the critical failure modes of the technology, and the existing failure data may no longer be directly applicable.

Therefore, information about the failure rates in WECs under real sea conditions is almost in-existent or it is not shared publicly due to IP reasons. Some information about sub-components failure rates can be found in Thies *et al.* (2011a). In this case based on a reliability block diagram, some failure rates are proposed for the different sub-components of the WEC (structure, moorings, transmission and PTO). The failure rates of these subsystems ranged from 0.47 times per year (transmission) to 2.42 times per year (for the PTO).

In this chapter, a simulation of different failure scenarios under the bathtub curve is performed. Due to the scarcity of the data, no components are detailed on this analysis, only three generic failures based on the different failure/downtime scenarios. According to Crabtree (2012) normally the failure rates and the downtime are often inversely proportional, what means that a very often failure has a low downtime and a very rare failure normally has a long downtime. Following this same procedure, the failure scenarios simulated on this subsection are detailed in Table 5.11. The simulation procedure is explained on figure 5.39. A failure simulation is first performed based on the parameters  $\beta$  and  $\lambda$  detailed on Table 5.11. Secondly, once the failure happens an algorithm calculates the waiting time until the repair operation is initiated. Secondly, a downtime simulation is performed based on the lognormal with parameters  $\mu$  and  $\sigma$ ; see Bovaird and H.Zagor (2006). Once the cycle is finished another simulation is performed up to 10.000 cycles.

These failure scenarios were simulated along the data points used in the previous section (from Reguero *et al.* (2012)). In order to obtain statistically significant results a series of 10.000 lifecycles (failure-repair) were simulated at each point for each of the scenarios described in Table 5.11. It should be noticed that although a distribution of waiting periods was obtained in the previous subsection, it was decided to perform the simulation again due to the fact that in this case the distribution used for the failure is Weibull (instead of Normal in the previous subsection). In figure 5.40 the mean downtime for these selected locations at the different

Scenario	Failure rate $\lambda$ (Weibull)	Downtime(Lognormal)	$\beta$
1	High (3/year)	Low ( $\mu = \sigma = 9h$ )	0.5
			1
			3
2	Low (0.25/year)	High ( $\mu = \sigma = 36h$ )	0.5
			1
			3
3	Medium (0.75/year)	Medium ( $\mu = \sigma = 16h$ )	0.5
			1
			3

**Table 5.11:** Combination of parameters for simulation

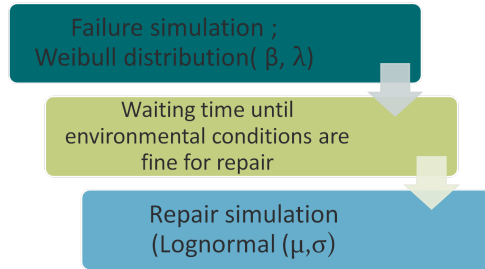


**Figure 5.39:** Schema of the simulation

studied scenarios is shown. Mean downtime is defined as the mean time interval between the component failure until its return to work after repair. This parameter includes the waiting time the repair team should spend until the environmental conditions are suitable for maintenance and the repair time itself. It should be taken into account that, similarly to the previous section, the threshold for unacceptable conditions was selected with  $H_s = 1.5m$  although in a more complete analysis more environmental factors should be taken into account.

Figure 5.40 shows the three scenarios with decreasing failure rate with time (top left), constant failure rate (top right) and increasing failure rate (bottom). As figure 5.40 shows the difference between the different parts of the bathtub curve ( $\beta$ ) is very small in all the locations. It can be concluded that when the failure rates are still uncertain an exponential distribution ( $\beta = 1$ ) is acceptable. Regarding the different scenarios with the distinct failure rates, the mean downtime is similar for all of them. Nevertheless, in all the locations the failure with  $\lambda = 0.25$  is the one with highest downtime, specially noticeable in the most severe locations such as Australia. This fact means that although the failure rates are low, the downtime is very high, and then the availability of this long weather windows along the year is extremely low. This issue leads to the conclusion that fails with very long repair time should be avoided by converters in order to keep availability as high as possible. It should be noticed that the mean downtime is not calculated on

a yearly basis, this means that the plotted mean downtime corresponds to the average downtime independently of the failure rate or the times this failure is produced during the year. On the other hand, the availability plot that is explained in the next paragraph corresponds to the yearly availability, that means that the availability is independently calculated for each of the years of the database and then it is averaged.

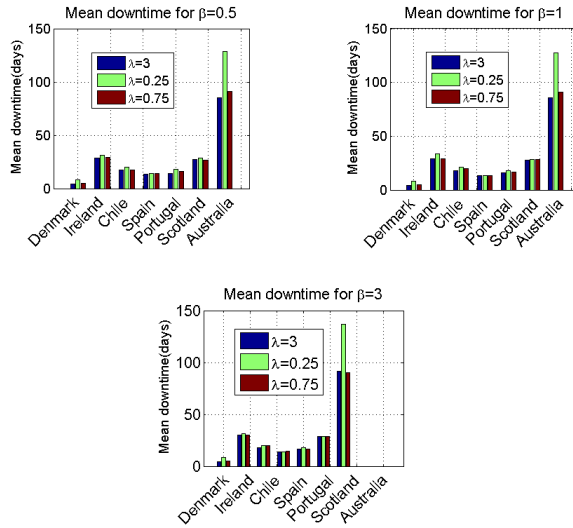


**Figure 5.40:** Mean downtime for the different aforementioned scenarios

In figure 5.41 the mean annual availability (defined as the mean percentage of time that a device is stopped, and then not producing energy, because either it is waiting for repair or is being repaired on a yearly basis) is shown. Oppositely to the last figure, here the differences within the different failure rates ( $\lambda$ ) are clearly represented. For instance, it is noticeable how the failure rate has a larger impact on availability on the rough climates, such as Ireland or Australia, indeed in Australia is reduced by 20% from  $\lambda = 3$  to  $\lambda = 0.75$ . In contrast with figure 5.40, when the availability is analyzed on a year per year basis, the failure rates becomes the most important parameter despite the duration of the operation. Then in this figure, the availability in all the locations decreases as the failure rates increases, no matter the duration of the weather window. With respect the influence of the shape parameter of the bathtub curve, it can be concluded that the first period (infant mortality) and the third period (wear out failures) are the most dangerous in terms failure and O&M assessment. However it could be seen that in average terms the influence of this parameters (shape of the bathtub curve) is limited and then for this kind of study an exponential distribution (constant failure rate) can be used. For

more specific issues, mainly related with specific locations and if the failure rate evolution of the specific components are known it will be useful to set the time evolution of the normalized O&M costs through the life cycle of a device.

In the analysis of this figure the difference between the downtime in this figure and the waiting periods of the table 5.9 in Australia and Chile is highlighted. The reason of this difference comes from the different nature of the problem analyzed. In the previous subsection the waiting period was computed as the time in between weather windows, considering that if a very long period of accessibility is available (and then several weather windows in a row) the waiting period in between is counted as 0. For this reason, in Table 5.9 Australia appears with a higher number of weather windows than Chile. Australia's conditions are much more seasonally dependent than Chile, and then in summer the periods of accessibility are long and the waiting period is lowered by the 0 values during summer. Despite this fact, in figure 5.40, the downtime in Australia is much higher than in Chile. This is due to the fact that the distribution of the weather windows along the year in Chile is equally distributed along the year, while in Australia there are several weather windows in a row during the summer and there could be no weather windows during the whole winter. For this reason the downtime appears much higher in Australia than in Chile.

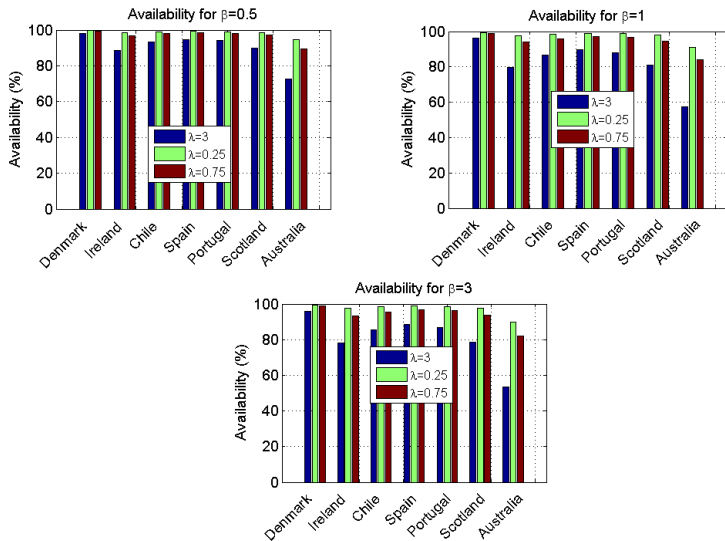


Figure 5.41: Availability(%) for the different aforementioned scenarios

#### 5.4.4 Maintenance Scenarios

Operation and maintenance may lead to a significant percentage of the cost of a wave energy project. The figures existing in literature (see O'Connor *et al.* (2013a)) could range from 10% to 30% of the final budget. Through this thesis it is clearly shown that most technologies are not ready for commercialization yet and they are still being tested at open sea conditions. Normally, the established test sites for wave energy prototypes are placed in high resource areas such as North of Scotland (EMEC), or Belmullet, within the Westwave project (West of Ireland). However, it is not clear if for the current state of the technology these high resource areas (and then rough wave climates) are recommended or areas with lower resource could be included into the test sites portfolio, in order to lower the costs of immature technologies in the open sea testing conditions. In this subsection, an assessment of the normalized O&M costs from a developers perspective is performed. Assuming that the normalized O&M costs correspond to a fixed part of the budget and assuming also a target cost of 0.04 Euros/kWh (taken from the offshore wind industry, see Khron *et al.* (2009)) two different scenarios in terms of normalized O&M costs are analyzed on this section in order to deepen into the understanding of balancing accessibility and resource. It should be noticed that although O&M during the night hours could be not possible some time, in this piece of work it has been assumed that night maintenance is feasible, based on the findings of Abdulla *et al.* (2011).

In table 5.12 the three scenarios are shown. Scenario 1 represents an O&M scenarios with fixed costs for all the locations. It tries to perform a fixed and fair comparison among the locations in terms of accessibility and availability. Scenario 2 represents a more real approach to O&M where the waiting costs are just reduced to the first 15 days (in the case of long waiting period areas). In this rough locations the developers arrange this kind of deals with the vessels companies in order to ensure repairing but not paying for excessive times. This scenario implies a favorable situation for the locations with a rough wave climate. On the other hand, Scenario 3 represents a combined approach with corrective and yearly preventive maintenance. In the rough locations, it is usual to perform an annual summer refit in order to check the components and find out if any repair is needed during the summer months, where the conditions for maintenance are better. This approach could lead to lower maintenance costs foreseeing the failures with the preventive maintenance and then avoiding long unavailable and inaccessible periods of time during winter.

On the last subsection, a failure-repair simulation was performed based on Table 5.11 and some failure scenarios with different failure rates and downtimes and the different parts of the bathtub curve. The influence of the shape of the weibull distribution on average terms was found to be limited, and for this reason, a new simulation with a fixed  $\beta$  parameter (1, that means that is an exponential distribution) is performed in this next section. Also, in order to perform another comparison the same duration of the repair operation is set for all the failures (12 h). Therefore, a range of failure rates (6,3,1,0.75,0.5,0.25,0.1,0.05 fails per year) with common repair duration

Scenario	Type of maintenance	Costs
1	Only corrective	Mobilization cost= 7000 EUR Vessel waiting cost= 625 EUR/h Vessel Repairing cost= 1250 EUR/h
2	Only Corrective	Mobilization cost= 7000 EUR If Waiting time<15 days (Vessel waiting cost= 625 EUR/h) If Waiting time>15 days (Vessel waiting cost= 625 EUR/h only for the first 15 days) Vessel Repairing cost= 1250 EUR/h
1	Corrective + Annual Preventive	Mobilization cost= 7000 EUR Vessel waiting cost= 625 EUR/h Vessel Repairing cost= 1250 EUR/h

**Table 5.12:** Combination of parameters for simulation

(12 h) simulated with an exponential distribution ( $\beta = 1$ ) is performed.

## Results

Based on the aforementioned assumptions, the results for Scenario 1 are presented. First of all, a figure with the availability values for three reference locations is shown (see 5.42). Availability is normally defined on time terms, taking into account the time when a prospective device will be stopped and then it will not produce energy. In this figure, this approach is compared with another definition of availability, based on resource assessment. Normally when a device is not working, because a component has failed and maintenance is not possible ( $H_s > 1.5m$ ), the resource that is not being harvested corresponds to the most powerful sea states, due to the threshold for the maintenance operation. Therefore, in this case availability (resource) is defined as the percentage of resource that is not captured by the device because the device is under maintenance or is waiting for repair (and then it is not harvesting energy).

As figure 5.42 shows the difference between the time availability and resource availability increases as the failure rate increases. It is noticeable how the availability of the resource is always lower than the time availability. This fact means that when a device is stopped and it is not harvesting energy, the energy that is not being captured does not correspond to the mean resource, it corresponds to the higher portion of the resource. It should be also noticed that the highest difference between resource and time availability corresponds to Denmark. This is due to the fact that, although this site has mild conditions, and the slope of the availability curve is mild as well, the time when the device is not available and not accessible corresponds to periods of time of very high resource, very separated from the mean resource. In Ireland and

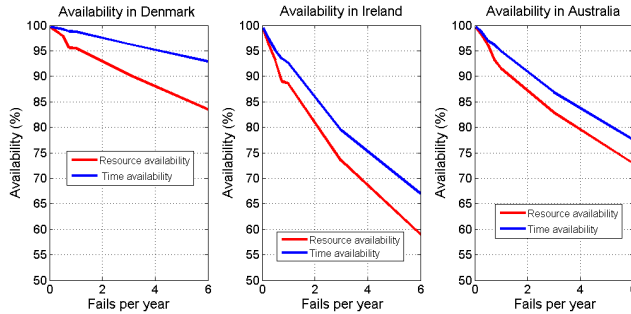
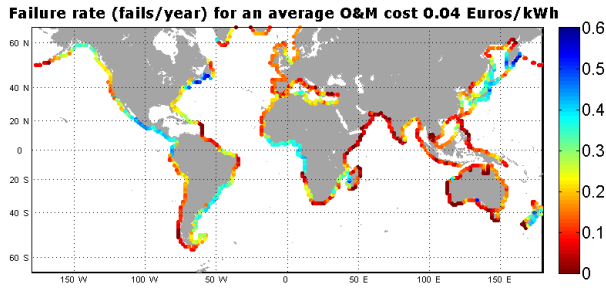


Figure 5.42: Resource and time availability in Denmark, Ireland and Australia

Australia, the slope of the curves is much higher although the difference between the time and resource availability is lower due to the severe conditions of both locations. It should be noticed that the availability currently proposed for offshore wind is around 90% (see Crabtree (2012)) and in the Australia and Ireland sites this level of availability is only obtained with 1 fail per year.

The results of the Scenario 1 are also shown in terms of the failure rate needed in order to spend a certain amount of money per kWh on O&M. In this case the cost analysis of the O&M has been performed the same was as the previous subsection with the cost scenarios described in Table 5.12. As explained before, a fixed cost of O&M is set to 0.04 Euros/kWh based on the state of the art of offshore wind (see Khron *et al.* (2009)). In order to make this map technology blind certain assumptions are made in terms of power capture. A capture width ratio (or efficiency of the conversion) of 20% has been assumed for all the data points, taking into account the CWR of current systems (see Hals (2011)). Also a 20 m water front has been assumed in order to compute the Annual energy Production. Also it should be pointed out that the power production takes into account the time where the device is not operating due to failure or during the waiting period.

In figure 5.43 the failure rate in fails per year is represented for the different coastal locations for an average O&M cost of 0.04 Euros per kWh. As the figure shows, the failure rates in all the locations are relatively low, taking into account that the current overall failure rates for offshore wind turbines are around 2 fails per year (see Van Bussel and Zaaier (2001)). It is noticeable how a large amount of locations need very low failure rates values (0.1-0.2 failures per year). On the other hand, it should be highlighted how some locations stand from the others with relatively high failure rates values (i.e. Mexico, Nova Scotia in Canada or Brasil). These areas have an excellent balance of resource and availability and then they should be considered as sites for the first 1:1 scale deployments, in order to prevent excessive normalized O&M costs.



**Figure 5.43:** Failure rates needed for an average normalized O&M costs of 0.04Euros/kWh

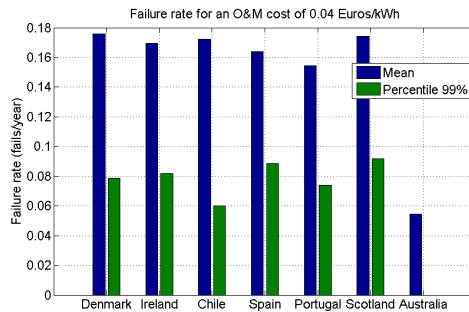


**Figure 5.44:** Failure rates needed for an average normalized O&M costs of 0.04 Euros/kWh on selected locations

In figure 5.44 some of the selected locations are further analyzed. As the figure shows, despite the differences on resource and availability on the different sites, the failure rates are very similar in all the locations. This means that availability/accessibility and resource are balanced in all these locations. For instance, the comparison between Ireland and Denmark should be pointed out. Denmark has an average resource of 12 kW/m while Ireland has an average resource of 62 kW/m. On the comparison made in figure 5.44, both locations achieve the same failure rates for an average normalized O&M costs of 0.04 Euros/kWh. This means that despite the differences on the ocean wave climates, both locations are similar in terms of reliability. Also the figures show the values of the failure rates needed in order to achieve a cost of 0.04 Euros/kWh with

a probability of 99%. As the figure shows, most failure rates values are reduced to half the value of the mean value, achieving values of 0.06 fails per year. These values are unrealistic as the standard failures of the components on the offshore wind industry range from 0.02 to 0.34 failures per year (see Van Bussel and Zaaier (2001)).

In figure 5.45 the failure rates of the locations considered in this study have been plotted in a histogram. As it shows, there are three different parts. A group of locations with failure rates lower than 0.12 failures per year, considered as high reliability locations, a group of locations with failure rates in between 0.12 and 0.32, that could be considered as intermediate reliability locations and finally a group of locations with low reliability (higher than 0.32 fails per year). The separation of the coastal location in these three groups is performed in figure 5.46. This figure highlights three different types of areas that could be inserted on the wave energy development scheme (see figure 5.47). Examples of low reliability needed areas, some sites such as the Pacific coast of Mexico, Nova Scotia in Canada, the Brazilian coast, the East part of New Zealand and Japan have a good balance between resource and availability and accessibility. Therefore, these areas, could be considered as sites with good characteristics for the first stages of sea trials of a device, when the reliability is still low, the failure rates are high and then the accessibility is a key factor. On the other side, there are areas, normally where the resource and accessibility are unbalanced, for instance all the Atlantic coast of Europe, the West coast of the US and the Chilean coasts. These sites need very reliable devices in order to be economically efficient in O&M terms. Therefore these areas can be recommended for wave energy development once the devices have been tested on the low and medium reliability areas. These areas could be useful for wave energy exploitation but its use as testing areas could be dangerous in terms of the high normalized O&M costs.

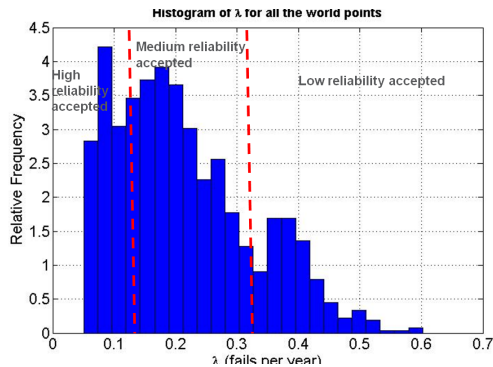


**Figure 5.45:** Histogram of failures per year for all the coastal locations

In figure 5.47 an schema of the proposed steps in the development path of a wave energy converter is shown. Once the device has been tested at a small and medium scale at some tank

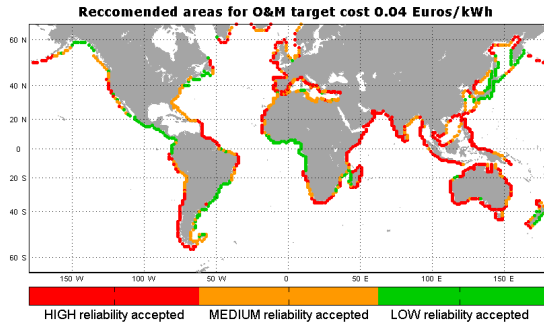


**Figure 5.46:** Recommended areas for wave energy development as a function of failure rates Scenario 1

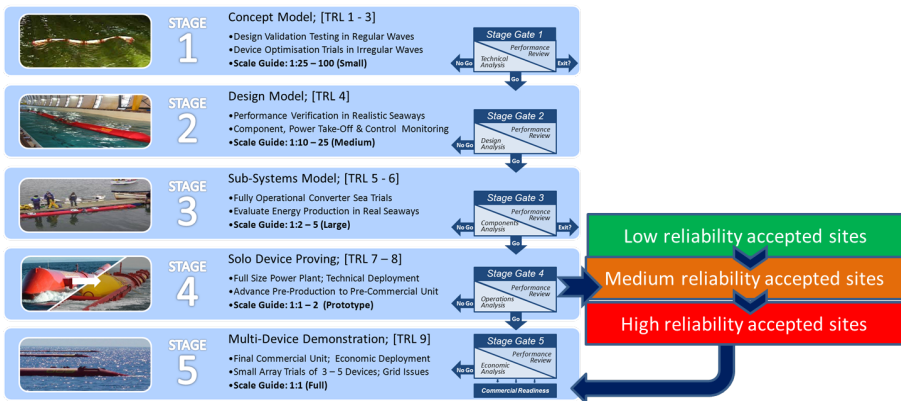


**Figure 5.47:** Stages of development for a wave energy prototype

facilities and after the individual components have been tested at 1:2 or 1:1 scale the period of full scale sea trial tests. As mentioned before it is recommended to split up the stage 4 in 3 different steps, a low reliability trial, when the devices have still a high failure rate, an intermediate step in areas with medium reliability and finally a full scale trial in areas with high resource and prospective development of multi-device farms.

After the results of scenario 1, the results of scenario 2 are analyzed. As table 5.12 shows, scenario 2 represents a milder scenario for rough locations, as the costs for the waiting time is limited to a maximum of 15 days. This scenario represents a closer to reality approach, based on some conversations of the author with vessel companies on different locations. Normally the developer and the vessel company agree on some terms in the case that the device fails in winter and the waiting time is very high.

The recommended areas for Scenario 2 are shown in figure 5.47 instead of the failure rates map in order to appreciate the difference among scenarios. In this second case the low reliability areas (green) remain the same as the Scenario 1. This means that despite the changes on the costs, the areas adequate for first deployments remain the same, and then it is concluded that these areas have a very good balance of resource and availability. In this Scenario 2 some of the areas that required high reliability systems under Scenario 1 (red ones) admit in Scenario 2 medium reliability systems (orange ones). In this scenario, for instance all the Atlantic coast of Europe relies on the medium reliability area. In this case only some low resource areas such as the Caribbean, most of the Indic coasts of Africa and Asia or some parts of the Mediterranean rely on the high reliability accepted category to achieve the fixed O&M cost of 0.04 Euros/kWh. In this case these areas are not balanced between resource (low) and accessibility (medium to high). Some areas such as the East part of Brasil have a mild resource but its accessibility is low compared to this level of resource.

The scenario 3 presents an approach of combined preventive and corrective maintenance. It is known that an adequate preventive maintenance could save time and cost in an offshore environment (see Rademakers *et al.* (2009)). There are lot of studies regarding how often the preventive maintenance should be performed. However, due to the immaturity of the wave energy industry there are no studies concerning this specific topic yet. Some works, such as Starling (2009) suggest to perform an annual preventive maintenance during the summer months. This preventive maintenance is normally advised in locations where the accessibility is low during winter months.

The preventive maintenance consists of a visit to the device, just to check if all the components are working properly or if any deficiency is found, then proceed to its repair. When this visit is performed there is a probability of detection of failure. This process has been simulated for offshore wind turbine with the equation proposed by Nielsen and Sørensen (2011), where the probability of failure detection is simulated based on the failure level (meaning how advance is the failure). The probability of detection is simulated by:

$$PoD = P_0(1 - \exp(\frac{-D}{\delta})) \quad (5.8)$$

where D is the damage level (days since the component was installed/mean life of the com-

ponent),  $P_0$  is the maximum probability of detection, and  $\delta$  is the expected value of smallest detectable damage. For this case study the same values as Nielsen and Sørensen (2011) were selected for  $\delta = 0.4$  and  $P_0 = 1$ . Annual preventive maintenance is specially beneficial on some locations (specially the ones with a severe climate) but not in all of them. Figure 5.49 shows the difference in O&M cost per kWh of Scenario 1 and Scenario 3 for one failure per year on average are shown. The negative values mean that preventive maintenance is not worth it and the positive values mean that preventive maintenance is worth in cost terms. As the figure shows most areas such as the Atlantic coast of Europe, the West coast of the US, the Chilean coast and the South and West Australian coasts have positive values so that a yearly preventive maintenance is recommended to save costs. In the opposite case, there are some areas with high accessibility in winter months (and normally low resource) such as the Mediterranean, the east coast of the US or the North coast of Australia where the impact of preventive maintenance is negative in terms of cost.

In figure 5.50 the failure rates for a mean normalized O&M costs of 0.04 Euros per kWh is shown. If this figure is compared with figure 5.43 some differences could be highlighted. Most severe locations as the Chilean coast or the Atlantic coast of Europe admit higher values of failure rates under Scenario 3 (near 0.25 failures/ year). It could be concluded that in most locations an annual preventive maintenance could reduce the reliability that the device needs to achieve in order to have a fixed normalized O&M costs.

Finally, the best case scenario of the three scenarios analyzed on this section is presented in figure 5.51 as the recommended areas for each stage of development of a wave energy converter. As this figure shows most green areas remain the same as in the scenario 1 and 2 figures. This means that whatever the cost or maintenance scenario is considered the areas recommended for devices on the first 1:1 scale test and low reliability are the same. These areas are mainly the Pacific coast of Mexico, Nova Scotia in Canada, the Brazilian coast (below  $20^{\circ}\text{S}$ ) and the east coast of New Zealand. With respect the medium and the high reliability category, it could be seen how a lot of areas in the red category in the first scenario migrated to the medium reliability scenario. This means that with an adequate planning and scheduled preventive maintenance, some areas such as the Atlantic coast of Europe may be considered as an important second step for sea trials. Lastly, the red areas correspond to areas where the balance between resource and accessibility is not achieved, either because these areas with very high resource and low accessibility or areas with very low resource and not quite high accessibility.

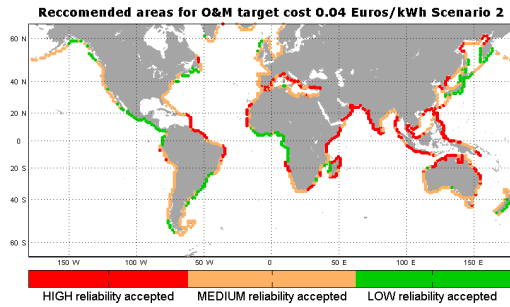


**Figure 5.48:** Recommended areas for wave energy development as a function of failure rates Scenario 2

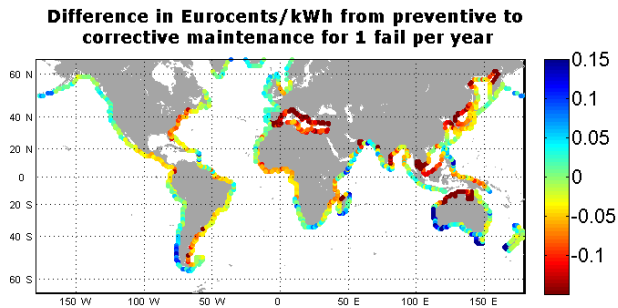


**Figure 5.49:** Difference in normalized O&M cost (Euros/kWh) of corrective and annual preventive maintenance with respect just corrective

### 5.4.5 Conclusions

This section examined the influence of failure assessment and O&M on the different stages of development of a WEC. Firstly, some failure simulations were performed based on the bathtub curve. It was concluded that in terms of the mean downtime, the failures that need a long weather window (more than 1 day) for its repair are dangerous because they increase their downtime, despite its rate of occurrence being low. On the other hand, regarding the mean

**Failure rate (fails/year) for an average O&M cost 0.04 Euros/kWh  
Scenario 3 (Corrective+Preventive maintenance)**

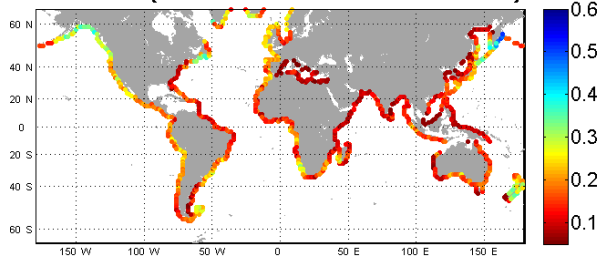


**Figure 5.50:** Failure rates needed for an average normalized O&M cost of 0.04Euros/kWh on selected locations Scenario 3

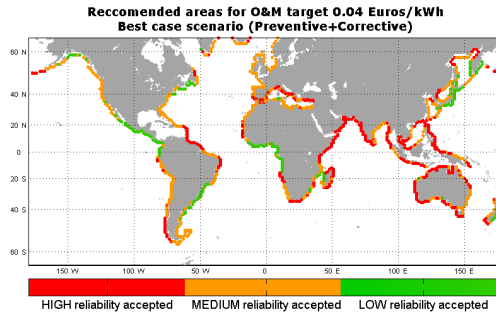


**Figure 5.51:** Recommended areas for wave energy development as a function of failure rates Scenario 3

yearly availability, it was found to be completely correlated with the failure rates, despite the duration of the weather window (the length of the weather window seemed to have a very mild influence on the mean yearly availability). In this analysis the different parts of the bathtub curve (decreasing, constant and increasing failure rate) were also analyzed. It was concluded that on average terms the three different parts lead to similar results and if the uncertainty on the failure rates, and therefore the simulation uncertainty (as it is currently in the marine energy field) an exponential distribution (constant failure rate in the bathtub curve) is advised in order

to simplify the procedure for a simple failure assessment.

In this section also an investigation about which coastal areas are more suited for testing WECs in stage 4 (1:1 scale sea trials) depending on the different reliability levels accepted by these WECs in terms of O&M costs was performed. A set of scenarios was investigated in order to assess the recommended areas for every stage of development. It was concluded that some areas, with a mild resource and a high accessibility such as Nova Scotia in Canada, or Brasil or the Pacific coast of Mexico, have an excellent balance for the first 1:1 scale deployments when the reliability of the devices is still low. Within a single WEC deployment, a path formed by three categorized areas has been suggested, areas where low reliability devices could be accepted (failure rate > 0.32 fails per year), areas where medium reliability devices are recommended (0.32 > failure rate / year > 0.12) and areas where devices with high reliability levels are required (failure rate < 0.12).

## 5.5 Factors that influence array layout on wave energy farms

### 5.5.1 Introduction

Nowadays, the most advanced wave energy prototypes are under real sea testing conditions and single units have been already deployed. Nevertheless, in the future, in order to reduce costs and achieve a better performance Wave Energy Converters (WECs) have to be deployed in the sea in the form of large arrays. These devices in arrays experience forces due to waves scattered and radiated from other devices, modifying the power production of WECs that can be increased or decreased respect to the theoretical sum of production of stand-alone WECs (Walker and Taylor (2005)). The analysis of array geometry in order to maximize the power production is a key research objective.

The interaction between radiated and diffracted waves can be constructive (summing amplitudes) or destructive (subtracting amplitudes). The interaction between WECs has been measured based on the interaction factor (or gain factor)  $q$  that is defined as the ratio between the output power of the array of  $N$  devices divided by the output power of an isolated device multiplied by the number of devices. When the interference is constructive  $q > 1$  and when is destructive  $q < 1$ .

The first study on WEC interactions corresponds to Budal (1977) where he introduced the concept of point absorber for array interaction taking into account that the scattered waves can be neglected and only radiated waves are essential for the analysis. Subsequent studies carried out by Falnes (1980) and Falnes and Budal (1982) affirmed that the  $q$  factor can be higher or lower than 1 depending on the wave period and the array configuration. The most recent studies correspond to Garnaud and Mei (2009) who investigated a set of equations

for dense arrays of heaving WECs. Child and Venugopal (2010) and Child (2011) showed two different methods for array optimization (Genetic algorithm and parabolic intersection methods) that were implemented considering wave directionality and array layout for generic point absorber. Some of the latest studies carried out on array configuration correspond to Babarit (2010) and Borgarino *et al.* (2012). Babarit (2010) demonstrated that in general, the  $q$  factor is variable in regular waves with respect to the period of incident waves, however in irregular waves the  $q$  factor is less dependent on wave period. They also studied the influence of long separating distances on a generic wave energy array and demonstrated that wake interactions are negligible for separating distances over 2000 m. Finally Borgarino *et al.* (2012) studied several configurations of wave energy arrays reaching the conclusion that in general, and considering a generic point absorber oscillating in heave or surge, triangle based arrays are the best configuration because they allow reaching optimum masking effects (destructive interaction). Wolgamot *et al.* (2012) studied the impact of directionality of regular waves over an array of heaving cylinders reaching the conclusion that wave direction is an important parameter in order to orient wave energy farms and achieve a maximum in production.

Nowadays, wave energy arrays have been studied under regular waves and with frequency domain models, however a more realistic approach is needed. Therefore, the objective of this subsection is to assess the different factors that influence wave energy array behavior under a time domain model with irregular waves in order to find the optimum one. The factors included in this study will be array configuration, separating distance, number of wave energy converters and wave directionality. Finally a new analysis will be performed taking into account the marine climate variability around the globe. Climates will be classified taking into account  $H_s, T_p$  and variance in wave directionality and then optimum array configurations will be discussed for each type of marine climate. Also optimum locations for these types of WECs are discussed.

### 5.5.2 Simulations

The study of factors that influence WECs array is carried out for the converter described in Figure 5.52. This converter was previously used on Chapter 4 for the long term power production assessment. It is a heave converter extracted from Babarit *et al.* (2012), which is a generic two body point absorber consisting of two objects: a deep draft spar buoy (1), that is only partially submerged and the surface buoy (2) that floats on the top of surface. Both objects are only allowed to move in heave and the union between the bodies is made through a linear PTO connection. In this case energy is extracted from the relative motion between the float and the buoy. The instantaneous power captured by the device is obtained using expression (5.9) assuming power production to be proportional to the square of the relative velocity between the two bodies:

$$P_i = C_{PTO}(\dot{z}_1 - \dot{z}_2)^2 \quad (5.9)$$

where  $z_1$  and  $z_2$  are, respectively, the vertical displacement of spar and surface buoys and the point indicates time derivative.

In the set of simulations explained in the next section, the  $C_{PTO}$  was set to the optimum for each sea state (maximum power production of every sea state). As in Chapter 4, the numerical model used to simulate this converter is a time domain model further explain on Appendix 1.

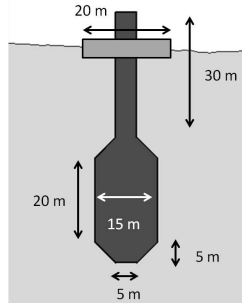


**Figure 5.52:** The two bodies heave Converter analyzed

The studied configurations are shown on figure 5.53. The first Array type (a) represents a linear configuration. With a  $0^\circ$  wave incidence it represents an attenuator array while with a  $90^\circ$  it represents a terminator array. Array type b is an equilateral triangle configuration and Array type c is a rhombus configuration consisting of two equilateral triangles. Finally Array type d is a square configuration consisting of two lines of WECs. As explained before the factors included in this study are array configuration, separating distance, number of WECs and wave directionality. In order to study these factors a set of simulations is proposed and defined in Table 6.1. The distance is expressed in terms of the corresponding wave length. This wave converter is designed to be tuned with a wave climate having a  $T_p$  around 10s then the wave length is expressed taking 10s as the basis. Then wave length associated to this period is  $L_{10}$  equal to 156 m.

These simulations were run with sea states characterized with significant wave height equal to 1 m and peak period ranging from 4.5 to 30 s in intervals of 0.3 s that represent the most common peak periods around the globe. The wave height was set to 1 m because the wave period is the key parameter in array analysis as studied in Babarit (2010). Falnes (1980) and Falnes and Budal (1982) determined that array layout and incident wave period are the most important parameters to be taken into account in array analysis.

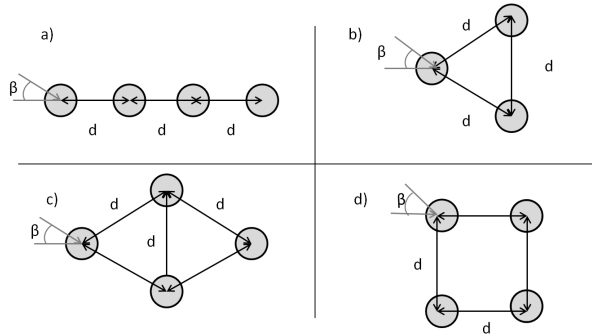


**Figure 5.53:** The different farms configurations simulated: a)Linear, b)Triangle, c)Rhombus, d)Square

Number of simulation	Number of WECs	Array configuration	Distance	Directionality $\beta(^{\circ})$
1	1	-	-	-
2 – 17	2	L	$L_{10}/4 - L_{10}/2 - L_{10} - 2L_{10}$	0 / 30 / 60 / 90
18 – 49	3	L / T	$L_{10}/4 - L_{10}/2 - L_{10} - 2L_{10}$	0 / 30 / 60 / 90
49 – 90	4	L / T / R / S	$L_{10}/4 - L_{10}/2 - L_{10} - 2L_{10}$	0 / 30 / 60 / 90

**Table 5.13:** Simulation sets, referring the symbols in array configuration to Linear (L), Triangle (T), Rhombus (R) and Square (S)

Nevertheless, a brief analysis was performed in order to understand the behavior of the device with respect to  $H_s$ . A range of simulations was run and the results are shown in Figure 5.54. Points are extracted from the model and lines show the best fit corresponding to a correlation coefficient specified in the legend. There are three different lines corresponding to different peak periods and power is represented with respect to significant wave height. This figure shows a parabolic behavior meaning that the power absorbed by the device is more or less proportional to  $H^2$ . As the influence of wave height is known, the analysis can be focused on wave period impact. We can therefore conclude that, the absorbed power behaves in the same way as the wave energy flux.

The aim of the simulations described above is to analyze the influence of the number of WECs, array layout, wave incident direction and distance between WECs on the power production of the wave energy farm studied with the sets of irregular sea states previously specified. In the next section, the results of this study are shown. It should be noticed that the maximum number of WECs considered is four. This is because it is considered that in a wave energy converter array the individual converter will be grouped in clusters in order to save costs sharing moorings

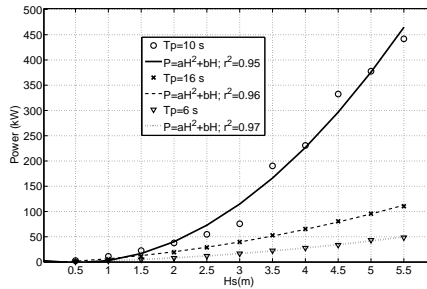


Figure 5.54: Power production vs  $H_s$  for different peak periods

or electrical infrastructure. Then in this study just a cluster of 4 devices is studied although a wave energy converter array could be formed by hundred of devices.

### 5.5.3 Results: sensitivity analysis

In this section, results are given in terms of the  $q$  parameter because it is the parameter that best describes the array interaction. This parameter represents the efficiency of the array configuration with respect to the individual WEC. As explained before  $q > 1$  represents constructive interference and  $q < 1$  represents destructive interaction. Figures 5.58 to 5.61 represent the different sets of simulations grouped by classes. The  $q$  parameter expressed in the y axis is referred to the mean  $q$  factor over the whole range of periods, written as  $q_m$ . This is not totally accurate because generally within a wave climate there is a predominant one, however in this chapter  $q_m$  is considered because this factor analysis is generically performed without taking into account any specific wave climate. This decision was taken based on the results obtained by Babarit *et al.* (2010) where the  $q$  factor seemed to have a low influence by the wave period on heaving WECs.

In order to show all the simulations and the results obtained, a figure for the 4 WEC linear configurations is presented. Figure 5.56 presents all the results of  $q$  factor obtained for the 4 WEC linear configurations (in order to show how the next figures are computed). In this figure, there are 4 plots each one corresponding to a separating distance among WECs and on each plot there are four lines corresponding to the different angles of incidence. In figure 5.56,  $q$  factor is not averaged (it is averaged in figures from 5.57 to 5.62, expressed as  $q_m$ ) and  $q$  factor is shown in terms of Separating distance (s)/Incident wave length (L), because this is the key parameter in terms of distance. In the first case of 39 m of separation, the  $q$  factor is very low for  $L/s > 4$  due to the destructive interference. In the case of a 78 m of separation ( $L_{10}/2$  with

respect the natural period of the WEC) the  $q$  factor is relatively high. In the case of 156 m and 312 m of separation  $q$  factor approximates to 1. This figure is very illustrative as it shows how sensitive the  $q$  factor is, therefore, interaction between WECs in terms of WEC distance will be analyzed averaging the  $q$  factor over the range of simulated periods ( $q_m$ ). It should be noted that from figures 5.57 to 5.62 the points with the different wave incident direction are joined by lines. However a linear interpolation is not assumed. It is known that slight changes on variations on separating distance (especially for small distances) could provoke great changes on  $q$  factor, then the  $q$  factor is not linear with respect the separating distance. However as the points are quite close on some figures they were joint by lines in order to help the vision of the plot, so these lines are considered just a viewing aid.

The influence of the factors on array performance are analyzed in the following subsection:

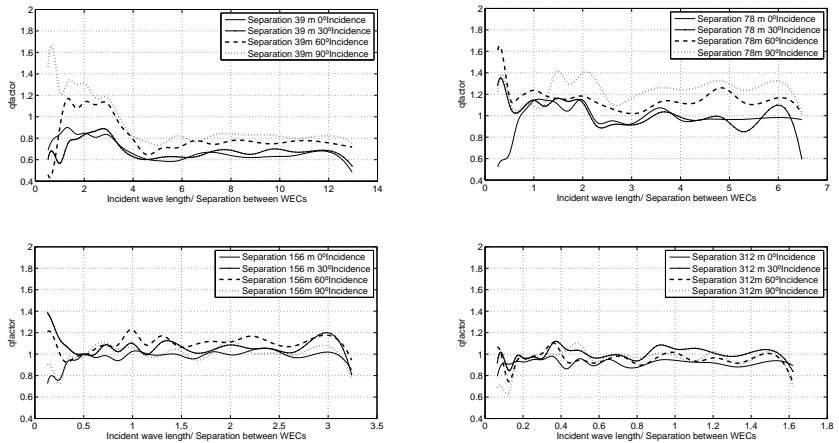


**Figure 5.55:**  $q$  factor for the specified separations in the subfigures and the specified incidence direction in the legend over the range of simulated periods

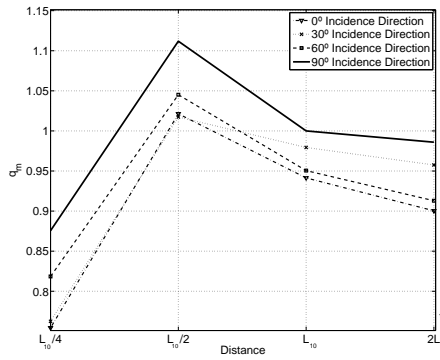


Figure 5.56:  $q_m$  factor for 2-body linear configuration

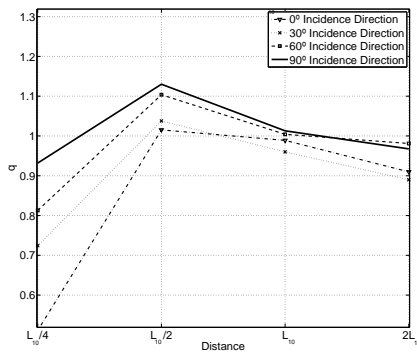


Figure 5.57:  $q_m$  factor for 3-body linear configuration

### Number of WECs

Analyzing figures 5.57, 5.58 and 5.60 is noticeable that  $q_m$  factor grows as the number of WECs generally increases when the interferences are constructive. For instance in figures 5.57, 5.58 and 5.60 an increase in  $q$  factor is shown (in  $L/2$  when constructive interference is achieved) for a linear configuration. Maximum  $q$  factor for 2 bodies configuration is 1.11 while the 4 body configuration has a maximum  $q_m$  factor of 1.23. It is concluded then that normally, an increase in the number of devices in an array means that there are more combinations of body pairs that undergo interaction and therefore a potentially greater number of interactions is possible. Nevertheless, when interference is destructive a growth in the number of WECs means a lower

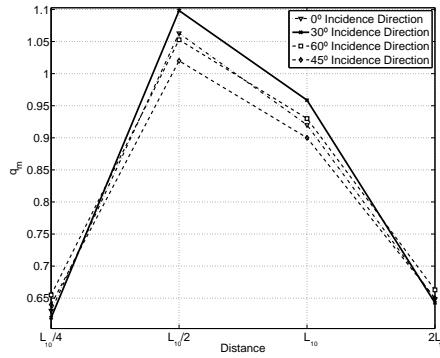


Figure 5.58:  $q_m$  factor for 3-body triangle configuration

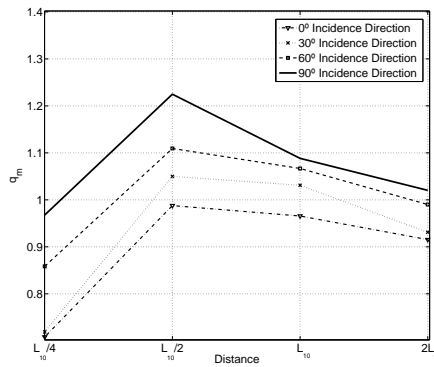


Figure 5.59:  $q_m$  factor for 4-body linear configuration

$q_m$ . If the number of interactions is greater then the effect of the destructive interference could be amplified. Therefore, it is demonstrated that the number of WECs amplifies the effect of array interactions, if the interaction is positive (constructive interference) then the effect of array configurations is highly beneficial, if the interaction is negative then the effect of increasing the number of WECs is negative for power production.

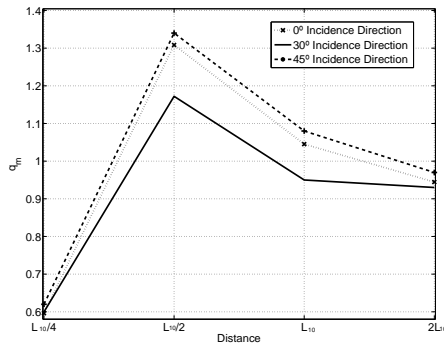


Figure 5.60:  $q_m$  factor for 4-body square configuration

#### Distance between WECs

Analyzing figures from 5.57 to 5.62 there is a clear behavior of the arrays in terms of separating distance. All the curves show more or less a similar pattern. Generally the lowest  $q$  factor correspond to  $L_{10}/4$ . In this case the WECs are in phase opposition because there is  $90^\circ$  of phase delay between the movements of the buoys. It is important to point out that in this case a smoothing of the power series occurs. However, we have noted that in all curves the highest  $q$  correspond to  $L_{10}/2$ . In this case the WECs are in phase with a separation of  $180^\circ$  and because of this fact the power is higher. The reason for this behavior is related with the crest and sine of the waves. Although irregular sea states are investigated in this section if the WECs are separated half of the wave length the motion of the bodies would be in phase because the waves reaches the WEC at the same position within the incident wave. This means that the waves radiated for a WEC reach the other WEC in phase with the incident wave, reinforcing the excitation forces.

All the curves show a drop of  $q_m$  factor from  $L_{10}$  to  $2L_{10}$ . As the distance increases the  $q_m$  factor approximates to 1.

It is important to point out that the influence of the moorings have not been considered in this piece of work. Although  $L_{10}/2$  was found to be the optimum distance between WECs theoretically in this case it is necessary to take into account the optimum mooring system layout.

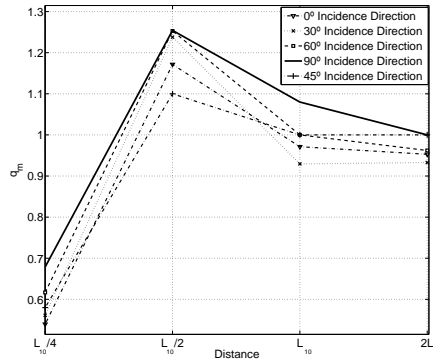
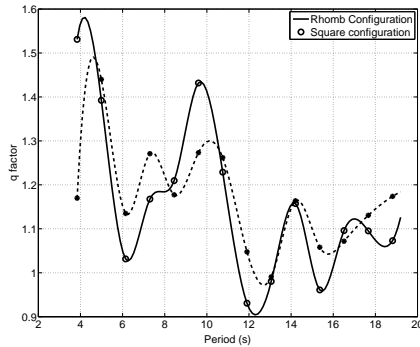


Figure 5.61:  $q_m$  factor for 4-body rhombus configuration

### Array Layout

Regarding the array layout 3 different configurations were analyzed: linear, triangular and square. The figures that represent the behavior with respect this parameter are 5.60, 5.61 and 5.62. In this case, the linear configuration is normally the worst in terms of  $q_m$  factor. There is only one line of WECs receiving the incoming waves and then the influence of the radiation is only unidirectional. On the other hand, triangular and square configurations receive the radiation of consecutive WECs in two directions and constructive interactions are more easily achieved. Comparing triangular and square configurations, we have noticed that both are similarly efficient although in the 4 WECs case the square configuration has a slightly higher  $q_m$  factor for the  $L_{10}/2$  case.

In order to clarify the different performance of rhombus and square layouts the  $q_m$  factor is represented over the range of studied periods in figure 5.62 for 4 WECs and  $0^\circ$  wave incidence and a separating distance of  $L_{10}/2$ . As the figure shows both configurations have a similar distribution and the optimum configuration depends on the most probable period. The  $q_m$  factor shows peaks in some periods due to the existing interaction distances as Ricci *et al.* (2006) suggested. In this figure, it is important to point out that the second highest  $q_m$  correspond to the periods near the natural one (10 s). The highest  $q_m$  corresponds to the periods near 5 s. This is due to the fact that 5 s has a wave length that corresponds to half of the WEC separation in the represented case. In the next sections these configurations will be investigated for different climates with different characteristics in terms of  $H_s$ ,  $T_p$  and wave direction.



**Figure 5.62:** Comparison of square and rhombus configuration for a 4 WEC wave farm,  $0^\circ$  incidence and separation  $L_{10}/2$  throughout the range simulated periods

### Wave Incidence Direction

The influence of wave direction depends on the array layout, therefore the analysis will be performed taking into account each layout:

- **Linear arrays:** The influence of wave direction on this type of layout is huge and it is the one that shows the most sensitivity to incident wave direction. Figures 5.57 or 5.59 show an important change of behavior with respect wave incident direction. The linear configuration can change from an attenuator array with  $0^\circ$  of incidence to a terminator with  $90^\circ$ . The worse configuration in terms of  $q_m$  factor is the attenuator array. In this case, WECs are aligned with incident wave direction and wave energy is dissipated by each converter. Consequently the energy absorbed by each converter is lower as the wave propagates, and then this energy loose is not compensated with the diffraction. The opposite case is the terminator array ( $90^\circ$  incidence). This case is the best one in terms of  $q_m$  factor. The devices radiate and constructive interference is achieved. The performance with the intermediate incidence angles ( $30^\circ$  and  $60^\circ$ ) shows the transition between the two extreme performances.
- **Triangular and rhombus arrays:** The influence of wave directionality on triangular arrays is lower than that of linear arrays. Interactions are more complex in these types of arrays than in linear ones (see figure 5.58). Lines in figure 5.61 with respect to 5.59 are less dependent on wave direction. Generally, when constructive interaction is achieved the most beneficial wave incident direction is  $30^\circ$ , meaning that the wave direction is aligned with one of the sides of the triangle. In the case of a rhombus configuration, formed by two equilateral triangles the best directions are  $90^\circ$  and  $60^\circ$ , the direction where one or two pairs of devices respectively are aligned with the wave direction in the

first case and in the second case perpendicular to one of the sides of the rhombus.  $45^\circ$  is the less productive direction because there is no alignment or coincidence between wave propagation and the array geometry. Alignment of wave incident direction and WECs is beneficial for power production, if the other factors also generate constructive interaction.

- Square arrays: The influence of wave directionality on square arrays is lower than in linear arrays (see figure 5.61). In this case  $0^\circ$  and  $90^\circ$  wave incident directions are the same due to the double symmetry and then only one of them is computed. Also because of this  $30^\circ$  and  $60^\circ$  waves are also the same. As the figure shows  $45^\circ$  is the most efficient configuration. In this case wave propagation is directly aligned with one of the sides of the square (and perpendicular to the other two).

Generally it is important to point out that the optimum wave incidence direction is related to the alignment of incident waves and WECs. To sum up it is important to reinforce that in linear configuration, the  $90^\circ$  incidence (terminator) is the most efficient wave direction. In the case of triangular arrays, a  $30^\circ$  incidence (parallel to one side) is the optimum. Regarding rhombus configurations, an incidence of  $90^\circ$  is the maximum (parallel to small diagonal) and in square configuration  $45^\circ$  (parallel to one side) is the optimum.

#### 5.5.4 Application to different weather scenarios

In this subsection the best configurations of the previous subsection are investigated considering different weather scenarios. Firstly, a weather classification is performed around the globe taking into account several ocean parameters. In order to successfully perform this analysis a global reanalysis data base was used: Global Ocean Waves (GOW) from Reguero *et al.* (2012). The global distribution of coastal marine climates has been classified based on the main parameters that describe the wave climate from the WEC performance point of view.

In the present analysis, the following four parameters have been chosen:

- $H_{sm}$ : Mean significant wave height. This parameter is the mean of the long term significant wave height mean regime. It is a parameter that gives direct information about the predominant wave height in a given location. In general, the higher  $H_{sm}$ , the more energetic the wave climate is.
- $T_{pm}$ : Mean peak period. This parameter is the mean of the long term peak period mean regime. The value of  $T_{pm}$  indicates the predominant peak period in a given coastal area. The value of  $T_{pm}$  increases as the predominance of swell sea states increases.
- $\sigma_{H_m}$ : Standard deviation of the mean wave propagation direction. This parameter is the standard deviation of the mean wave direction long term mean regime. The  $\sigma_{H_m}$  parameter is an indication of the variability of the wave direction in a given area. For instance, unidirectional sea states will show low  $\sigma_{H_m}$ .

- $F_{em}$ : Mean energy flux. This parameter is the wave energy flux mean regime. The value of  $F_{em}$  is the indication of how energetic is the wave climate.

In order to perform the weather classification, the K-Means algorithm (KMA) has been used. The K-Means clustering technique is capable of dividing the input data set to several subsets, where each of them are represented by a centroid. The aim of this algorithm is to adjust the centroids to the data by minimizing the sum of distances to the corresponding centroid. When the sum of distances of the rest of the points of the subset are minimum the method ends (see Figure 5.63). KMA provides the best representation of the average wave conditions. A more detailed explanation of the method can be found in Camus *et al.* (2011).

### Methodology for the weather classification

According to the methodology described by Mendez *et al.* (2009), once the parameters have been selected, the normalization is required, providing equal weights for each of them. This process is shown in Figure 5.63. The scalar parameters  $X_i = \{H_{sm}, T_{pm}, F_{em}\}$ , are normalized by scaling the values of the variables between [0,1] with a simple linear transformation, which requires the minimum and maximum value of the three scalar variables.

$$X_i^{min} = \min(X_i) \quad (5.10)$$

$$X_i^{max} = \max(X_i) \quad (5.11)$$

For the circular variables  $\theta_i = \sigma_{H_m}$ , (defined in radians or in sexagesimal degrees using the scaling factor  $\pi/180$ ), the range of  $\sigma_{H_m}$  is  $[0-\pi]$  radians, this variable has been normalized by dividing the direction values between  $\pi$ , therefore  $\theta_i$  range is between [0,1]. After these transformations, the dimensionless input data  $X_i$  are defined as:

$$X = \frac{(X_i - X_i^{min})}{(X_i^{max} - X_i^{min})} \quad (5.12)$$

$$\theta = \frac{\theta_i}{\pi} \quad (5.13)$$

After the variable normalization, the K-Means algorithm is applied. The centroids obtained in the KMA are defined as  $C^f = [H_s^f, T_p^f, F_e^f]$ ;  $f = 1, \dots, Ngroups$ . In this study, the K-Means algorithm was applied in order to classify the high-dimensional data space into 10 wave climate typologies. The last step is the denormalization of the clusters obtained, applying the opposite transformation of the normalization step. These ten climate types have been described by an occurrence matrix for each incidence direction. These data are necessary in order to obtain the production matrix for each site using the methodology explained here. The ten climate types are shown in figure 5.64.

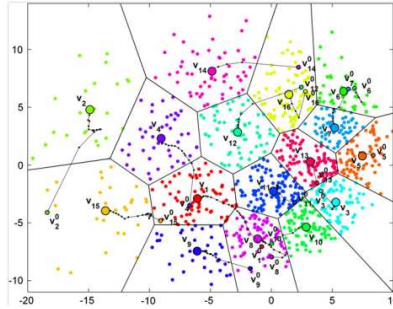


**Figure 5.63:** KMA clustering: initialization  $\{v_{10}, \dots, v_{160}\}$ , updating tracks and final centroids  $\{v_1, \dots, v_{16}\}$  with their corresponding clusters. Camus *et al.* (2011)

In table 5.14 the mean parameters that characterize the climate classification performed before are shown (mean  $H_s$  and mean  $T_p$ ) and Figure 15 shows the occurrence matrices and the direction rose for climates 2,6, 7 and 9 that are the ones compared in the next subsection.

Climate 1 is the most energetic one and corresponds, for example to South Chile in the Pacific Ocean giving the highest mean wave height (3.5 m). Moreover this climate is nearly unidirectional and with a very spread occurrence matrix with several extreme events. Climate 2 (see figure 5.64 for location of wave climates) can be located for instance in some parts of Indonesia and is characterized by a bidirectional climate with a very spread occurrence matrix. Climate 3 corresponds, for instance, to Central and the North part of South America and has low wave heights and peak periods near 9 s. Climate 4, for example, corresponds to the Mexican Coast in the Pacific and is characterized by a very concentrated occurrence matrix with high periods near 11 s. Climate 5 corresponds to the Argentinean Coast in the Atlantic and one important characteristic is the low periods (around 7.4 s) and the spreading of the occurrence matrix. Climate 6 which corresponds to Central America in the Pacific is characterized by a concentrated occurrence matrix but above all it is really unidirectional. Climate 7 corresponds to North Atlantic in Europe (see figure 13) is very multidirectional climate and is also characterized by a very spread occurrence matrix as well. Climate 8 is located, for instance, on some areas of South East-Africa. This climate is characterized by a very spread occurrence matrix with low periods (7.4 s) and it is also very multidirectional. Moreover, Climate 9 which corresponds to South Pacific in Australia is a unidirectional climate with a very concentrated occurrence matrix. Lastly, climate 10 corresponds to Mediterranean area and is the one with the lowest wave energy due to the low wave height and the low peak period existing in this area. Figure 5.66 shows the occurrence matrix and the directional spectra of climates 2,6,7 and 9.

	Climate parameters		q factor		
	Mean $H_s(m)$	Mean $T_p(s)$	Linear	Square	Rhombus
Climate 1	3.5	9.6	0.9977	1.3137	1.3501
Climate 2	2	8.5	1.1570	1.3268	1.2931
Climate 3	1.2	9.2	1.1541	1.1745	1.2875
Climate 4	2	11.2	1.1644	1.3966	1.2949
Climate 5	1.3	7.4	1.1991	1.2536	1.3469
Climate 6	1.67	10	1.1892	1.3295	1.2658
Climate 7	1.94	9.4	1.1532	1.2991	1.3215
Climate 8	1.3	8.4	1.1558	1.2851	1.2734
Climate 9	2.2	11	1.2170	1.3080	1.2715
Climate 10	0.9	5.8	1.1900	1.1054	1.3703

**Table 5.14:** Climate parameters and mean  $q_r$  for each climate type for the configurations specified

#### Analysis of q factor for the different weather scenarios

After the climate classification, power matrices were computed for the best configurations in the previous section : 4-body wave energy farms for linear, rhombus and square configurations. These power matrices are multiplied by the occurrence matrices of each location, taking into account wave incident direction in order to obtain the production matrices and assess the best configuration for each climate. It is important to point out that these calculations are performed with the most productive wave farm direction aligned with the most probable wave incidence of each climate. For instance, if in a specific climate the most probable direction is  $320^\circ$ , then for example for the square configuration, the sides of the square will be aligned with this direction in order to get maximum production. This fact is very important when comparing results from the studied configurations.

Figure 5.65 shows the distribution of the mean  $q_r$  factor (mean q factor for the analyzed climate) around the coastal areas of Earth for the three wave farm configurations. As shown in the figure, in general the triangular configuration is the most effective in terms of q factor.

Figure 5.67 shows the pdfs of the  $q_r$  factor obtained through the combination of the occurrence matrix and q matrix (obtained by the power matrix of the wave farm and the power matrix of the individual WEC). Results for the long term mean,  $q_r$ , obtained from these regimes are shown in table 5.14 for all the climates. These mean  $q_r$  factors have been obtained from the probability density functions of q factor shown in figure 5.67. In figure 5.67 the area with the highest of probability corresponds to the natural period of the WEC (10 s). In terms of wave height the highest area of probability is dominated by the occurrence matrix and in general corresponds to  $H_s < 2$ . Note that this WEC device is tuned to a climate with a period near 10

s, nevertheless this study is locating the same WEC, with the same hydrodynamic properties, in different climates. Therefore, it should be highlighted that due to this fact the WEC is not tuned with every climate explained in this section.

Looking at figure 5.66, it can be pointed out that climate 7 is very multidirectional and Table 5.14 shows that the triangular configuration is the most efficient. On the other hand climate 9 is very unidirectional and then square configuration has higher  $q$  factors. Also it is important to point out that dispersion of events in occurrence matrix  $H_s-Tp$  is important. For example, climate 4 and 9 have a very concentrated occurrence matrix, however climate 5 and 7 have a very disperse occurrence matrix. This fact affects the efficiency of the array. This device is designed to be tuned to a climate with a peak period near 10 s, then as the occurrence matrix is more concentrated around this point the efficiency will be higher. Consequently, the climates where this farm is more efficient are climates 4,6 and 7. This corresponds to the North America in the Pacific Ocean and Europe in the North Atlantic (see figure 5.64 for a better explanation).

When comparing climates 6 and 7, we see that they are totally different climates in terms of wave direction and occurrence matrix. Climate 7 has a very disperse occurrence matrix with very energetic events (more extreme wave heights) and very multidirectional, while climate 6 has a much more concentrated occurrence matrix with less extreme events and very unidirectional. Between these 2 climates the wave farm analyzed is more efficient in climate 6 due to the absence of extreme events and the regularity of the incoming waves (swell) as well as the low variability of the directionality. Another remarkable issue is the high  $q_r$  factor obtained in climate 10 corresponding to the Mediterranean area. This fact is due to the existence of very small periods where the array layout is quite efficient.

For the linear configuration climate 9 provides the highest  $q_r$  factor, because this climate is unidirectional. However the  $q_r$  factor value is much lower than that obtained in square and rhombus configurations. In the square configuration the highest  $q_r$  factor corresponds to climate 4 with a value of 1.3966. This climate has an occurrence matrix very concentrated around 10 s and then the device is totally tuned with the wave climate. Finally, the rhombus configuration has the highest  $q_r$  factor on climate 10, which corresponds to the Mediterranean area. This is due to the existence of a natural period of the device near 5 s.

Finally, it is important to point out that square based arrays are optimum for unidirectional wave climates because  $q_r$  factor across  $q$  matrix is higher in square based arrays, however the deviation of  $q$  factors between this angle and the other angles of incidence is high. This means that in square based arrays wave incident direction is a very important variable to take into account due to the difference in  $q_r$  factors for each direction. However in the case of triangle

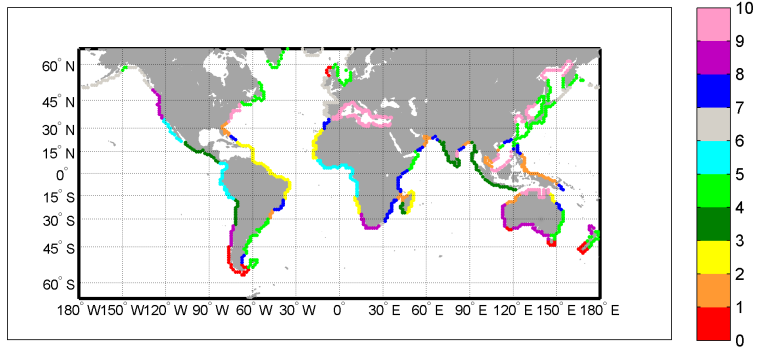


**Figure 5.64:** Weather climates types derived from classification taking into account wave height, the peak period, the wave energy flux and the deviation of directionality

based arrays, wave incidence direction has a much lower influence and the variance of  $q_r$  factor for the different incidence direction is low. This is because of the double symmetry of the array. Therefore square based arrays are optimum for climates with unidirectional characteristics. On the other hand linear arrays were found to be the least efficient configuration in terms of  $q$  factor. These types of configurations are very sensitive to directionality because they change from an attenuator to a terminator. These arrays are indicated for unidirectional climates where the waves comes perpendicular to the orientation of the array (terminator array). Nevertheless, in this case, the square configurations are more efficient than linear, which is why the linear configuration is not recommended for array layout.

On the other hand, triangular based arrays are optimum for multidirectional wave incidence. while these arrays have lower  $q$  factor for optimal wave direction than square arrays, the

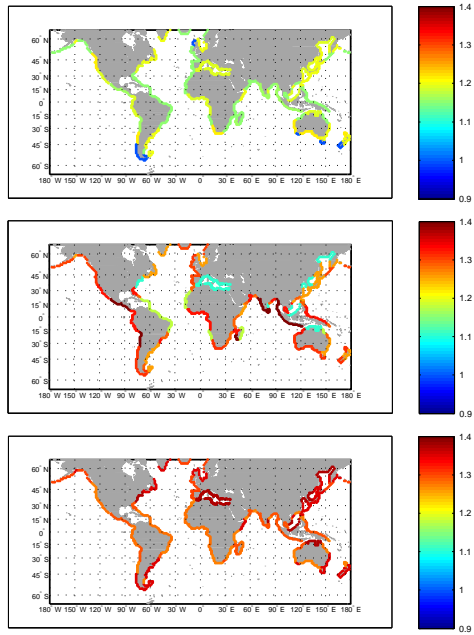


**Figure 5.65:**  $q_r$  factor maps for the linear(above), square(center) and rhombus(bellow) configuration

decrease of  $q_r$  factor for non-optimal directions is lower in triangular based arrays than in the square ones, leading to the conclusion that triangular-based configurations are indicated for multidirectional climates

### 5.5.5 Conclusions

Different factors that influence array layout in wave energy farms were studied in this subsection. The distance between WECs has been found to be an important factor in order to reach higher  $q$  factors.  $L_{10}/2$  has set the optimum distance due to a delay of  $180^\circ$  (in phase) between WECs. Several array layouts were investigated. Linear configuration was found to be the worst one in terms of  $q$  factor while triangular and square configurations had similar efficiencies depending on the wave climate of the area. Taking into account wave directionality, triangular based arrays were optimum for multidirectional wave regimes and square arrays for unidirectional wave regimes due to the higher  $q$  factor of square arrays for the optimal unique

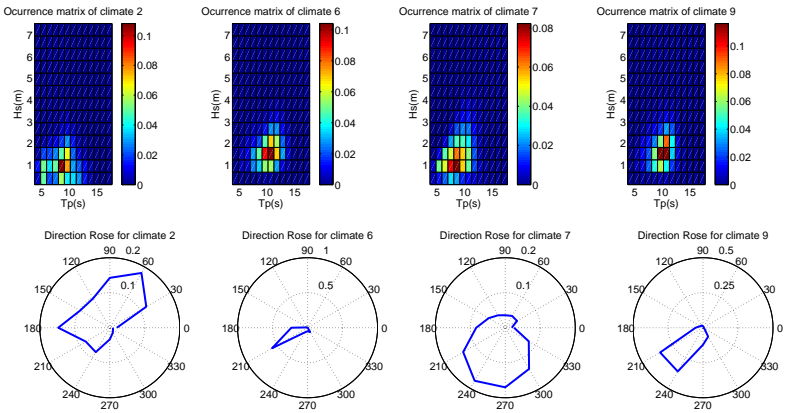


Figure 5.66: Occurrence matrices and Direction Rose of Climates selected for comparison 2,6,7 and 8

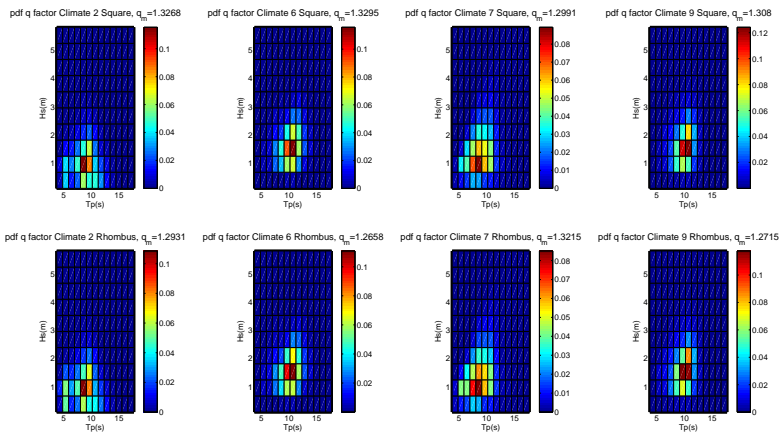


Figure 5.67: Probability density functions for q factor (gain factor) for rhombus and square configurations

direction.

The dispersion in the occurrence matrix of a particular wave regime is found to be an important factor in order to reach higher efficiencies on the wave farm analyzed. Wave regimes concentrated around the natural period of the device are the most effective.

In this subsection only 2, 3 and 4 WEC arrays have been investigated due to limitations in the numerical model WADAM. However an increase in the number of the devices has been found to be positive in terms of  $q$  factor due to the increase in interactions between WECs when constructive interference is achieved. Further research is needed with wave farms comprising several tens of WECs.

## Economics of wave energy

---

### 6.1 Introduction

In this chapter the current state of wave energy from an economic perspective is analyzed. Firstly, the costs of a wave energy device will be broken out on the different concepts and the risk and uncertainties that wave energy is facing nowadays from an economic perspective will be further analyzed in this chapter. Secondly, based on the assumption that wave energy is not yet cost-competitive with other renewable sources and that further improvements are needed to reduce the Levelized Cost of Energy (LCOE), two case studies are presented. In these case studies the current cost of two wave energy converters will be assessed and the areas with a higher impact on LCOE are thoroughly investigated.

### 6.2 Risks and Uncertainties on wave energy economics

#### 6.2.1 Introduction

The ocean wave energy sector has significant potential to contribute substantially to the global electricity generation if sufficient investment is provided (see Clement *et al.* (2002)). Furthermore, wave energy represents a good alternative as a renewable source due to the low environmental impacts (see Lin and Yu (2012)) and the extensive sites available for the placement of wave farms. Current wave energy targets for 2020 are quite ambitious (e.g. 1000 MW for 2020 in the UK or 500 MW for Ireland) making economic assessment of wave energy farms a key issue in the search of financial resources (see Beels *et al.* (2011)).

A methodology for economic analysis of wave energy projects is therefore required and it is an essential tool for assessing the potential profitability of wave energy projects from the perspective of developers, local administration and investors. Beside costs, developers, investors and public administration's major concern is the assessment of project uncertainties. According to Ayyub (2010) there are three major sources of uncertainty that can affect the profitability of an investment projects.

The first one is related to the high internal variability of the data: met-ocean historical records show a highly variable behavior (see Reguero *et al.* (2013)) which origins uncertainty about

how seasonal, interannual and long term variability of wave energy flux may affect production over the farm's expected life.

The second source of uncertainty has to do with the fact that most technologies have rarely been tested under real conditions; consequently only simulations of future response and efficiency are possible. Future estimates should consider the reduction in uncertainties thanks to the experience acquired through the learning processes associated with the deployment of WECs.

The last source of uncertainty considered is linked to socioeconomic issues including, among others: institutional support, availability of subsidies for emerging green technologies, future social acceptance or commercial conditions under which energy will be supplied to users.

Therefore, a study of the uncertainties that affect wave energy development is required in order to provide investors a guide to the potential risks assumed on wave energy development.

Several authors have carried out studies regarding the economic performance of wave energy projects; Beels *et al.* (2011), Dalton *et al.* (2012), O'Connor *et al.* (2013a)), almost all of them concerning a specific type of technology. Beels *et al.* (2011) was one of the first to study several arrangements for the Wave Dragon device taking into account the operational and maintenance costs as a function of the marine climate.

Teillant *et al.* (2012) studied the economical performance of a generic wave energy device through operational simulations. However, in general all the studies published to date base their cash flow analysis on the power matrix. However, de Andres *et al.* (2013a) showed that the power matrix is not accurate enough to study the long term behavior of a WEC or its economic performance due to the absence of a power production series. One of the latest studies corresponds to Castro-Santos *et al.* (2015), where an LCOE GIS model was built. It was concluded that the North West part of Portugal have currently a LCOE ranging from 81 Eurocents per kWh to 1.19 Euros/kWh.

Several authors have studied the economic feasibility of wave energy projects reaching the same conclusion, namely that current feed in tariffs are not sufficient to make the development of wave energy farms cost-effective. A sensitivity analysis of the inputs of the economic analysis was performed and optimal locations for specific technologies are suggested as a function of these parameters (O'Connor *et al.* (2013d)).

O'Connor *et al.* (2013a) also studied the implications of operational costs on the economic analysis taking into account the concepts of accessibility and availability of a specific location. Finally Dalton *et al.* (2012) performed a case study sensitivity analysis taking into account the impact of the learning curve, supply and demand curves and future cost of cash. The conclusion of this study was that the current feed in tariffs for wave energy in countries such as Ireland are insufficient to develop cost-effective projects. Ireland feed in tariff, available until 2015, has been set to 0.22 Euros/kWh and spans a 15 year project. However this tariff has been shown to be insufficient for currently available devices, specifically for the Pelamis Device studied by

Dalton *et al.* (2012). A feed in tariff of 0.45 Euros/kWh was found to be more realistic so as to reach an attractive internal rate of return.

The goal of this chapter is to carry out an uncertainty analysis of the most relevant financial indicators to be considered in wave energy farm developments and focus on the aspects that had not been studied previously by other authors. The three sources of uncertainty considered are treated differently:

- Introducing parametric scenarios for prices and feed in tariffs. A sensitivity analysis to different socioeconomic scenarios is carried out.
- Uncertainties regarding technological evolution are addressed considering a learning coefficient as is usually done in other energy economic analysis.
- Much emphasis is put in this work in assessing uncertainties stemming from inter-annual variability of wave climate, one of the most unpredictable sources of uncertainty to date.

Without loss of generality a case study is presented and then the uncertainty analysis is carried out for a specific wave energy converter technology based on a two body heave converter as described in de Andres *et al.* (2013a).

## 6.2.2 Methodology

### Technology selection

The first step consists of the selection of the technology. The WEC selected is a two body heave converter which extracts energy from the relative motion of both bodies in the heave mode (see Figure 1), previously used in Chapters 4 and 5. This WEC extracts energy with a linear generator with 1 MW of nominal power. The device is based on Babarit *et al.* (2012). This type of technology is currently under development by two different companies. It should be highlighted that although the methodology is applied to this converter, this methodology can be generalized to any WEC technology.

### Wave farm location

The second step in the methodology is the design of a wave energy farm consisting of a number of these devices. Wave energy is an expensive option when compared with other renewable sources. However, under some specific conditions this cost could be admissible. For instance, isolated electrical systems are highly dependent on fossil fuel resulting in high energy costs due to long distances from mainland or developed areas.

In this context, renewable energy sources are very useful in order to achieve self-sufficiency and avoid the overexpenses due to transportation of fossil fuels. A wave energy resource assessment around La Palma (Canary Islands, Spain) island was carried out in IHCantabria

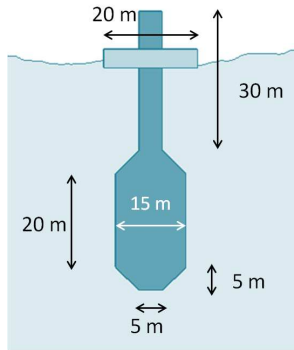


**Figure 6.1:** Two body heave converter analyzed

(2011), reaching the conclusion that the northwest coast of La Palma is the most suitable place for the farm Hernández-Brito *et al.* (2012) (see figure 6.2). The selected area is located at a point in La Palma Island with coordinates 28.81N and 18.01W for its accessibility and clean exposure to wave energy flux (due to the incidence of the Atlantic swell). This site is 1500 m from the shoreline, at a 150 m depth and has a yearly mean wave resource of 22 kW/m (see IHCantabria (2011)). The wave climate data of this point was provided by Reguero *et al.* (2012) from a reanalysis database, including the wave height, peak period and wave direction from 1948 to 2008. In figure 6.3 the occurrence matrix of this location is shown.

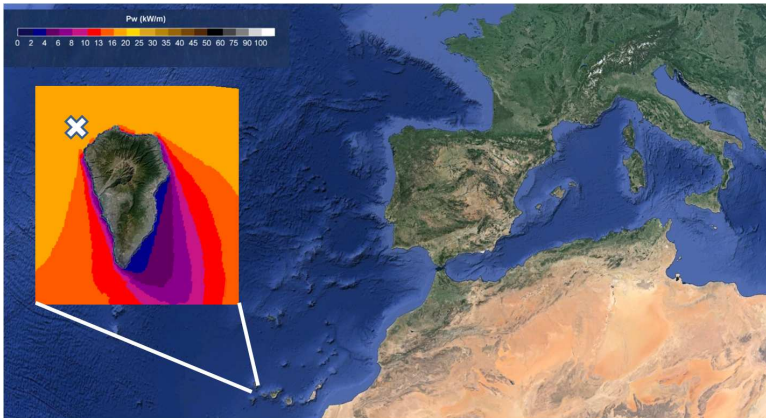


**Figure 6.2:** Location of the wave farm and yearly mean wave energy resources around La Palma Island extracted from IHCantabria (2011)

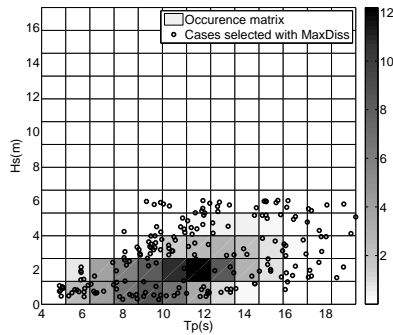


**Figure 6.3:** Occurrence matrix (in percentage) and 196 selected sea states for the selected site

### Wave farm production

The methodology to obtain the long-term power production is explained in figure 6.4, based on the methodology presented in Chapter 4. This method provides a way to obtain the life cycle power production of a device with the same computational effort than the classical method based on the multiplication of the power matrix and the occurrence matrix, being able to estimate the long-term power production time series. Firstly, the climate data is taken from a global reanalysis database, GOW, with sixty year climate data (see Reguero *et al.* (2012)). A sea state selection technique is applied to this set of data. The MaxDiss selection technique is used from Camus *et al.* (2011) in order to select the most representative sea states only (figure 6.3). These selected sea states are the input for the time domain model assuming a Jonswap spectrum with gamma 3.3.

Numerically, in order to compute the power production two steps are needed, firstly, the floating converter is analyzed with DNV (2008), a Boundary Element Model (BEM), that obtains the added mass, damping and excitation force coefficients. These coefficients are the input for the time domain model described in de Andres *et al.* (2013a). With this time domain model, the power production is obtained for the selected sea states. Finally, in order to reconstruct the long-term power production series, an interpolation technique is applied. The Radial Basis Function interpolation technique (RBF) has been used to obtain the complete power series.

In order to select the farm layout for this analysis, the previous chapter investigated the most important factors that influence array performance (de Andres *et al.* (2013b)). Optimal configurations for wave energy farms were proposed as a function of the wave climate. In this case, a wave energy farm composed of 4 WECs is analyzed. Then, a rhombus configuration is selected for this location based on the results of the previous chapter.

Based on the methodology described, the production of the wave farm is computed. The time domain model is run for these sea states resulting in hourly time series of the wave farm production for the last 60 years. This is the input to carry out the long term power production analysis. In figure 5 the series of mean wave energy production obtained with the methodology explained previously is represented.

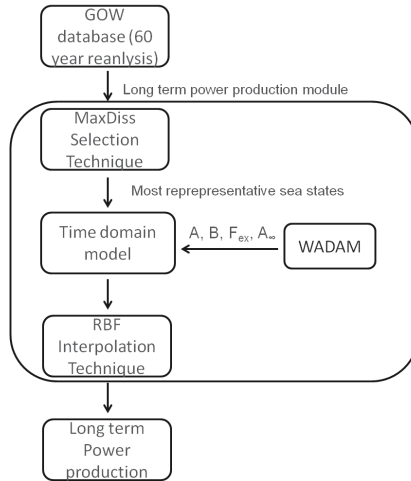


Figure 6.4: Diagram of the energy production model

### 6.2.3 Long term production analysis

In order to perform the analysis of the uncertainty of financial indicators on wave energy farms a database, of a great number of life-cycle energy productions is required. This is necessary because the interannual variability of power production is important, thus the project profitability is significantly variable. Based on Espejo *et al.* (2011), for a given lifetime of  $n_y$  years (25 years),  $n_y$  years bootstrap sub-samples from the original  $t_s$  years (60 years) are selected. The selection is based on Monte Carlo random sampling with replacement.

The methodology is based in the following Figure 6.6:

1. From the long term power production module, explained in Figure 6.4, a sixty year power production series is obtained
2. Random selection is performed based on the previous assumptions (random bootstrapping, Montecarlo technique to generate 25 life cycle time series of power production)
3. 10,000 lifecycles of 25 year duration are generated

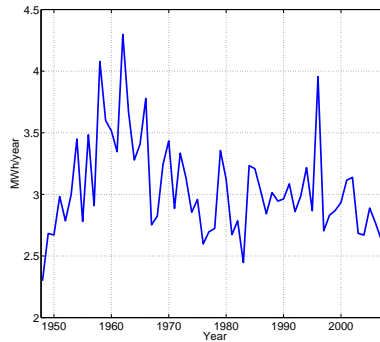


**Figure 6.5:** Yearly production of the 4 WECs 4 MW wave farm 1948 to 2008

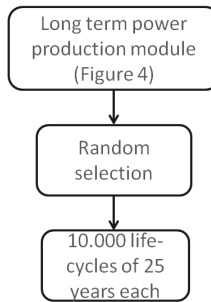


**Figure 6.6:** Process of generation of the life-cycles for the statistic analysis (Monte Carlo)

A 25 year time is set, as this is the period that this kind of infrastructure is assumed to last in the sea (with an estimated replacement of the devices at the middle of the service life). In this work it is assumed that no replacement of the mooring system is needed based on the experience presented in Harris *et al.* (2004).

### Project Budget

In this subsection, a brief description of the theoretical assumptions and the estimates the parameters needed for the economic analysis is given. First, the Engineering, Procurement, Construction and Installation (EPCI) budget of the wave farm is presented in Table 1. The WEC is assumed to be built of steel and a concrete ballast. Steel price is fixed at 5 Euros/Kg. For concrete a cost of  $98.35\text{Euro}/\text{m}^3$  is assumed. The cost of the linear generator is set to 600.000 Euros/MW (see Danielsson (2003)). This last assumption is an important source of

Concept	Subconcept	Amount (Euro)
Power Take-Off	Procurement Onshore installation	2,400,000 0
Platform (Shell)	Manufacturing	6,671,880
Equipment and Systems on board Station-keeping System		498,953
	Mooring procurement	851,273
	Anchoring	154,723
	Vessel Mobilization Cost	200,000
	Mooring procurement	765,000
Electrical infrastructure		
	Offshore Substation	288,666
	Onshore Substation	218,666
	Array cable procurement	168,000
	Array cable installation	765,000
	Export cable procurement	525,000
	Export cable installation	765,000
	Onshore cable procurement	630,000
	Onshore cable installation	490,000
Logistics and Installation		
	Tug Vessel	270,000
	Supply Vessel	360,000
	Mobilization cost	300,000
	Other	93,000
Engineering		191,494
Contingencies		1,321,494
TOTAL		17,840,000

**Table 6.1:** Budget for the considered 4 WECs 4 MW wave energy farm

uncertainty due to the lack of experience in this field and the limited availability of commercial PTOs for this type of devices in the market. This cost is selected based on the state of the art of the generators in existing WEC prototypes or demonstration projects. The prices of the logistics and installation and electrical infrastructure are based on a personal communication with the author. For this calculation the wave farm of 4 devices is considered. The weight of the structure are 293,320 Kg of steel (for the shell) and 2200  $m^3$  of concrete for the ballast. As stated before it is assumed that the export cable length is 4.3 km, the array cable distance is 1.6 km and the onshore cable length is 1 Km.

As shown in Table 6.1 the budget of the project is quite high. The percentage of steel is nearly 37%, representing an important stake of the cost. It would be possible to assume that for WECs which have been through several optimization phases this percentage could be reduced.

In order to complete the economic analysis, operating expenses (OPEX) have to be added.

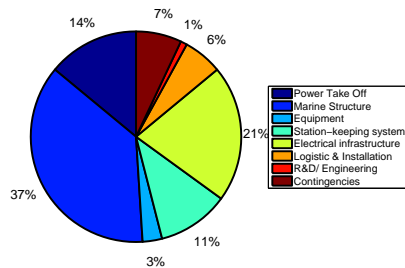


**Figure 6.7:** Distribution of cost items for the EPCI budget for the selected wave energy farm

OPEX refers to the operation and maintenance costs also taking into account the insurance cost. OPEX assessment is a difficult task due to the absence of experience in the operation and maintenance of these devices. In order to provide a value a review of the existing percentages with respect to the initial cost of the project is carried out. O'Connor *et al.* (2013a) presented a table compiling OPEX costs in available projects suggesting values ranging between 1.4 % and 7 % of the total project initial cost. In this study an average value of 5 % is taken based on a conservative approach. A total replacement of the devices is proposed at the middle of the life-cycle. A conservative value has been assumed due to the lack of experience regarding the durability of these types of structures at sea.

No project financing is considered and payment of the initial cost of the project is set at year 0 in the cash-flow analysis as it is conventionally assumed in project financing studies( f.i Newnan and Lavelle (1998)). This assumption is also assumed on O'Connor *et al.* (2013a). It is known that this assumption is probably unrealistic. However on this study the influence of other factors is highlighted and the influence of the debt/equity financing will be studied on future studies.

**Discounted cash-flow algorithm**

The discounted cash flow technique is a method assessing the value of a project, company or asset by measuring the expected future cash flows derived from its operation, introducing the time value of money to capture the opportunity cost of the money tied up in the project. All future cash flows are estimated and discounted to give their present values (*PVs*). The sum of all future cash flows, both incoming and outgoing, is the present value of the project (*PV*), which summarizes in a single value the overall distribution of cash flows derived from the project. The future value, *FV*, of a series of cash flows refers to the future value, at future time *n* (total periods in the future), of the sum of the future values of all cash flows, *CF*.

The cash flow analysis is based on the following formula:

$$PV = \frac{FV}{(1+r)^t} \quad (6.1)$$

where *PV* is the present value, *FV* refers to the future value, *r* represents the discount rate and *t* means the number of time periods.

For the uncertainty analysis of the financial performance that will be presented in the next section a set of 3 financial indicators is chosen. The first indicator in order to evaluate the profitability of a specific project is the net present value (NPV) that is the sum of all the present values of the cash-flows corresponding to the project.

$$NPV = \sum_{t=1}^{n_y} \frac{FV}{(1+r)^t} = -I_0 + \sum_{t=1}^{n_y} \frac{AnnualRevenue - OperationCost}{(1+r)^t} \quad (6.2)$$

where  $I_0$  represents the initial cost of the project assumed to be paid at time  $t = 0$ . *AnnualRevenue* and *OperationCost* refers to the annual income obtained by selling the energy generated at year  $t$  ( $q_t$ ) (kW) at a price  $p_t$  (Euro/kW), and to the annual operation and maintenance costs respectively and  $r$  refers to the discount rate.

The second indicator is the internal rate of return (IRR) that is the rate of return that makes the net present value of all cash flows from a particular investment equal to zero. It is expressed with the next formula:

$$NPV = \frac{FV}{(1+IRR)^t} = 0 \quad (6.3)$$

The last financial indicator to take into account is the payback period (PBP), which provides the minimum number of years needed to recover the initial investment on a project.

$$\sum_{t=0}^{PBP} NPV \geq 0 \quad (6.4)$$

### 6.2.4 Statistical analysis of financial indicators

The aim of this section is to analyze the uncertainty of the selected financial indicators for the wave energy farm project considered. Following the methodology proposed in this work, we define the socioeconomic scenario based on the following assumptions:

1. Energy price, defined as the cost of electricity at the point of connection to a load or electricity grid, is set to 0.1 Euros/kWh.
2. A nominal interest rate of 8% is fixed with a 3% expected inflation resulting in a 5% real interest rate. This is assumed to be Real Rate of Interest a company is willing to accept and will be used as the discount rate.
3. Initial project's costs are incurred and paid at year 0, that means that no external financing is needed for the construction period (this assumption could be unrealistic, however the influence of debt/equity business models will be studied on subsequent works).
4. OPEX is supposed to account for 5 % of the initial cost of the project. This is an average value obtained from literature.
5. A first estimate of 0.55 Euros/kWh is set for the feed in tariff in order to obtain profits from the investments. Lower values were tested, however, these tariffs produced unrealistic results due to the large proportion of negative IRR and PBP. A detailed sensitivity analysis of the results to different feed in tariffs is presented in the next section.

With these assumptions, the cash flow analysis is performed for each of the 10.000 simulated life-cycle, obtaining then a series of 10.000 IRR, NPV and PBP values. In figure 6.8 the mean cash flow is shown with a bar diagram. The green dark bars represent the free cash flow accumulative path while the green clear bars represent the income (sales and feed in tariff); the blue bars represents the revenue (Income minus the OPEX) and the blue solid and red dotted lines represent the maximum and minimum free cash flow. The time evolution of the mean cash flow suggest that the mean net present value of the investment is positive. However, the blue and red lines represent the maximum and minimum NPV showing that a negative NPV is also possible. A complete replacement of the devices is foreseen at the thirteenth year resulting in a change in the sign of the cash-flow series is observed. The maximum free cash flow line becomes positive before the replacement reflecting net positive contribution to NPV. Note that the separation between the minimum and maximum values is the highest. This implies that at the end of the cash flow the maximum NPV is positive and the minimum NPV is negative. The difference between maximum and minimum is 2.5 Million Euros. This indicates a great uncertainty induced by the interannual variability of the wave climate. This variability is expressed in terms of the coefficient of variation (standard deviation divided by the mean) in table 6.2.

Consequently, it can be concluded that the variability derived from randomness in energy fluxes produces the uncertainty in the economic performance of the farms and this can be measured through the statistical distribution of the economic indicators selected. In figure 6.9 the mean,

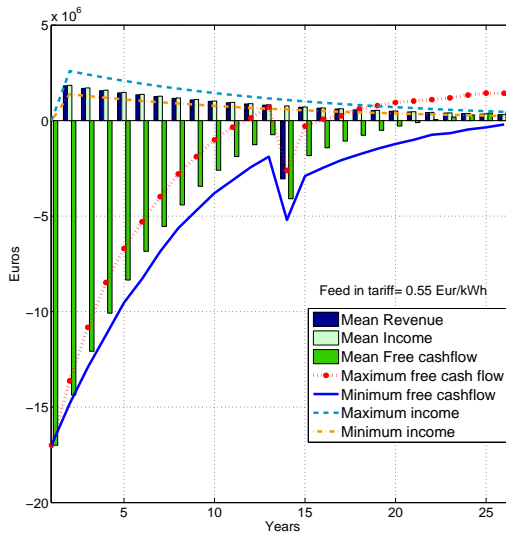


**Figure 6.8:** Mean cash-flow for the 10000 generated life-cycle.

standard deviation and coefficient of variation of wave energy flux are represented. From this figure, it can be concluded that coefficient of variation of wave energy resource should be an important value for wave energy projects location assessment due to its high importance in financial returns. Therefore, as a recommendation for the promotion of wave energy project, locations with a low coefficient of variation and low standard deviation are suggested, for instance near the low latitudes in the Southern hemisphere (for instance on the Chilean coast where the average wave power is high and the coefficient of variation is low).

In Figure 6.10 different life-cycles are compared. For case 1, a life cycle with a high production is simulated, and hence a positive NPV is obtained. It is observed that the positive balance is reached after 22 years of operation. In the second case where a less productive life-cycle is chosen, we observe that the accumulated NPV does not reach a positive value. Therefore, it can be concluded that the variability of financial indicators has been analyzed as a result of the influence of the wave climate. Then, it is also concluded that in order to study the performance of a wave energy farm a long data series is needed in order to capture all the met-ocean variability.

The present methodology provides a statistical approach analysis of IRR, NPV and PBP by simulating life-cycle production. In figures 6.11 to 6.13 the Cumulative Density Function

Element	Coefficient of Variation
Wave flux	1.39
Power production	0.128
IRR	0.08
PBP	0.12

**Table 6.2:** Coefficient of variation of wave flux, wave production IRR and PBP

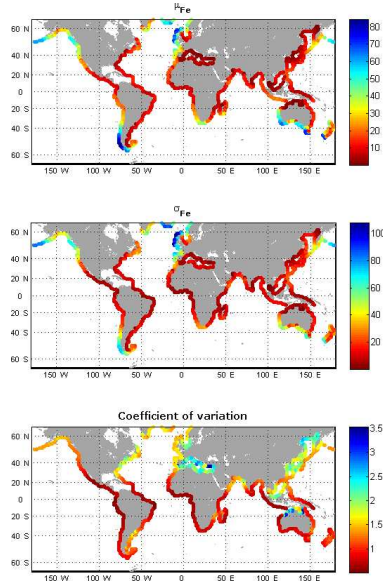


**Figure 6.9:** Mean, standard deviation and coefficient of variation of wave flux

(CDF) of the financial indicators IRR, NPV and PBP are shown. In Figure 6.11 the CDF of IRR and the adjustment to a log-normal distribution are represented (the best fit for these data). It is important to point out that based, on the previous assumptions, the mean IRR is nearly 5.6 %, that is a very low value for an investment (Newnan and Lavelle (1998)). This means that although the benefits can reach a maximum value of 8% this investment represents a high financial risk. The high standard deviation of the distribution (0.45).

Figure 6.12 represents the CDF of the NPV distribution. The best fit for this data is also a log-normal distribution. The Expected value for this indicator is 828.905 Euros, and the standard deviation for this variable is also high, 624.415 Euros. In the interval between  $\mu(NPV) \pm \sigma(NPV)$  ( $828905 \pm 624415 \text{Eur}$ ) we find the 66% of the data.

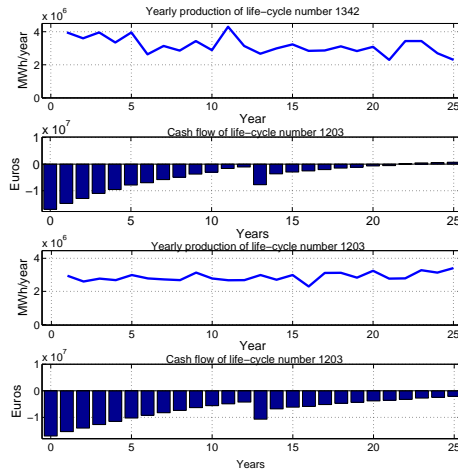


Figure 6.10: Comparison between 2 life-cycles: top panels, the yearly accumulated production and lower panels associated the cash flow

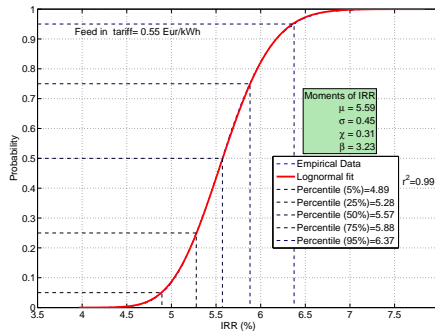


Figure 6.11: Cumulative distribution function for the IRR with a lognormal distribution

Lastly, In figure 6.13, the CDF of the PBP is shown. In order to fit these data ,the PBP that were greater than project lifetime (25 year) were not taken into consideration (only 0.025 % of the cases). Then this graph presents the truncated distribution. These data fit a t-student distribution. The mean PBP is 21.22 years, and the standard deviation is 2.5 years. These results indicate that the NPV reach positive values near the end of the lifetime.

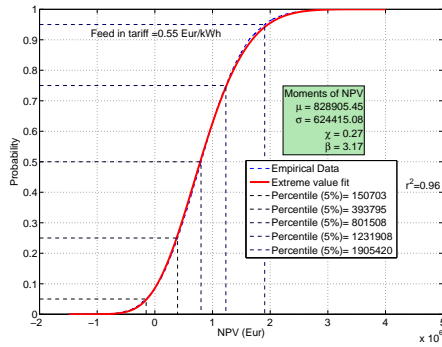


Figure 6.12: Cumulative distribution function for the NPV with a lognormal distribution

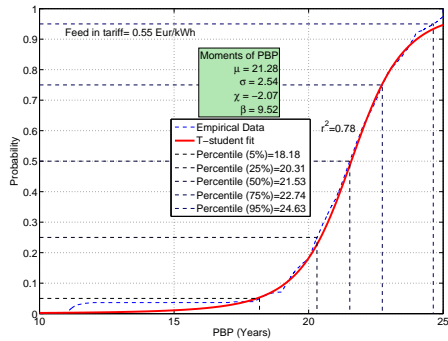


Figure 6.13: Cumulative distribution function for the PBP with an extreme value distribution

From the analysis of this figure, the anomalous situation that emerges when the initial investment is recovered before the general replacement is treated; see figure 6.8, when the maximum cash flow line intersects with the x axis before the mid life replacement. This fact influence the first part of the curve, where the fit of the t-student is worse due to these anomalies (the probability of this fact is very low and then the fit is not good because of this reason).

### 6.2.5 Sensitivity analysis: feed in tariff

In this section a sensitivity analysis is performed on the feed in tariffs. As said before, existing feed in tariffs are not sufficient to guarantee positive profits for the WECs. In this section a set of feed in tariffs will be studied in order to obtain the minimum tariff for the device studied in this paper. The learning process is introduced through a learning curve coefficient affecting the investment costs in the future.

To this point, all the results are derived from the analysis of a 4 WECs wave farm. However, the improvement obtained from repetitive construction cycles has to be considered in order to approximate to the actual field conditions.

The approach to the problem will be based on two steps, initially the sensitivity analysis on feed in tariffs is performed without a learning process. This way the effect of different feed in tariffs on the financial performance of the project is isolated, which is shown in Figure 6.14. Note how the minimum feed in tariff required to achieve a positive mean IRR is 0.4 Euros/kWh. Also if a 10% IRR is required a feed in tariff of 0.8 Euro/kWh is needed to reach that value. This corroborates the theory explained in Dalton *et al.* (2012) regarding the insufficiency of the actual feed in tariffs. Also another noticeable issue is the difference between the minimum and maximum IRR for each feed in tariff. For example if a feed in tariff of 0.5 is fixed then the difference between the minimum and maximum IRR is 4 %. This also corroborates the idea explained in the previous subsection on the huge influence that marine climate has on financial indicators. It is important to highlight that the IRR does not reach positive occurrences until feed in tariffs over 0.3 Euros/kWh.

Another noteworthy issue is how the difference between maximum and minimum is higher as the feed in tariffs increase. This is a strong evidence of the variability of power production. As the feed in tariff increases, the revenue is also increased, making the power production more significant in the cash flow analysis. In fact, feed in tariffs amplify variability in production when transforming kW into euros. Consequently, a high feed in tariff maximizes the importance of power production in cash flow and it increases variability.

In figure 6.14, the NPV is also analyzed (taking into account the hypothesis outlined in previous section). The point at which the mean net present value starts to be positive correspond approximately to a 0.6 Euros/kWh, that is a very high feed in tariff comparing with the current values. Moreover, for the same feed in tariff, the difference between the minimum and maximum NPV is relatively high, approximately 5 million Euros for a feed in tariff of 0.5 Euros/kWh.

As mentioned earlier, in a second step the learning curve is taken into account. Learning curve accounts for the process of learning in an industrial process and how it affects the cost of the devices (Wright (1936)), referred to the bulk orders of devices. Then it is logical that as the number of produced units gets higher, the cost per unit will decrease based on the learning produced per unit. The experience shows that learning process in human activities produce an

increase in productivity hence decreasing unit costs. There are very few studies that take into account learning curve in wave energy conversion. In this paper the curve suggested by Dalton *et al.* (2012) is used. This curve is specified in the following equation:

$$P = N^{\ln(lc)/\ln(2)} \quad (6.5)$$

being  $N$  being the number of WECs produced and  $lc$  is the learning curve factor that measures improvements gained when production is doubled (in this case). In this study 3 scenarios are considered. For the optimistic scenario a  $lc$  of 0.91 is considered, for the middle 0.86 and for the pessimistic a 0.82. For instance, the middle scenario, with a factor of 0.86 means that when the number of units is doubled the reduction in cost is 14 %. As previously established , this learning curve focuses on the technical uncertainty of actual conditions, and allows modeling its impact on financial results. With time and repetition higher levels of efficiency are reached and lower unit costs are obtained.

In Figure 6.15 the learning curve impact in the cash-flow analysis is represented. The figure represents the three scenarios specified in the previous paragraph. The 3D plot represents the internal rate of return for the different feed in tariffs and the accumulated number of manufactured units . As the figure shows for all the scenarios for the lowest feed in tariffs and the lowest number of units the internal rate of return is not calculated because it is negative. In the middle scenario it can be seen that for the currents tariffs of 0,22 Euros/kWh (Ireland) a high number of units (nearly 20) need to be considered in order to get an IRR of 10 % or similar. If the percentage of learning is analyzed, this represents a 48% of learning with respect the first unit, then the cost is expected to diminish 82 % with respect to the first unit. Due to the lack of information, this study was done with a theoretical expression and in reality a drop of the cost in a 48 % is unknown and uncertain. For higher tariffs such 0,4 Euros/kWh a lower number of units is needed in order to get the same IRR.

Figure 6.16 shows some iso-internal rates of return curves corresponding to the middle scenario. These curves are horizontal sections of the central figure 15 surface. As the feed in tariff grows the internal rate of return has an asymptote, which is obvious as device performance becomes less dependant on the learning process. It is remarkable that the for the base feed in tariff of 0,22 Euros/kWh, 20 units (a 48% drop in the cost) are needed for 10 % IRR , 32 units (a 52% drop in the cost) for the 12 % IRR and 80 units (a 62% drop in the cost) for the 15 % IRR. This fact, gives an idea about the technological risk of this type of inversions and how the feed in tariffs that currently exist are not sufficient for the development of this technology.

This section summarizes the issues and the numbers regarding the subsidies that administrations apply to renewables in order to promote its development. However, the last goal for this study is to provide an abacus for the administrations in order to choose the right feed in tariff (specified for the wave farm of this study) for each case. For this task a set of pdfs is shown in figure 6.17

for each feed in tariff. These figures can help governments to determine the appropriate feed in tariff to assure a given IRR with a given confidence level. For instance, in the first subfigure with a tariff of 0.25 Euros/kWh an 8% IRR is possible but the probability is very low (0.1 %). This figure give the administration an abacus in order to choose with statistical parameters the right tariff. In this figure it should be highlighted that the shape of the pdf changes as the feed in tariff increases. The pdf moves towards higher IRR and also the pdf has a flatter shape. Figure 6.17 show how the pdfs mean and standard deviation increase as the feed in tariff increases. The reason is because as the feed in tariff increases the importance of revenues by the energy production increases in the cash flow algorithm and then the variability of production has a major influence on the distribution of IRR. For instance, if nowadays a 10 % is needed with a high level of confidence (95%) a feed in tariff of 0.5 Eur/kWh is needed.

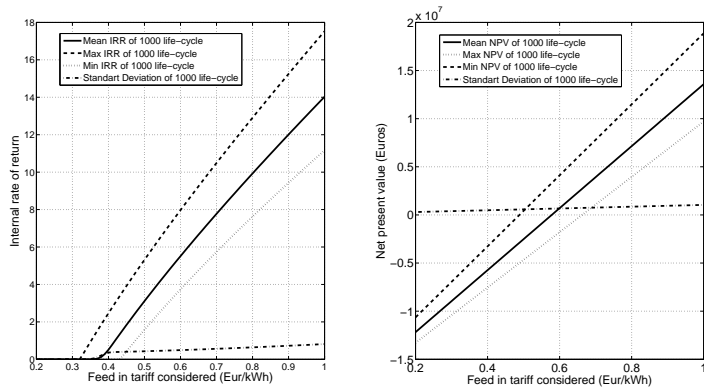


**Figure 6.14:** Internal rate of return and Net present value vs different feed in tariffs

### 6.2.6 Feed in tariff uncertainty

In the previous sections the uncertainty of marine climate on the financial feasibility of the studied wave energy project was evaluated. The feed in tariff mechanism was studied and a range of feed in tariffs was tested in order to demonstrate the importance of the feed in tariff on the viability of the novel wave energy projects. In this previous case the feed in tariff mechanism was simplified to a constat value during the life cycle of the project. However, this assumption could be risky in the real world and then more realistic feed in tariff scenarios are needed to evaluate the uncertainty that the feed in tariff decisions imply on the project feasibility.

Firstly, in figure 6.18 the feed in tariffs for different renewable technologies across the European countries are shown. This figure is extracted from Klein *et al.* (2008). As shown in this table,

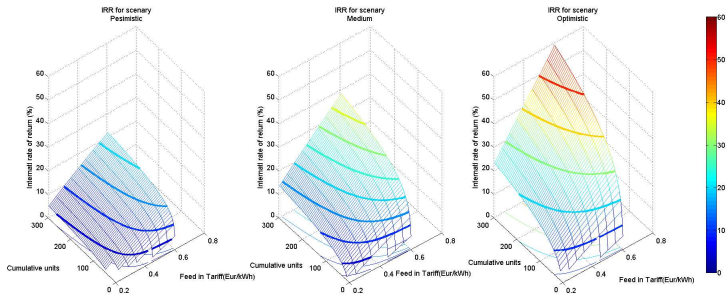


**Figure 6.15:** Internal rate of return vs number of units and feed in tariff for the different scenarios (optimistic, medium and pessimistic) proposed (the gross lines represent the isolines of IRR)

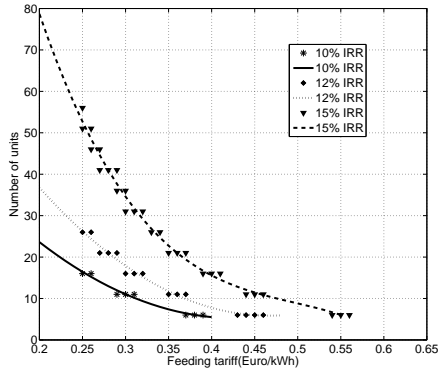


**Figure 6.16:** Curves of iso-internal rate of return for number of units produced vs feed in tariff applied

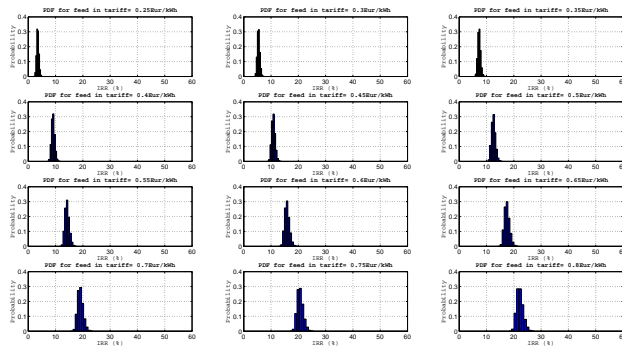


Figure 6.17: PDF of IRR for the different feed in tariffs

when the feed in tariffs are set they are maintained during a fixed number of years. Once the limit is reached the feed in tariff is revised or entirely eliminated depending on the state of the technology and the political status. The scale of financial support towards renewable energy normally ranges around 10-25 years.

The duration of the support also affects the novel wave energy. For instance, the UK recently adopted the Contracts of Difference (CdFs) as the support mechanism towards novel renewables replacing the old Renewable Energy Obligations (ROCs). The contracts of difference are intended to remove the potential for windfall benefits while retaining the level of support necessary to make low-carbon investment viable. The Feed-in Tariff element of the package "tops-up" any shortfall between the amount the generator receives per unit of electricity and a pre-defined "strike price" in the long-term Contract for Difference. Once the strike price is exceeded, the generator is required to pay the surplus back. The result is that generators neither suffer nor benefit from price volatility as illustrated on Figure 6.19.

In the case of wave energy, the CdFs are confirmed for 15 years (see Renewable UK *et al.* (2013)). This support towards wave energy changed with the adoption of CdFs. The shortening of the contract length from 20 years under the Renewable Obligations to 15 years under the FiT CfD has a significant impact on the rate of returns expected from projects, heightening the required support level by around 16% under a 15 year contract. Thus a reduction in contact length to 15 years would necessitate uplift of the strike price to 325 - 350 pounds per MWh for tidal stream energy and 350 -375 pounds per MWh for wave energy.

This change on the financial support system affects the feasibility of the projects on two ways. Firstly, when setting tariffs shorter than the average expected life-cycle of the projects if the same level of support is desired it should be taken into account that from a government

		Tariff level in 2008 [€ Cents/kWh] and duration of support for different technologies						
Country		Small hydro	Wind onshore	Wind offshore	Solid biomass	Biogas	PV	Geothermal
Austria (fixed)		3.2 – 5.7 10–15 yrs.	7.8 10–15 yrs.	–	11.3 – 15.7 10–15 yrs.	11.5 – 17.0 10–15 yrs.	32.0 – 49.0 10–15 yrs.	7.4 10–15 yrs.
Bulgaria (fixed)		4.1 – 4.4 –	8.0 – 9.0 –	–	8.3 – 11.0 –	8.3 – 9.4 –	36.7 – 40.0 –	–
Cyprus (fixed)		6.3 no limit	9.2 15 yrs.	9.5 15 yrs.	6.3 no limit	6.3 no limit	20.4 – 38.6 15 yrs.	–
Czech Republic	(fixed)	6.6 – 9.9 15 yrs.	9.4 – 12.5 15 yrs.	–	9.3 – 16.1 15 yrs.	8.9 – 14.9 15 yrs.	25.1 – 51.5 15 yrs.	17.2 15 yrs.
	(premium)	2.0 – 5.4 15 yrs.	7.1 – 10.3 15 yrs.	–	4.4 – 11.2 15 yrs.	4.0 – 10.0 15 yrs.	22.0 – 48.4 15 yrs.	12.9 15 yrs.
Denmark (fixed)		–	–	–	8.0 10 yrs.	8.0 10 yrs.	20.0 – 25.0 20 yrs.	6.9 20 yrs.
Estonia	(fixed)	7.42 12 yrs.	7.42 12 yrs.	7.42 12 yrs.	7.42 12 yrs.	7.42 12 yrs.	7.42 12 yrs.	7.42 12 yrs.
	(premium)	11.0 12 yrs.	11.0 12 yrs.	11.0 12 yrs.	11.0 12 yrs.	11.0 12 yrs.	11.0 12 yrs.	11.0 12 yrs.
France (fixed)		6.6 – 8.6 20 yrs.	8.2 15 yrs.	13.0 20 yrs.	4.9 – 6.1 15 yrs.	4.5 – 14.0 15 yrs.	30.0 – 55.0 20 yrs.	12.0 – 15.0 15 yrs.
Germany <sup>1)</sup> (fixed)		7.65 – 12.67 20 yrs.	9.2 20 yrs.	13.0 – 15.0 20 yrs.	7.79 – 22.67 <sup>2)</sup> 20 yrs.	7.79 – 29.67 <sup>2)</sup> 20 yrs.	31.94 – 43.01 20 yrs.	10.5 – 20.0 20 yrs.
Greece (fixed)		7.3 – 8.5 12 yrs.	7.3 – 8.5 12 yrs.	9.0 12 yrs.	7.3 – 8.5 12 yrs.	7.3 – 8.5 12 yrs.	40.0 – 50.0 12 yrs.	7.3 – 8.5 12 yrs.
Hungary (fixed)		10.5 no limit	10.5 no limit	–	10.5 no limit	10.5 no limit	10.5 no limit	10.5 no limit
Ireland (fixed)		7.2 15 yrs.	5.7 – 5.9 15 yrs.	5.7 – 5.9 15 yrs.	7.2 15 yrs.	7.0 – 7.2 15 yrs.	–	–
Italy (fixed)		22.0 <sup>3)</sup> 15 yrs.	22.0 <sup>3)</sup> 15 yrs.	–	22.0–30.0 <sup>3)</sup> 15 yrs.	18.0–30 <sup>3)</sup> 15 yrs.	44.5 – 49.0 20 yrs.	20.0 <sup>3)</sup> 15 yrs.
Latvia (fixed)		11.0 – 14.1 10 yrs.	12.6 – 13.0 10 yrs.	–	13.0 – 16.7 10 yrs.	13.0 – 16.7 10 yrs.	–	–
Lithuania (fixed)		5.8 10 yrs.	6.4 10 yrs.	6.4 10 yrs.	5.8 10 yrs.	5.8 10 yrs.	–	–
Luxembourg (fixed)		7.8 – 10.3 10 yrs.	7.8 – 10.3 10 yrs.	–	10.4 – 12.8 10 yrs.	10.4 – 12.8 10 yrs.	28.0 – 56.0 10 yrs.	–
Netherlands (fixed)		–	–	–	14.7 10 yrs.	–	–	–
Portugal (fixed)		7.5 – 7.7 15 yrs.	7.4 – 7.5 15 yrs.	7.4 15 yrs.	10.2 – 10.9 15 yrs.	11.5 – 11.7 15 yrs.	31 – 47 15 yrs.	–
Slovakia (fixed)		6.0 – 8.4 12 yrs.	5.1 – 8.6 12 yrs.	–	7.9 – 12.9 12 yrs.	6.5 – 7.9 12 yrs.	25.1 12 yrs.	9.3 12 yrs.
Slovenia	(fixed)	6.0 – 6.2 10 yrs.	5.9 – 6.1 10 yrs.	–	6.8 – 7.0 10 yrs.	5.0 – 12.1 10 yrs.	6.5 – 37.5 10 yrs.	5.9 10 yrs.
	(premium)	8.2 – 8.4 10 yrs.	8.1 – 8.3 10 yrs.	–	9.0 – 9.2 10 yrs.	6.7 – 14.3 10 yrs.	8.7 – 39.7 10 yrs.	8.1 10 yrs.
Spain	(fixed)	7.8 25 yrs.	7.3 20 yrs.	–	10.8 – 15.9 15 yrs.	10.0 – 10.8 15 yrs.	23.0 – 44.0 25 yrs.	6.9 20 yrs.
	(premium)	6.5 – 8.5 no limit	7.1–8.5 no limit	14.1– 16.4 no limit	10.4 – 16.6 no limit	9.4 no limit	–	9.5 no limit

1) For installations commissioned 2009 according to the new EEG from June 2008.  
2) The maximum value given for Germany is only available if all premiums are cumulated. This combines the enhanced use of innovative technologies, CHP generation and sustainable biomass use in a relatively small plant (see Chapter 3.6.1.1 and 3.2.3). This maximum value is rarely reached.  
3) The Italian feed-in tariffs are available only for plants with a capacity below 1 MW (except for photovoltaics).

Figure 6.18: Level and duration of support for RES-E plants commissioned 2008

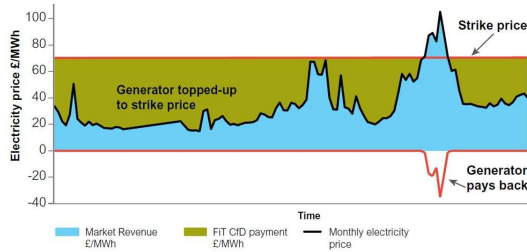


**Figure 6.19:** Contracts for difference schema from Renewable UK *et al.* (2013)

perspective an increase on the tariff should be applied.

Secondly, from a project developer perspective, when analyzing the feasibility of projects a change on the political support and then on the feed in tariff should be analyzed on the feasibility study. Changes of the duration of the support should be taken into account and the uncertainty produced should be examined.

This feed in tariff real case has been applied to the WEC case studied in this chapter. The feed in tariff mechanism was plotted in Figure 6.20. This Scenario 1, consists of a constant tariff (0.55 Eur/kWh) until the tariff is stopped before the end of the life cycle of the project. In this figure, 4 cases are plotted, 5, 10, 15 and 20 years of support. Figure 6.22 represents the cashflow associated to the 3 subcases presented in previous figure. As can be seen the cashflow for the different scenarios is totally different and a decrease on the profitability of the project is obtained with the shortened tariff. Also for the four sub-scenarios presented here the tariff needed in order to obtain the same NPV than the reference case study (Figure 6.8) is performed and it is explained on table 6.3. A decrease of the financial support of 5 years (less than the project life cycle) here leads to a recommended increase on the FiT of an 8% if the level of support towards the company wants to be maintained.

	Scenario 1.1 (5 years)	Scenario 1.2 (10 years)	Scenario 1.3 (15 years)	Scenario 1.4 (20 years)
Feed in Tariff (Eur/kWh)	1.47	0.87	0.69	0.59
Feed in Tariff percentage increase	166%	58%	25%	8%

**Table 6.3:** FIT needed to obtain the same NPV than reference case in Figure 6.8

On the other hand there are some countries where a stepped feed in tariff mechanism is used. On this mechanism the plants receive a fixed tariff during the first 5 or 10 years of operations and then the tariff decreases during the rest of the life of the plant. This support scenario is plotted on Figure 6.21. The way the tariff is constant during the 5 first years of operation of the

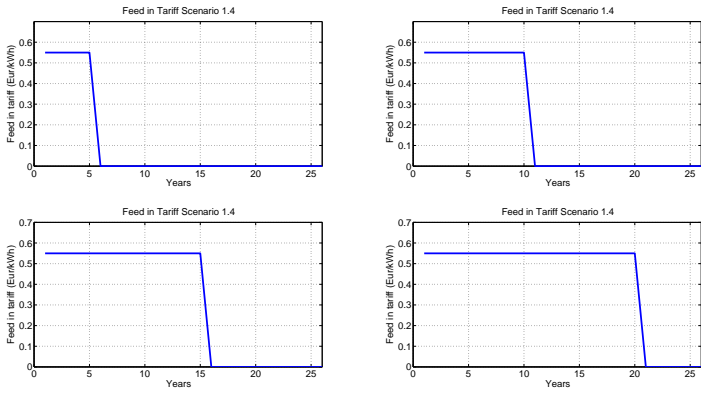


Figure 6.20: Feed in tariff Scenario 1

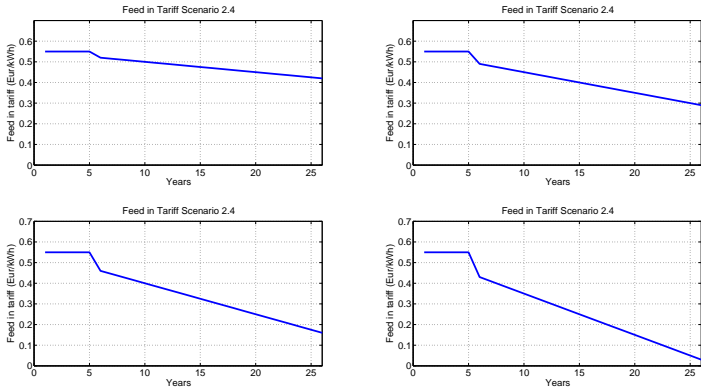


Figure 6.21: Feed in tariff Scenario 2

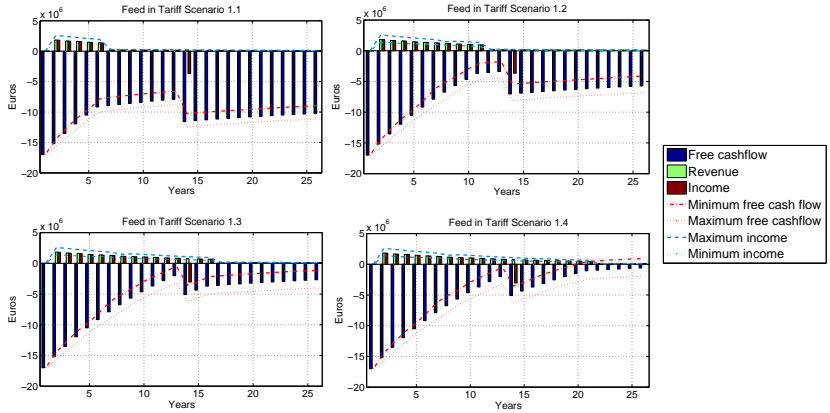


Figure 6.22: Cash flow associated with Feed in tariff Scenario 1

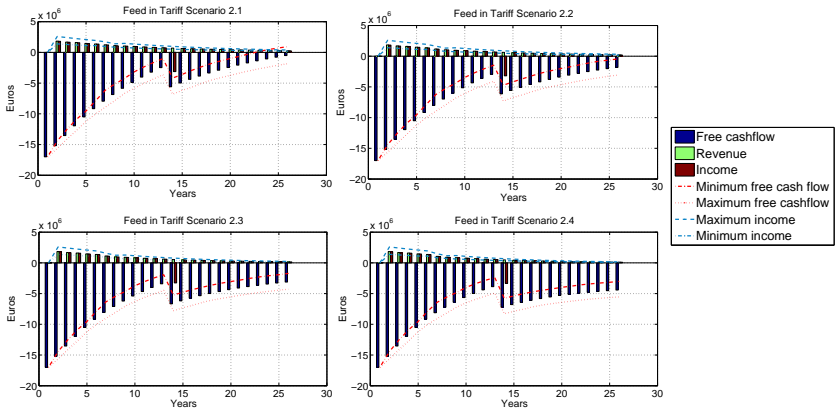


Figure 6.23: Cash flow associated with Feed in tariff Scenario 2

plant can also be seen along with the tariff that decreases gradually during the years that are left. The associated cashflows to this feed in tariff scenario (Scenario 2) are plotted on Figure 6.23. As can be seen the change on the final NPV of the project is milder than the previous case (Scenario 1) when the support changed to 0 at a certain point.

In the previous section, the way the marine climate affects the variability and the uncertainty of the feasibility indicators of wave energy projects was highlighted. However, the political uncertainty regarding the financial support towards the project should also be taken into account. On the previously defined scenarios - Scenario 1, constant support until certain time when no support is provided and Scenario 2, constant support until certain time when stepped support happens -a calculation regarding the influence of these political decisions on the feasibility of the project is performed (see Table 6.4). In this table the uncertainty of the different factors/scenarios is represented through the standard deviation. The way the uncertainty on the NPV is higher for the Scenarios 1 and 2 than the marine climate should be highlighted. It could be concluded that political decisions have a great impact on the feasibility of these novel projects and the creation of a fixed and stable regulatory framework is key in order to avoid risks and more uncertainties. From a developer perspective met-ocean conditions variability is unavoidable and thus it needs to be included and analyzed on the feasibility studies. However the political framework (feed in tariff) stability should be also taken into account when analyzing the feasibility of the projects. Also, as demonstrated with the Scenario 1, feed in tariffs lasting less than life cycle of the financed projects are not recommended because they increase the uncertainty for developers and further investment is needed then if the support wants to be maintained.

	Met- ocean conditions	Cease of feed in tariff (Scenario 1)	Stepped feed in tariff (Scenario 2)
Standard deviation	600.000 Eur	3.000.000 Eur	1.600.000 Eur

**Table 6.4:** FIT needed to obtain the same NPV than reference case in Figure 6.8

### 6.2.7 Conclusions

The aim of this chapter was to examine the uncertainty of the economic analysis on wave energy farms. A cash flow algorithm is developed in order to analyze these uncertainties. A methodology to find out how the wave climate affects the financial performance of a wave energy project is presented first based on a sea state selection technique, a non-linear interpolation technique and a random bootstrapping. The results show that the variability of financial indicators is huge due to the variability of wave climate. The CDFs of IRR, NPV and PBP are fitted to a log-normal distribution, characterized by low mean and high variances. The need for

long term climate data series is shown, and its importance is highlighted in order to explain the influence of climate variability in wave farms economic analysis.

The political-legal source of uncertainty, covered in the next section, focuses on the feed in tariff influence. The current feed in tariffs are shown to be insufficient in order to get low risk profitable inversions. Besides the maximization of the influence of power production variability as the feed in tariff increases is demonstrated. It has been concluded that the feed in tariff is not a very efficient funding mechanism for early stage wave energy technologies. In relation to the learning curve inclusion on the economic study, the analysis proves that, in order to achieve economic feasibility of a wave energy farms project, the learning process needs to be taken into account and large scale farms need to be studied.

Also the influence of the uncertainty of feed in tariff decisions was analyzed for this case study. It was demonstrated how the feed in tariffs decision cause a high uncertainty on the financial indicators. It has also been concluded that financial support should match the average life cycle of the studied farm in order to set a constant and fixed regulatory framework in order to avoid unnecessary uncertainties.

## 6.3 Pathways towards a reduced LCOE in Ocean Energy

### 6.3.1 Introduction

Ocean energy is still in a prototype testing stage and there has been few commercial deployment to date. One of the reasons for this lack of deployment is that the electricity production, in kWh, from the current prototypes is still expensive in comparison with other renewable energy sources such as wind energy. There are very few scientific studies regarding the evolution and the current status of the Levelised Cost Of Energy (LCOE) for present day ocean energy technologies. According to research carried out by Carbon Trust, it was concluded that ocean energy could achieved a cost of 15 pence/kWh by 2050, see CarbonTrust (2011), with a global deployment potential of 46.5 GW. However, there are few studies that clearly show the innovation pathway needed to achieve this goal.

In the previous subsection the influence of met-ocean variability and feed in tariff on the LCOE was investigated. It was concluded that, for the prototype studied within this research, a feed-in-tariff of 0.45 Eurocents/kWh would be needed in order for an ocean energy project to be profitable. It was subsequently demonstrated that the technology under investigation in this section is still far away from commercialization.

Previsic and Shoel (2013) investigated the current status of wave energy regarding the LCOE. They identified some key areas with cost-reduction potential for a specific type of converter. They concluded that wave energy could achieve the target of 15 cents/kWh in the near future.

Venture capital investors are discouraged to invest in ocean energy not only due to the substantial capital required, but also because of the uncertainty and unpredictability of the costs and future revenue streams Leete *et al.* (2013) - all of which present significant risk.

It is evident that by systematically identifying the risks and uncertainties, together with their potential impacts on overall cost of energy, a study of the optimal routes forward for commercialization of the sector can be presented.

As explained, there are some studies regarding the current state of the economic performance of tidal/wave prototypes. However there is very little research to date about the path that developers need to follow in order to achieve commercialization. The Energy Technologies Institute (ETI)/UKERC Marine Energy Technology Roadmap (see ETI and UKERC (2014)) presents 40 technology and deployment issues and prioritizes them from the perspective of the ETI. While this reflects the needs of the industry, there is no route map for defining timelines for the development of each identified issue, or prioritization of the aspects that are considered to be a key step towards achieving a lower LCOE. In an ideal case, funding should be targeted on the areas where the impact on reducing the LCOE is higher.

There are ocean energy industry based reports that reveal projected costs for 20MW arrays, after cumulative deployment of 20MW has already taken place SIOcean (2012), but currently there is no literature investigating the current costs of ocean energy converters, as will be experienced by the very first deployments of the technology. In order to achieve final investment decision for the first deployments, a greater understanding of the current costs must be taken into consideration by stakeholders capable of impacting ocean energy development, as cost reductions associated with future learning will not be realized without deployment of the initial small arrays.

This subsection presents a case study of two actual wave energy converters where the current costs and the planned improvements are analyzed.

### **6.3.2 Wave energy prototypes case study**

In order to define the key areas with a greater impact on the LCOE a case study analyzing two different existing wave energy technologies has been proposed. The goal of this study is to understand the areas with a greater impact on LCOE and then identify the R&D hot spots for developers in the near future. Also it is aimed to present some credible figures of the LCOE of actual technologies. For this case study a fixed multi point absorber as well as a floating multi-body pitching device has been selected for comparison. The multi-point absorber considered in this study consists of a set of floats attached to a piloted platform through an arm and it extracts energy from the heaving motion of the buoy. This prototype is a follower and then it is not very dependent on the period of the waves, but its highest power performance corresponds to low periods (4-5 s). On the other hand the attenuator considered in this study is

formed by a set of floating cylinders with joints in between. It extracts motion from the relative pitching and yawing motion between cylinders. The performance of this prototype is higher in the 8 - 9 s period area and wave heights higher than 2 m. It should be noticed that the names, exact characteristics and power matrices of the devices are not included in this chapter due to confidentiality issues. The data for the economic analysis as well as the power matrix of both devices has been obtained through conversations with the developers.

For the LCOE analysis of both prototypes the LCOE tool from Julia Fernandez Chozas web page has been used. In this particular case, this tool is used for the sake of simplicity and the easiness adaptation to different locations. Furthermore, despite the goal of previous section, in this section the goal of the LCOE analysis is average terms, not on the inter-annual variability and then this tool simplifies the analysis compared to the methodology developed on the previous section.

In this tool, the computation of the Annual Energy Production is based on the classical method of multiplying the scatter plot by the power matrix of the devices. For this economic analysis the data regarding the energy yield of the devices is explained in Table 6.5. The multi-point absorber is assumed to be deployed for this study in Hanstolm (Denmark), while the attenuator is assumed to be deployed at EMEC. The scatter plot has been obtained from COE Tool from Julia Fernandez Chozas web page for both cases. The power matrices have been obtained for the Multi point absorber case from conversation with the developer and for the attenuator case from Dalton and Lewis (2011). It should be noticed that these figures are taken considering only one unit and the no learning is applied on these costs. Within this tool, the LCOE calculation is based on the cash flow analysis presented in the previous section. The total costs of the device are obtained taking into account the CAPEX obtained through the summation of all the capital costs and the OPEX as a percentage of the CAPEX. An interest rate of 10 % is set for both cases based on the recommendations in Julia Fernandez Chozas web page.

Firstly, for this study it is intended to investigate how the different variations of the current prototypes will affect the LCOE and, ultimately, what LCOE could be realistically expected for the future. For this reason several variations have been studied. For the multi-point absorber case the base case study has been selected with the following characteristics:

- Structure made with fibre glass
- Resistive control
- Hydraulic efficiency of PTO =0.7

For the attenuator the base case is set with:

- Reactive control
- Structure made with steel
- O&M strategy without optimization
- Restrained availability (80%)

	Multi point absorber	Attenuator
Location	Hanstolm (Denmark)	EMEC(UK)
Average depth	30 m	75 m
Average resource	5.8 kW/m	28.5 kW/m
Estimated lifetime	20 years	20 years
Rated power of the device	1 MW	750 kW
Initial cost (structural cost of the device + PTO)	11 MEuros	3.8 MEuros
Mooring system		0.4 MEuros
Electrical connection	0.3 MEuros	0.5 MEuros
Installation	3.5 MEuros	1.7 MEuros
Total CAPEX	17 MEuros	8.3 MEuros
Annual OPEX	(0.5% CAPEX) 0.18 MEuros	(3% CAPEX) 0.18 MEuros

**Table 6.5:** Characteristics of the selected devices

	Case number	Characteristics	Energy Yield (MWh/year)
Mutipoint absorber	1M	Base Case	340
	2M	Base Case + Reactive control	500
	3M	Case 2 + 10 % Improvement on PTO efficiency + Reactive control	1028
	4M	Case 3 + Optimum control + Reactive control	1144
	5M	Case 4 + Ultra High perform concrete	1144
Attenuator	1A	Base case	1185
	2A	Base case + concrete	1185
	3A	Case 2 + optimization of O&M strategy	1185
	4A	Case 3 + enhanced control	1539
	5A	Case 4 + increase on availability	1729

**Table 6.6:** FIT needed to obtain the same NPV than reference case in Figure 6.8

It should be pointed out that the reference case study represents the current state of the technology and it was impossible to compare both prototypes with similar characteristics as they are on different TRL levels.

It should be noticed that in Table 6.7, in order to find out the net influence of each case on the LCOE each case takes into account the previous improvements specified in the other cases. For the calculation of the LCOE, an interest rate of 10% due to the novelty of the technology has been selected. The procedure in order to do the cash-flow analysis has been performed following the methodology outlined in the previous section.

In Figure 6.24 the LCOE for both prototypes is analyzed. For the multipoint absorber, the base case is very expensive (5 Euros/kWh) because the control strategy that is applied is not efficient and the prototype is made from glass fibre reinforced plastic (which is relatively expensive). For the second case the control strategy is changed to a reactive control (2 constants, damping and stiffness control strategy), instead of resistive (1 constant control strategy), and, as can be seen on Table 6.7, the power production sees an increase of almost a 30% (the LCOE is reduced by almost 30%). In addition, it is worth mentioning that, for the multipoint absorber case, the improvement of 10% on the hydraulic efficiency of the PTO leads to a LCOE reduction of 50%.

Also, in both cases the LCOE reduction is very significant when cheaper materials are applied to the main hull of the converter. On the multipoint absorber case, ultra high performance concrete is applied and it leads to a LCOE decrease of 40 % (with respect the 4M case) while the attenuator case, similar material improvements and cost reductions lead to a LCOE decrease of approximately 30%.

In regard to attenuator case, the improvement with a highest impact on LCOE is the optimization of the control strategy of the converter. It is concluded that both converters need to improve their power capture in order to enhance their power production and facilitate an advance towards commercialization.

However, in terms of comparing the two devices, this comparison is unfair as the deployment locations for both devices are very different (Hanstolm has a resource of just 5.4 kW/m and EMEC has a resource of 28.5 kW/m). In order to address this, as a continuation from the previous case study, six locations are selected, in order to make a fair comparison for the devices and find out the most appropriate locations for each prototype. The selected locations are specified in Table 6.7.

The data for EMEC, BIMEP, Humboldt Bay and SEM REV has been obtained from COE Tool from Julia Fernandez Chozas web page. The data for Nova Scotia has been obtained from a buoy located at the coordinates (43.71, 59.85) named "wel429", located on a site with depth of 37 m. For the location in Chile, as there wasn't open source buoy data available, the data was selected from a Global reanalysis database used in the previous chapter, at the coordinates (-73.5,26).

Locations	Average resource (kW/m)	Availability (%) for multipoint absorber case ( $H_s < 4m$ )	Availability (%) for attenuator absorber case ( $H_s < 6m$ )
EMEC (UK)	28.5	92	94
BIMEP (Spain)	20.5	97	99
Humbold Bay (USA)	26.1	95	98
SEM-REV (France)	15.7	95	99
Nova-Scotia (Canada)	16.3	97	99
Chile	30	82	92

Table 6.7: WEC characteristics for case studies

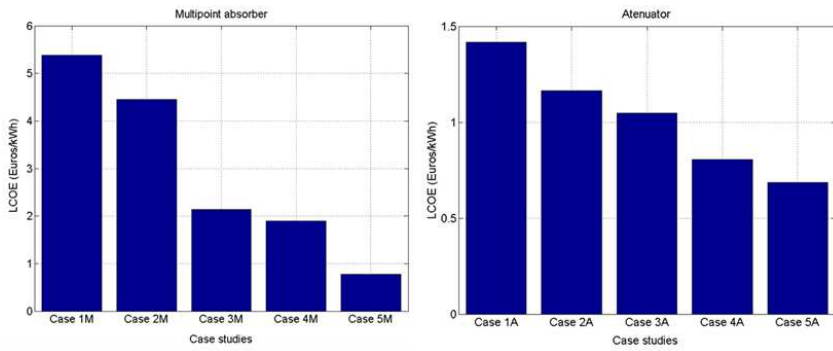


Figure 6.24: LCOE for the different cases

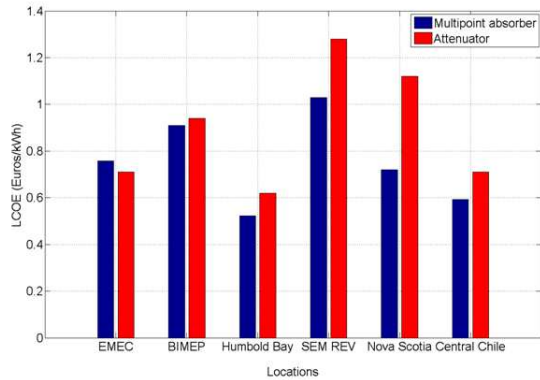
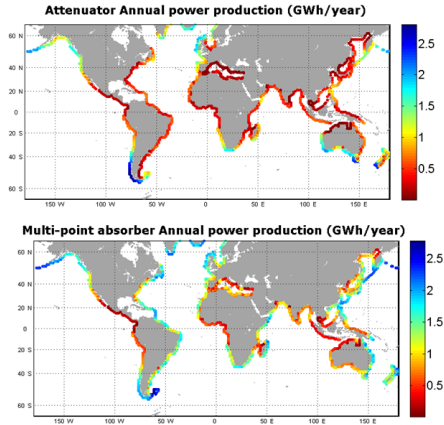


Figure 6.25: Cost of Energy on the different selected locations



**Figure 6.26:** Yearly power production for the two analyzed converter

For these comparisons at a geographical level, the cases 5M and 5A are selected. The costs are kept the same for all the locations (although it is known that the materials cost and labor costs can vary from country to country). It should be highlighted that no feed in tariff has been applied on this study in order to make a fair economic performance comparison among the economic performance among the different locations. The feed in tariff is considered within the political will aspects of the country case study carried out previously. Figure 6.25 shows the LCOE in Eurocents/kWh for each technology within each of the aforementioned locations. It should be noticed that for all the cases except EMEC, the multipoint absorber has a lower LCOE than the attenuator. The highest differences are found on Nova Scotia and SEM-REV locations. The multipoint absorber is designed for relatively mild climates and for low energy periods. On the other hand the attenuator is designed for rougher climates and higher energy periods. Then, as this graph shows, both converters have different markets and, as such, their design is different and their prospective target markets should not collide or interfere.

From the power performance point of view it should be highlighted that, on Table 6.7, the location with highest resource was Chile and the locations with the lowest resource was SEM REV (France). However, on the LCOE chart the location with the lowest LCOE is Humboldt Bay in USA. This is due to the fact that Chile, despite its great resource, has a lower availability and therefore net power yield over the period of one year. On the other hand the Nova Scotia case should be highlighted. The resource is low (16.3 kW/m) compared to the other locations, however, for the multipoint absorber case the LCOE is the third lowest. This fact leads to the idea that locations with low resource can still be successful for waver energy development if the converter is matched for these particular met-ocean conditions.

Figure 6.25 also leads to the idea of market targeting for wave energy converters. As the design approach and the working principle are different, the performance of the converters is highly different at each of the geographic locations considered within this study. This idea of market targeting is clearly shown in Figure 6.26 where the annual power production of each converter is represented. The appreciated differences on the LCOE on the previous figure come from the distinct energy yields of the converters at the different sites. The areas with high resource such as Ireland have in both converters a high power production, however the difference between the two maps should be highlighted. For instance, in the attenuator map the coast of Chile has a very high production because this area is characterized by strong swells with high periods. On the other hand, the multi-point absorber converter has a mild production on this area. This converter has a good performance on some sites with milder conditions such as Denmark, Nova Scotia (Canada), East coast of North and South America.

Further studies of wave energy development on specific converters are needed in order to gauge the attractiveness of different converter designs for specific wave climates.

### 6.3.3 Conclusions

In this case study the LCOE of two different actual wave energy converters was analyzed. The LCOE tool from Julia Fernandez Chozas was used for this section due to the simplicity and its easy adaptation to different location characteristics. Within this case study, the impact of some improvements on the LCOE both converters was studied in order to unveil the areas with the highest cost reduction potential in the near future. In this analysis, both converters showed that the hydraulic efficiency of the PTO has a significant impact on LCOE (up to 50 %) and also the optimization of the control techniques could lead to an important reduction on LCOE (up to 25 %). In regard to the attenuator, for being an offshore device, the increase on availability and the optimization of the O&M also has a significant impact on LCOE (up to 30 %). Also the multi-point absorber showed a more pronounced decrease of the LCOE in comparison with the attenuator because it is on an earlier stage of the technology. It is concluded that an optimization of the energy harvest through improvements of the PTO control techniques and the PTO efficiency is a key step to LCOE reduction for both converters.

On the other hand, the devices were compared on 6 different locations with different wave resource characteristics. The LCOE results showed that the behavior of the converters is completely different on the different locations. For instance the performance of the multi-point absorber is excellent in low to medium resource areas such as Nova-Scotia while the attenuator performance is good in high resource areas with high peak periods. It has been demonstrated that for wave energy, different technological solutions offer different levels of attractiveness based on the specific resource available in a given geographic location. The technologies considered within this section should therefore not be seen as competitors to one another; actually an adequate market targeting strategy could lead to a range of successful technologies

on different locations. While both technologies currently find themselves much earlier in the development life-cycle than tidal energy, there is much potential for the unlocking of significant cost reduction.

# Conclusions

---

This thesis covers several topics in regard to the techno-economic analysis of wave energy conversion. The ultimate purpose of this thesis is to provide a set of useful pieces of work ranging from the design process to the operating stage of a Wave Energy Converter. This thesis studies the techno-economics of a wave energy converter, keeping in mind the Euro/kWh as the main indicator with a focus on the influence of the met-ocean conditions on the behavior of a converter. A set of recommendations/procedures is extracted as conclusions of this thesis in order to apply them on the design/site selection/operation procedures of a wave energy converter.

In Chapter 2 the current state of wave energy is described presenting the numerous types of wave energy converters existing at the moment. A review of the readiness technologies as well as the paths followed towards commercialization is performed, concluding that although wave energy has been proved to be feasible during the last decades, the prototypes are on the testing phase and no technology has been successfully to be confirmed competitive yet. Many different converters with different activating principles are still being considered and no convergence has been achieved contributing to a very sparse funding. Therefore, a gap on the techno-economic analysis of wave energy converters has been perceived of which this thesis attempts to deepen the understanding of the techno-economic issues on wave energy conversion. From this general gap, three more detailed gaps have been identified:

1. A lack of consensus regarding a computationally efficient and accurate methodology for long term power assessment, valid for several devices and several wave conditions
2. An insufficiency of understanding of the influence of different met-ocean conditions on a wave energy converter, from the design stage, to the operation stage.
3. A scarcity of detailed economic and financial analysis of wave energy projects, bearing in mind the current stage of the technology and the particularities of the wave resource (variability)

This thesis then addresses these gaps and focuses on three main aspects:

1. The development of a computationally efficiency power assessment methodology and its comparison with respect the classical power assessment method

2. The study of the influence of met-ocean conditions from the design phase to the operating stage of a wave energy converter
3. The economic study of current wave energy prototypes (Levelized cost of Energy).

Firstly, due to the lack of long term power production data for wave energy converter a computationally efficient methodology in order to obtain the long term power production series was developed. This methodology uses a sea state selection technique in order to select the most distinct and representative sea states from a sea state spectral long term time series. These selected sea states are the input for a numerical model and the power production for the cases is assessed. Afterwards, a non-linear interpolation technique (RBF functions) is used in order to reconstruct the whole power production series along the met-ocean data series. In the first example for a two body heaving buoy, it was found that the classical power assessment method underestimates the Annual Energy Production by a 46 % while the proposed methodology only underestimates the AEP by a 11% with a similar computation time.

This technique was further applied to several converters under different sea state conditions at different locations around the world. The methodology was found to work well with the different types of WECs, locations and types of data, although it proved to work more accurately with non-resonant converters, as its response is smoother with respect the wave period and with a lower number of cases a very good precision is achieved.

Within the use of this methodology the influence of the classic power assessment methodology assumptions regarding the analytical spectra was also analyzed and some conclusions were extracted:

1. The assumption of analytical spectra proved to be inaccurate for resonant devices while it was acceptable for follower devices.
2. The use of analytical spectra (JONSWAP) was confirmed to be very inaccurate at locations with very probable mixed SWELL-WIND SEA sea states.
3. The power matrix method was found to underestimate the AEP on all the locations from -45% to -7%.
4. The proposed methodology was probed to give accurate long term data series for both analytical spectra and real spectra from buoys and it was demonstrated to improve the estimation of the AEP from 10% to 30% with respect the classical method.
5. The methodology was probed to be very accurate with 3 parameter selection,  $H_s$ ,  $T_p$  and  $\epsilon_0$ , especially in the locations with many bimodal spectra.
6. The assumption of JONSWAP spectra in a resource estimation (following the the International Energy Agency's formula for the sea state mean energy flux) for a specific  $H_{m0}, T_p$  set lead to an overestimation of the resource of 30% in all the locations. Therefore, the need of long term quality data (buoy or multi-component spectra) for an accurate long term power estimation is also highlighted.

Secondly, the influence of met-ocean conditions on the design/operation process of a converter

is analyzed. The latest failures on some real prototypes and the very modest figures of power production of some prototypes show a lack of understanding of how the met-ocean conditions influence the design/operation process of a wave energy converter.

Therefore, in chapter 4 the design phase of a generic wave energy converter is analyzed from the location targeting perspective. The geometric tuning of a converter from a geographical perspective was analyzed. This study from a global perspective led to the conclusion that tuning a converter for each location is positive in terms of efficiency but not advantageous in economic terms (kW per Ton indicator). It was demonstrated that the locations where the most probable period is very high (>10 s) need very heavy structures in order to achieve tuning, and then it is not recommended when keeping in mind the material costs. In conclusion, considering that the cost of other factors that influence the overall cost of WECs (the number of PTOs for a given power, O&M) increase for smaller WECs, the main goal of a WEC design should be to select structures with a moderate size although they are not tuned to the local wave climate.

Also in Chapter 5 the influence of the wave conditions during the operation stage of a converter are analyzed due to the identified gap on the understanding of the importance of operation and maintenance in the location targeting process of a Wave Energy Converter. The Operation and Maintenance (O&M) parameters are analyzed on a global basis in order to find the balance between resource and accessibility. The analysis of weather windows and waiting periods showed that apart from the resource these parameters should be taken into account for site selection. Some areas such as the south part of Australia showed very limited accessibility during the whole year (less than 5 %) while some areas in Europe, such as Ireland with the same resource (Ireland) showed an order of magnitude higher accessibility. The variability of the accessibility was also studied on this section, showing that locations as Chile, despite offering a low number of weather windows, its distribution is equally spaced along the year, while other locations such as Australia show a great seasonality with practically 0 accessibility during some winter months. The O&M cost analysis carried out in this section showed that although the wave resource is important in order to predict the income of the WEC power production, it is advised to take the weather windows and waiting period into account, specially for the current stage of the technology within the low reliability stage, in order to accurately estimate the annual costs that the device would require for maintenance.

Finally, due to the absence of studies on the targeting of locations for wave energy development, bearing in mind both resource and accessibility, a generic failure analysis is performed in order to target the locations with an adequate balance between resource and severity of the wave conditions. A set of scenarios was investigated in order to assess the recommended areas for every stage of development. It was concluded that some areas, with a mild resource and a high accessibility such as Nova Scotia in Canada, or Brasil or the Pacific coast of Mexico, have an excellent balance of resource and availability/accessibility for the first 1:1 scale deployments when the reliability of the devices is still low. Within a single WEC deployment, a path formed

by three categorized areas has been suggested, passing from low reliability accepted areas to medium and finally to high reliability areas, in order to take the most advantage of the wave conditions in every location. Some locations with mild resource (10 to 15 kW/m) offer great opportunity to test the devices and enhance its performance and reliability in order to achieve high resource areas in the future.

Finally, as the WECs are assumed to be developed in arrays in the near future, an study of the main wave factors that influence array design is performed. Separation distance between the WECs was found to be a key factor in order to achieve constructive interference. Also wave incidence direction was studied and climates with a more unidirectional trend were found to work better for WEC arrays.

Thirdly, the lack of real economic figures (LCOE) for real prototypes, and the absence of a methodology to analyze the influence of the inter-annual variability on the economics of a wave energy project was identified on Chapter 6. The effect of the uncertainties on met-ocean conditions on the finance of a particular wave energy project is further analyzed. The results show that the variability of financial indicators is extremely high due to the variability of wave climate. The yearly climate conditions uncertainty lead to a standard deviation of 0.73 with respect the mean net present value of the particular case study analyzed. A need of computing the year by year power production through the proposed methodology is highlighted in order to be considered as an input for reliable economic analysis. Furthermore, the influence of the political framework regarding feed in tariffs is analyzed on the cash flow of a particular project with a case study, leading to the conclusion of the importance of the stability of the regulatory markets (at least for the average life time of projects- 20 to 25 years) in order to provide the adequate tools for the development of wave energy. It was concluded that financial support should match the average life cycle of the studied farm in order to set a constant and fixed regulatory framework and avoid unnecessary uncertainties.

Finally, an analysis of the Levelised Cost of Energy (LCOE) of two current prototypes was performed. The impact of the planned improvements on the devices on the LCOE were analyzed showing some real figures of LCOE for the near future (around 1 Euro/kWh). It was concluded that enhancing the energy harvest is a key step in order to reduce the LCOE (either through control techniques or improving PTO efficiency). It was shown how small growth on the hydraulic efficiency of the PTO has a significant impact on LCOE (up to 50 % for a 10% efficiency increase) and also the optimization of the control techniques could lead to an important reduction on LCOE (up to 25 %).

To sum up, the R&D focus in order to achieve a lower LCOE as soon as possible should be on PTO optimization, control techniques in order to enhance the harvest as well as focus on finding cheaper materials for the prototypes. Furthermore, an analysis of these prototypes on different coastal areas was performed showing the importance of finding optimum locations for each type of device (depending on the activating principle) in order to achieve optimum

performance. It is concluded that due to the different performance of some of the current converters, they are matched to different locations around the world, and then the market of each developers has minimum collision with the other developers.

In conclusion, a set of recommendations/conclusions have been extracted on some key topics regarding techno-economic assessment of wave energy converters. Three main gaps were identified on this thesis, regarding power assessment on wave energy converters, the influence of met-ocean conditions on the design and operation phase of a Wave Energy Converter and the economic analysis of wave energy projects. This thesis then addressed these gaps and proposed innovative solutions, mainly a new methodology for wave power assessment, some guidance regarding location targeting for wave energy conversion based on local wave conditions and a new methodology for economic assessment of wave energy converters.

# Future research

---

This thesis has tried to improve the current knowledge about techno-economic assessment of wave energy converters, however some important aspects were put aside because either they were out of the scope of this thesis or because these aspects were discovered while this research was being carried out and the associated time constraints. These aspects will compose the future research lines of this thesis, which are summarized in the following bullet points:

- On the fourth chapter of this thesis the importance of having quality spectral data was highlighted, however on this thesis only multi-component reanalysis spectrums on four locations and one set of real spectrums were used to determine the influence of the quality of the data on the power production assessment. A use of a broader set of real buoys spectra (or at least multi-component reanalysis spectra) on different coastal locations around the world will be useful to identify where exactly and how the analytical spectrums used on the classical power assessment methods influence the final power production figures. Also the use of real spectrums would be useful to further improve the proposed long term power estimations and maybe find a substitute to the bidimensional  $(H_s - T_p)$  power matrix.
- Within the fourth chapter, a simplified analysis was carried out avoiding the influence of the wave direction on the methodology. It will be very interesting to see how the wave direction is added as a fourth parameter in the methodology. Furthermore, it will be very relevant to see how it influences the performance of devices such as a flap, very sensitive to the wave direction.
- Finding an easy method in order to estimate the power performance of a converters on a specific location based on the performance data of a previous location has been highlighted to be very important. This problem is already being studied by the International Electromechanical Committee within the PT 62600-102. A contribution to this committee is expected based on the research performed in this thesis and future research that will be carried out within this committee.
- On the first section of the fifth chapter the matchability of a wave energy converter was analyzed. However a very specific converter was used with a constant ratio diameter/draft was selected for this analysis. It will be useful to repeat the same analysis with different converter variations as well as with converters with different action principles in order to

prove that the selection of small structures is beneficial independently of the harvesting mode.

- On the same aforementioned section it was concluded that small structures should be designed from the material/power production point of view. However at the end of the section a comparison of how the results change when the O&M costs were included was performed. The data for this study were assimilated from the wind industry because of the lack of these type of data on the wave energy sector. It will be useful on future research to perform this study of optimum sizing with real data from prototypes at the sea.
- On the second section of the fifth chapter the analysis of O&M was carried out on a global basis, however some assumptions were made on this study. Only the significant wave height was taken in to account on this study, and in the future more variable such as the wave period and the wind speed should be taken into account in order to do a proper analysis. Also, on this study only sea state parameters were used for O&M, however some recent studies from HMRC have developed new methods to estimate accessibility based on North Atlantic Treaty Organization (2000), Dobie (2000) and Crossland and Rich (2000) taking into account the specific sea keeping conditions for staff performing O&M on floating structures. The O&M study performed on this thesis could be improved taking into account these aspects and specifying the O&M conditions for different converters.
- The third section on the fifth chapter analyzes the optimum locations for wave energy development from a reliability perspective based on a simple failure analysis. This analysis was based on certain assumptions and it could be further improved with a more advanced failure modeling as well as using real failure rates from real prototypes. Also, the inclusion of fatigue on the study could lead to more realistic failure scenarios on the most severe locations.
- On the fourth section of chapter 5 the optimum layout configuration was analyzed for a set of 4 heaving devices. It could be useful to include more devices with different activating principles on future research and also to validate this data with laboratory tests.
- On the fifth chapter an economic analysis of a wave energy prototype was done considering the uncertainties that wave energy is facing nowadays. On the second part of this chapter a comparison on economic terms of two real devices was made. It will be useful to make a fair comparison of more real devices in order to help the industry to find economic-reliable devices. Also it was concluded that market targeting is an important issue for wave energy developers and then it could be useful to include on future research an study of the optimum locations for each type of converter depending on the power matrix type.

# Scientific contributions of this thesis

---

Part of the PhD process requires actively disseminating the findings of the research in the form of posters, publication and presentations. On this chapter the scientific publications related with this thesis are summarized. Part of the contributions from this thesis consist of collaborations with researchers from other research centers, then the author would like to thank Ronan Costello and Jochem Weber from National University of Ireland (Maynooth) and Andrew MacGillivray and Henry Jeffrey from the Institute of Energy Systems, University of Edinburgh for their valuable contribution on some of these papers.

### Journal Papers:

1. De Andrés, A., Guanche, R., Armesto, J., Del Jesus, F., Vidal, C., Losada, I. J., (2013) Time domain model for a two-body heave converter: model and applications. *Ocean Engineering*, 72,116-123.
2. De Andrés, A., Guanche, R., Armesto, J., Del Jesus, F., Vidal, C., Losada, I. J., (2013) Long term power estimation of a Wave Energy converter. *Revista del sector marítimo, Ingeniería Naval, Volumen 2*, 2.01
3. De Andres, A., Guanche, R., Meneses, L., Vidal, C., Losada, I. J. (2014). Factors that influence array layout on wave energy farms. *Ocean Engineering*, 82, 32-41
4. Guanche, R., de Andres, A. D., Simal, P.D., Vidal, C., Losada, I. J., (2013). Uncertainty analysis on financial indicators on wave energy farms. *Renewable Energy*, 68, 570-580
5. De Andres, A., Guanche, R., Vidal, C., Losada, I. J. (2014). Adaptability of a generic wave energy converter to different climate scenarios, *Renewable Energy (under revision)*, RENE-D-14-01337
6. De Andres, A., Guanche, R., Weber, J., Costello, R. (2014). Finding gaps on power production assessment on WECs: wave definition analysis, *Renewable Energy (under revision)*, RENE-D-14-01260
7. Guanche, R., Andres, A., Vidal, C., Losada, I. J. (2014). Study of optimum locations for wave energy development with emphasis on O&M parameters. *Renewable Energy (under revision)*
8. MacGillivray, A. , de Andres, A. ,Guanche, R. , Jeffrey H. (2014) . Factors affecting LCOE of Ocean energy technologies: a study of technology and deployment attractive-

ness. Technological Forecasting and Social Change (under revision)

Conference Papers:

1. De Andrés, A., Guanche, R., Armesto, J., Del Jesus, F., Vidal, C., Losada, I. J., (2013). Metodología para el análisis de la producción de la vida útil de un captador de energía undimotriz. Jornadas de Costas y Puertos 2013, Cartagena (España)
2. De Andrés, A., Guanche, R., Armesto, J., Del Jesus, F., Vidal, C., Losada, I. J., (2013). Methodology for performance assessment of a two body heave converter. Proceedings of the 32nd OMAE Conference, Nantes (France)
3. de Andres, A. , Guanche, R. . Techno-economic assessment of a wave energy converter (2013). 8th INORE Symposium, Pembroke Dock (Wales)
4. de Andres, A. , Guanche, R. . Analysis of O&M parameters and influence of sea state characterization on WECs performance from a global perspective (2014). 9th INORE Symposium, La Vega (Spain)
5. De Andres, A., Guanche, R., Vidal, C., Losada, I. J. (2014). Analysis of the geometric tunability of a WEC from a worldwide perspective. Proceedings of the 33rd OMAE Conference, San Francisco (USA)
6. de Andres, A. , MacGillivray, A. , Guanche, R. , Jeffrey H. (2014) ,Identifying risk and Uncertainties - Pathways towards a Lower LCOE in Marine Energy, Proceedings of the 5th International Conference of Ocean Energy, Halifax (Canada)
7. De Andres, A., Guanche, R., Vidal, C., Losada, I. J. (2015).Location targeting for wave energy development from an Operation and Maintenance Perspective. Proceedings of the 34th OMAE Conference, St Johns (Canada)-Abstract accepted
8. De Andres, A., Guanche, R., Diaz-Simal, P., Vidal, C., Losada, I. J. (2015)Uncertainties on the techno-economic feasibility assessment of wave energy projects. Proceedings of the EWTEC Conference, Nantes(France)-Abstract accepted
9. De Andres, A., Jeffrey, H., Guanche, R.(2015). Finding locations for wave energy development as a function of reliability metrics Proceedings of the EWTEC Conference, Nantes(France)-Abstract accepted

## Appendix 1: Time domain model

---

On this appendix a time domain model developed in order to simulate a two body heaving converter is explained. The The WEC geometry to be analyzed is shown on the sketch of Figure A.1, is a generic two body point absorber consisting of two objects: a buoy (2) , that is only partially submerged and a float (1) that floats on the top of surface. Both objects are only allowed to move in heave and the interconnection between the bodies is made via a linear PTO connection.

The time domain model is based on the second Newton law given by equation B.2

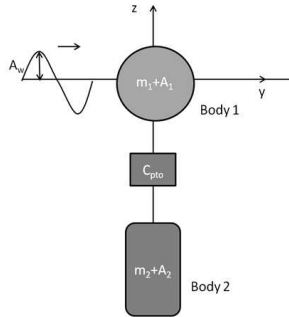


**Figure A.1:** Simplified model

$$\sum F = m\ddot{z} \quad (\text{A.1})$$

where in eq. B.2  $F$  represents the external forces,  $m$  is the body mass,  $z(t)$  is the vertical displacement of the body ( $z$  origin at the Still Body Level, SBL) and the dots symbolize the order of partial time derivation. In the case of a generic floating WEC under wave excitation, the external forces in equation (1) were formulated by Cummins (1962), see equation A.2.

$$m\ddot{z} = F_{excitation} + F_{PTO} + F_b + F_{rad} + F_{vis} \quad (\text{A.2})$$

The external forces represented in eq. A.2 are, 1) the wave excitation term,  $F_{excitation}$ , that results from the integration of the pressure over the wet surface of the body when is held still in the water, 2) the force exerted by the PTO,  $F_{PTO}$ , 3) the hydrostatic buoyancy force,  $F_b$ , due to the submergence variation caused by the WEC oscillations, 4) the radiation force,  $F_{rad}$ , due to the waves radiated by the WEC motion and 5) the viscous friction force,  $F_{vis}$ , caused by the turbulent drag generated by the WEC motion in the fluid. The excitation force,  $F_{excitation}$  is obtained using the frequency-domain BEM WADAM. WADAM extracts the value of the amplitude of the excitation force on the frequency domain and then in this model this values are composed in order to obtain the excitation force vector as an input for the state-space system. The buoyancy force,  $F_b$ , is represented in equation A.3 using the hydrostatic restoring coefficient  $G$  (obtained by the multiplication of the density of the water, the acceleration of gravity and the surface area of the device at the water plane) multiplied by the position of the device.

$$F_b = -Gz(t) \quad (\text{A.3})$$

The radiation force,  $F_{rad}$ , is expressed following Yu and Falnes (1998) in the expression A.4

$$F_{rad} = -A_{\infty}\ddot{z}(t) - \int_0^t K(t-\tau)\dot{z}(\tau)d\tau \quad (\text{A.4})$$

where  $A_{\infty}$  is the constant added mass when the frequency tends to infinity. The second term is the convolution integral where  $K(t)$  represents the fluid memory effects.

The viscous friction force,  $F_{vis}$ , is represented following Hals *et al.* (2007) by equation A.5 as a drag force that depends on the vertical velocity difference between the body and the fluid.

$$F_{vis} = -B\frac{\pi}{8}C_dD_p^2(\dot{z} - v_z)(\dot{z} - v_z) \quad (\text{A.5})$$

where in A.5  $C_d$  is the drag coefficient,  $D_p$  is the diameter of the body and  $v_z$  is the undisturbed flow velocity. Values for the drag coefficient are chosen based on an experimental work by Sauder and Moan (2007) where the viscous forces were measured for different amplitudes and frequencies. In this work  $C_d = 4$  was used.

The PTO force,  $F_{PTO}$ , is assumed to be proportional to the relative vertical motion between the two bodies considered as is expressed in equation A.6.

$$F_{PTO} = C_{PTO}\dot{z}_{rel} \quad (\text{A.6})$$

Inserting equations A.3 to A.6 in the Cummins equation A.2, equations A.7 and A.8 are obtained for the two bodies considered in this model referred here by the sub-index 1 and 2, respectively

$$\begin{aligned} (m_1 + A_{\infty 1})\ddot{z}_1(t) - A_{\infty 12}\ddot{z}_2(t) &= F_{excitation_1}(t) - Gz_1 \\ &\quad - C_{PTO}[\dot{z}_1(t) - \dot{z}_2(t)] - \int_0^t K_1(t - \tau)z_1(\tau)d\tau \\ &\quad - \int_0^t K_{12}(t - \tau)z_2(\tau)d\tau - F_{vis_1}(t) \end{aligned} \quad (\text{A.7})$$

$$\begin{aligned} (m_2 + A_{\infty 2})\ddot{z}_2(t) - A_{\infty 21}\ddot{z}_1(t) &= F_{excitation_2}(t) - Gz_2 \\ &\quad - C_{PTO}[\dot{z}_2(t) - \dot{z}_1(t)] - \int_0^t K_2(t - \tau)z_2(\tau)d\tau \\ &\quad - \int_0^t K_{21}(t - \tau)z_1(\tau)d\tau - F_{vis_2}(t) \end{aligned} \quad (\text{A.8})$$

The most challenging task in the resolution of equations A.7 and A.8 is the computation of the convolution integrals inside the radiation force equation A.4. An efficient resolution technique is to replace the convolution integral with a state-space system, see Henriques *et al.* (2012) or Alves (2012). A general state-space has the form:

$$\begin{aligned} \dot{\mathbf{X}}(t) &= \mathbf{A}\mathbf{X}(t) + \mathbf{B}u(t) \\ y(t) &= \mathbf{C}\mathbf{X}(t) \end{aligned} \quad (\text{A.9})$$

where  $u(t)$  and  $y(t)$  are called input and output respectively of the state space and  $\mathbf{X}(t)$  is the state vector. Each convolution integral in equations A.7 and A.8 is approximated by a state-space:

$$I_{ij}(t) = \int_0^t K_{ij}(t - \tau)\dot{z}_j(\tau) \approx \begin{cases} \dot{\mathbf{X}}_{ij}(t) = A_{ij}\mathbf{X}_{ij}(t) + \mathbf{B}_{ij}\dot{z}_j(t) \\ I_{ij}(t) \approx y(t) = \mathbf{C}_{ij}\mathbf{X}_{ij}(t) \end{cases}, \quad (\text{A.10})$$

$i = 1, 2$ ,  $j = 1, 2$  where  $\dot{z}_j(t)$  is the input of the system.

The problem now is to calculate matrix  $A_{ij}$  and vectors  $\mathbf{B}_{ij}$  and  $\mathbf{C}_{ij}$  to approximate the convolution integral. The methodology is explained for  $i = j = 1$ . The first step therefore is

to choose a set of frequencies  $\{\omega_i\}_{i=1}^n$ , and compute their damping coefficients,  $\{B(\omega_i)\}_{i=1}^n$ , added mass coefficients,  $\{A(\omega_i)\}_{i=1}^n$ , and added mass at infinity,  $A_\infty$  with a BEM code. Ogilvie (1964) provides the relations between the impulse response function in time domain  $K(t)$ , and the added mass,  $A(\omega)$ , and damping coefficients,  $B(\omega)$  in frequency domain. Using Fourier transform, it is possible to write the corresponding transfer function in frequency domain as a function of the added mass and damping coefficients, Taghipour *et al.* (2008):

$$K_{wadam}(i\omega_n) = B(\omega_n) + i\omega[A(\omega_n) + A_\infty], \quad n = 1, 2, \dots, N, \quad (\text{A.11})$$

where  $i$  is the imaginary unit. The least square technique is then applied to find a rational function  $\hat{K}$  that approximates  $K_{wadam}$  for the given set of frequencies  $\{\omega_i\}_{i=1}^n$  following the restrictions given by Perez and Fossen (2011). The approximation is restricted to imaginary values, so writing  $s = i\omega$ , the rational function is defined as (Perez and Fossen (2011)):

$$\hat{K}(s, \theta) = \frac{P(s, \theta)}{Q(s, \theta)} = \frac{p_{n-1}s^{n-2} + p_{n-2}s^{n-2} + \dots + p_1s}{s^n + q_{n-1}s^{n-1} + \dots + q_0}. \quad (\text{A.12})$$

When the coefficients  $\theta = \{p_{n-1}, p_{n-2}, \dots, p_1, q_{n-1}, q_{n-2}, \dots, q_0\}$  are found using the least square method, the matrix and vectors of the state-space which approximates the convolution integral can be written as:

$$A_{11} = \begin{bmatrix} 0 & 0 & 0 & \dots & 0 & -q_0 \\ 1 & 0 & 0 & \dots & 0 & -q_1 \\ 0 & 1 & 0 & \dots & 0 & -q_2 \\ \vdots & \vdots & \vdots & \ddots & \vdots & \vdots \\ 0 & 0 & 0 & \dots & 1 & -q_{n-1} \end{bmatrix}; \quad \mathbf{B}_{11} = \begin{bmatrix} 0 \\ p_1 \\ p_2 \\ \vdots \\ p_{n-1} \end{bmatrix}; \quad \mathbf{C}_{11} = \begin{bmatrix} 0 & \dots & 0 & 1 \end{bmatrix} \quad (\text{A.13})$$

Now, all components of the state-space given in equation (A.10) are known, and the convolution integral can be replaced by the output,  $y_{11}(t)$ , of the state-space. However, the heave velocity of the body,  $\dot{z}_1(t)$ , which is the input of this state-space system is obtained solving the general motion equation (equations (7) and (8)) of the two body WEC every time step. For this purpose, another state-space system is defined (A.15): the general state-space system, Alves (2012). This state-space describes the general equations of motion (equations (7) and (8)) of the 2 body WEC, taking into account all the forces included, and all the convolution integrals,  $I_{ij}(t)$ . In order to extend the obtained state-space to a general one, the general state vector collects the state vectors of all convolution integrals and includes the vector of the position,  $z$ , and its derivative,  $\dot{z}$ :

$$\mathbf{X}(t) = [[\mathbf{X}_{11}] [\mathbf{X}_{12}] [\mathbf{X}_{21}] [\mathbf{X}_{22}] [z] [\dot{z}]]. \quad (\text{A.14})$$

Finally the general equations of motion (equations A.7 and A.8) can be rewritten in an unique state-space as:

$$\begin{cases} \dot{\mathbf{X}}(t) = \mathbf{A}\mathbf{X}(t) + \mathbf{B}F_{excitation}(t) \\ y(t) = \mathbf{C}\mathbf{X}(t) \end{cases} \quad (\text{A.15})$$

Where the input of the state-space is the excitation force,  $F_{excitation}(t)$ , the output is the movement of the 2 body WEC,  $z(t)$ , and matrix  $A$  and vectors  $B$  and  $C$  are given by:

$$A = \begin{bmatrix} [A_{11}] & [0] & [0] & [0] & [0] & [B_{r1}] \\ [0] & [A_{12}] & [[0] & [0] & [0] & [B_{r2}] \\ [0] & [0] & [A_{21}] & [0] & [0] & [B_{r21}] \\ [0] & [0] & [0] & [A_{22}] & [0] & [B_{r2}] \\ [0] & [0] & [0] & [0] & [0] & [1] \\ \left[\frac{C_{r1}}{M}\right] & \left[\frac{C_{r12}}{M}\right] & \left[\frac{C_{r21}}{M}\right] & \left[\frac{C_{r2}}{M}\right] & \left[\frac{G}{M}\right] & [C_{PTO}] \end{bmatrix} \quad (\text{A.16})$$

$$B = \begin{bmatrix} [0] & [0] & [0] & [0] & [0] & [-M^{-1}] \end{bmatrix}^T \quad (\text{A.17})$$

$$C = \begin{bmatrix} [0] & [0] & [0] & [0] & [1] & [0] \end{bmatrix} \quad (\text{A.18})$$

where  $A_i$  in A.16 are the radiation sub-matrices corresponding to the sub-indexes,  $M$  is the mass and added mass matrix, and  $C_{PTO}$  is the PTO and friction sub-matrix. In this global state-space system vectors  $B$  and  $C$  are transformed into matrices. The differential equation system from eq. A.15 is solved using a Runge Kutta Method (ode45) implemented in MATLAB.

## Appendix 2: Frequency domain model

---

### B.1 Frequency domain model for Section 5.2

The frequency domain models are useful for the early stages of development of a converter because of the low computational requirements. By considering that nonlinearities are small, the superposition principle can be used. Then, a linear model is constructed.

This type of model has been widely explained and previously used Falnes (2002), R.Taghipour (2008), . The equations of motion for a rigid body system (with 6 degrees of freedom, DOF) in sea waves can be described with the following equation:

$$\begin{aligned}
 -\omega^2 m |z| e^{i\omega t} = A(\omega) f_{exc}(\omega) e^{i\omega t} - G |z| e^{i\omega t} + \omega^2 M(\omega) |z| e^{i\omega t} \\
 - i\omega B(\omega) |z| e^{i\omega t} - i\omega D(\omega) |z| e^{i\omega t} - K(\omega) |z| e^{i\omega t} \quad (B.1)
 \end{aligned}$$

where

- $\omega$  is the radial frequency in rad/s;
- $m$  is the mass of the floating object;
- $A(\omega)$  is the amplitude of the incident wave;
- $f_{exc}(\omega)$  is the complex amplitude of the excitation force of a wave with a frequency  $\omega$  and unit wave;
- $G$  is the hydrostatic coefficient;
- $M(\omega)$  is the added mass considered as a function of  $\omega$ ;
- $B(\omega)$  is the hydrodynamic damping coefficient considered as a function of  $\omega$ ; and
- $K(\omega)$  and  $D(\omega)$  are the PTO coefficients that depend on  $\omega$ .

This equation is time dependent because of the term  $e^{i\omega t}$ . However, this term can be neglected because it is present in all other terms of the equation. Then, equation 1 can be rewritten as a time independent equation:

$$-\omega^2 m |z| = A(\omega) f_{exc}(\omega) - G |z| + \omega^2 M(\omega) |z| - i\omega B(\omega) |z| - i\omega D(\omega) |z| - K(\omega) |z| \quad (\text{B.2})$$

If the previous equation is expressed for one floater with 6 DOFs, this equation can be written in the following matrix form:

$$[-\omega^2(m+M) + G + i[\omega(B+D)]] \times [Z] = [F_{ex}] \quad (\text{B.3})$$

where

- $m$  is the inertia matrix of the floating object;
- $M$  is the added mass matrix of the floating object that accounts for the added mass of each DOF  $i$  when a displacement is produced in a DOF  $j$ . If several bodies are considered, then the added mass matrix contains the added mass that it is produced on a body  $a$  on a DOF  $i$  when a displacement is produced on body  $b$  in a DOF  $j$ ;
- $G$  is the matrix of hydrostatic coefficients;
- $B$  is the damping matrix of the floating object that contains the added mass of each DOF  $i$  when a displacement is produced in a DOF  $j$ . If several bodies are considered, then the added mass matrix contains the added mass that is produced on a body  $a$  on a DOF  $i$  when a displacement is produced on body  $b$  in a DOF  $j$ ;
- $D_{PTO}$  is the power take-off matrix in which the coefficients appear as the degree of freedom that reflects how the converter extracts energy; and
- $Z$  is the complex amplitude of motion of each degree of freedom. In this equation, the incident wave height is assumed to be 1 m. Afterwards, the real incident wave will be considered.

Once the system of equations is solved, the amplitude of motion for each degree of freedom variable is computed. Then, the absorbed power can be calculated. The time series of displacements that accounts for the amplitude of motion by computing the frequency domain model is as follows:

$$\eta(t) = \sum_{i=1}^n A_i(\omega_i) a_{D_i}(\omega_i) \sin(\omega_i t + \varphi_i) \quad (\text{B.4})$$

where  $A_i(\omega_i)$  is the amplitude of the incident wave,  $a_{D_i}(\omega_i)$  is the amplitude of motion obtained by the frequency domain model for the DOF that extracts the energy for a certain frequency and  $\varphi_i$  is the phase of the motion. The power time series can be obtained as the following equation:

$$P(t) = D \sum_{i=1}^n A_i(\omega_i) a_{D_i}(\omega_i) \sin(\omega_i t + \varphi_i)]^2 \quad (\text{B.5})$$

where D the optimum PTO constant for the frequency  $\omega_i$ . For a sea state of N spectral components, the mean power of a sea state can be calculated as follows:

$$\bar{P} = \frac{1}{S} \int_0^S P(t) dt = \frac{D}{S} \int_0^S \left[ \sum_{i=1}^N A_i(\omega_i) a_{D_i}(\omega_i) \cos(\omega_i t + \varphi_i) \right]^2 dt] \quad (\text{B.6})$$

$$\begin{aligned} \bar{P} = \frac{1}{S} \int_0^S P(t) dt = \frac{D}{S} \int_0^S D \sum_{i=1}^N [\omega_i A_i(\omega_i) a_{D_i}(\omega_i) \cos(\omega_i t + \varphi_i)]^2 dt] \\ + \frac{D}{S} \int_0^S D \sum_{i=1}^N 2\omega_i \omega_j A_i A_j a_{D_i} a_{D_j} \cos(\omega_i t + \varphi_i) \cos(\omega_j t + \varphi_j) dt] \quad (\text{B.7}) \end{aligned}$$

The average of the second integral can be assumed to be zero if S is large; therefore, the solution of the first square cosine integral is S/2. Then, the mean power absorbed by a floating converter within a sea state can be computed with the following expression:

$$\bar{P} = \frac{D}{2} \sum_{i=1}^n (\omega_i A_i(\omega_i) a_{D_i}(\omega_i))^2 \quad (\text{B.8})$$

Applying this procedure, the power matrix of a device can be obtained. For each sea state, a unique PTO constant is applied. The PTO constant is the value that maximizes the mean absorbed power for a regular wave train with a period equal to the peak period ( $T_p$ ) of the sea state. Consequently, only one PTO constant exists per sea state.

## B.2 Frequency domain model for Section 4.2

1

This model is the frequency domain model used to simulated the devices on section 4.2. It is a frequency domain model that solves the same equations than the previously explained one. However, it exists some differences regarding the motion limits based on the varice of the position.

$$\sigma^2 = \text{var}(a_{D_i} A_i(\omega_i)) = \frac{1}{2} \sum_{\omega} |a_{D_i} A_i(\omega_i)|^2 \quad (\text{B.9})$$

---

1. This model was used in collaboration with Ronan Costello and Jochem Weber from NUI Maynooth, see chapter 9 Scientific Contributions

There is no expression for the maximum position that a WEC will take in any given sea state but given the variance of position, the position with any chosen exceedence may be calculated from an inverse cumulative normal distribution function. We define  $x_{(n\%)}$  as the position where  $n\%$  of values in the position time series are in the range  $-x_{(n\%)} < x < x_{(n\%)}$ . The implementation of the inverse normal cumulative distribution functions used was the Matlab implementation from Tracy *et al.* (2007). This knowledge of variance and exceedence values is used to apply relevant constraints to the position in power producing modes of motion, in other words PTO end-stops.

The above equations were implemented in a Matlab program, in execution for each device in each sea state the computer program used a simplex optimization algorithm to manipulate the power take off damping (and optionally stiffness) to minimize -P subject to the constraint that the  $x_{(98\%)}$  exceedence value is less than a specified maximum. The results is that in most smaller sea states the optimum damping is chosen but in larger sea states higher damping values than those that correspond to maximum power are sometimes chosen by the optimization in order to limit the extreme positions.

---

## Bibliography

---

- Abdulla, K., Skelton, J., Doherty, K., O’Kane, P., Doherty, R., and Bryans, G. Statistical availability analysis of wave energy converters. *Proceedings of the International Society of Offshore and Polar Engineers*, 2011.
- Alves, M. *Numerical Simulation of the Dynamics of Point Absorber Wave Energy Converters using Frequency and Time Domain Approaches*. PhD thesis, Universidade Técnica de Lisboa, February 2012.
- Ambühl, S., Kramer, M., Kofoed, J. P., Sørensen, J. D., and Ferreira, C. B. Reliability assessment of wave energy devices. *Safety, Reliability, Risk and Life-Cycle Performance of Structures and Infrastructures*, pages 5195 –5202, 2014a.
- Ambühl, S., Kofoed, J. P., and Sørensen, J. D. Stochastic modeling of long-term and extreme value estimation of wind and sea conditions for probabilistic reliability assessments of wave energy devices. *Ocean Engineering*, 89(0):243 – 255, 2014b.
- Ayyub, B. *Elicitation of Expert Opinions for Uncertainty and Risks*. Taylor & Francis, 2010. ISBN 9780849310874.
- Babarit, A. and Hals, J. On the maximum and actual capture width ratio of wave energy converters. *Proceedings of the European Wave and Tidal Energy Conference, Southampton*, 2011.
- Babarit, A., Borgarino, B., Ferrant, P., and Clément, A. Assessment of the influence of the distance between two wave energy converters on energy production. *Renewable Power Generation, IET*, 4(6):592–601, November 2010.
- Babarit, A., Hals, J., Muliawan, M., Kurniawan, A., Moan, T., and Krokstad, J. Numerical benchmarking study of a selection of wave energy converters. *Renewable Energy*, 41(0):44 – 63, 2012.
- Babarit, A. Impact of long separating distances on the energy production of two interacting wave energy converters. *Ocean Engineering*, 37(89):718 – 729, 2010.
- Beels, C., Troch, P., Kofoed, J. P., Frigaard, P., Kringelum, J. V., Kromann, P. C., Donovan, M. H., Rouck, J. D., and Backer, G. D. A methodology for production and cost assessment of a farm of wave energy converters. *Renewable Energy*, 36(12):3402 – 3416, 2011.
- Borgarino, B., Babarit, A., and Ferrant, P. Impact of wave interactions effects on energy absorption in large arrays of wave energy converters. *Ocean Engineering*, 41(0):79 – 88, 2012.

- Bovaird, R. and H.Zagor. Lognormal distribution and maintainability in support systems research. *Naval Research Logistics Quarterly*; 8(4):343 - 356, 2006.
- Brown, A., Paasch, R., Tumer, I., Lence-Bluhm, P., Hovland, J., von Jouanne, A., and Brekken, T. Towards a definition and metric for the survivability of ocean wave energy converters. *Proceedings of ASME 2010 14th International Conference on Energy Sustainability*, 2010.
- Budal, K. Theory for absorption of wave power by a system of interacting bodies. *J.Ship Res.*, 21(0):248 – 253, 1977.
- Camus, P., Mendez, F. J., and Medina, R. A hybrid efficient method to downscale wave climate to coastal areas. *Coastal Engineering*, 58(9):851 – 862, 2011.
- CarbonTrust. Accelerating marine energy. Technical report, Carbon Trust, 2011.
- Carnegie Web page. Carnegie. WWW page, 2014. URL <http://www.carnegiwave.com/?url=/ceto/what-is-ceto>.
- Castro-Santos, L., Garcia, G. P., Estanqueiro, A., and Justino, P. A. The levelized cost of energy (lcoe) of wave energy using {GIS} based analysis: The case study of portugal. *International Journal of Electrical Power & Energy Systems*, 65(0):21 – 25, 2015.
- CERN. Putnam, energy in the future, 1953; j. laherrere, peak oil and other peaks, CERN 2005, BP statistical review. Technical report, CERN-BP, 2008.
- Child, B. F. *On the configuration of arrays of floating wave energy converters*. PhD thesis, The University of Edimburgh, 2011.
- Child, B. and Venugopal, V. Optimal configurations of wave energy device arrays. *Ocean Engineering*, 37(16):1402 – 1417, 2010.
- Clement, A., McCullen, P., Falcao, A., Fiorentino, A., Gardner, F., Hammarlund, K., Lemonis, G., Lewis, T., Nielsen, K., Petroncini, S., Pontes, M.-T., Schild, P., Sjöström, B.-O., Sorensen, H. C., and Thorpe, T. Wave energy in europe: current status and perspectives. *Renewable and Sustainable Energy Reviews*, 6(5):405 – 431, 2002.
- Crabtree, C. Operational and reliability analysis of offshore wind farms. Technical report, Durham University, Supergen Wind, 2012.
- Crossland, P. and Rich, K. Validating a model of the effects of ship motion on postural stability. *Gosport: UK Defense Evaluation and Research Agency*, 2000.
- Cummins, W. E. The impulse response function and ship motions. *Schiffstechnik*, 9:101 – 109, 1962.

- Dalton, G. and Lewis, T. Performance and economic feasibility analysis of 5 wave energy devices off west coast of Ireland. *Proceedings of the 9th European Wave and Tidal Energy Conference, Uppsala*, 2011.
- Dalton, G., Alcorn, R., and Lewis, T. A 10 year installation program for wave energy in Ireland: A case study sensitivity analysis on financial returns. *Renewable Energy*, 40(1):80 – 89, 2012.
- Danielsson, O. *Design of liner generator for a wave energy plant*. PhD thesis, University of Uppsala, January 2003.
- Davey, T., Harrison, G., and Stallard, T. Procedures for economic evaluation. Technical report, Equitable Testing and Evaluation of Marine Energy Extraction Devices in terms of Performance, Cost and Environmental Impact, 2009.
- de Andres, A., Guanche, R., Armesto, J., del Jesus, F., Vidal, C., and Losada, I. Time domain model for a two-body heave converter: Model and applications. *Ocean Engineering*, 72(0): 116 – 123, 2013a.
- de Andres, A., Guanche, R., Meneses, L., Vidal, C., and Losada, I. J. Factors that influence array layout on wave energy farms. *Ocean Engineering(submitted)*, 2013b.
- Department of Energy and Climate Change. Tech. rep hm government: Marine energy action plan 2010 Ú executive summary & recommendations. Technical report, Department of Energy and Climate Change., 2010.
- DNV. *SESAM Users Manual, WADAM*, 2008. URL <http://www.dnv.cl/services/software/products/sesam/sesamhydrod/wadam.asp>.
- Dobie, T. The importance of the human element in ship design. *New Orleans: University of New Orleans*, 2000.
- Doherty, K. Learning by doing. *Renewable UK: Wave and Tidal 2014 Proceedings*, 2014.
- Edinburgh Wave Power Group webpage. Edinburgh Wave Power Group. WWW page, 2009. URL <http://www.mech.ed.ac.uk/research/wavepower/>.
- Espejo, A. *Variabilidad espacial y temporal del recurso surf: metodología y resultados*. PhD thesis, University of Cantabria, May 2011.
- Espejo, A., Mínguez, R., Tomas, A., Menendez, M., Mendez, F., and Losada, I. Directional calibrated wind and wave reanalysis databases using instrumental data for optimal design of off-shore wind farms. In *OCEANS, 2011 IEEE - Spain*, pages 1 –9, June 2011. doi: 10.1109/Oceans-Spain.2011.6003592.

- ETI and UKERC. Marine energy technology roadmap. Technical report, Energy Technologies Institute, 2014.
- EWEA. The european offshore wind industry - key trends and statistics 2013. Technical report, The European Wind Energy Association, 2014.
- Falcao, Antonio. Wave energy utilization: A review of the technologies. *Renewable and Sustainable Energy Reviews*, 14(3):899 – 918, 2010.
- Falnes, J. A review of wave-energy extraction. *Marine Structures*, 20(4):185 – 201, 2007.
- Falnes, J. Radiation impedance matrix and optimum power absorption for interacting oscillators in surface waves. *Applied Ocean Research*, 2(2):75 – 80, 1980.
- Falnes, J. *Ocean Waves and Oscillating Systems - Linear Interactions Including Wave-Energy Extraction*. Cambridge University Press, 2002. ISBN 978-0-521-78211-1. URL <http://app.knovel.com/hotlink/toc/id:kp0W0SLI18/ocean-waves-oscillating/ocean-waves-oscillating>.
- Falnes, J. and Budal, K. Wave-power absorption by parallel rows of interacting oscillating bodies. *Applied Ocean Research*, 4(4):194 – 207, 1982.
- Fernandez-Chozas, J. *Technical and Non-Technical issues towards the commercialisation of wave energy converters*. PhD thesis, Aalborg University, 2013.
- Flocard, F. and Finnigan, T. Increasing power capture of a wave energy device by inertia adjustment. *Applied Ocean Research*, 34(0):126 – 134, 2012.
- Franke, R. Scattered data interpolation: Tests of some method. *Mathematics of Computation*, 38(157):pp. 181–200, 1982.
- Fronde WEC . Fronde. WWW page, 2014. URL <http://www.see.ed.ac.uk/~eeto/Modules%20-%20do%20not%20use/45-07/Handouts/wave/The%20Fronde%20Wave%20Energy%20Generator.pdf>.
- Garnaud, X. and Mei, C. C. Wave-power extraction by a compact array of buoys. *Journal of Fluid Mechanics*, 635:389–413, 2009.
- Gilloteaux, J. and Ringwood, J. Control-informed geometric optimisation of wave energy converters. *IFAC Conference on Control Applications in Marine Systems (CAMS), September 2010, Rostock*, 2010.
- Goggins, J. and Finnegan, W. Shape optimisation of floating wave energy converters for a specified wave energy spectrum. *Renewable Energy*, 71(0):208 – 220, 2014.

- Gonzalez-Reguero, B. *Numerical modeling of the global wave climate variability and associated environmental and technological risks*. PhD thesis, University of Cantabria, January 2013.
- Guedes-Soares, C. Spectral modeling of sea states with multiple wave systems. *Journal of Offshore Mechanics and Arctic Engineering*, 114(4):278–284, 1992.
- Guedes-Soares, C. Probability distributions of wave heights and periods in measured two-peaked spectra from the portuguese coast. *Proceedings of the 20th International Conference on Offshore Mechanics and Arctic Engineering*, 2001.
- Hals, A. B. J. On the maximum and actual capture width ratio of wave energy converters. *Proceedings of the European Wave and Tidal Energy Conference*, 2011.
- Hals, J., Taghipour, R., and Moan, T. Dynamics of a force-compensated two-body wave energy converter in heave with hydraulic power take-off subject to phase control. In *Proceedings of the 7th European Wave and Tidal Energy Conference*, 2007.
- Hanson, J. and Phillips, O. Automated analysis of ocean surface directional wave spectra. *Journal of Atmospheric and Oceanic Technology*, 18:277–293, 2001.
- Harris, R., Johanning, L., and Wolfram, J. Mooring systems for wave energy converters: A review of design issues and choices. *3rd International Conference on Marine Renewable Energy, Blyth, UK*, 2004.
- Henriques, J., Lopes, M., Gomes, R., Gato, L., and Falcão, A. On the annual wave energy absorption by two-body heaving wecs with latching control. *Renewable Energy*, 45(0):31 – 40, 2012.
- Hernández-Brito, J., Monagas, V., González, J., Schallenberg, J., and Llinás, O. Vision for marine renewables in the canary islands. In *4th International Conference on Ocean Energy, 17 October, Dublin*, october 2012.
- IHCantabria. *ENOLA Project*. 2011. URL "<http://www.enola.ihcantabria.com/>".
- Iturrioz, A. *Modelado numérico de sistemas de extracción de energía del oleaje basados en la tecnología de Columna de Agua Oscilante*. PhD thesis, Universidad de Cantabria, Santander, Spain, 2014.
- Jensen, P., Morthorst, P., Skiver, S., and Rasmussen, M. Economics of wind turbines in denmark -investment and operation and maintenance cost for selected generations of turbines. *Renewable Energy*, 2002.
- Julia Fernandez Chozas web page. Julia Fernandez Chozas. WWW page, 2014. URL <http://http://www.juliafchozas.com/es/>.

- Kaimei website. Japan Agency for Marine-Earth Science and Technology. WWW page, 2014. URL <http://www.jamstec.go.jp/e/>.
- Kalnay, E., Kanamitsu, M., Kistler, R., Collins, W., Deaven, D., Gandin, L., Iredell, M., Saha, S., White, G., Woollen, J., et al. The ncep/ncar 40-year reanalysis project. *Bull. Amer. Meteor. Soc.*, 77(3):437–471, 1996.
- Kerbiriou, M., Prevosto, M., Maisondieu, C., and Clement, A. Influence of an improved sea-state description on a wave energy converter production. In *Proceedings of the 26th International Conference on Offshore Mechanics and Arctic Engineering; 2007; San Diego, California, USA., 2007a*.
- Kerbiriou, M., Prevosto, M., Maisondieu, C., and Clement, A. Influence of sea-states description on wave energy production. In *Proceedings of the European Wave and Tidal Energy Conference; 2007; Porto, 2007b*.
- Khron, S., P.Morhost, and S.Awebuch. The economics of wind energy. Technical report, European Wind Energy Association, 2009.
- Klein, A., B.Pfluger, A.Held, and M.Ragwitz. Evaluation of different feed-in tariff design options: Best practice paper for the international feed-in cooperation. Technical report, Fraunhofer, 2008.
- Kofoed, J., Pecher, A., Margheritini, L., Antonishen, M., Bittencourt, C., Holmes, B., Retzler, C., Berthelsen, K., Crom, I. L., Neumann, F., Johnstone, C., McCombes, T., and Myers, L. A methodology for equitable performance assessment and presentation of wave energy converters based on sea trials. *Renewable Energy*, 52(0):99 – 110, 2013.
- Kramer, M., E.Vidal, L.Marquis, and P.Frigaard. Status and perspectives for the wavestar demonstrator at hanstholm. *Proceedings of the European Wave and Tidal Energy Conference, Aalborg*, 2013.
- Leete, S., Xu, J., and Wheeler, D. Investment barriers and incentives for marine renewable energy in the uk: An analysis of investor preferences. *Energy Policy*, 60(0):866 – 875, 2013.
- Limpet: the guardian News Ltd. Limpet: the guardian News. WWW page, 2008. URL <http://www.theguardian.com/environment/2008/apr/06/windpower.scotland>.
- Lin, L. and Yu, H. Offshore wave energy generation devices: Impacts on ocean bio-environment. *Acta Ecologica Sinica*, 32(3):117 – 122, 2012.
- Mackay, E. B., Bahaj, A. S., and Challenor, P. G. Uncertainty in wave energy resource assessment. part 1: Historic data. *Renewable Energy*, 35(8):1792 – 1808, 2010.

- Mendez, F., Camus, P., Medina, R., and Cofino, A. Analyzing the multidimensional wave climate with self organizing maps. In *OCEANS 2009 - EUROPE*, pages 1 –9, may 2009. doi: 10.1109/OCEANSE.2009.5278285.
- NAVITAS web page. NAVITAS tool from HMRC. WWW page, 2014. URL <http://www.ucc.ie/en/hmrc/projects/navitas/>.
- Newnan, D. and Lavelle, J. *Essentials of Engineering Economic Analysis*. Engineering Press, 1998. ISBN 9781576450284.
- Nielsen, J. J. and Sørensen, J. D. On risk-based operation and maintenance of offshore wind turbine components. *Reliability Engineering & System Safety*, 96(1):218 – 229, 2011. Special Issue on Safecom 2008.
- Nobre, A., Pacheco, M., Jorge, R., Lopes, M., and Gato, L. Geo-spatial multi-criteria analysis for wave energy conversion system deployment. *Renewable Energy*, 34(1):97 – 111, 2009.
- North Atlantic Treaty Organization. Nato stanag 4154 , en-general criteria and common procedures for seakeeping performance assessment-ed 2 amd 2. Technical report, IHS, 2000.
- Ocean Power Technologies Web page. OPT POWER buoy. WWW page, 2014. URL <http://www.oceanpowertechnologies.com/>.
- O'Connor, M., Lewis, T., and Dalton, G. Operational expenditure costs for wave energy projects and impacts on financial returns. *Renewable Energy*, 50(0):1119 – 1131, 2013a.
- O'Connor, M., Lewis, T., and Dalton, G. Weather window analysis of irish and portuguese wave data with relevance to operations and maintenance of marine renewables. *Proceedings of the International Conference on Ocean, Offshore and Arctic Engineering; 2013; Nantes.*, 2013b.
- O'Connor, M., Lewis, T., and Dalton, G. Weather window analysis of irish west coast wave data with relevance to operations and maintenance of marine renewables. *Renewable Energy*, 52(0):57 – 66, 2013c.
- O'Connor, M., Lewis, T., and Dalton, G. Techno-economic performance of the pelamis p1 and wavestar at different ratings and various locations in europe. *Renewable Energy*, 50(0):889 – 900, 2013d.
- Ogilvie, T. Recent progress towards the understanding and prediction of ship motions. In *Sixth Symposium on Naval Hydrodynamics*, pages 3–79, 1964.
- Pecher, A. *Performance Evaluation of Wave Energy Converters*. PhD thesis, Aalborg University, 2012.

- Perez, T. and Fossen, T. Practical aspects of frequency-domain identification of dynamic models of marine structures from hydrodynamic data. *Ocean Engineering*, 38:426 – 435, 2011.
- Pitt, E. Assessment of performance of wave energy conversion systems. *The European Marine Energy Centre Ltd (EMEC) (2009) no. Marine Energy Guides*, p. 1Ú28, 2009.
- Previsic, M. and Shoele, K. Cost reduction pathways for wave energy. *Proceedings of the 10th European Wave and Tidal Energy Conference, Aalborg*, 2013.
- Price, A., Dent, C., and Wallace, A. On the capture width of wave energy converters. *Applied Ocean Research*, 31(4):251 – 259, 2009. *Renewable Energy: Leveraging Ocean and Waterways Renewable Energy*.
- Rademakers, L., Braam, H., Obdam, T., and vd Pieterman, R. Operation and maintenance cost estimator (omce) to estimate the future o&m costs of offshore wind farms. 2009.
- Rasclé, N. and Arduin, F. A global wave parameter database for geophysical applications. part 2: Model validation with improved source term parameterization. *Ocean Modelling*, 70(0):174 – 188, 2013a. *Ocean Surface Waves*.
- Rasclé, N. and Arduin, F. A global wave parameter database for geophysical applications. part 2: Model validation with improved source term parameterization. *Ocean Modelling*, 70(0):174 – 188, 2013b.
- Rashid, A. and Hasanzadeh, S. Status and potentials of offshore wave energy resources in chahbahar area (nw omman sea). *Renewable and Sustainable Energy Reviews*, 15(9):4876 – 4883, 2011.
- Reguero, B., Menendez, M., Mendez, F., Mínguez, R., and Losada, I. A global ocean wave (GOW) calibrated reanalysis from 1948 onwards. *Coastal Engineering*, 65(0):38 – 55, 2012.
- Reguero, B., Mendez, F., and Losada, I. Variability of multivariate wave climate in latin america and the caribbean. *Global and Planetary Change*, 100(0):70 – 84, 2013.
- Reliability data handbook (OREDA) Det Norske Veritas (DNV), O. Offshore Reliability data handbook (oreda). Technical report, Det Norske Veritas (DNV), 1997.
- Renewable UK, Associates, B., and Hassan, G. G. Wave and tidal energy in the uk; conquering challenges, generating growth. Technical report, RenewableUK, 2013.
- Renzi, E. and Dias, F. Resonant behaviour of an oscillating wave energy converter in a channel. *Journal of Fluid Mechanics*, 701:482–510, June 2012.
- Ricci, P., Alves, M., Falcão, A., and Sarmiento, A. Optimization of the geometry of wave energy converters. In *Proceedings of the OTTI International Conference on ocean energy (2006) Bremerhaven*, 2006.

- Rodriguez, G., Guedes-Soares, C., and Pacheco, M. Wave period distribution in mixed sea-states. *Journal of Offshore Mechanics and Arctic Engineering*, 126(1):105–112, 2004.
- R.Taghipour. *Efficient Prediction of Dynamic Response for Flexible and Multi-Body Marine Structures*. PhD thesis, Norwegian University of Science and Technology Faculty of Engineering Science and Technology Department of Marine Technology, October 2008.
- Salter, S. Wave power. *Nature*, 4:249:720, 1974.
- Sauder, T. and Moan, T. Experimental investigation of the hydrodynamic characteristics of a novel column design for semi-submersible platforms. In *The Seventeenth (2007) International Offshore and Polar Conference*, 2007.
- Saulnier, J. Deliverable 6: Annual variability of wave energy. , research training network towards competitive ocean wave energy. *Report No.: MRTN-CT-2004-50166.*, 15, 2004.
- Saulnier, J.-B., Clement, A., de O. Falcao, A. F., Pontes, T., Prevosto, M., and Ricci, P. Wave groupiness and spectral bandwidth as relevant parameters for the performance assessment of wave energy converters. *Ocean Engineering*, 38(1):130 – 147, 2011a.
- Saulnier, J.-B., Prevosto, M., and Maisondieu, C. Refinements of sea state statistics for marine renewables: A case study from simultaneous buoy measurements in portugal. *Renewable Energy*, 36(11):2853 – 2865, 2011b.
- Seabased. Seabased web page. WWW page, 2014. URL <http://www.seabased.com/en/>.
- Seatricity . Seatricity web page. WWW page, 2014. URL <http://www.seatricity.net/>.
- S.H.Salter. The swinging mace. In *Proceedings of the workshop Wave Energy R&D; 1992*. p. 197-206., 1992.
- SIOcean. Ocean energy: State of the art. Technical report, University of Edinburgh; Carbon Trust; JRC; European Ocean Energy Association; RenewableUK; Wavec; DHI, 2013.
- SIOcean. Ocean energy: State of the art. Technical report, SIOcean, 2012.
- Smith, G. and Taylor, J. Preliminary wave energy device performance protocol. *The Department of Trade and Industry (DTI) (2007) MRF/02/00005/00/00-URN 07/807*, 2009.
- Snarey, M., Terrett, N. K., Willett, P., and Wilton, D. J. Comparison of algorithms for dissimilarity-based compound selection. *Journal of Molecular Graphics and Modelling*, 15 (6):372 – 385, 1997.
- Starling, M. Guidelines for reliability, maintainability and survivability of marine energy conversion systems. Technical report, European Marine Energy Centre, 2009.

- Steenstrup, P. Wave star energy - new wave energy converter. *Proceedings of the International Conference Ocean Energy*, 2006.
- Taghipour, R., Perez, T., and Moan, T. Hybrid frequency-time domain models for dynamic response analysis of marine structures. *Ocean Engineering*, 35(7):685 – 705, 2008.
- Teillant, B., Costello, R., Weber, J., and Ringwood, J. Productivity and economic assessment of wave energy projects through operational simulations. *Renewable Energy*, 48(0):220 – 230, 2012.
- Thies, P. *Advancing reliability information for Wave Energy Converters*. PhD thesis, University of Exeter, August 2014.
- Thies, P., Flinn, J., and Smith, G. Is it a showstopper? reliability assessment and criticality analysis for wave energy converters. *Proceedings of the European Wave and Tidal Energy Conference, 2011, Uppsala (Sweden)*, 2011a.
- Thies, P. R., Johannig, L., and Smith, G. H. Towards component reliability testing for marine energy converters. *Ocean Engineering*, 38(2Ü3):360 – 370, 2011b.
- Thies, P. R., Smith, G. H., and Johannig, L. Addressing failure rate uncertainties of marine energy converters. *Renewable Energy*, 44(0):359 – 367, 2012.
- Tracy, B., Devaliere, E., Hanson, J., Nicolini, T., and Tolman, H. Wind sea and swell delineation for numerical wave modeling. *Proceedings of the 10th International Workshop on Hindcasting and Forecasting, November 11-16, 2007, at Turtle Bay, Oahu, H, 2007*.
- UKERC. Marine (wave and tidal current) renewable energy technology roadmap. Technical report, UK Energy Research Centre, 2007.
- UnitedNations. World population prospects: The 2008 revision. Technical report, United Nations, 2009.
- Van Bussel, G. and Zaaier, M. Reliability, availability and maintenance aspects of large-scale offshore wind farms, a concepts study. In *Proceedings of MAREC*, volume 2001, 2001.
- Vicinanza, D., Margheritini, L., Kofoed, J. P., and Buccino, M. The ssg wave energy converter: Performance, status and recent developments. *Energies*, 5(2):193–226, 2012.
- Vicinanza, D., Contestabile, P., Norgaard, J. Q. H., and Andersen, T. L. Innovative rubble mound breakwaters for overtopping wave energy conversion. *Coastal Engineering*, 88(0): 154 – 170, 2014.
- Vidal, C. *Estudio de las Disponibilidades de Energía del Oleaje en el mar Cantábrico. Selección y Análisis en Modelo Matemático y Físico de un Sistema Hidroneumático Fijo Colector para el Aprovechamiento de la Energía del Oleaje*. PhD thesis, Universidad de Cantabria, España, Junio 1984.

- Vidal, E., Hansen, R., and Kramer, M. Early performance assessment of the electrical output of wavestar's prototype. *Proceedings of the International Conference of Ocean Energy, Dublin*, 2012.
- Walker, D. and Taylor, R. E. Wave diffraction from linear arrays of cylinders. *Ocean Engineering*, 32(17):2053 – 2078, 2005.
- Walker, R., Johanning, L., and Parkinson, R. Weather windows for device deployment at uk test sites: availability and costs implications. *Proceedings of the European Wave and Tidal Energy Conference, Southampton*, 2011.
- Wang, D. and Hwang, P. An operational method for separating wind sea and swell from ocean wave spectra. *Journal of Atmospheric and Oceanic Technology*, 18:2052–2062, 2001.
- Weber, J. WEC technology readiness and performance matrix finding the best research technology development trajectory. *International Conference of Ocean Energy Proceedings*, 2012.
- Whitakker, T., Beattie, W., Folley, M., Boake, C., A.Wright, and M.Osterried. The limpet wave power project- the first years of operation. *Renewable Energy*, 2006. URL <http://web.sbe.hw.ac.uk/staffprofiles/bdgsa/shsg/Documents/2004sem/limpet.PDF>.
- Wolgamot, H., Taylor, P., and Taylor, R. E. The interaction factor and directionality in wave energy arrays. *Ocean Engineering*, 47(0):65 – 73, 2012.
- Wright, T. P. Factors Affecting the Cost of Airplanes. *Journal of Aeronautical Sciences*, 3: 122–128, 1936.
- Yemm, R. Update of pelamis at EMEC. *Renewable UK: Wave and Tidal 2014 Proceedings*, 2014.
- Yu, Z. and Falnes, J. State-space modelling of dynamic systems in ocean engineering. *Journal of Hydrodynamics*, 1(1):1–17, 1998.